EFFECT OF MESENCHYMAL STEM CELLS ON EQUINE OVARIAN FOLLICULAR DEVELOPMENT AND GENE EXPRESSION

A Dissertation

by

SICILIA TATIANA GRADY

Submitted to the Office of Graduate and Professional Studies of
Texas A&M University
in partial fulfillment of the requirements for the degree of

DOCTOR OF PHILOSOPHY

Chair of Committee,	Katrin Hinrichs
Committee Members,	Scott V. Dindot
	Qinglei Li
	Ashlee E. Watts
Head of Department,	Larry J. Suva

August 2017

Major Subject: Biomedical Sciences

ABSTRACT

Aging affects the reproductive efficiency of females. In rodent models, injection of mesenchymal stem cells (MSCs) improves function and induces trophic mRNA expression in ovaries compromised by chemotherapy. However, little information is available on the effect of MSCs in the aging ovary, an application which if effective in increasing fertility, would have an impact in both human and equine reproduction. The aim of the research outlined in this dissertation was to investigate this area. We hypothesized that injection of MSCs into the ovaries of old mares would increase follicle numbers and increase expression of genes related to follicle growth. We examined for the first time the use of fluorescent quantum dots (QDs) to label equine MSCs, to see if this would allow them to be tracked after injection. We found that QD-labeled MSCs retain their ability to proliferate and differentiate. The QDs were maintained in MSCs induced to differentiate into chondrocytes (non-proliferating), but the percentage of labeled cells and the fluorescence intensity decreased to essentially non-detectable within 3 to 5 days in rapidly proliferating cells. Co-culture of equine ovarian tissue with MSCs was not effective due to tissue degradation in culture; however, we used this trial to develop effective methods for isolation of RNA from the extremely fibrous equine ovarian tissue. In a preliminary study on intra-ovarian MSC injection, there was an apparent increase in follicle numbers 4 weeks after injection in 2 randomly-selected young mares. Based on these results, a more comprehensive study was performed on old and young mares to determine if MSC injection affects ovarian function. There was no

significant increase in follicle numbers after MSC injection in either old or young mares, nor was there an increase in serum levels of anti-Müllerian hormone, a marker for numbers of growing follicles. Results of RNA sequencing of ovarian tissue showed that injection of MSCs in old mares was associated with a minor increase in gene expression of factors that might relate to ovarian function.

CONTRIBUTORS AND FUNDING SOURCES

CONTRIBUTORS

This work was supervised by a dissertation committee consisting of Dr. Katrin Hinrichs (advisor), Dr. Ashlee E. Watts of the Department of Large Animal Clinical Sciences, Dr. Qinglei Li of the Department of Veterinary Integrative Biosciences, and Dr. Scott V. Dindot of the Department of Veterinary Pathobiology. The analyses in Chapters III, V and VII were conducted in part by Dr. Gus Wright. The analyses in Chapters III and VII were conducted in part by Dr. James Thompson and Dr. Cecilia Penedo. The analyses in Chapters VI and VIII were conducted in part by Dr. Drew Hillhouse and Kranti Konganti.

Transvaginal ultrasound-guided follicle aspirations, oocyte handling and culture were performed in part by the Equine Embryo Lab Personnel; intracytoplasmic sperm injection and embryo culture were performed by Dr. Young Ho Choi. Mesenchymal stem cell culture, freezing and thawing for intra-ovarian injections were performed in part by Hsing Fann.

All other work conducted for this dissertation was completed by the student independently.

FUNDING SOURCES

Graduate study was supported by a Merit Scholars Fellowship from the College of Veterinary Medicine & Biomedical Sciences, the Clinical Equine ICSI Program at

Texas A&M University, the Link Equine Research Fund from Texas A&M University, a Lechner Scholar Award from Texas A&M University, a Postdoctoral Trainee Research Grant and a Graduate Student Core Facility Experiential Learning Program Grant from the College of Veterinary Medicine & Biomedical Sciences, and a Travel Award from the College of Veterinary Medicine & Biomedical Sciences Graduate Student Association.

TABLE OF CONTENTS

Page

LIST OF FIGURES

FIGURE Page

FIGURE Page

LIST OF TABLES

CHAPTER I

INTRODUCTION

Aging affects female reproductive efficiency. While neuroendocrine and uterine and/or oviductal factors may affect fertility, a decrease in oocyte quality and exhaustion of ovarian follicle stores are the major causes of age-related reproductive failure [1]. This is especially relevant to human medicine as each year millions of women undergo fertility treatments due to age-related loss of fertility. In women, ovarian senescence begins as early as 31 to 35 yr of age; the proportion of women who remain fertile rapidly declines afterward, from 50% at age 40, to 15% by age 45 [2].

The mare may serve as an excellent model for reproductive aging. In mares, reproductive senescence begins around 20 yr of age, and it is estimated that only 37% of mares older than 24 yr of age display any ovarian activity [3]. Most research on reproductive aging has been performed with rodent models, which have ovarian function and senescence timelines that differ in many aspects from that in women.

Each year millions of women are rendered sterile by chemotherapy-associated oocyte loss. Interestingly, there have been reports showing an unexpected return of ovarian function and fertility after chemotherapy in women who underwent bone marrow transplantation as a component of their therapy [4-7]. Several animal studies have been conducted to try to explain this phenomenon. Studies performed on mice, rats and rabbits indicate that systemic or intra-ovarian injection of bone marrow-derived mesenchymal stem cells (MSCs) increases ovarian follicle numbers and induces mRNA

and protein expression of genes that may improve the function of ovaries compromised by chemotherapy [8-14]. However, little information is available on the effect of MSC injection on the aging ovary, an understanding of which would have a potential impact on millions of women undergoing assisted reproduction because of age-related infertility. Furthermore, considerable interest exists in the equine industry to establish pregnancies from older, valuable mares. Thus, the mare offers a useful model to explore the possibility that bone marrow-derived MSCs could restore ovarian function in aging females.

The studies in this dissertation aim to determine 1) the effects of intra-ovarian injections of bone marrow-derived MSCs on the ovarian function of old and young mares; 2) if MSCs persist in the ovaries after injection, and 3) the effects of bone marrow-derived MSCs on equine ovarian gene expression.

CHAPTER II

LITERATURE REVIEW

DEVELOPMENT OF THE OOCYTE AND FOLLICLE AND FACTORS AFFECTING OOCYTE QUALITY

Introduction

Normal fertility depends on complex biological processes including the production of gametes, the fertilization process, the initial growth of the embryo, the transition from embryo to fetus, and the growth of the fetus. Aging affects female reproductive efficiency [1, 15, 16]. Ovarian aging in women is characterized by a reduction in follicle and oocyte numbers, failure of follicular growth, and a decrease in oocyte developmental competency [16, 17]. While there are neuroendocrine and uterine and/or oviductal factors that affect fertility, the decrease in oocyte quality and exhaustion of ovarian follicle stores appear to be the major causes of age-related reproductive failure. This has been clearly demonstrated by the ability of women well past reproductive age to become pregnant and carry successfully to term when embryos produced from young donor oocytes are transferred to their uteri [17-20]. Similarly, in mares, oocytes from young donors transferred to the oviducts of inseminated recipients have higher developmental rates than those from old donors, suggesting that oocytes from old mares have lower or impaired developmental competence [21].

Folliculogenesis and Follicle Number

In mammals, oocyte precursors are produced during embryogenesis. Primordial germ cells arise extra-gonadally and migrate from the yolk sac through the hindgut endoderm up the dorsal mesentery and into the genital ridges where, after undergoing several mitotic divisions, they form oogonia, the population of cells from which all future gametes will arise. Oogonia resulting from the rapid mitotic proliferation of primordial germ cells become primary oocytes when they enter prophase of meiosis; thereafter they are incapable of further mitotic division. Meiosis begins between late intra-uterine and early post-natal life, the timing varying among species. At the time the primary oocytes become arrested in prophase of the first meiotic division they are enclosed by pre-granulosa cells to form primordial follicles [15, 22]. This meiotic arrest lasts the lifetime of the oocyte, except in those rare oocytes destined to ovulate. Follicles grow in pre-pubertal females; however, no nuclear progression occurs in oocytes until they are in antral follicles stimulated by the preovulatory LH surge. Thus, since women can ovulate into their fifties, the oocytes ovulated at that time remained arrested for 50 yr or more at the same stage of meiosis that they entered before birth.

In female rats, the total population of germ cells peaks 4 days before birth (i.e. the 18th day of gestation) and rapidly declines so that only about 30% of germ cells (now oogonia) survive to 2 days after birth [23]. In humans, it is estimated that by 20 weeks of gestation each fetal ovary contains 5 to 7 million primordial follicles and this number decreases to about 1 million at birth [22]. The rise in the population of germ cells is associated with high mitotic activity whereas the subsequent decline is due to the

spontaneous degeneration (i.e., apoptosis) of germ cells, especially of oogonia that do not become surrounded by follicle cells. Germ cell apoptosis is regulated by opposing functions of members of the B-cell lymphoma/leukemia (BCL) protein family [24]. The BCL2 and BCLX proteins are antiapoptotic, whereas BAX promotes cell death. In mice, deletion of BCL2 results in fewer oocytes and primordial follicles, but no differences in the number of primary and preantral follicles [25], whereas loss of BAX increases the number of germ cells [26]. The involvement of caspases (proteases that upon activation cleave cellular proteins leading to apoptosis) in follicle atresia was shown by targeted disruption of the caspase 2 gene (*Casp2*); loss of *Casp2* results in significantly more primordial follicles and resistance to the chemotherapeutic agent doxorubicin in mice [27]. Thus, during fetal development and in the perinatal period, apoptosis is important in reducing the primordial follicle pool.

Between birth and puberty, there is continued recruitment of follicles from the primordial pool, but all growing follicles undergo atresia due to lack of gonadotropin support. Because of this, in humans the numbers of primordial follicles decline to about 25% of the numbers at birth during the years before puberty [15, 16]. After puberty, those follicles that leave the primordial pool but do not reach ovulatory maturity (the majority of follicles that leave the pool), estimated to be around 400 follicles for each one that ovulates [28], undergo atresia. Because of both pre-pubertal loss and loss of the vast majority of follicles leaving the primordial pool after puberty, fewer than 0.1% of the oocytes present at birth will actually be ovulated during a woman's reproductive life [29].

In mammals, granulosa cells are the major cell type of the follicle, and they undergo apoptosis during atresia. Evaluation of apoptosis using the TUNEL histochemical assay or DNA laddering in atretic follicles of pig [30, 31], rat [32, 33], human [34], horse [35], and sheep [36] ovaries revealed DNA fragmentation and ladder formation in granulosa cells, indicating that apoptosis is involved in follicular atresia. There is an inevitable decline in the numbers of oocytes with age because the numbers of oocytes within the ovary are fixed at birth; once the oogonia have committed to meiosis, there is no mechanism for producing more of them [22]. Recently, the dogma of a non-renewable pool of primordial follicles that declines with age has been challenged by a claim that neo-oogenesis from female germline stem cells ("oogonial stem cells") present in the ovarian surface epithelium can occur in the adult ovary of mice [14]; this will be discussed more thoroughly below.

Follicle recruitment is the process by which a primordial follicle makes an irreversible commitment to growth. Once this process has started, follicle growth continues until the follicle undergoes atresia or, in a minority of cases, ovulates. Many follicles are recruited each month but only one reaches ovulatory maturity in monoovulatory species. In women, follicles are recruited continuously until the original store is exhausted, shortly after menopause. The number of follicles that begin growing each day depends on the number of primordial follicles remaining in the ovary and, therefore, decreases with age [22].

Primordial Follicle Recruitment and Activation

Although the trigger and molecular mechanisms that promote growth in some follicles while the rest remain in primordial stage is unclear in humans, studies using genetically-modified mouse models have identified signaling pathways and transcription factors involved in the regulation of follicular activation (i.e., transition from primordial to primary follicle) and survival. Mice with mutations at the white spotting (*Kit*) or steel loci (*Kit ligand*) lack germ cells in their gonads [37-39]. Interactions between *Kit ligand* and the KIT tyrosine receptor appear to be critical in early folliculogenesis. During postnatal ovarian development, *Kit* is expressed in oocytes and *Kit ligand* is expressed in pre-granulosa and granulosa cells throughout folliculogenesis [40-44]. *Kit/Kit ligand* interactions have been implicated during follicular growth from the primordial pool. Newborn mice injected with an antibody to *Kit* (ACK2) that blocks its interaction with *Kit ligand* exhibit restricted progression of primordial follicles to primary follicles [44]. Conversely, treatment of neonatal rat ovaries with recombinant *Kit ligand* accelerates follicular activation, resulting in an increased number of growing follicles [45]. Although these studies suggest that *Kit* signaling is necessary during follicular development and follicular activation, the mechanisms by which *Kit* signaling contributes to the primordial-to-primary transition are not entirely known; however, there is evidence suggesting that the *Kit/Kit ligand* pathway induces the PI3K (phosphatidylinositol 3-kinase)/AKT (protein kinase B) pathway, leading to phosphorylation and thus inactivation of forkhead box O3 (*Foxo3*), an inhibitor of primordial follicle activation [46]. The conversion of the membrane phospholipid PIP2

(phosphatidylinositol 4,5-bisphosphate) to the second messenger PIP3 (phosphatidylinositol 3,4,5-trisphosphate) is catalyzed by PI3K, which leads to AKT activation. *Foxo3* is a member of the FOXO subfamily of forkhead transcription factors, which are downstream targets of AKT; activation of AKT phosphorylates and functionally suppresses FOXO transcription factors by causing their nuclear exclusion [46]. When mouse or rat oocytes are treated with *Kit ligand*, Foxo3 is phosphorylated in a PI3K/AKT-dependent manner; treatment with a PI3K inhibitor prevents AKT activation and subsequent *Foxo3* phosphorylation [47].

Additional genetic studies support a critical role for the PI3K/AKT pathway in regulation of *Foxo3*. Oocyte-specific deletion of *Pten* (phosphatase and tensin homolog deleted on chromosome 10), which opposes the actions of PI3K by converting PIP3 to PIP2, causes premature activation of primordial follicles, with an ovarian phenotype nearly identical to *Foxo3* deletion (i.e., enlarged ovaries, marked increase in growing and atretic follicles, and absence of primordial follicles) [48-50]. Loss of *Pten* in oocytes results in enhanced PI3K activity, AKT hyperactivation, and functional suppression of FOXO3 secondary to hyperphosphorylation, resulting in follicle activation. Concurrent loss of *Pten* and *Foxo3* in oocytes does not have a synergistic effect on follicle activation, indicating that phosphorylation of FOXO3 is the main regulator of its activity [50]. The PI3K inhibitor LY294002 suppressed primordial follicle activation in ovaries with *Pten*-deficient oocytes but had no effect in *Foxo3* null mutant ovaries, suggesting a linear PTEN-PI3K-AKT-FOXO3 pathway [49]. It is unknown whether *Kit* is an upstream modulator of this pathway *in vivo*, or at least one of the many receptor tyrosine

kinases that might initiate this signaling cascade to promote primordial follicle recruitment; however, in female mice with a mutated KIT receptor that prevents activation of PI3K, folliculogenesis is impeded beyond the primary stages of development [51], similar to mice with constitutively active *Foxo3,* which are infertile due to impeded follicular development beyond primary follicles [52]. The mechanisms by which nuclear *Foxo3* prevents primordial follicle activation and arrest at the primary follicle stage remain unknown [53].

Whereas *Foxo3* is the key oocyte factor critical for suppressing primordial follicle activation, forkhead box L2 (*Foxl2*), another forkhead domain transcription factor, is crucial in maintaining granulosa cell identity through the repression of testis-specific genes [54]. Foxl2 also has a role in modulating the transition from squamous to cuboidal granulosa cells that occurs during the primordial-to-primary follicle transition. Non-functional mutations in *Foxl2* cause type I blepharophimosis/ptosis/epicanthus inversus syndrome (BPES) which is associated with premature ovarian failure. In the ovary, *Foxl2* is expressed in pre-granulosa cells surrounding primordial follicles, and in granulosa cells throughout folliculogenesis. *Foxl2* knock-out mice form primordial follicles, but differentiation of granulosa cells from the squamous to cuboidal state is blocked, and granulosa cell proliferation is interrupted [55, 56]. Unexpectedly, however, at 2 weeks of age, most primordial follicles are activated in the ovaries of *Foxl2* knock-out mice, as demonstrated by expression of transforming growth factor beta family member (TGFβ) *Gdf9* (growth differentiation factor 9), a marker of oocyte activation. This activation is accompanied by widespread follicular atresia and a near absence of

primordial follicles by 8 weeks of age because the defective granulosa cells fail to progress along the follicular growth pathway and fail to support growing oocytes [55].

As noted above, *Gdf9* is a member of the TGFβ family associated with oocyte activation; however, another TGFβ family member, AMH (anti-Müllerian hormone), produced by granulosa cells of growing follicles, appears to suppress primordial follicle recruitment. In the rodent and human ovary, AMH and its type II receptor, AMHR2, are expressed in granulosa cells of primary and growing pre-antral follicles; type II receptors phosphorylate and activate type I receptors, which then bind and activate transcriptional regulators [57]. Although female mice lacking AMH are fertile, juveniles show an increase in growing follicles, and by 4 months this increase is reflected in a reduction of primordial follicles compared to wild-type litter-mates. By 13 months of age, *AMH* knock-out females have few remaining primordial follicles [58]. These *in vivo* findings are supported by *in vitro* studies showing that neonatal ovaries cultured in the presence of recombinant AMH show fewer growing follicles [59]. Thus, AMH appears to inhibit the recruitment of primordial follicles, and in its absence, there is a faster depletion of primordial follicles [58, 59]. The mechanism by which AMH inhibits primordial follicle recruitment has not been elucidated [60]. Although no information is available that clearly demonstrates AMH type II receptor expression in primordial follicles, a direct effect of AMH on the primordial follicles themselves cannot be excluded. Alternatively, the primary action of AMH may be autocrine in nature, as granulosa cells of small follicles express both AMH and its type II receptor. The small follicles may be stimulated by AMH to produce factors that act on the primordial follicles [58]. Since

AMH null mice have low levels of FSH (follicle-stimulating hormone), and yet greater numbers of growing follicles, it has also been hypothesized that follicles are more sensitive to FSH in the absence of AMH. The possible inhibitory effect of AMH on follicular sensitivity could play a role in the process of follicular selection. Diminished expression of AMH within the growing follicles would reduce the threshold level for FSH, allowing follicles to continue growing and to ovulate in the next cycle. Another theory suggests a role of AMH in modulating the function of FSH; treatment with AMH decreases FSH-stimulated aromatase expression in human granulosa cells [61, 62] and decreases FSH receptor expression [62], thus showing a relevant effect of AMH in modulating ovarian follicular responses to gonadotropins.

The heterodimeric complex made by TSC1 and TSC2 (tuberous sclerosis complex 1 and 2, respectively) is the most important regulator of mTORC1 (mammalian target of rapamycin complex 1) [63, 64]. TSC1 and TSC2 are products of two distinct tumor suppressor genes, *Tsc1* and *Tsc2*, respectively. It has been shown that oocyte-specific deletion of *Tsc1* [65] or *Tsc2* [66] leads to a global activation of all primordial follicles, causing follicular depletion and premature ovarian failure in mice. The driving force underlying the overactivation of primordial follicles in the ovaries of these knock-out mice is elevated mTORC1 activity, suggesting that suppression of mTORC1 activity by the TSC1-TSC2 complex in oocytes is required for maintenance of the quiescent state of primordial follicles. At the same time, these findings also indicate that elevated mTORC1 activity in the oocyte is required for follicular activation [65, 66].

The results from the above genetic mouse models suggest that the PTEN-PI3K-AKT-FOXO3 signaling pathway, AMH activity, and suppression of mTORC1 activity, and likely other pathways yet to be identified, converge to repress primordial follicle recruitment, and this inhibitory effect must be overcome for follicles to leave the primordial pool.

Oocyte Quality

Oocyte quality deteriorates with age [17]. In women, the importance of decreased oocyte quality in age-related decline of fertility was confirmed by studies that showed that after receipt of embryos produced from oocytes from young donors, women > 40 yr of age were able to conceive, carry, and give birth with success rates similar to young women [17-20]. Meiosis in oocytes consists of 2 divisions and of 2 different stages of temporary arrest. As mentioned above, meiosis starts in oogonia in the human fetal ovary at 11 to 12 weeks of gestation. During this time, the oogonia enter prophase and become oocytes; the chromosomes replicate and the homologous chromosomes undergo pairing. An exchange of material between the chromatids of different homologs occurs via the formation of chiasmata in a process known as recombination or crossing over [67]. The oocytes then progress to the diplotene stage of prophase and enter meiotic arrest. They remain at this stage until ovulation, which may occur much later (10 to 50 yr in women). At the time of or soon after the oogonia initially enter meiosis, the oocytes become surrounded by pre-granulosa cells, forming primordial follicles. When primordial follicles leave the pool, the oocyte remains arrested in prophase I during

follicle growth. It is not until the oocyte is within a dominant preovulatory follicle in a sexually mature female, in response to the luteinizing hormone (LH) surge, that the oocyte resumes meiosis. At this time, the nuclear membrane breaks down and the chromosomes condense and line up on the first metaphase plate (MI). During anaphase, the bivalents separate, each moving to the opposite poles of the meiotic spindle. Thus, in humans, 23 bivalents, each composed of two sister chromatids, enter the polar body while the remaining 23 remain within the oocyte. After this, a second meiotic spindle and metaphase plate (MII) form immediately. The remaining chromosomes align and the cell cycle arrests again until fertilization, when fusion with the sperm triggers the resumption of meiosis and release of the oocyte from MII [68]. The sister chromatids separate; half are extruded as the second polar body and half are retained within the oocyte as its 1n chromosome complement. Thus, meiosis in the oocyte takes a long period of time to be completed, since this process starts during fetal life and is completed only in matured oocytes that undergo fertilization.

Alterations during the process described above can lead to aneuploidy (an abnormal number of chromosomes) through two main mechanisms: 1) nondisjunction (failure of homologous chromosomes or sister chromatids to separate and segregate normally) during the first or second meiotic divisions or 2) premature separation of sister chromatids [69]. Although aging does not appear to affect the ability of oocytes to become fertilized *in vitro*, maternal age in women has been associated with an increased incidence of aneuploidy. In women < 25 yr of age, the expected aneuploidy rate is 5%, while this is nearly 60% in oocytes of women > 43 yr of age [70].

Many factors in addition to aneuploidy affect the quality of oocytes in aging females. Oocyte cytoplasmic factors and mitochondrial abnormalities also affect oocyte quality, as does the quality of the cells making up the follicle and supporting the oocyte in its growth. Recent work suggests that patterns of gene expression of cumulus cells (CCs) and the metabolites present in follicular fluid (FF) have the potential to be used as markers of oocyte quality; these are reviewed below.

Follicle-Stimulating Hormone

Elevated FSH levels in older women are one of the first signs of reproductive aging [71], and increased levels of FSH have been hypothesized as a possible cause of increased aneuploidy [72, 73]. In mouse models, repeated ovarian stimulation with FSH results in an increased number of MII oocytes with spindle malformations [74]. Studies in mouse cumulus-oocyte complexes cultured in increasing concentrations of FSH have shown that exposure to high levels of FSH accelerates the timing of nuclear maturation and induces chromosomal abnormalities [75]. Oocytes with aneuploidy are associated with follicles with increased follicular-fluid FSH levels [76]; these findings are supported by *in vitro* studies showing that high FSH levels in the *in vitro* fertilization (IVF) medium during *in vitro* oocyte maturation significantly increase aneuploidy rates [77]; however, the mechanisms by which elevated FSH appears to cause oocyte aneuploidy remain unknown [73, 77].

The integrity of bivalents is crucial for accurate chromosome segregation. However, there is a high proportion of bivalents that are disintegrated in the oocytes of

older women [78-81]. Sister chromatids in mouse and human oocytes lose cohesion with age, which may lead to incorrect alignment of bivalents on the meiotic spindle and segregation errors during meiosis [78-84]. Cohesion along crossover sites keeps bivalents intact in MI and centromere cohesion holds sister chromatids together during all stages of meiosis until MII. A defect in cohesion distal to crossover sites may result in a shift of chiasmata placement or premature separation of bivalents in MI, whereas reduced centromere cohesion may result in premature separation of sister chromatids in MII [85]. Studies in mice have identified cohesion loss as a major contributor to age-related aneuploidy [83, 86-88]. Cohesin complexes in mouse oocytes are already present during DNA replication in the early stages of meiosis. Therefore, cohesin complexes must remain in place and functional throughout the period of oocyte arrest to ensure correct chromosome segregation in meiosis. The levels of Rec8, a subunits that forms the cohesin complex, are markedly decreased on the bivalents of oocytes from aged mice [82, 83] and these oocytes show an increase in segregation errors [83]. Human oocytes from aged females show age-related structural changes similar to those observed in mice [78-81]; however, the molecular mechanisms that cause these age-related changes in chromosome architecture in human oocytes remain unknown [79].

Mitochondrial Dysfunction

Mitochondrial dysfunction is another factor that affects oocyte quality. The theory of ovarian aging, first proposed by Tarin [89], implies a reduced ability of oocytes and granulosa cells to counteract reactive oxygen species (ROS), which are

among the most important physiological inducers of cellular injury associated with aging. Mitochondria are major generators of ROS and abnormal accumulation of intra-mitochondrial ROS can result in mitochondrial DNA (mtDNA) mutations [90]. ROS-induced mtDNA mutations lead to the production of inefficient proteins that increase the mitochondrial production of ROS, creating a vicious cycle [91]. Animal models with accelerated mtDNA mutations show significantly reduced longevity, and exhibit a phenotype consistent with human aging, including reduced fertility [92, 93]. When nuclei from mouse oocytes with induced oxidative mitochondrial damage are transferred into healthy enucleated ooplasts, nuclear function is rescued, leading to an increase in normal meiosis, fertilization, and blastocyst formation [94]. Alterations in mtDNA copy number and mutation load and in mitochondrial function have been demonstrated in aged mammalian oocytes and are thought to be either a contributing factor or a hallmark of oocyte aging [95-100]. In aged mice, mitochondria of primary follicle-enclosed oocytes are smaller than those of young mice. Mature MII oocytes from old mice have significantly less mtDNA and have elevated expression of mitochondrial unfolded protein response gene *Hspd* (heat shock protein family D), compared to oocytes from young mice. Aged mature oocytes also have higher ROS levels than do mature oocytes from young mice [101].

Human and mouse oocytes from females of advanced age also have abnormal mitochondria with large vacuoles [98] and have increased mitochondrial aggregates, which are correlated with poor-quality oocytes and decreased fertilization [102]. Additionally, mouse, hamster, and human oocytes from old females have decreased ATP

content, correlated with a similar decrease in mtDNA copy number and number of mitochondria [98]. Oocytes from older women, compared to those from younger women, also have upregulation of proapoptotic genes including CD40 ligand (*CD40*), and tumor necrosis factor receptor superfamily members 10a and 21 (*Tnfrsf10a, Tnfrsf21*). Oocytes from old females also show downregulation of antiapoptotic genes including *Bcl2* and caspase 8-and-fas-associated death domain-like apoptosis regulator (*Cflar*); these findings suggest that aging initiates apoptosis in oocytes [103].

Mitochondrial dysfunction can also affect formation of the meiotic spindle. In mice, a decrease in mitochondria-derived ATP induced by oxidative stress causes disassembly of MII spindles [104]. And in human germinal-vesicle stage oocytes, ROS production induced by mitochondrial stress also disrupts subsequent spindle formation and size [105]. Thus, it is possible that oxidative damage from increased ROS production by dysfunctional mitochondria of aged oocytes could lead to segregation errors and aneuploidy as a consequence of abnormal spindle function.

Cumulus Cells

Cumulus cells (CCs) are a highly specialized cell type that surround the mammalian oocyte from antrum formation through the early stages of embryo development in the oviduct. During this period of close contact, CCs maintain paracrine and bidirectional cell-to-cell communications with the oocyte and appear to be indispensable for acquisition of oocyte developmental competence; the early removal of CCs significantly reduces blastocyst rates [106]. Furthermore, the properties and

functions of CCs are regulated by the oocyte itself and reflect the degree of maturation of the oocyte [107, 108]. Oocyte competence can be divided into 2 levels: meiotic competence, the ability of the oocyte to complete meiosis to MII, and developmental competence, the ability of the oocyte to be fertilized, and to produce blastocysts able to produce viable and healthy progeny [109-112].

Because of their relationship with oocyte competence, CCs are increasingly being investigated as potential markers to predict oocyte quality, an application which could lead to greater ability to select oocytes with increased fertilization, implantation and pregnancy rates during IVF treatments. Despite the improvement in our understanding of events occurring during oocyte maturation, accurate selection of good-quality oocytes remains challenging. In women and cattle, morphological criteria associated with the oocyte (ooplasm transparency, diameter), the CCs (number of layers, compactness), the follicle (follicle size, follicular vascularization), and the early embryo (fragmentation, number of blastomeres, multinucleation) are often used to predict developmental and implantation competence [113-117]; however, these criteria are subjective and lack the required precision to select highly-competent oocytes or embryos. Thus, several groups have focused their research on the analysis of CC gene expression to identify markers that represent quantitative and non-invasive (once the cumulus-oocyte-complex has already been removed from the follicle for IVF) tools for the assessment of oocyte developmental competence in humans [118-124].

In a study applying a microarray approach, new potential regulators and marker genes involved in human oocyte maturation and CC function were identified; these

genes, suggested as potential marker of oocyte competence, included *Bard1* (BRCA1 associated RING domain 1), *Rbl2* (RB transcriptional corepressor like 2), *Rbbp7* (RB binding protein 7), *Bub3* (budding uninhibited by benzimidazoles 3) and *Bub1b* (budding uninhibited by benzimidazoles 1 homolog beta) [118]. In a later study, this same group demonstrated that morphologically-normal oocytes from patients with recurrent fertilization failure display abnormal patterns of gene expression, especially of those genes involved in meiosis, cell growth and apoptosis [119]. Alterations in gene expression have also been reported in morphologically abnormal embryos [120]. Patterns of CC gene expression on microarray evaluation significantly associated with embryo morphology and pregnancy outcome have also been reported; these include the up-regulation of *Bcl2l11* (BCL2-like 11 involved in apoptosis) and *Pck1* (phophoenolpyruvate carboxykinase 1 involved in gluconeogenesis) and down-regulation of transcription factor *Nfib* (nuclear factor 1 b) [121]. Using real-time PCR, transcription of 5 genes in CCs, previously shown to be affected by the preovulatory LH-surge, was shown to be associated with oocyte competence [122]. Nuclear maturation of the oocyte was associated with increased expression of *Star* (steroidogenic acute regulator), *Cox2* (cyclooxygenase 2), *Areg* (amphiregulin), *Scd1* (stearoyl-CoA desaturase 1) and *Scd5* in CCs; the expression of *Star*, *Cox2* and *Areg* is induced by the preovulatory LH peak while *Scd1* and *Scd5* are involved in oocyte lipid metabolism. [122]. Real-time PCR has also been used to correlate CC gene expression with subsequent embryo development; CCs isolated from oocytes which produced high quality Day-3 embryos were found to have higher transcript levels of *Cox2*, *Has2*

(hyaluronan synthase 2), and *Grem1* (gremlin 1) than those detected in CCs from oocytes that developed into poor-quality embryos [123, 124]. Thus, measurement of transcripts of these genes in CCs could complement morphological evaluation of the cumulus-oocyte complex and provide a useful tool for selecting oocytes with higher potential of fertilization and development in vitro. A further set of 6 genomic markers differentially expressed in CCs of human oocytes in association with successful pregnancies has been identified using 2 different microarray platforms, and validated by real-time PCR [125]. These include *Ar* (androgen receptor), which acts as an intracellular transducer signal and/or a transcription factor that interacts with transcription regulators and is also involved in CC steroidogenesis [126]; *Calu* (calumenin) and *Calm1* (calmodulin 1), two ubiquitous calcium-binding proteins shown to be important for the calcium pathway which has been reported to interact with progesterone, PKA and PI3K which in addition to other actions induce a chemical attraction of the spermatozoa to the oocyte during fertilization [127]; *Ubqln1* (ubiquilin 1), *Casp9* (caspase 9) and *Tom1* (target of Myb1 membrane trafficking protein), which are associated with catabolic and proteasome activities shown to be required for oocyte maturation, CC expansion, ovulation, and fertilization [128-131].

Current studies on the CC transcriptome are focusing on explaining the mechanisms by which differences in CC gene expression are associated with altered oocyte competence as well as on linking the different potential pathways involved. Recently it has been reported that activation of the EGF (epidermal growth factor) pathway by *Areg*, an EGF-related ligand, in CCs stimulates PI3K/AKT signaling in

mouse oocytes [132, 133]. As mentioned above, *Areg* is induced by the LH surge and has been shown to promote oocyte maturation and developmental competence during *in vitro* maturation [122]. Activation of PI3K/AKT cascade results in an increased translation of maternal mRNAs and an increase in corresponding protein accumulation in mouse oocytes; this increase in protein levels is associated with increased fertilization rate and improved embryo development [132, 133]. The increase in protein translation also promotes the release of factors such as GDF9, BMP15 (bone morphogenic protein 15), and IL7 (interleukin 7) from oocytes, which act on CCs, regulating their function, thus completing a feedback regulatory loop [134]. This timed secretion before ovulation likely modulates molecular events in CCs that are necessary for the development of a competent oocyte.

These studies highlight the importance of the bidirectional communication between the oocyte and CCs and highlight gene expression of CCs as a potential tool to assess oocyte quality.

Follicular Fluid

Follicular fluid (FF) provides an important microenvironment for the development of oocytes. Follicular fluid is a product of both the transfer of blood plasma constituents that cross the blood-follicle barrier and of the secretory activity of granulosa and thecal cells [135]. It has been suggested that the biochemical characteristics of the FF surrounding the oocyte may play a role in determining oocyte quality and the subsequent potential to achieve fertilization and embryo development, or at least reflect

the status of the oocyte [136-141]. In cows, differential abundance of 8 proteins in the follicular fluid has been found in less fertile cows (i.e., cows that fail to conceive following six inseminations) compared to control cows; these proteins include SERPINA1 (serpin family A member1), TIMP2 (tissue inhibitor of metalloproteinases 2), ITIH1 (inter-alpha-trypsin inhibitor heavy chain 1), HSPG2 (heparin sulfate proteoglycan 2), C8A (complement C8 alpha chain), COL1A2 (collagen type 1 alpha 2 chain), F2 (coagulation factor II, thrombin), and IL1RAP (interleukin 1 receptor accessory protein) [137]. Although the specific role of each protein has yet to be determined, it is possible that they could influence (or reflect) follicular function and oocyte quality. Recent research has focused on protein analysis and metabolomics, i.e., the analysis of all low molecular-weight substances contained in FF at a given time. This approach could be more useful than the direct study of gene expression, mRNAs or proteins because metabolites can reveal the response of the follicle to all influences affecting its development, and more than one metabolite are likely to be involved in determining oocyte quality [142]. In mice, oocytes able to absorb larger amounts of glucose and actively convert it into lactate show the highest fertilization potential [136]. Follicular fluid from aged women (> 40 yr) and aged cows (≥ 10 yr) has been reported to contain high concentrations of advanced glycation end-products (AGEs) [138, 139]. Glycation is the non-enzymatic reaction between reducing sugars and proteins, lipids or nuclei acids. Electrophilic carbonyl groups of reactive sugars react with free amino groups of amino acids forming a non-stable Schiff base. Further rearrangement leads to formation of a more stable ketoamine. Schiff bases and ketoamines are reversible

reaction products; however, they can react irreversibly with amino acid residues of peptides to form protein crosslinks. They can also undergo further oxidation, dehydration, polymerization and oxidative breakdown reactions which give rise to AGEs. AGEs are glycated proteins or lipids that form as a result of glycation during normal metabolic processes [143]. The accumulation of AGEs in FF of aged women was negatively correlated with follicular growth, fertilization and embryonic development, while in cows, supplementation of *in vitro* maturation medium with FF from aged cows decreased oocyte fertilization and embryo development rates and increased oocyte ROS levels [139]. AGEs induce apoptosis through the production of ROS in human epithelial cells [144]. Maturation medium of mouse oocytes containing MG (methylglyoxal), an AGE precursor, induces oxidative stress which leads to DNA damage, meiotic delay and spindle aberrations, and the sensitivity to oxidative stress by MG increases with maternal age [140, 141]. Furthermore, expression of AGE receptor in human ovarian granulosa cells is correlated with age [145, 146] and may be responsible for decreased glucose uptake by granulosa cells leading to altered follicular growth [146]. These studies suggest that soluble AGEs may play a role in the decline of ovarian function and oocyte quality during aging; however, further studies are needed to determine what other factors present in FF may affect oocyte competence.

The results from the CC and FF studies suggest that non-invasive biomarkers may be prognostic of the quality of an oocyte to develop into an embryo that successfully implants and sustains pregnancy. However, further studies are needed to

determine if these markers can be used as a clinical tool to select the most competent oocytes in assisted reproductive technologies.

Ovarian Stem Cells

Recently, Johnson *et al.,* [14] proposed the existence of oocyte-generating stem cells in mouse adult ovaries. This finding remains controversial. These "oogonial stem cells" have been implied as being present via immunohistochemical and grafting experiments in that report and in subsequent studies. The main findings from Johnson *et al.,* and subsequent reports from the same laboratory were that histological analysis of adult mouse ovaries revealed the presence of large ovoid cells, resembling germ cells of fetal mouse ovaries; however, these cells were in the surface epithelial cell layer covering the ovary and not associated with any cells in any type of structure resembling a follicle [14]. Immunohistochemical staining for DEAD box polypeptide 4 (*Ddx4*), a gene thought to be expressed exclusively in germ cells [147], was positive, suggesting that the ovoid cells were of a germline lineage [14]. Expression of synaptonemal complex protein 3 (SCP3), a meiosis-specific protein structure that is essential for synapsis of homologous chromosomes, was examined in adult mouse ovaries. Immunohistochemical localization of SCP3 revealed individual immunoreactive cells in the surface of the ovary; however, minimal to no expression of this protein was observed in non-gonadal tissues [14]. Finally, ovarian fragments harvested from normal adult mice were grafted onto the ovaries of transgenic females expressing green fluorescent protein (GFP). After 3 to 4 weeks, the ovarian fragments were collected and examined.

Confocal microscopic analysis revealed follicle-enclosed, GFP-positive cells surrounded by GFP-negative granulosa cells in the fragments. The authors suggest that germ cells from the host transgenic mouse infiltrated the grafted tissue and initiated folliculogenesis [14]. However, it is not clear whether the GFP-positive cells were in fact normal oocytes as their developmental potential was not tested.

White *et al.,* [148] described a fluorescent-activated cell sorting-based protocol that was used with adult human ovarian cortical tissue to isolate mitotically-active cells having a gene expression pattern consistent with germ cells. The isolated cells expressed germline markers including PR domain containing 1 (*Prdm1*), developmental pluripotency-associated 3 (*Dppa3*), interferon-induced transmembrane protein 3 (*Ifitm3*), telomerase reverse transcriptase (*Tert*), and *Ddx4*; and lacked expression of differentiated oocyte markers including NOBOX oogenesis homeobox (*Nobox*), zona pellucida glycoprotein 3 (*Zp3*) and *Gdf9*. Injection of the isolated cells, engineered to express GFP, into human ovarian cortical biopsy tissue led to the formation of follicle-like structures containing GFP-positive cells 1 to 2 weeks after xenotransplantation of the cortical tissue into immunodeficient female mice; when the cortical tissue was removed from the mice, these structures remained detectable through 72 h of culture. The authors suggest that their findings provide evidence that GFP-expressing human oogonial stem cells spontaneously generated germline cells that became enclosed by granulosa cells that were present in the adult human biopsy tissue [148]. However, as for the previous study, the authors in this study did not test for function of the structures that they called follicles and oocytes. Thus, the existence of oogonial stem cells remains

controversial and it is still unclear whether, if these stem cells do exist, they are in fact capable of oogenesis and folliculogenesis, and if they exist in other species.

The Mare as a Model for Reproductive Aging

All of the age-related changes discussed above result in reduced fertility. Reproductive aging is especially relevant to human medicine, as each year millions of women undergo fertility treatments due to age-related loss of fertility [149]. Female fertility is defined as the ability to achieve a successful pregnancy after 12 months or more of attempted conception [150]. In women, ovarian senescence begins as early as 31 to 35 yr of age; the proportion of women who remain fertile declines rapidly afterward, from 50% at age 40, to 15% by age 45 [2]. In the United States, of all the assisted reproductive technology procedures performed in 2013, 57% were performed on women between 35 and 44 yr of age [151].

Most research on reproductive aging has been performed with rodent models, but the ovarian function and senescence timelines in these species differ in many aspects from that in women. The mare offers advantages as a model for women, as in both species, oocytes are maintained in meiotic arrest for decades, and follicle development and ovulation timing are similar, suggesting a comparable sequence of events. For instance, the cycle length is similar (3 weeks in mares vs 4 weeks in women), only 1 follicle ovulates per cycle, and, as noted above, decreased oocyte quality has been identified in both species as the main factor in age-related infertility [1, 21]. Trans-vaginal follicle aspiration can be performed in mares as in women, allowing simple and

repeatable non-terminal evaluation of follicle cells, fluid and oocytes. In addition, considerable interest exists in the equine industry to establish pregnancies from older, valuable mares. These mares may be kept by breeders until they start to show age-related infertility and thus older mares are typically readily available for study. This allows us to perform research on individuals that may more accurately reflect the changes present during ovarian aging in women.

As in women, characteristic reproductive changes occur in aging mares. In mares, reproductive senescence begins around 20 yr of age, and it is estimated that only 50% of mares older than 20 yr of age and 37% of mares older than 24 yr of age display normal ovarian activity [3, 152-155]. When they do cycle, aged mares have a delayed entry into the breeding season and have longer estrous cycles [3, 156]. Carnevale *et al.,* [21] reported lower pregnancy rates after artificial insemination in old mares (20 to 26 yr) compared to young mares (31% vs. 83%, respectively). Carnevale *et al.,* [157] also reported lower pregnancy rates in a retrospective analysis of a commercial oocyte transfer program; oocyte transfers from donors < 15 yr resulted in a 50% pregnancy rate, while oocyte transfers from donors > 23 yr resulted in a 16% pregnancy rate. Additionally, lower foaling rates (53%) have been reported for old mares (≥ 20 yr) compared to young mares (85%), and to produce a foal, old mares have been reported to be bred 2.3 more cycles than young mares [3]. Ovarian inactivity, characterized by the presence of small, hard ovaries with no visible follicles, is also associated with increased age in mares, as reported in a slaughterhouse survey [158].

As seen in women, a decrease in follicle numbers and failure of follicular growth

are also found in the older mare. Old mares (≥ 20 yr) have longer interovulatory intervals than young mares due to a lengthened follicular phase; the growth rate of the ovulatory follicle in old mares is slower than that for young mares, and old mares also ovulate smaller follicles than young mares [156]. The decreased follicular development in old mares, like that in women, is also likely related to follicle depletion, as FSH is elevated in old mares suggesting decreased negative feedback from follicular inhibin due to lack of follicle activity [152]. The number of antral follicles that can be imaged by ultrasonography in old mares is decreased compared to that of young mares [159].

As in women, in addition to a decrease in follicle numbers, a decline in oocyte quality has also been documented in older mares. Oocyte transfers from young donors (6 to 10 yr) to young recipients had higher embryo development rates (92%) than did oocyte transfers from old donors (20 to 26 yr) to young recipients (31%) [21]. Day-3 oviductal embryos from old mares have fewer cells and more morphological abnormalities than do embryos from young mares [156]. The results from these studies suggest that there is an age-related decline in oocyte quality which affects embryo development. In a study using light and electron microscopy, more oocytes from old mares (> 19 yr) than young mares (3 to 10 yr) had morphological abnormalities including fragmentation, large vesicles in the ooplasm, atypical shapes, areas of ooplasm without organelles, and sections of oolemma with scarce microvilli [160]. Altermatt *et al.,* [161] evaluated oocytes collected from preovulatory follicles of young (4 to 9 yr) and old (≥ 20 yr) mares by light microscopy to determine morphological measurements. In old mares, the zona pellucida (ZP) was thinner than that in young mares, and the

perivitelline space and inner ZP volume were larger and associated with oocytes that failed to develop after intracytoplasmic sperm injection; the authors suggested that during natural fertilization these changes could constitute a functional impairment associated with sperm binding or penetration of the ZP. The results from these studies indicate that oocytes from old mares undergo degenerative changes. Ruggeri *et al.,* [162] showed the presence of actin vesicles in oocytes collected from old (20 to 25 yr) mares. Actin is a major cytoskeletal component and plays a key role in the migration of the meiotic spindle in mouse oocytes [163, 164]. Actin vesicles are spherical filamentous actin structures which act as pushing forces and are part of the actinomyosin contractile forces during oocyte maturation [165-167]. Actin cytoskeleton remodeling and localization is involved in human oocyte maturation, and *in vitro* maturation affects the actin network and amount of actin present before fertilization [167]. Although the role of actin in equine oocyte maturation and fertilization has not been studied, the presence of actin vesicles in oocytes from old mares could suggest abnormal remodeling of the cytoskeleton of those oocytes [162].

As mentioned above, mitochondrial damage and low mtDNA copy numbers also negatively influence oocyte developmental competence and contribute to decreased fertility in women [94, 98, 101, 102]. Oocytes of aged mares, like those of aged women, have a lower mtDNA copy number [99, 168] and a higher prevalence of morphological mitochondrial abnormalities; oocyte mitochondria from aged mares are often enlarged with damaged cristae [99]. Thus, mitochondrial dysfunction and degeneration also appears to be associated with aging in mares.

As reviewed above, the composition of FF has been suggested as a possible marker of oocyte quality. In mares, analysis of FF revealed the presence of microvesicles and exosomes which contain microRNAs (miRNAs) [169]. Bioinformatics analysis revealed that three miRNAs were significantly higher in FF from old mares compared to that of young mares. The main pathway targeted by these three miRNAs is TGFβ signaling which, as discussed above, is critical for proper follicular development and growth. These findings suggest that in old mares, miRNAs present in FF could suppress this pathway leading to decreased oocyte competence [169]. In support of these results, another study from the same group evaluated gene expression of selected TGFβ family targets/components in granulosa cells from young and old (20 to 26 yr) mares [170]. Analysis revealed significant differences of *Il6* (interleukin 6) and *Col1a2* in young mares, and *Id2* (inhibitor of DNA binding 2), *Stat1* (signal transducer and activator of transcription 1) and *Cdc25a* (cell division cycle 25A) in old mares; the expression level of these 5 genes was altered after induction of follicular maturation. *Col1a2* is involved in cell proliferation and regulation of the cell cycle, and decreased levels of this gene in old mares further supports the possibility of downregulation of TGFβ signaling as a factor in the age-related decrease in oocyte quality [170]. Differences in gene expression in granulosa cells [168, 171], CCs and oocytes from old and young mares after administration of equine recombinant LH have also been evaluated [168]. In these studies, levels of *LHr* (luteinizing hormone receptor) in granulosa cells of young mares declined (this decline is caused by exogenous LH or the preovulatory LH surge and lasts until cells luteinize and the CL forms after which levels of LHr increase), but there was

no time effect in old mares, suggesting an age-related delay in response to LH by follicular cells and oocytes. Granulosa cells of old mares also had higher expression levels of *Areg* and *Ereg* (epiregulin; an EGR-related ligand) [168] which, as reviewed above, activate the EGF pathway to stimulate PI3K/AKT signaling in CCs; *Star*, *Tpa* (tissue-type plasminogen activator), and *Txn2* (thioredoxin-2) [171]. These age-related changes in metabolic, steroidogenic and inflammatory genes could mark alterations in follicular functions of old mares. Cumulus cells from old mares also had higher expression levels of phosphodiesterases (PDEs) Pde4d and Pde3a. These PDEs are essential for oocyte maturation as they regulate cAMP (cyclic adenosine monophosphate; a second messenger involved in intracellular signal transduction and of major importance in resumption of meiosis in preovulatory oocytes) in response to gonadotropins; these results suggest the possibility of premature oocyte maturation in aged mares, which could affect their reproductive success [172]. Finally, oocytes from old mares had lower expression levels of *Gdf9* and *Bmp15*, which, as described above, regulate the function of CCs; these lower levels of oocyte-secreted factors could contribute to the decreased developmental competence observed in oocytes from old mares [168].

In summary, aging causes a decrease in female reproductive efficiency. In both women and mares, a decrease in follicle numbers and oocyte quality is the major cause of age-related infertility. Factors that affect the oocyte quality in aging women and mares include aneuploidy, oocyte cytoplasmic factors, and mitochondrial abnormalities. Therefore, the mare offers an excellent model for reproductive aging.

MESENCHYMAL STEM CELLS

Stem cells are distinguished from other cell types by their ability to self-renew through cell division and to differentiate into multiple lineages during early life and growth [173]. When a stem cell divides, each new cell has the potential to either remain a stem cell or become another type of cell with a more specialized function. In addition, in many tissues they serve as an internal repair system, dividing to replenish other cells as long as the organism is alive [174].

Adult stem cells are undifferentiated cells found in many organs and differentiated tissues with a limited capacity for self-renewal and differentiation. The differentiation capacity of these cells, under certain physiologic or experimental conditions, is usually limited to cell types in the organ of origin. The main function of adult stem cells in a living organism is to maintain and repair the tissue in which they are found [174]. Bone marrow contains two kinds of stem cells: 1) hematopoietic stem cells, which give rise to all types of blood cells in the body, and 2) mesenchymal stem cells (MSCs; also called bone marrow stromal cells), which can differentiate into osteoblasts [175], chondrocytes [176], and adipocytes [177]. Mesenchymal stem cells also exist in other tissues such as umbilical cord blood [178], adipose tissue, and muscle [179].

Mesenchymal stem cells, particularly those derived from bone marrow (BM-MSCs), are increasingly being used in regenerative therapies because of their capacity to repair tissue damages due to injury and disease. In horses, BM-MSCs have been shown to enhance early chondrogenesis in articular defects [180], as well as to improve the biomechanical, morphological and compositional parameters in naturally-occurring

[181] and experimentally-induced [182] tendon injuries. Wilke *et al.,* [180] examined the effects of BM-MSC implantation on cartilage healing characteristics in horses. Twelve full-thickness cartilage lesions in the femoropatellar articulations of six horses were treated by injection of a fibrin vehicle with MSCs or fibrin vehicle alone in control joints. One month after injection, arthroscopic assessments and defect biopsies were performed, and 8 months after injection the animals were euthanized. Cartilage repair was evaluated by histology, histochemistry, collagen type I and type II immunohistochemistry, collagen type II *in situ* hybridization, and matrix biochemical assays. In the full-thickness articular defects, MSC grafting resulted in early improvement of defect healing. However, this was not sustained over the course of the 8-month study. Arthroscopic assessments and biopsies at 1 month showed improved tissue filling of MSC-grafted defects; however, biochemical and morphologic assessment at 8 months showed few differences between MSC-implanted defects and those implanted with fibrin vehicle without MSCs [180]. Smith *et al.,* [181] studied the effects of BM-MSCs in the treatment of naturally-occurring superficial digital flexor injuries in 12 horses. Horses were randomly assigned to receive MSCs or saline, then after a 6-month exercise program the horses were euthanized and their tendons assessed for structural stiffness, appearance and molecular composition. Tendons treated with MSCs exhibited statistically significant improvements in the key parameters examined compared to the saline-injected control tendons. Injections of MSCs resulted in the formation of tissue resembling normal tendon matrix rather than the fibrous scar tissue formed after natural inflammation and repair. Schnabel *et al.,* [182] examined the effects

of BM-MSCs in collagenase-induced tendinitis lesions created in the superficial digital flexor tendon of horses. Horses were euthanized 8 weeks after MSC injection and their tendons were mechanically tested and evaluated for biochemical composition and histologic characteristics. Similar to the findings of Smith *et al.,* in naturally-occurring tendon injuries [181], the results from this study showed that MSC injections into tendinitis core lesions resulted in significant histological tendon healing and a trend towards improved biomechanical characteristics of healing tendon [182].

Mesenchymal stem cells have also been successfully used in models of injury in other species, typically with the proposed mechanism of stimulating endogenous repair pathways. They have been used in rat models of kidney disease to accelerate glomerular recovery damage to mesangial cells, important structural and functional cells in the glomeruli, by releasing paracrine growth factors [183], mouse models of diabetes mellitus to decrease mesangial thickening and macrophage infiltration and to enhance insulin secretion by increasing proliferation, migration and differentiation of endogenous cells [184], mouse, sheep, canine, and swine models to restore ventricular function after acute myocardial infarction by increasing vascularity and secreting paracrine growth factors [185-188] and rodent models of neurological disorders to promote repair and regeneration of nervous tissue [189].

In reports in which MSCs were tracked *in vivo*, MSCs were shown to enhance tissue repair despite low or transient engraftment levels [182, 190]. Only a small proportion of MSCs were found to home and persist in the target sites, and typically MSCs were not detectable after 7 to 14 days after transplantation [191].

Mesenchymal stem cells secrete soluble factors which can alter the tissue microenvironment including: interleukin 1 receptor antagonist (*Il1rn*) which inhibits inflammatory responses [192]; vascular endothelial growth factor (*Vegf*) which induces angiogenesis [193, 194]; basic fibroblast growth factor (*bFgf*), hepatocyte growth factor (*Hgf*), brain-derived neurotropic factor (*Bdnf*) and nerve growth factor (*Ngf*) which promote the survival and proliferation of endogenous cells [184, 195, 196]; and insulin-like growth factor-1 (*Igf1*) and interleukin-6 (*Il6*) which decrease apoptosis [9, 197, 198]. Notably, MSCs can also alter the host tissue microenvironment by transferring mitochondria. Spees *et al.,* [199] used cells pre-treated with ethidium bromide so that mitochondrial DNA became mutated and depleted making the cells incapable of aerobic respiration and growth. Mutated cells were co-cultured with GFP-labeled human BM-MSCs. The results from this study showed that after co-culture with MSCs, some of the mutated cells acquired functional mitochondria which were confirmed to be from the MSCs by genetic analysis of the rescued cells [199]. However, the results from this study did not establish the mechanism by which mitochondria were transferred from MSCs to mutated cells.

The results from these studies- showing a significant repair of diseased or injured tissue despite low levels of MSC engraftment, and identifying known tissue-repair factors secreted by MSCs- suggest that MSCs do not contribute physically to tissue regeneration by differentiating themselves. Instead, MSCs appear to promote tissue repair via paracrine effects of the secreted factors which stimulate proliferation of endogenous cells, and decrease inflammation and immune reactions. Thus, the ability of

MSCs to alter the host tissue microenvironment may contribute more significantly to the repair of tissue than does their ability to differentiate into other cells.

Since the groundbreaking identification of MSCs by Friedenstein *et al.,* [200] in 1970 and the first detailed description of the trilineage potential of MSCs by Pittinger *et al.,* [201], many attempts have been made to better define what a MSC is. To address this issue, the Mesenchymal and Tissue Stem Cell Committee of the International Society for Cellular Therapy has proposed a set of standards to define human MSCs. The three criteria to define MSCs include adherence to plastic when maintained in standard culture conditions using tissue culture flasks, multipotent differentiation potential to osteoblasts, adipocytes, and chondrocytes under standard *in vitro* differentiating conditions, and specific surface antigen expression. Surface antigen expression allows for the rapid identification of a cell population and has been used extensively in immunology and hematology. The CD (cluster of differentiation) system is commonly used in immunophenotyping, because it allows cells to be defined based on the molecules that are present on their surface. Each CD indicates cell-surface protein or epitope (section of protein) that is recognized by an antibody. Human MSCs express (are positive for) CD105, CD73 and CD90 and lack expression of (are negative for) CD45, CD34, CD14 or CD11b, CD79α or CD19 and HLA-DR. These positive and negative markers are used to distinguish MSCs from other cells in the bone marrow compartment. The negative markers include surface antigens that are expressed by hematopoietic cells, while the positive markers are absent from most hematopoietic cells [202]. However, no such uniform immunophenotyping criteria are available for equine MSCs. This is further

hampered by the lack of equine-specific or cross-reacting monoclonal antibodies to CDs. De Schauwer *et al.,* [203] screened 30 commercial monoclonal antibodies (raised in mouse and rat to human, mouse and dog) with flow cytometry to determine their ability to recognize equine epitopes and confirmed their specificity by confocal fluorescence microscopy. In this study, they found that equine MSCs were positive for CD44, CD29 and CD90, negative for CD45 and CD79α, and had variable expression for CD73 and CD105 [203]. Equine MSCs have been found to have variable expression of MHC II, possibly due to a combination of factors including the animal of origin, bone marrow aspirate quality, immunologic background at a given time, and culture conditions [204]. This 8-marker panel is commonly used for the immunophenotyping of equine MSCs, although due to variability in immunophenotype, the physical attributes (shape and adherence to plastic) and the functional characteristics (ability to undergo trilineage differentiation) are currently the definitive measure of MSC identity.

Cryopreservation

Cryopreservation of MSCs is critical for both research and clinical applications. The ability to preserve MSCs long-term permits the banking of cells to facilitate coordination of therapy with a patient care regimen, and allows the completion of quality and safety testing before use, as well as simplifying transportation of cells. In order to use cryopreserved cells successfully, MSCs need to be stored with minimal loss of cell viability and differentiation capacity and ideally their immunophenotype needs to remain unchanged.

Although there is no consensus protocol for preserving MSCs, most cryopreservation procedures use a variation of a technique involving addition of a penetrating cryoprotectant such as dimethyl sulfoxide (DMSO) and a source of plasma protein, cooling at a defined rate, and storage at cryogenic temperatures (below -150 ºC) using mechanical refrigerators or liquid nitrogen refrigerators [205]. Preservation of the structural integrity of cells involves the use of very low temperatures. However, when cells are stored at low temperatures freezing damage can occur through the formation of intracellular ice, which can lead to cell death. Avoiding the formation of intracellular ice is therefore essential for the successful cryopreservation of cells. The cryoprotectant DMSO colligatively decreases the freezing point and interferes with ice crystal formation, thereby reducing the formation of intracellular ice [206]. Colligative effects depend upon the number of molecules, which is why most cryopreservation laboratories use high concentrations of DMSO (10% v/v) [205, 207]. However, the effectiveness of lower DMSO concentrations in human cell cryopreservation has been reported [208, 209]. Cryopreservation with DMSO does not alter the differentiation capacity of MSCs [207] nor the expression of MSC markers [210].

Handling of MSCs during thawing can affect their viability. When frozen-thawed MSCs are centrifuged for removal of cryoprotectant and resuspension, viability decreases over time, with the rate of viability decrease varying depending on holding temperatures and holding media [211]. The rate of dilution during thawing also affects MSC viability [210, 212] due to osmotic injury from fast addition of dilution medium [210].

Quantum Dot Labeling

As reviewed above, regenerative therapies have seen rapid advances in the use of adult BM-MSCs for tissue repair because of their potential to promote angiogenesis and survival and proliferation of endogenous cells. However, the distribution and fate of MSCs once introduced *in vivo* are not well understood. This is in part due to the limited methods available to track and identify delivered MSCs *in vivo*. Current methods for labeling MSCs include ultra-small iron particles [213], radioactive labels [214], organic fluorescent dyes loaded exogenously into cells [215], and fluorescent proteins expressed by the cells [216]. Previous attempts at tracking delivered MSCs have been hampered by the autofluorescence of host tissue and limitations of existing labeling techniques including chemical and metabolic degradation, reduced photostability and signal quality [217]. Quantum dots (QDs), nanoparticles made of semiconducting material, have emerged as fluorescent alternatives to organic dyes because they are non-toxic, are more resistant to photochemical and metabolic degradation, and do not interfere with cellular function or proliferation [218]. Cells uptake QDs through endocytosis based on their surface coatings; QDs then distribute in the cytoplasm in perinuclear endosomes and lysosomes. The mechanism by which cells expel QDs is controversial and poorly defined in literature; however, QDs do not interfere with normal cell physiology and cell differentiation [219].

Quantum dots have been reported to persist for up to 8 weeks in human MSCs delivered into canine hearts [220]. Full-thickness defects were surgically induced and scaffolds seeded with QD-labeled MSCs were used to repair them. After 8 weeks, the

animals were euthanized and a region of myocardium circumscribing the scaffold was excised. Transmural sections within the scaffold region were imaged to identify QD-labeled MSCs. Costa *et al.,* [221] infused QD-labeled goat MSCs into goat mammary glands and mouse testicles. Mammary gland and testicle tissue biopsy samples were obtained 30 days after infusion and examined 30, 60 and 90 days after collection. Histological examination under fluorescence microscopy of the tissues revealed the presence of QD-labeled MSCs at all time points evaluated. Whereas *in vivo* studies with QD-labeled human MSCs have reported long term persistence of QDs in target tissues, human MSCs maintained in standard *in vitro* culture conditions have shown a rapid loss of fluorescence signal. Seleverstov *et al.,* [222] reported a significant loss of fluorescence in QD-labeled human MSCs in culture 2 to 7 days after labeling and Wang *et al.,* [223] recently reported a significant reduction in fluorescence in QD-labeled human MSCs after 24 h of culture. Flow cytometry indicated that cell proliferation was the main factor leading to decreased fluorescence [223]. Whole-body detection of QDs was achieved by Larson *et al.,* [224] by injecting QDs intravenously into mice; using multiphoton imaging QD-containing vasculature was visible through the intact skin to the base of the dermal layer in live mice; however, whole-body detection of QD-labeled MSCs in higher organisms has not been reported, as larger quantities and volumes of cells may be required to enable this application [225].

MESENCHYMAL STEM CELLS AND FERTILITY RECOVERY

Each year millions of women are rendered sterile by chemotherapy-associated ovarian failure. The risk of developing premature depletion of functional ovarian follicles as a consequence of chemotherapy is dependent on several factors. Some chemotherapy agents are considered more gonadotoxic than others [226, 227]. Dosage of the treatment used is also important [227, 228] as is the age of the patient [229-231]. While damage to follicles occurs at all ages, the age-related difference is probably due to the fact that older women have a smaller primordial follicle reserve at the start of treatment compared with that of younger women [231].

Among the most ovo-toxic of the chemotherapy drug groups are the alkylating agents (cyclophosphamide (CTX), busulphan and dacarbazine), platinum complexes (cisplatin and carboplatin), and taxanes (paclitaxel) [232-236]. The fact that chemotherapy induces oocyte death is a conundrum, as chemotherapy agents target replicating DNA and dividing cells, and oocytes and the surrounding cells of the primordial follicle neither replicate DNA nor divide.

The most recent theory of chemotherapy-induced destruction of follicles suggests that *in vivo*, chemotherapy agents including CTX trigger an initiation of primordial follicle growth, which occurs simultaneously with growing follicle apoptosis induced by this chemical [237]. As described above, the activation of primordial follicles is mediated by an upregulation of the PI3K/PTEN/AKT signaling pathway [48-50]. The mechanism by which chemotherapy induces activation of the PI3K/PTEN/AKT pathway may be via direct influence on the primordial follicles, or indirectly via chemotherapy-

induced destruction of larger follicles. In mice, treatment with CTX has been shown to cause severe primordial follicle loss and growing follicle apoptosis, resulting in depletion of the ovarian reserve [238]. Ovaries of CTX-treated mice also showed increased phospho-Akt and phospho-mTOR levels as well as increased phosphorylation of the downstream P70S6-rpS6-eIF4B proteins. Thus suggesting that CTX treatment over-activated the PI3K/Akt/mTOR signaling pathway in the ovary leading to excessive primordial follicle activation and recruitment into a vicious cycle of growth, development, and apoptosis, causing exhaustion of the ovarian reserve [238]. *In vivo* treatment of mice with AS101 (a non-toxic compound that acts on the PI3K/PTEN/AKT pathway [239]) reduced CTX-induced loss of primordial follicles and decreased CTX-induced apoptosis of granulosa cells of growing follicles [237]; these results also suggest that destruction of primordial follicles by CTX is through activation of primordial follicles mediated by disruption of the PI3K/PTEN/AKT pathway.

Destruction of growing follicles results in a decrease in AMH and thus a loss of suppression of the primordial follicle pool. This loss of suppression results in activation of primordial follicles [240]. As mentioned above, AMH is produced by granulosa cells of small growing follicles and is a negative regulator of follicle activation; studies in knockout mice have shown that loss of AMH leads to excessive activation and depletion of the primordial follicle pool [58]. Analysis of AMH mRNA expression has shown that immediately following *in vivo* treatment of mice with CTX, the transcript levels of AMH were reduced by half [241]. When recombinant human AMH was added to *ex vivo* culture systems together with CTX, ovaries maintained higher numbers of primordial

follicles, with a loss of only 17% after one week in culture compared with the 53% loss of primordial follicles in ovaries exposed to CTX without AMH [241]. Chemotherapy drug-induced apoptosis in the ovary has been demonstrated in growing follicles, and has been shown to originate in the proliferating granulosa cells [242]. In cells, including mature oocytes, apoptosis is mediated by ceramide, BAX, and the caspases [243-245]. In mice, targeted disruption of *Casp2*, which activates *Bax*, results in retention of more primordial follicles and resistance to doxorubicin [26]. Tumor protein p63 is specifically expressed by oocytes of primordial follicles, and in particular the p63 isoform TAp63 is a key mediator of the DNA damage/apoptosis pathway regulating the response of primordial follicle oocytes to DNA injury [246-248]. The p63 pathway is upregulated when primordial oocytes are exposed to external triggers of DNA damage such as chemotherapy drugs [249]. Increased TAp63 activates apoptosis via BAX; thus loss of p63 in mouse oocytes results in resistance to the apoptotic effects of cisplatin [250]. The activation of apoptosis is also mediated by TAp73 [250], either directly or through the activation of p53-upregulated modulator of apoptosis (PUMA) and phorbol-12-myristate-13-acetate-induced protein 1 (NOXA) [251]. Oocyte-specific deletion of PUMA or both PUMA and NOXA in mice prevents chemotherapy-induced apoptosis and can result in the production of healthy offspring in chemotherapy-treated mice, indicating that the protected oocytes are capable of DNA repair and subsequent normal function [251].

Another mechanism by which chemotherapy drugs induce follicle loss is via indirect damage to the ovarian stroma and the vascular system [252, 253]. In women,

ovarian blood flow was significantly reduced immediately after chemotherapy [254] and in mice, doxorubicin administration induced a significant acute reduction in ovarian blood volume and narrowing of the small vessels [255]. Examination of human ovarian tissue previously exposed to *in vivo* chemotherapy revealed evidence of thickening and hyalinization of cortical stromal blood vessels, proliferation of small and disorganized blood vessels in the ovarian cortex, and subcapsular focal cortical fibrosis [256]. Although larger follicles may be more sensitive to acute ischemic changes due to the requirements of proliferating granulosa cells, experimental models support the dependence of primordial follicles on adequate vascularization [257]. Ovarian stroma and ovarian extracellular matrix are important for normal ovarian function, follicle growth, and survival [258, 259], and in human ovarian tissue xenotransplants there is an inverse correlation between ovarian vascular density and primordial follicle apoptosis [257]. The fact that the blood supply to the ovary is an end-artery system makes it more likely that these stromal and vascular changes might impair ovarian function and contribute to the loss of primordial follicle reserve [252, 260].

Interestingly, there have been reports showing an unexpected return of ovarian function and fertility after chemotherapy in women who underwent bone marrow transplantation (BMT) as a component of their therapy. Salooja *et al.,* [4] reported that of 10 women receiving a high-dose chemotherapy regimen followed by single BMT, 4 developed ovarian failure and six resumed spontaneous cyclical menstruation. Five of the 6 menstruating women became pregnant between 4 and 40 months following BMT. Sanders *et al.,* [261] described that of 187 women 43 women who had received BMT

following a high-dose chemotherapy regimen, 32 recovered normal ovarian function and 9 of these women had 12 pregnancies. In a different report, Sanders *et al.,* [6] also described that of 708 women who had received high-dose chemotherapy followed by BMT, 110 recovered normal ovarian function and 32 became pregnant. In a retrospective analysis, Hershlag *et al.,* [7] reported that 4 patients with ovarian failure induced by high-dose chemotherapy established pregnancies following BMT. In humans, data on pregnancies in patients post-chemotherapy shows no increase in fetal malformations or pregnancy loss, indicating that prevention of infertility with reestablishment of normal hormonal function and viable pregnancies following BMT is a realistic possibility. It is not known whether these pregnancies resulted from oocytes that did not sustain any DNA damage or from oocytes that underwent DNA repair.

Several animal studies have been conducted to investigate the return of ovarian function following chemotherapy. In 2007, Lee *et al.,* [8] demonstrated that BM-MSCs injected via the tail vein to chemotherapy-treated adult female mice rescued long-term fertility. Females administered non-lethal doses of busulfan and CTX without BMT became infertile whereas mice that underwent BMT achieved 4 to 6 pregnancies (per mouse) over the course of 7 months although the number of pups per litter was lower than that for non-treated control females. Two months after chemotherapy and MSC injection, fertility decreased. In the study of Lee *et al.,* [8], bone marrow was harvested from transgenic females expressing green fluorescent protein (GFP). Two months after MSC injection, the ovaries of recipients possessed GFP-positive cells within apparent immature follicles, although the percentage of the total immature follicle pool containing

GFP-positive cells was low (1.4%). However, these cells only appeared in apparent immature follicles up to the pre-antral stage and were not observed in preovulatory follicles, and all offspring were derived from the recipient germline. This supports findings in other tissues, that the tissue microenvironment is repaired by the transplanted BM-MSCs or by factors released by the transplanted cells, and not by the differentiation of BM-MSCs into functional cells [8].

In other studies using similar protocols, transplanted MSCs were not found within follicle-like structures, but did persist in ovarian stromal tissue and even in the theca. Wang *et al.,* [11] showed that in mice intravenous injection of human umbilical cord MSCs increased the number of follicles and decreased apoptosis of granulosa cells in females with CTX-induced premature ovarian failure. Ovaries were collected 1 week after MSC injection and the presence of normal follicles was determined. Ovaries of mice receiving MSCs after chemotherapy had more oocyte-containing follicles at different stages of development and had a significantly lower percentage of TUNEL-positive (TUNEL staining identifies and quantifies the apoptotic cell fraction) granulosa cells than ovaries of mice that received chemotherapy only. Injected MSCs were labeled with the fluorescent tracker CM-Dil dye; 1 week after injection of MSCs, the labeled cells could be traced in the ovaries although these cells did not develop into follicles, granulosa cells or oocytes. Abd-Allah *et al.,* [262] showed that intravenous injection of BM-MSCs increased the number of follicles in female rabbits with CTX-induced ovarian failure. Six weeks after CTX injection follicle count was performed on ovarian sections. CTX injection resulted in a significant decrease in the number of all types of

follicles. However, in the MSC-injected group, a significantly higher number of follicles was detected when compared to the CTX injection group. Donor MSCs were harvested from male rabbits and the SRY gene was detected by PCR in the ovarian tissue of recipient females. Fu *et al.,* [9] reported that in female rats with CTX-induced ovarian damage, intra-ovarian injection of BM-MSCs improved ovarian function, as indicated by the restoration of the estrous cycle, increased serum estradiol levels and follicle numbers as counted on slides of ovarian sections, and reduced granulosa cell apoptosis which was analyzed by TUNEL staining. Donor MSCs were transfected with GFP; GFP-positive cells were found in the ovarian interstitium of recipient females 2 weeks after injection and persisted for 8 weeks. However, GFP-positive cells were not found in any follicles. Takehara *et al.,* [10] used a rat model with CTX-damaged ovaries and showed that intra-ovarian injection of adipose-derived MSCs induced angiogenesis, as shown by immunostaining of ovarian sections for CD34, expressed on vascular endothelial cells, and increased the number of follicles and corpora lutea in treated females. Eight weeks after MSC injection, females were euthanized and their ovaries were removed; histological sections were prepared and the number of follicles and corpora lutea was calculated and compared between the MSC-injected animals and the animals that received chemotherapy only. The injected MSCs were derived from male rats, and the Y chromosome was localized in the theca layer in the recipient ovaries 8 weeks after MSC injection using fluorescent *in situ* hybridization (FISH) to detect the distribution of cells exhibiting Y chromosomes in the ovarian tissues.

In another model of ovarian dysfunction, Ghadami *et al.,* [263] reported that the intravenous injection of BM-MSCs from wild-type mice restored estrogen hormone production and folliculogenesis in FORKO (follicle-stimulating hormone receptor knockout) mice. FORKO mice have a targeted disruption of the receptor for FSH (follicle-stimulating hormone) and show reduced fertility and early reproductive senescence due to disordered estrous cycles, decreased estrogen levels and absence of folliculogenesis. In this study, blood samples collected before and after MSC injection showed a 4- to 5.5-fold increase in estrogen in treated animals compared to FORKO mice that did not received MSC injections. After inducing ovulation with pregnant mare serum gonadotropin and human chorionic gonadotropin, oviductal flushings were performed. However, oocytes were not detected in oviductal flushings of the treated FORKO mice, suggesting that the MSC-induced resumption of folliculogenesis, based on serum estrogen concentrations, was not accompanied by ovulation. Lack of ovulations was also confirmed by the absence of corpora lutea on histological examination of the ovaries.

As described above, during the process of ovarian aging there is a decrease both in the quantity and quality of the ovarian follicle pool which leads to a decrease in fertility. This similarity to findings in chemotherapy-treated ovaries leads to the questions of whether MSC transplantation may help rescue ovarian function in aged females. Unfortunately, there is limited information on the effects of MSCs in females with decreased fertility due to aging. Selesniemi *et al.,* [12] showed that once-monthly intravenous injections of young adult BM-MSCs increased the number of full-term

pregnancies and sustained the fertile potential of aged female mice long past the normal time of reproductive senescence (typically begins around 8 months of age). On average, 75% of 11.5-14.5-month old, and 52% of 14.5-17.5-month old MSC-injected females remained fertile. In comparison, 56% of 11.5-14.5-month old, and 31% of 14.5-17.5-month old control females achieved full-term pregnancies and delivered offspring. Injected MSCs harvested from young adult female mice (6 to 10 weeks of age) were transfected with GFP; there was little evidence of engraftment and all offspring were derived from the recipient germline. As reviewed previously, BM-MSCs secrete cytokines which improve cellular function and decrease the apoptosis of somatic cells after cytotoxic insult. It is possible that in the non-insult model of aging, the secreted factors from the injected MSCs could also act as anti-apoptotic signals in aging ovaries [12]. A case report by Mohammed Ali *et al.,* [13] described the intra-ovarian injection of peripheral blood mononuclear cells in a 49-yr old woman with a 30-yr history of infertility. An increase in serum levels of anti-Müllerian hormone (AMH) followed by a pregnancy occurring 5 months after treatment, and a live birth, were reported. The authors of this report suggest that peripheral blood mononuclear cells stimulate mitotically-active oogonial stem cells and generate new oocytes *in vivo*. However, these are only assumptions as there is no evidence presented in the report to validate this hypothesis. Finally, in a recent pilot study, Buigues *et al.,* [264] isolated autologous BM-MSCs and injected them into one ovarian artery of 10 women of advanced maternal age with decreased fertility; the contralateral ovary of each woman was considered to be a control. Serum AMH and antral follicular count (AFC) were monitored for up to 5

months after the injection. An enhancement of AFC of ≥ 3 follicles was considered as a successful outcome. Injection of MSCs improved the AFC in 40% of the patients in the first two weeks after MSC injection; in 30% of the patients, in addition to an increase in AFC there were two consecutive increases in AMH.

In the studies reviewed above, increased follicular activity was detected in the ovaries of recipient females as early as 2 weeks after MSC injection; however, it takes a mouse primordial follicle about 1 month to grow and reach ovulatory maturity (this period is approximately 4 months in women) [22]. Thus, it is unlikely that the injected MSCs were triggering oogenesis or even growth of primordial follicles. Furthermore only one study reported the presence of injected MSCs in apparent follicles [8], but these cells did not develop or ovulate, suggesting that it is unlikely that they were functional oocytes and may have appeared in the follicles via migration. Therefore, based on the results of these studies, it appears that MSCs are unlikely to differentiate into follicle components or drive primordial follicle development, but rather may function through a paracrine pathway to protect endogenous cells within primary or larger follicles.

In summary, chemotherapy causes activation of primordial follicles and apoptosis of granulosa cells of growing follicles leading to oocyte and follicle loss. Several factors secreted by MSCs are known to promote the survival and decrease the apoptosis of endogenous cells. It is possible that these factors are acting on the granulosa cells of ovarian follicles and protecting them from the deleterious effects of chemotherapy. Similarly, ovarian aging causes cytological changes including oocyte atresia and degeneration of granulosa cells and mitochondria. It is possible that the

factors secreted by MSCs can act on the granulosa cells of aging follicles and protect them. Furthermore, it has been shown that MSCs can transfer mitochondria to other cells. Thus, there is a possibility that the injected MSCs could transfer healthy mitochondria to replace the damaged mitochondria of aging follicles.

Mesenchymal Stem Cells and Ovarian Gene Expression

As described above, MSCs secrete a variety of growth factors, some of which have been found to affect follicular growth in ovaries; these factors include *Vegf*, which induces angiogenesis, promotes cell migration, and inhibits apoptosis of rat cumulus cells [265], *Hgf*, which induces angiogenesis and tissue regeneration [266], and *Igf1*, which suppresses apoptosis and causes proliferation of porcine cumulus cells [267].

After intra-ovarian injection of adipose-derived MSCs into rat ovaries damaged by CTX, Takehara *et al.,* [10] extracted total RNA from ovaries and performed quantification of gene expression by RT-PCR according to the standard-curve method. Ovaries from females receiving CTX and MSCs had greater mRNA expression of *Vegf, Hgf*, and *Igf1* than did ovaries from females that received CTX but not MSCs. MSC-injected ovaries also had a higher expression of steroidogenic acute regulator (*Star*) which enhances the conversion of cholesterol to pregnenolone, the first step in production of sex steroids. Additionally, in MSC-injected ovaries, the production of all the HGF, VEGF and IGF-1 proteins reached levels seen in normal control ovaries. Wang *et al.,* [11] also extracted total RNA from normal control ovaries and ovaries from females that received systemic injection of umbilical cord MSCs after CTX, and

performed qRT-PCR to determine levels of gene expression. The RNA expression pattern of ovaries from MSC-injected females was similar to that of ovaries of control mice, with only 33 genes differentially expressed including; *Nuf2* which has a role in chromosome segregation during meiotic prophase, *Ptgds* which is important for reproductive tract development, *Megf10* which plays a role in cell proliferation and apoptosis, and *Saa1* which is highly expressed in response to inflammation and tissue injury. In contrast, 91 genes were differentially expressed between normal control ovaries and ovaries from CTX-treated females that did not receive MSCs. Additionally, Wang *et al.,* [11] reported that umbilical cord MSCs rescued the expression of important proteins from the aldo-keto reductase family 1 which catalyze the conversion of progesterone to 20-alpha dihydroprogesterone, a reaction thought to be important for luteolysis and overall reproductive health. Amounts of this protein were very low in the CTX-treated group; however, after MSC therapy, they increased to normal levels. In both of these studies, the changes in gene expression were associated with increased ovarian activity, i.e., increased follicle numbers and corpora lutea in MSC-treated mice and rats [10, 11], and increased fecundity in MSC-treated mice (13.6 litters in MSC-treated females compared to 9.4 litters in saline-injected control females) [10]. Finally, in a pilot study Buigues *et al.,* [264] quantified the soluble factors released by BM-MSCs used for ovarian artery injections in aged women; among the factors identified, fibroblast growth factor-2 (FGF-2) and thrombospondin (THSP-1) were positively correlated with the enhancement of AFC.

These studies indicate that intra-ovarian or systemic injection of MSCs into

ovaries induces mRNA and protein expression of genes that may improve the function of ovaries compromised by chemotherapy. However, little information is available on the effect of MSC injection on the aging ovary, an application which, if effective at increasing fertility, would have an impact on millions of women undergoing assisted reproduction because of age-related infertility.

CONCLUSIONS AND AIMS

The findings from the papers reviewed indicate that MSCs secrete trophic factors and appear to restore the ovarian function of females who have decreased follicle numbers and oocyte quality due to chemotherapy. Age-related changes also result in decreased follicle numbers and oocyte quality reducing fertility in aging females, and it is possible that BM-MSCs could restore or improve ovarian function in aging females. The mare offers a useful model to explore this possibility as age-associated changes in fertility in the mare parallel those in women.

The studies presented in this dissertation aimed to evaluate for the first time, using the mare as a model, whether intra-ovarian injections of BM-MSCs may improve ovarian function in aging females, and if so, the mechanism by which these effects are accomplished, i.e., to: 1) determine whether intra-ovarian injections of BM-MSCs increase the number of antral follicles visible on ultrasonography; 2) determine whether QD-labeled BM-MSCs colonize the ovaries and if so, which areas; 3) determine whether *in vitro* co-culture of BM-MSCs with ovarian explants increases the expression of genes related to growth and repair; and 4) determine whether ovarian tissues recovered after *in*

vivo BM-MSC injection show different gene expression from non-injected mares. We hypothesized that injection of MSCs into the ovaries of mares would increase follicle numbers and increase the expression of genes related to follicle growth. The results from these studies could have potential implications in both human and equine reproduction.

CHAPTER III

PROOF OF CONCEPT: INTRA-OVARIAN INJECTION OF BONE MARROW-DERIVED MESENCHYMAL STEM CELLS IN MARES

INTRODUCTION

Adult bone marrow-derived mesenchymal stem cells (BM-MSCs) have emerged as a key element in regenerative medicine therapies due to their ability to aid in repair of damaged tissue and their potential to treat degenerative disease [180-184, 189, 268, 269]. In rat and mouse ovaries compromised by chemotherapy, injection of MSCs enhances ovarian function, as determined by follicle number, and induces mRNA and protein expression of genes that may improve ovarian function [10, 11]. However, little information is available on the effect of MSCs on the aging ovary, an understanding of which would have a potential impact on millions of women undergoing assisted reproduction because of age-related infertility. The mare offers a useful model to explore this possibility, as age-associated changes in fertility in the mare parallel those in women. In addition, the procedure also has potential clinical relevance in the mare, as considerable interest exists in the equine industry to establish pregnancies from older, valuable mares. To the best of our knowledge, intra-ovarian injections of MSCs in mares have not been performed previously. This preliminary study was performed to determine the feasibility of injection of autologous and allogeneic BM-MSCs into the stroma of the ovary in the live mare.

MATERIALS AND METHODS

Animals

This study was performed from January to December 2014. Two mares, age 7 yr, were housed in pens at the College of Veterinary Medicine Research Park and had *ad libitum* access to hay and fresh water throughout the study, and supplemental grain. All procedures were approved by the Texas A&M University Institutional Animal Care and Use Committee and were performed using guidelines set forth by the *United States Government Principles for the Utilization and Care of Vertebrate Animals Used in Testing, Research and Training*.

Experimental Design

The mares were randomly assigned to receive one of 2 MSC treatments: self (SF; autologous) or allogeneic (AL). Blood was collected from each mare and processed to recover serum, which was frozen. Bone marrow aspirates were harvested from the SF mare at two different time points during the study. MSCs were isolated from the aspirates and expanded in culture, labeled with fluorescent nanoparticles (Quantum dots; QDs) and cryopreserved in serum autologous to the mare to be injected.

Two intra-ovarian injections of MSCs, 5 months apart, were performed in each mare. The mares were monitored by physical examination and ultrasonography of the reproductive tract per rectum at 1, 3 and 7 days after each intra-ovarian injection of MSCs, then by ultrasonography per rectum every 14 days thereafter for 8 months. Starting 14 days post-injection, follicles greater than 8 mm in diameter were aspirated by

ultrasound-guided transvaginal aspiration (TVA) every 14 days to evaluate oocyte competence for nuclear maturation and development to the blastocyst stage *in vitro* after intracytoplasmic sperm injection (ICSI).

Seven months after the second injection, the ovaries of both mares were removed by ovariectomy via colpotomy. The ovaries were examined for gross pathology, histopathology, and presence of QDs, and ovarian tissue samples from the AL mare were submitted to the UC Davis Veterinary Genetics Laboratory for analysis of genomic and mitochondrial chimerism.

For analysis of follicle number, the number of follicles aspirated at each TVA in the two injected mares, and in the mares in the remainder of the research herd (control mares) which had not received intra-ovarian injections but which underwent similar follicular TVAs every 14 days, was recorded.

Serum Samples

Blood, 120 ml from each mare, was obtained via venipuncture of the jugular vein using 60-ml syringes and an 18-G needle. After collection, blood samples were kept at 4 ºC for 30 min and allowed to clot. The blood samples were then centrifuged for 10 min at 4000 x g and the serum was collected with a 20-ml syringe and an 18-G needle, filtered through a 0.2-µm filter, transferred into 15-ml conical tubes (Sigma-Aldrich, St. Louis, MO) and frozen at -20 ºC for later use.

Bone Marrow Harvest and Cell Culture

Bone marrow was harvested from sternal aspirates from the SF mare on two occasions, four months apart. To do this, the mare was sedated with intravenous (IV) administration of 0.4 mg/kg xylazine. The intersternebral spaces were identified by palpation on the ventral midline of the cranial thorax at the level of the elbows and the harvest sites were clipped of hair and aseptically prepared. Ten ml of 2% lidocaine were infiltrated through the subcutis and muscle layers and into the periosteum to provide local anesthesia. A Jamshidi Illinois sternal/iliac-aspiration needle (10-cm, 15-G) was introduced through the lidocaine-blocked area until it made contact with the surface of the sternebra. A slow, back-and-forth, rotational movement was used to advance the needle until it was firmly seated in the bone at a depth of 1 to 2 cm. The stylet was removed and a 60-ml syringe containing 10 ml of 1,000 IU/ml heparin in sterile saline was attached to the hub and aspiration was applied. This was repeated and a total of 100 ml of bone marrow were collected per procedure.

Red blood cell lysis of the aspirates was achieved by adding 60 ml of ammonium chloride (7.7 mg/ml NH_4Cl in phosphate buffered saline buffered with 206 mg/ml TRIS (hydroxymethane-aminomethane); pH 7.2) to the 120 ml of aspirate/heparin, suspending the cells by pipetting, and centrifuging at 300 x g for 5 min. The supernatant was aspirated and the remaining nucleated cellular portion of the marrow was resuspended to 120 ml with standard MSC culture medium consisting of Dulbecco's modified Eagle's medium (DMEM 1 g/l glucose; Mediatech, Manassas, VA) supplemented with 10% fetal bovine serum (FBS; HyClone Inc, Logan, UT), 2.5% HEPES buffer (Corning, St.

Louis, MO), 1 ng/ml basic fibroblast growth factor (bFGF; Sigma-Aldrich) and 1% antibiotic-antimycotic (10,000 U penicillin, 10,000 µg/ml streptomycin, 25 µg/ml amphotericin B; GIBCO; Invitrogen, Carlsbad, CA). This suspension was plated at 30 ml/175-cm^2 flask and maintained at 37 °C in a humidified atmosphere of 5% CO_2. The medium was refreshed and non-adherent cells discarded three times per week. When the monolayers reached 70% confluence, adherent MSCs were resuspended by treatment with 0.05% trypsin, counted with a hemocytometer, and reseeded as "Passage 1" (P1) at a density of 5 to 8 x 10^3 cells/cm^2. P1 cells were allowed to multiply to 70% confluence before trypsinization and successive passage.

Cells from P4 were trypsinized, resuspended in Dulbecco's phosphate-buffered saline (DPBS; BioWhittaker; Lonza, Walkersville, MD) and counted with a hemocytometer. To aid in identification of MSCs after injection, a commercially-available fluorescent nanoparticle kit (Qtracker 605 Cell Labeling Kit, Q25001MP; Invitrogen) was used to label the cells with QDs following the directions provided by the manufacturer. Briefly, a QD labeling solution was prepared by mixing 1 µl each of Qtracker Reagent A and B in a 1.5 ml microcentrifuge tube (10 nM/l concentration of QDs) and incubated for 5 min at room temperature. Standard MSC culture medium (0.2 ml) was added to the QD labeling solution and the solution was vortexed for 30 sec. A 1-ml cell suspension containing 1 x 10^6 cells in MSC culture medium was added to the QD labeling solution. The cells in QD labeling solution were incubated at 37 °C for 60 min, after which they were washed twice with serum-free medium consisting of DMEM supplemented with antibiotics and 1% ITS premix (1 mg/ml insulin, 0.55 mg/ml

transferrin, and 0.5 μg/ml selenium; VWR, Radnor, PA).

After being washed, the cells were frozen in cryopreservation medium containing 95% serum, autologous to the mare that would receive the injection, and 5% dimethyl sulfoxide (DMSO) at a concentration of 10 x 10^6 cells/ml. Cryovials containing this suspension were placed in a Cryo 1 °C Freezing Container (Thermo Scientific; VWR, Radnor, PA) for 24 h at -80 °C before transfer to liquid nitrogen where they were stored until used.

Characterization of MSCs

The MSCs used in this study (from Mare SF) were characterized based on the criteria proposed by the International Society for Cellular Therapy [202] by their ability to adhere to plastic (as seen in cell culture, above), chondrogenic differentiation potential, and specific surface antigen expression based on the literature discussed in Chapter II, i.e., positive for CD44, CD29 and CD90, negative for CD45 [203], with variable expression of MHC II [204]. Cells from the first BM aspirate performed in this mare were characterized.

In Vitro Colony-Forming Assay

To assess the proportion of MSCs in the first BM aspirate, the number of colony-forming units (CFUs) per 1,000 BM cells, after red blood cell lysis, was determined. The proportion of viable cells was determined by staining a 100-μl sample with propidium iodide (PI; 1.35 mg/ml) and fluorescein diacetate (FDA; 67.57 mg/ml) in DPBS.

Immediately after staining, 10 µl of the cell suspension were placed in the chamber of a Neubauer hemocytometer and visualized by fluorescence microscopy (Olympus, Center Valley, PA). Non-viable cells were detected by nuclear staining with PI, as this fluorescent stain is excluded from cells with intact membranes. The FDA stain indicated viability, as enzymatic activity of live cells is required to activate FDA's fluoresce and cell-membrane integrity is required for the intracellular retention of the fluorescent product. The live (green) and dead (red nucleus) cells were counted. A total of 10 squares (corner and middle squares of each counting grid) were counted. The concentration of the cell suspension was determined and the amount of cell suspension calculated to contain 1,000 viable cells was seeded onto a 10-cm tissue culture dish containing 9 ml of standard MSC culture medium. The dish was maintained at 37 °C in a humidified atmosphere of 5% CO_2 in air. Medium was changed every other day. After ten days, the cells were rinsed with phosphate-buffered saline (PBS) and stained with 3% crystal violet solution for 8 min to visualize colonies. The number of colonies was determined by counting manually without magnification.

In Vitro Chondrogenic Differentiation

QD-labeled MSCs were induced to differentiate into chondrogenic pellets by centrifuging 2.5 x 10^5 cells in chondrogenesis-induction media (DMEM with 4.5 g/l glucose, supplemented with 1% FBS, 2.5% HEPES buffer, 1% antibiotic-antimycotic (GIBCO), 10 ng/ml transforming growth factor beta (TGF-β3; Life Technologies), 0.6 µg/ml dexamethasone (Sigma Aldrich), 50 µg/ml L-ascorbic acid, 40 µg/ml proline

(Sigma Aldrich), and 1% ITS premix (VWR). Pellets were maintained in static culture at 37 °C in a humidified atmosphere of 5% CO_2 for 21 days with medium changes every other day. On day 21 the pellets were fixed with 4% paraformaldehyde (PFA; Sigma Aldrich) at room temperature for 10 min, after which they were embedded in paraffin. Sections were stained with hematoxylin and eosin (H&E) and visualized under light microscopy to determine the presence of round chondrocytes embedded in extracellular matrix. This was performed in triplicate for the first aspirate.

Phenotype Analysis by Flow Cytometry

Cells of P3 from the first aspirate were immunophenotyped by assessing immunoreaction using mouse anti-horse antibodies to MHC class II (Product No: MCS1085PE; Bio-Rad, Raleigh, NC), CD44 (Product No: MCA1082F; Bio-Rad), CD29 (Product No: 6603177; Beckman Coulter, Brea, CA), CD90 (Product No: DG2011; VMRD Inc, Pullman, Washington), and CD45 (Product No: HR-DG2009; VMRD). The antibodies against MHC II, CD44 and CD29 were fluorescently-labeled with fluorescein isothiocyanate (FITC). The antibodies against CD90 and CD45 were not labeled with FITC and a secondary goat anti-mouse IgG antibody, labeled with phycoerythrin (PE), was used for visualization.

MSCs were aliquoted at 1 x 10^6 cells per Eppendorf tube in 50 µl staining buffer. To stain MSCs with directly-labeled antibodies (MHC II, CD44, and CD29), antibodies were diluted at 1:100 and incubated with the cells for 45 min at 4 ºC. Cells were

centrifuged at 400 x g for 5 min, then washed with 200 µl DPBS and centrifuged again before being resuspended in 500 µl DPBS for analysis.

To stain MSCs with non-labeled antibodies (CD90 and CD45), the dilutions used were 1:400 for CD90 and 1:10 for CD45. The cells were incubated on ice for 15 min before centrifugation (400 x g) for 3 min. Cells were then washed twice with 100 µl DPBS before being resuspended. One hundred microliters of secondary antibody at a dilution of 1:100 were added and the cells were incubated on ice in the dark for 15 min before centrifugation at 400 x g for 5 min. Cells were washed with 200 µl DPBS and centrifuged again before being resuspended in 500 µl DPBS for analysis.

All cell suspensions had 5 µl 7-aminoactinomycin (7-AAD; Biolegend, San Diego, CA) added immediately prior to analysis, for assessment of viability. 7-AAD has a strong affinity for DNA but does not readily penetrate intact cell membranes; therefore, it can be used to determine cell viability because only cells with compromised membranes will be stained with 7-AAD. A sample of unlabeled MSCs and MSCs labeled only with secondary antibody were also analyzed by flow cytometry as controls.

Acquisition of the cell surface marker data was performed using a Becton Dickenson FACS Caliber flow cytometer using Cell Quest Version 3.3 (BD San Jose, CA). FITC, PE and 7-AAD were detected using a 488 nm laser with a 515/30 bandpass filter, 585/42 bandpass filter, and 650 Long Pass filter, respectively. At least 10,000 live events were collected. Data analysis was performed using FlowJo 9.8 Mac version (TreeStar Corp., Ashland, OR).

Intra-ovarian Injections

For intra-ovarian injection, the mares were sedated by IV administration of 0.005-0.01 mg/kg detomidine. Immediately prior to the MSC injection, 10 mg butorphanol tartrate and 120 mg n-butylscopolammonium bromide were administered IV. Previously-cryopreserved autologous or allogeneic MSCs, suspended in serum autologous to the mare receiving the injection, were thawed in a 37 °C water bath for 3 min. One ml of cell suspension containing 1.0 x 10^7 cells was divided among 4 1-ml syringes (250 µl of cell suspension per syringe). The syringes were attached, one at a time, by tubing to an 18-G x 60-cm single-lumen transvaginal needle to perform the injections. The volume of the tubing and needle was measured prior to the injections in order to determine the volume of the apparatus itself, and thus the volume of medium needed to ensure that the entire 250 µl of the cell suspension were delivered into the ovary. This volume varied with the individual apparatus used, and was ~2 ml. When the injections were performed, the 250 µl of cell suspension was ejected into the line and this was followed by the predetermined amount of DPBS medium.

Intra-ovarian injection was performed using a transvaginal, ultrasound-guided technique as originally described for TVA by Brück *et al.,* [270] and modified by Jacobson *et al.,* [271]. Briefly, a curvilinear transducer housed in a vaginal probe handle was introduced through the vulva and vestibule and placed with the transducer in the anterior fornix of the vagina. The ovary to be injected was grasped per rectum and pulled toward the transducer. When the ovary was visualized on the ultrasound screen, the needle was advanced through the cranial vaginal wall and into the ovary. The needle was

passed into the ovarian stroma, avoiding visible follicles, and the cell suspension was gently expressed as the needle was withdrawn from the ovary. This procedure was performed in 4 different locations per ovary. After both ovaries were injected, the mares received 500 mg flunixin meglumine and 6.6 mg/kg gentamicin IV, and 22,000 U/kg penicillin G procaine intramuscularly (IM).

Aspiration of Follicles for Oocyte Recovery

Ultrasound-guided TVA of all immature follicles ≥ 8 mm in diameter was performed on both mares every 14 days after MSC injection as described above for intra-ovarian injection, but with the modification that when the ovary was visualized on the ultrasound screen, a 12-G x 60-cm double-lumen oocyte aspiration needle (Cook Veterinary Products, New Buffalo, MI) was advanced through the cranial vaginal wall and into the ovary. Each visible follicle was aspirated and flushed 6 times with M199 Hank's salts with 25 mM HEPES (GIBCO) containing 0.4% FBS (GIBCO), 8 IU/ml heparin (Sigma Aldrich) and 25 μg/ml gentamicin (GIBCO). After TVA was completed, each mare was administered 500 mg flunixin meglumine IV.

Recovered flushed media and oocytes were filtered through an embryo filter (EmCon filter, Immuno Systems, Inc., Spring Valley, WI) and oocytes were located using a dissection microscope.

Assessment of Follicle Number

Every follicle ≥ 8 mm diameter visible on ultrasonography was aspirated by TVA. All the TVAs were performed by the same team; ovaries were manipulated by the same operator while a second operator manipulated the needle. The follicle numbers were determined from the count of aspirated follicles of both ovaries.

In Vitro Maturation and Intracytoplasmic Sperm Injection of Recovered Oocytes

Recovered oocytes were held overnight in EH holding medium (40% M199 Earle's salts (GIBCO), 40% M199 with Hanks' salts, and 20% FBS) at room temperature as previously described by Choi *et al.,* [272]. After overnight holding, oocytes were transferred to maturation medium (M199 with Earle's salts, 5 mU/ml FSH (Sioux Biochemicals, Sioux Center, IA), 10% FBS and 25 μg/ml gentamicin) for 24-30 h before ICSI. Oocytes were cultured in droplets at a ratio of 10 μl medium per oocyte, under light mineral oil (Sage, Origio; Knardrupvej, Denmark.) at 38.2 °C in a humidified atmosphere of 5% CO_2 in air. After the maturation period, oocytes were denuded of cumulus by pipetting in a solution of 0.05% hyaluronidase (Sigma Aldrich), and oocytes with an intact membrane and a polar body underwent ICSI.

Intracytoplasmic sperm injection was performed as previously described by Choi *et al.,* [273] under micromanipulation using a Piezo drill. After ICSI, oocytes were held in post-ICSI holding medium (CZB-H [274] or M199/Earle salts with 10% FBS) for 2 h at 38.2 °C in 5% CO_2 in air. After the post-injection holding period, presumptive zygotes were cultured in a commercial human embryo culture medium (GB; Global medium,

LifeGlobal, Guilford, CT) supplemented with 10% FBS [273] in microdroplets under oil (1 µl of medium/embryo). The culture environment was 6% CO_2, 5% O_2 and 89% N_2 at 38.2 °C. Medium change and cleavage examination were conducted at Day 5, and only cleaved embryos were cultured further. Medium was changed to GB with 20 mM added glucose at Day 5. Embryos were checked daily from Day 7 to Day 10 post-ICSI for blastocyst development as evidenced by the formation of a presumptive trophoblast layer immediately inside the zona pellucida and decreased density centrally. As a control for the in vitro maturation and ICSI procedures, an ICSI-control replicate was performed concurrently with a replicate of oocytes from MSC-injected mares, at least once every two weeks.

Ovariectomy and Ovarian Tissue Processing

Seven months after the second injection, the ovaries of the mares were surgically removed. The mares were sedated by IV administration of 250 mg acepromazine, 0.005-0.01 mg/kg detomidine, and 10 mg butorphanol. Immediately prior to surgery, each mare received 20 mg/kg ampicillin, 6.6 mg/kg gentamicin, and 500 mg flunixin meglumine IV, and 1 ml of tetanus toxoid vaccine IM.

Ovariectomies were performed via colpotomy as described by Slone [275]. Briefly, the tail of the mares was wrapped and secured, the rectum was evacuated of feces, and the perineal area was aseptically prepared. The vagina was distended with air and a blind stab incision was made in the right craniodorsal vaginal wall using the tip of a #10 scalpel blade. The incision was digitally enlarged and blunt scissors were used to

thrust through the peritoneum; the incision was enlarged enough for the entire hand to enter the peritoneal cavity. The ovarian pedicle was identified and anesthetized by holding gauze soaked with 2% lidocaine around the pedicle for 3 min. The gauze was secured with umbilical tape to prevent loss in the peritoneal cavity. The ovary was removed with an écraseur (Jorgensen Laboratories, Loveland, CO) and the opposite ovary was then anesthetized and removed in the same way through the same incision. Administration of penicillin G procaine (22,000 IU/kg, IM), gentamicin (6.6 mg/kg, IV), and flunixin meglumine (500 mg, IV) was continued for 5 days, and 10 mg of butorphanol was administered as needed if the mare showed signs of pain such as elevated heart or respiratory rates, agitation, or lack of appetite.

After removal, the ovaries were examined for gross pathology and each ovary underwent sagittal bisection. A scalpel blade was used to dissect 15 x 15 x 1 mm fragments from different sections of the ovary, which were placed in Bouin's solution at room temperature, and after 24 h were placed in 70% ethanol until histological processing. The ovarian fragments were embedded in paraffin and cut into 7-µm thickness sections which were stained with periodic acid-Schiff (PAS) and hematoxylin (H&E) [276]. Four slides from each ovary of each mare were submitted to the Texas A&M Veterinary Medical Diagnostic Laboratory (TVMDL) for histopathological analysis. Four additional slides from each ovary of each mare were examined under a fluorescent microscope for the presence of QDs.

Additional 2 x 2 mm fragments were obtained from each ovary of the AL mare and were frozen at -20 °C. Ovarian tissue from the AL mare, as well as hair samples

from the AL and SF mares, were submitted to the Veterinary Genetics Laboratory at the University of California for genomic microsatellite profiling and mitochondrial genotype analysis to assess genomic microsatellite identification markers and sequence of the mitochondrial D-loop hypervariable region, to detect genomic or mitrochondrial chimerism indicating the presence of the transferred allogeneic cells (cells from mare SF).

Statistical Analysis

Differences in number of follicles for MSC-injected and control mares among the treatment periods were determined using Bayesian modeling in WinBUGS 1.4.3. The follicle count for each mare was modeled as a Poisson distribution. The Poisson parameters were modeled as a function of the expected follicle count, a mare-specific random effect, and a treatment effect. The one-week period before the first injection and the 8-week period (4 TVAs) before the second injection were considered the "pre-treatment" period; the 4-week period following MSC-injections was considered the "treatment" period; and, the 10-week (5 TVAs) and 6-week (3 TVAs) periods following the first and second injections, respectively, was considered the "post-treatment" period. The increase (or decrease) in follicles was compared in the MSC-injected mares between pre-treatment, treatment, and post-treatment periods, and in control mares during the concurrent times.

The oocyte recovery rate (oocytes recovered per follicle aspirated on TVA), proportions of oocytes reaching metaphase II in culture, and the proportion of oocytes

developing to blastocyst after ICSI were compared among the Pre-treatment, Treatment and Post-treatment periods within mare group (MSC-injected or control mares) using Chi-square analysis, with Fisher's exact test used when a value < 5 was expected for any parameter. Significance was defined as $P < 0.05$.

RESULTS

Mare Health and Ovarian Status

Intra-ovarian injections of autologous or allogeneic MSCs were not associated with any observed signs of discomfort or systemic illness in the mares. Temperature, pulse and respiration rates were within normal limits for the 7-day period in which they were evaluated after injection. Both mares continued to appear bright, alert and responsive, and in good health for the 12 months after the first injection (7 months after the second injection) until ovariectomy.

Examination of the ovaries of the mares, removed after two MSC injections into each ovary, showed no gross pathology. Histopathologic examination revealed infiltration of the lining of some degenerating follicles by neutrophils and lymphocytes interpreted by the pathologist as mild to moderate folliculitis and considered to be of no clinical significance, in both ovaries of both mares. It was not possible to determine if the inflammatory changes were the results of normal follicle atresia or a result of ovarian puncture for TVA or MSC injection.

There were no QDs detected in the ovarian sections examined (4 sections per ovary per mare). Genetic analysis of tissue from the AL mare revealed microsatellite ID and mitochondrial genotype for only this mare (no alleles present from the MSC donor).

Colony-Forming Assay, Chondrogenic Differentiation and Phenotypic Analysis

The MSCs isolated and used for intra-ovarian injections formed 89 colonies per thousand original bone marrow aspirate cells. The MSCs showed evidence of differentiation to a chondrogenic cell lineage when pelleted and cultured in appropriate medium, as seen by the histological presence of round chondrocytes embedded in extracellular matrix (Figure 3.1). Immunophenotypic analysis of MSCs at P3 by flow cytometry revealed that MSCs had a high expression (99%) of CD29 and CD90 markers, low expression (3 to 4%) of CD44 and CD45 markers, and mixed expression of MHC II (Figure 3.2), consistent with results from De Schauwer [203] and Schnabel [204].

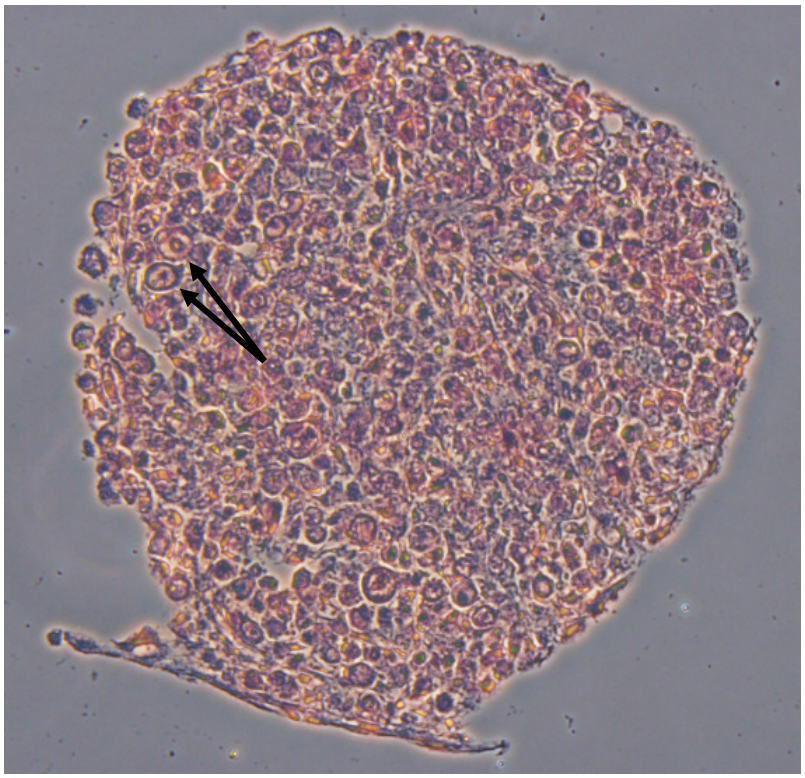

Figure 3.1 Chondrogenic pellet after MSC differentiation. Overview of the entire pellet section shows the typical round morphology of chondrocytes (arrow heads) embedded in abundant extracellular matrix. Stained with H&E. Original magnification 100 X.

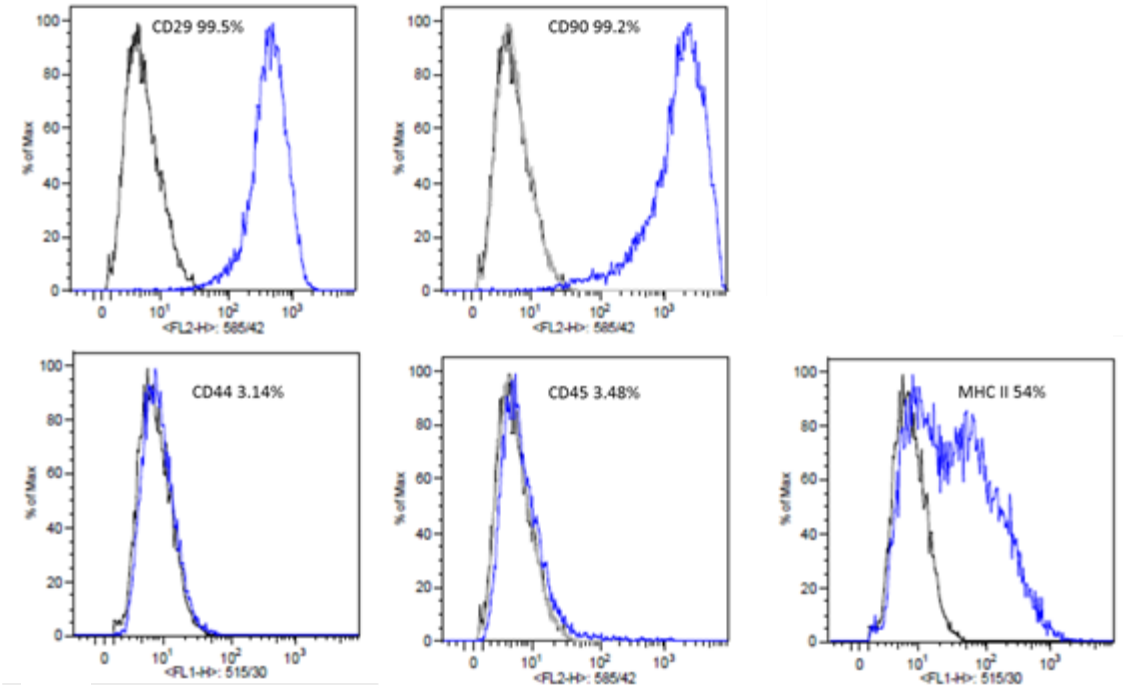

Figure 3.2 Flowcytometric histogram analyses of cell surface markers in P3 BM-MSCs. The black lines represent negative control staining and the blue lines represent cell surface marker staining of MSCs. The percentage of positive cells is indicated in each histogram.

Follicle Numbers

There was a marked increase in the number of ovarian follicles identified in MSC-injected mares in the 4 weeks after MSC injection for both injections (Figure 3.3). There was a significantly higher follicle number during the Treatment period than for these mares in either the Pre-treatment or Post-treatment periods ($P < 0.0001$ and $P = 0.0025$, respectively; Figure 3.4). The number of follicles in the Post-treatment period was also significantly higher than in the Pre-treatment period ($P = 0.003$). Prior to injection the subject mares had a mean of 6 follicles (4.25, 8.5; lower 2.5% and upper 97.5% limits, respectively) per two ovaries. This increased to 15.25 (11, 19.5) during the

Treatment period. The mean number of follicles during the Post-treatment period was 10 (7.5, 12). In the Control mares, the mean number of follicles during the period concurrent with the Treatment period was 10.6 (8, 13) which was not significantly different from the number of follicles in the control mares during the periods concurrent with the Pre-treatment (11.24 (6.25, 15); P = 0.81) or Post-treatment periods (12.56 (8, 13); P = 0.67).

Oocyte Recovery, Maturation and Blastocyst Formation

Over the period of the study, 16 TVA sessions were performed in the treated mares. There was no difference in oocyte recovery rate between the MSC-injected and Control mares in any period (Table 3.1). The overall oocyte maturation rate was higher in control mares (61.2%, 85/139) than in MSC-injected mares (47.1%, 64/136; P = 0.02), and the overall blastocyst rate tended to be higher for Control (32.8%, 21/64) than for MSC-injected (18.8%, 12/64) mares. However, there were no significant differences in oocyte recovery, maturation or blastocyst rates in either MSC-injected or Control mares among periods (Table 3.1).

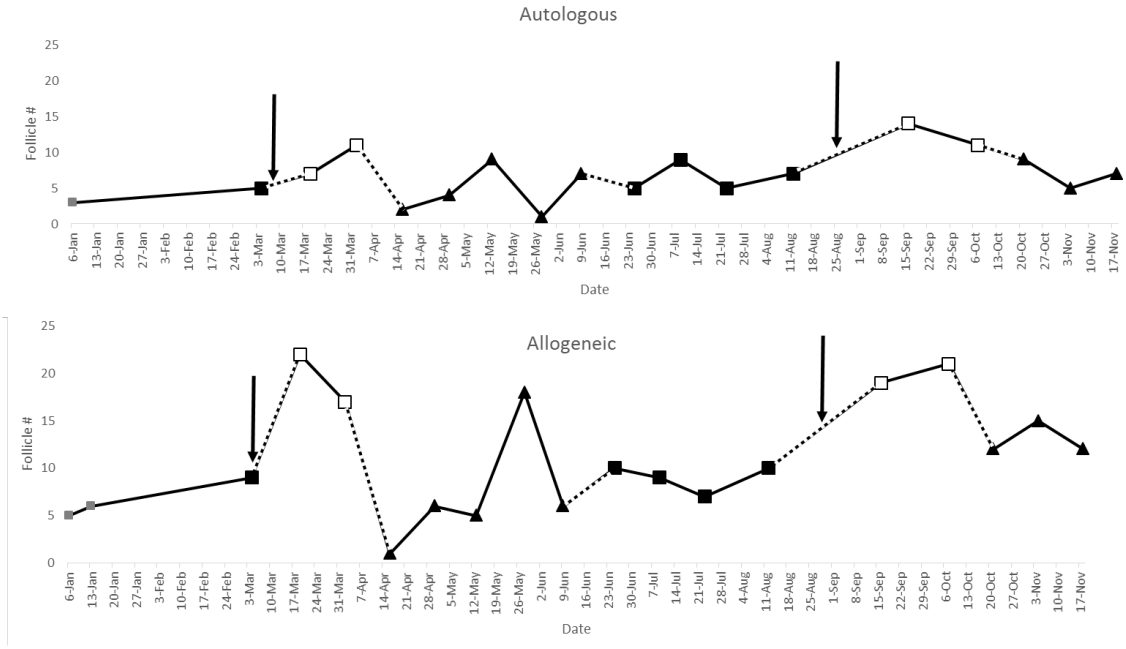

Figure 3.3 Total follicle numbers of autologous (SF) and allogeneic (AL) mares throughout the study. Follicle numbers were those recorded on performing TVA. Arrows: dates on which MSC injections were performed. Pre-Treatment: filled square markers; Treatment: open square markers; Post-treatment: triangular markers. Gray squares denote follicle numbers determined prior to the onset of the study that were not included in the analysis.

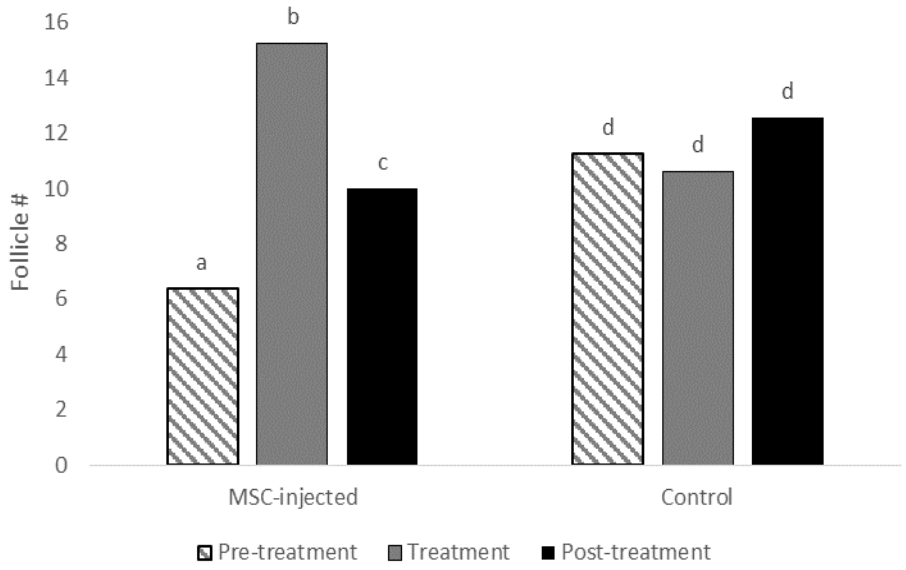

Figure 3.4 Number of follicles in MSC-injected mares and control mares over the period of the study. Pre-treatment period: the 1 week preceding the date of the first injection and the 4 weeks preceding the date of the second MSC injection in treatment mares; Treatment: the 4 weeks following MSC injection to treatment mares; Post-treatment: the 5 weeks after the first injection and the 3 weeks after the second injection. a, b, c: within MSC-injected mares, values with different superscripts differ significantly ($P < 0.01$). Within control mares, there was no significant effect of period ($P > 0.05$).

Table 3.1 Rates of oocyte recovery, *in vitro* maturation to metaphase II (MII), and of blastocyst formation after ICSI of MSC-injected and control mares.

	MSC-injected			Control		
	Oocyte recovery	**Maturation to MII**	**Blastocyst**	**Oocyte recovery**	**Maturation to MII**	**Blastocyst**
Pre-treatment	47.4% (37/78)[a]	48.6% (18/37)[a]	16.7% (3/18)[a]	43.2% (41/95)[b]	48.4% (15/31)[b]	
Treatment	46.7% (57/122)[a]	45.6% (26/57)[a]	23.1% (6/26)[a]	51.5% (69/134)[b]	65.2% (45/69)[b]	34.9% (15/39)[b]
Post-treatment	35.3% (42/119)[a]	47.6% (20/42)[a]	15% (3/20)[a]	42.9% (102/238)[b]	64.1% (25/39)[b]	28.6% (6/21)[b]

There was no ICSI performed in control mares during the pre-treatment period. There were no significant differences in oocyte recovery, maturation or blastocyst rates in either MSC-injected or control mares among periods ($P > 0.05$). In control mares, missing values represent oocytes used for separate projects.

DISCUSSION

The results from this study suggest that intra-ovarian injections of allogeneic and autologous MSCs are safe to perform in mares, as no detrimental effects were seen in mare health or ovarian status in injected mares. The mild folliculitis found on histological examination could have been the result of the repeated TVAs (the injected mares underwent 16 TVAs in the yr before ovariectomy) or of the MSC injections.

Although the main purpose for this study was to evaluate the feasibility of intra-ovarian injection of MSCs in mares, the apparent increase in follicle numbers in the two MSC-injected mares in the 4 weeks after injection led us to analyze whether this effect was significant. Because this analysis was not planned *a priori*, the numbers of evaluations in the different periods are not uniform.

Injections of MSCs in other species have been associated with an improvement in ovarian function, as determined by an increase in follicle number and fecundity, in females with ovaries compromised by chemotherapy [8-11, 262, 263]. In the present study there was a significant increase in follicle numbers in treated mares when evaluated 14 and 28 days after MSC injection. Because this increase in follicle numbers was seen so soon after MSC injection, it is unlikely that the MSCs are differentiating into oocytes or follicle components. Instead, it is possible that MSCs stimulate the growth of large secondary follicles or antral (tertiary) follicles already present within the ovary, resulting in an increase in numbers of antral follicles identifiable on ultrasonography. Oocyte recovery, maturation and blastocyst rates remained unchanged in the treated mares following MSC injections. These data indicate that intra-ovarian injection of BM-MSCs does not affect the developmental competence of oocytes.

The MSCs used for the intra-ovarian injections in the present study were obtained from a 7 yr old mare, and characterized by their adherence to plastic, ability to differentiate into a chondrogenic lineage, and specific cell-surface markers. Although equine MSCs have been shown to express CD44 (a hyaluronate receptor involved in cell-cell interactions, cell adhesion and migration [277]), the MSCs used in the present study did not exhibit this marker. However, proper identification of equine MSCs remains a challenge due to the lack of suitable antibodies. Although a panel of markers has been proposed and is routinely used for the proper identification of equine MSCs, it has been suggested that expression of CD markers can be influenced by cell culture conditions and isolation methods [203, 204]. Thus, the cells' ability to differentiate into

different mesenchymal tissue types, as shown by chondrogenic differentiation in this study, has been suggested to be the best method to characterize MSCs [278, 279].

The lack of chimerism detected in the ovaries of the AL mare 7 months after the second injection suggests that the injected MSCs did not persist or multiply within the ovary. However, it is possible that MSCs were present in the ovarian tissue but at levels that were below the threshold that could be detected by the analyses run. We evaluated both microsatellite ID markers and mitochondrial genotype in the AL mare, as it has been suggested that mitochondria from injected MSCs may be transferred to host cells [199]. The analyses were negative for both DNA species, thus there was no evidence of chimerism in the ovaries. However, the possibility exists that MSC-derived cells were present in the ovaries, just not in the ovarian sections evaluated.

We also attempted to determine if MSCs colonize the ovary by labeling the cells with fluorescent nanoparticles (QDs) and then identifying cells containing these particles after ovary removal. However, examination of ovarian sections post-ovariectomy did not reveal the presence of QDs. It is not possible to determine where the QD-labeled MSCs were injected, so the possibility exists that QDs were present and localized only to the area of injection, and were not in the examined ovarian sections. Although equine BM-MSCs have been shown to migrate *in vitro*, these cells migrate at a slower rate than do adipose-derived MSCs [280]. *In vivo* it has been shown that equine BM-MSCs remain close to their site of injection in artificially-induced tendon lesions [281]. It is possible that QDs would have been found if the ovaries had been removed sooner after the MSC injection; however, to the best of our knowledge, there is no information on how long

QDs persist in equine MSCs *in vitro* or *in vivo*. To investigate this, we conducted a study (see Chapter V) to determine the duration for which the QDs were detectable in equine MSCs that were either proliferating or not proliferating in culture.

Currently, little information is available on the effect of MSCs in the aging ovary [12, 13]. If validated in a larger experiment, the information generated in this study could have potential implications in both human and equine reproduction. Based on the results of the present study, a more comprehensive study involving a larger sample size that included both young and old mares was performed and is described in Chapter VII of this dissertation.

CHAPTER IV

EFFECT OF DIFFERENT POST-THAW CONDITIONS ON EQUINE MESENCHYMAL STEM CELL VIABILITY

INTRODUCTION

Adult mesenchymal stem cells (MSCs) are increasingly being used in regenerative therapies because of their capacity to repair tissue damaged due to injury and disease. In horses, bone marrow-derived mesenchymal stem cells (BM-MSCs) have been shown to enhance early chondrogenesis in articular defects [180], as well as to improve the biomechanical, morphological and compositional parameters in age-related [181] and experimentally-induced [182] tendon injuries. In other species, MSCs have been successfully used in models of lung injury [268], kidney disease [183], diabetes [184], myocardial infarction [269], and neurological disorders [189]. Mesenchymal stem cells can be grown *in vitro* to high numbers and cryopreserved for long term storage [207, 282, 283]. Cryopreservation allows elective storage of cells that may be transplanted to patients at a later point in a course of treatment.

There is no consensus protocol for preserving MSCs. At low temperatures, damage can occur because of the formation of intracellular ice which can lead to cell death. Avoiding formation of intracellular ice is therefore essential for successful cryopreservation. Most cryopreservation procedures use a penetrating cryoprotectant such as dimethyl sulfoxide (DMSO) and a source of plasma protein, cool at a defined

rate, and store at cryogenic temperatures (below -150 ºC) using mechanical or liquid-nitrogen refrigerators [205].

For clinical applications, MSCs must also remain viable after thawing. However, after thawing, a decrease in MSC viability over time has been reported, with the rate of viability decrease varying between different post-thaw holding temperatures and holding media [211, 282, 284]. The rate of dilution during thawing also affects MSC viability [210, 212] as osmotic injury occurs after rapid addition of dilution medium [210].

For the intra-ovarian injections performed in the studies described in this dissertation, equine MSCs were cryopreserved in 95% autologous (to the horse being injected) serum and 5% DMSO prior to use. The cells were injected immediately after thawing, then placed on ice and viability was assessed when the remaining cells in the cryovial were taken back to the laboratory. Because of the time needed for mare handling and ovarian injection, assessment of cell viability was delayed for up to 60 min, and it is possible that delay to assessment and prolonged exposure to DMSO affected the observed viability, in comparison to the viability at the time of injection. This study was conducted to evaluate the effects of time and post-thaw conditions on MSC viability.

MATERIALS AND METHODS

One cryovial of previously frozen MSCs (10 x 10^6 cells) was thawed in a 37 °C water bath for 3 min. The cells were then resuspended and the cryovial was placed in an ice bath at 4 °C. The cell suspension in the cryovial was divided into 4 treatment groups: DMSO) 400 µl of cell suspension remaining in the freezing medium (5% DMSO in

serum); Rinse) 400 µl of cell suspension rinsed to remove DMSO (see below); Dil1) 50 µl of cell suspension mixed with 950 µl serum to rapidly dilute DMSO; Dil2) 50 µl of cell suspension mixed with 50 µl serum and after 5 min another 900 µl serum to dilute DMSO in a step-wise manner. Cell viability for each group was assessed immediately and at 15, 30, 45, 60, and 120 min. The cells and solutions used were maintained on ice (~ 4 °C) between time points and 6 replicates were performed.

To rinse the DMSO out in the Rinse group, the 400 µl of cell suspension was placed in a 50-ml conical tube and 400 µl of Dulbecco's phosphate-buffered saline (DPBS; Life Technologies) was added; after 5 min, additional DPBS was added to the 50-ml conical tube to q.s. to 20 ml. The cells were resuspended, then the suspension was centrifuged at 300 x g for 5 min. The supernatant was aspirated and the cells were resuspended in 300 µl DBPS.

Assessment of Viability

Viability of MSCs was assessed by staining a 100-µl sample of cells from each treatment group at each time point using propidium iodide (PI; 1.35 mg/ml) and fluorescein diacetate (FDA; 67.57 mg/ml) in DPBS, as described in Chapter III. The live (green) and dead (red nucleus) cells were visualized by fluorescence microscopy and counted. A total of 10 squares (corner and middle squares of each counting grid) were counted per sample.

Statistical Analysis

Data were analyzed by a two-way (factorial) ANOVA model using JMP Pro ver. 11 for Windows (SAS Institute Inc, Cary, NC). Data were log-transformed prior to statistical analyses to minimize interactions between means and variances. Treatment, time, and treatment x time interactions were included in the model. Multiple comparisons were performed using the post-hoc Tukey's HSD method to determine differences in viability among all treatments and time points. Differences were considered significant when $P < 0.05$.

RESULTS

There was no significant effect of dilution treatment on cell viability at any of the time points evaluated. All treatments behaved similarly over time, as there was no treatment x time interaction ($P = 0.7735$). A trend toward a decrease in viability over time was observed within all four treatment groups; however, this decrease was significant only for the DMSO group (Figure 4.1); Post-hoc Tukey's HSD tests showed that the viability at 120 min in the DMSO group was significantly lower than the viability in the DMSO group at all other time points (Appendix Table A-1).

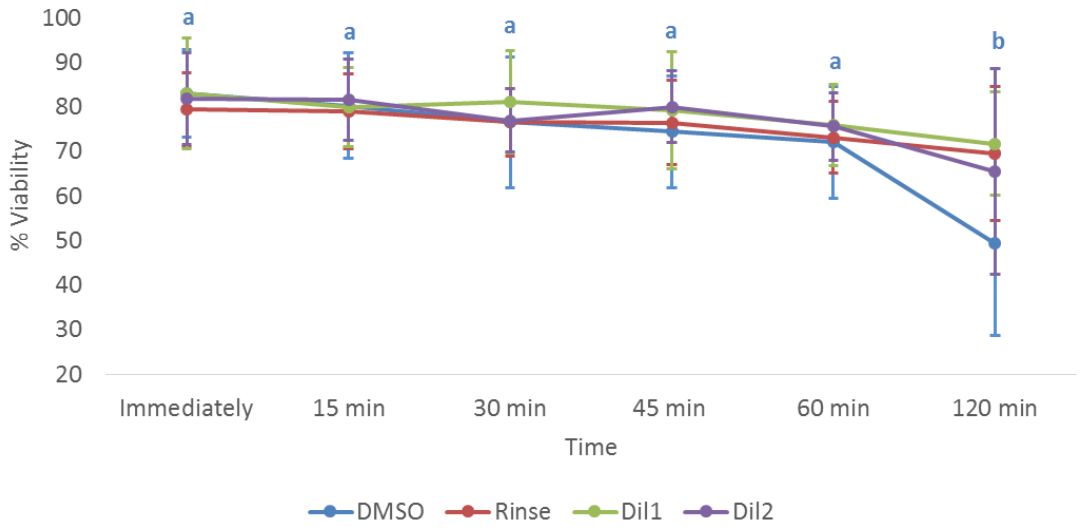

Figure 4.1 MSC viability measured for each treatment group at each time point throughout the trial. Values represent the mean ± s.d. for six independent replicates from different animals. a,b: within the DMSO treatment, values with different superscripts differ significantly ($P < 0.05$); all other values are not significantly different.

DISCUSSION

To use MSCs effectively for cellular therapy in regenerative medicine, it is essential to transport, hold, and store MSCs in optimal conditions to maintain their viability, and to be able to assess the viability of the cells that are used. In this study, we analyzed the viability of frozen-thawed MSCs in four different conditions over time. Our results indicate that viability of MSCs held on ice decreases slowly over time up to 60 min post-thaw in every medium tested; after which there is a rapid decrease in viability in cells that remain in 5% DMSO. This is in agreement with other studies that have shown a decrease in MSC viability over time after thawing [211, 282, 284]. Thus, if cells remain in 5% DMSO, it is best to evaluate viability prior to 60 min post-thawing to obtain an accurate measure. If the DMSO is removed from the cells or if the DMSO is

diluted, MSCs can be held on ice without a significant decrease in viability for up to 120 min post-thawing. Although it has been reported that osmotic injury from rapid addition of dilution medium can affect MSC viability [210], we found no significant differences in MSC viability between samples in which DMSO was diluted rapidly and those diluted in a step-wise manner, using equine serum.

In conclusion, following freeze-thaw, MSCs held on ice demonstrate a slow decrease in viability, which is more apparent if cells remain in DMSO. Rinsing cells to remove DMSO or adding serum, either rapidly or in a step-wise manner, to dilute DMSO can be used to hold MSCs with no significant effect on viability, for up to 120 min. Thus, if cells are injected and it is anticipated that more than 60 min will elapse before the remaining cells can be assessed for viability, it would be advisable to add previously frozen/thawed serum to the remaining cells and to maintain the cells on ice (at ~ 4 ºC) until viability can be determined. It is possible that viability, as shown in the present study, does not correlate directly with functional measures of stem cell potency. Therefore, inclusion of other analyses such as cell-surface markers and differentiation assays may have yielded significant differences among the different conditions evaluated in the present study.

CHAPTER V

PERSISTENCE OF QUANTUM DOTS IN DIVIDING AND NON-DIVIDING EQUINE MESENCHYMAL STEM CELLS

INTRODUCTION

Quantum dots (QDs) are fluorescent nanoparticles that can be used as markers for long-term *in vitro* and *in vivo* cell imaging applications [218, 285]. The quantum dot product, Qtracker® (ThermoFisher Scientific; Invitrogen; Carlsbad, CA) is frequently used for stem cell labeling [218] because it is resistant to metabolic degradation [285], has minimal cytotoxic effects, and does not interfere with cell proliferation [217]. Visualization of QDs in labeled rat mesenchymal stem cells (MSCs) is possible in cardiomyocyte co-cultures for up to seven days [217], and QDs have been demonstrated to be present in canine hearts 8 weeks following delivery of QD-labeled human MSCs [220].

Stem cell therapy is commonly used clinically in horses but little research has been done on the persistence or function of MSCs after injection in this species. In our study on intra-ovarian injection of bone marrow-derived MSCs (BM-MSCs; experiment detailed in Chapter III), to help determine if injected MSCs colonize the equine ovary, and, if so, in which areas, the MSCs used were labeled with QDs. However, to the best of our knowledge, there is no information available on the behavior of QDs in dividing or in differentiated equine BM-MSCs.

To determine this, we conducted an *in vitro* study on QD persistence, i.e., the ability to identify QDs in MSCs over time. Live MSCs were labeled with QDs and the persistence of QDs in both dividing cells (in cell culture conditions) and non-dividing cells (in chondrogenic pellets) was evaluated. We hypothesized that dilution of QDs as a result of cell division would lead to decreased detection of QD-labeled MSCs as cells proliferated in culture, whereas they would persist in non-dividing cells. Additionally, we evaluated the effect of QDs on the trilineage differentiation potential and the immunophenotypic markers of MSCs by inducing QD-labeled MSCs to differentiate into adipocytes, chondrocytes and osteocytes and performing flow-cytometric immunophenotypic analysis on QD-labeled MSCs.

MATERIALS AND METHODS

Previously-frozen BM-MSCs were thawed and re-plated in standard MSC culture medium consisting of Dulbecco's modified Eagle's medium with 1 g/l glucose (DMEM; Sigma-Aldrich, St. Louis, MO) supplemented with 10% fetal bovine serum (FBS; Sigma-Aldrich), 1 ng/ml basic fibroblast growth factor (bFGF; Sigma-Aldrich) and 1% antibiotic-antimycotic (10,000 U penicillin, 10 mg streptomycin, 25 µg amphotericin B/ml; GIBCO; Invitrogen). The cells were plated at a density of 5-8 x 10^3 cells/cm^2 and cultured at 37 °C in a humidified atmosphere of 5% CO_2. Once the cells reached 70% confluence, they were trypsinized and divided into two groups, control and QD-labeled.

Cells in the QD treatment were labeled with QDs using the Qtracker® 625 Cell Labeling Kit (ThermoFisher Scientific) following the directions provided by the

manufacturer. Briefly, 2 µl of a 10-nM QD-labeling solution were added to 0.2 µl of medium containing 1 x 10^6 cells in suspension. The cells were incubated at 37 °C for 60 min, after which they were washed twice with serum-free medium consisting of DMEM supplemented with antibiotics and a culture supplement providing 1 mg/ml insulin, 0.55 mg/ml transferrin, and 0.5 µg/ml selenium (ITS; BD Biosciences, Sparks, MD). The cells in both Control and QD groups were then placed in either standard monolayer culture conditions (dividing cells) or were induced to differentiate into chondrogenic pellets (non-dividing). Three replicates were performed.

In a parallel study, control and QD-labeled cells were induced to differentiate into adipocytes, chondrocytes and osteocytes, then stained and evaluated for evidence of differentiation. Furthermore, QD-labeled cells after 4 passages in proliferative culture were immunophenotyped by flow cytometry.

Monolayer Culture

Cells in the QD treatment were imaged using a fluorescent inverted microscope (excitation 405-585 nm) 1 h after labeling to ensure uptake of QDs, as evidenced by the presence of red fluorescent dots in the cytoplasm of the cells. QD-labeled and control MSCs were plated in cell culture flasks in standard MSC culture medium and cultured at 37 °C in a humidified atmosphere of 5% CO_2 in air. The cells within culture flasks were evaluated every other day until QDs were no longer detected. Multiple flasks were prepared and each flask was imaged only once, to eliminate the effect of photobleaching. The medium was replaced every other day and the flasks were passaged at 70-80%

confluence throughout the study. At every passage, the cell concentration was determined using a hemocytometer (as described in Chapter IV) and a sample of MSCs was cryopreserved in 95% autologous serum and 5% DMSO at a concentration of 10 x 10^6 cells/ml. Cryopreserved cells were later thawed and evaluated by flow cytometry to determine changes in mean fluorescence intensity (MFI; measures the mean fluorescence intensity of a population of cells) as well as the proportion of viable, labeled cells over time; viability was assessed by adding 5 µl of 7-aminoactinomycin (7-AAD; Biolegend, San Diego, CA) to the cell suspensions. This compound has a strong affinity for DNA but does not readily penetrate intact cell membranes; therefore, it can be used to determine cell viability because only cells with compromised membranes will stain with 7-AAD.

The proportion of cells showing QD-associated fluorescence was detected using a Beckman Coulter MoFlo Astrios high-speed cell sorter (Beckman Coulter, Brea, CA). The 405-nm laser and the 620/29 bandpass filter were used and the PMT voltage was set to 390 volts. Dead cells labeled with 7-AAD were detected using the 488-nm laser and the 664/22 bandpass filter; the PMT voltage was set to 575 volts. At least 20,000 live cell events were collected per sample.

Chondrogenic Differentiation

Induction of chondrogenic differentiation was performed as described in Chapter III. Multiple pellets were prepared and three pellets were removed from culture every two weeks for evaluation. Following removal of the pellets and cutting of chondrogenic

sections, the sections were stained with the nuclear dye 4',6-diamidino-2-phenylindole (DAPI) and imaged with a fluorescent microscope (Ex/Em 405-585/625 nm) to determine the presence of QDs. Additional sections were stained with Toluidine Blue to assess chondrogenic differentiation by identification of cartilaginous extracellular matrix, which stains purple (metachromasia), and fibrous tissue, which stains blue. To stain with Toluidine Blue, the chondrogenic sections were first deparaffinized by dipping them into xylene for 15 min, 100% ethanol for 10 min, 95% ethanol for 10 min, 80% ethanol for 5 min and then into deionized water. Toluidine Blue staining was accomplished by dipping the sections into Toluidine Blue solution for 5 min followed by rinsing with deionized water, 95% ethanol for 2 min, 100% ethanol for 2 min, and xylene for 4 min. Excess xylene was blotted off and a coverslip was applied while the specimen was still moist. Pictures of the sections were taken with a phase-contrast microscope immediately after the cover slip was applied.

Adipogenic Differentiation

To induce adipogenic differentiation, MSCs were seeded onto 10-cm plates at a density of 1000 cells/cm^2 in standard MSC culture medium. Once the cells reached 70% confluence, the medium was exchanged for adipogenic induction medium consisting of DMEM/F12 (VWR) supplemented with 3% FBS, 1% antibiotic-antimycotic, 5% rabbit serum (Life Technologies), 33 µM biotin (Sigma-Aldrich), 17 µM/l pantothenate (Sigma-Aldrich) , 1 µM/l insulin (Sigma-Aldrich), 1 µM/l dexamethasone, 225 µl isobutylmethylxanthine (Sigma-Aldrich) and 89 µl rosiglitazone and cultured for 72 h.

After 72 h the medium was exchanged for adipogenic maintenance media (adipogenic induction medium without isobutylmethylxanthine and rosiglitazone) for an additional 72 h. Induced cells were stained with Oil Red O (Sigma-Aldrich) to detect lipid droplets within the cells, which stain red. To stain with Oil Red O, the medium in induced plates was aspirated and the cells were rinsed with phosphate buffered saline. The cells were then fixed in the plates with 5 ml of 4% paraformaldehyde for 20 min at room temperature. After 20 min the plates were rinsed with distilled water and soaked with 5 ml of 60% isopropanol for 5 minutes at room temperature. After 5 min, the isopropanol was aspirated and each plate was stained with 5 ml of Oil Red O solution for 5 min at room temperature. The Oil Red O-stained plates were rinsed with distilled water and set out to dry. Pictures of each plate were taken under a phase contrast microscope within 2 h of staining.

Osteogenic Differentiation

To induce osteogenic differentiation, MSCs were seeded onto 10-cm plates at a density of 1000 cells/cm^2 in standard MSC culture medium. Once the cells reached 70% confluence, the medium was exchanged for osteogenic induction medium consisting of DMEM/F12 supplemented with 10% FBS, 1% antibiotic-antimycotic, 10 µM/l ß-glycerophosphate (Sigma-Aldrich), 20 nM/l dexamethasone, and 50 µg/ml L-ascorbic acid. The plates were maintained in culture for 21 days. After 21 days, the plates were stained with 2% Alizarin Red (Sigma-Aldrich) to identify the presence of calcified extracellular matrix and bone nodules, which stain red. To stain with Alizarin Red, the

induced cells were rinsed with phosphate buffered saline and fixed with 5 ml of 70% ethanol for 20 min at 4 °C. After 20 min the ethanol was aspirated from the plates and the plates were allowed to dry completely for 1 to 2 h. After drying, each plate was stained with 5 ml of 2% Alazarin Red solution for 10 min at room temperature. After 10 min the plates were rinsed with distilled water and set out to dry. Pictures of cells in each plate were taken under a phase-contrast microscope within 2 h of staining.

Immunophenotype Analysis by Flow Cytometry

Immunophenotype analysis was performed as described in Chapter III.

Statistical Analysis

Data were analyzed using JMP Pro ver. 11 for Windows (SAS Institute Inc, Cary, NC). Data were log-transformed prior to analyses to minimize interactions between means and variances. Paired t-tests were performed to determine differences in MFI between P1 and P2 and between P2 and P3. Differences were considered significant when $P < 0.05$.

RESULTS

Dividing MSCs

In dividing MSC cultures, flow-cytometric analysis showed a rapid decrease in the percentage of QD-labeled cells, as well as in the MFI, as passage number increased (Table 5.1). The initial MFI at P1 varied among trials, between 154 and 1796; however

the percentage of cells labeled with QDs at P1 was consistently high (between 98.1 and 99.9%). Both the proportion of labeled cells and the MFI dropped precipitously between P1 and P2, and again between P2 and P3. The proportion of labeled cells and the MFI then stayed at fairly consistent low levels for 2 to 5 more passages. For P2 and P3, the MFI measured by flow cytometry was less than the MFI expected due to dilution associated with cell division, calculated based on the MFI of the previous passage, the number of cells seeded and the number of cells present at confluence (Table 5.2). The time between passages and the number of cells present at each passage was similar for QD-labeled and control cells (Table 5.3), indicating that QD labeling did not cause increased cell death or reduced cell division.

Visual assessment of cell cultures under fluorescent microscopy supported the flow-cytometric results; the proportion of cells labeled with QDs as well as the number of QDs per cell decreased from P1, when an estimated 100% of the cells were labeled with QDs to P2 (estimated 50% of cells labeled with QDs) and continued to decrease rapidly thereafter (Figure 5.1).

Non-dividing MSCs

In contrast to the rapid decrease in fluorescence seen in dividing MSC cultures, non-dividing MSCs (chondrogenic pellets) remained labeled with QDs, without an apparent decrease in intensity on visual examination under fluorescence microscopy, for the duration of the study (up to 8 wk; Figure 5.2). Notably, while the majority of the

pellet retained QDs, the cells on the periphery of the pellet lost QD labeling within 2 weeks.

Table 5.1 Percentage of QD-labeled cells and measured MFI for cells in monolayer culture conditions.

	Cell line A		Cell line B		Cell line C		
P	**Labeled cells (%)**	**MFI**	**Labeled cells (%)**	**MFI**	**Labeled cells (%)**	**MFI**	**MFI Mean ± s.d.**
1	99.9	651.0	99.6	1796.0	98.1	156.0	867.7^{a} ± 847.2
2	51.5	31.6	78.4	83.9	82.0	38.0	51.2^{b} ± 28.5
3	11.0	4.4	20.1	5.4	24.4	2.9	4.2^{c} ± 1.3
4	2.1	4.4	5.8	4.9	8.5	2.2	3.8 ± 1.5
5	0.3	3.0	5.5	5.4	1.9	2.1	3.5 ± 1.7
6	0.1	4.7	13.0	6.9			5.8 ± 1.5
7	0.1	3.9					3.9

Cells from a different horse were used for each replicate. Within the Mean column, values with different superscripts differ significantly ($P < 0.05$).

Table 5.2 Expected MFI for cells in monolayer culture conditions.

	Cell line A			Cell line B			Cell line C		
P	**Initial # of cells**	**Final # of cells**	**Exp MFI**	**Initial # of cells**	**Final # of cells**	**Exp MFI**	**Initial # of cells**	**Final # of cells**	**Exp MFI**
1	$1.02x10^7$		651.0	$1.02x10^7$		1796.0	$5.40x10^6$		156.0
2	$1.02x10^7$	$2.04x10^7$	325.5	$1.02x10^7$	$5.76x10^7$	318.0	$5.40x10^6$	$1.23x10^7$	68.5
3	$1.10x10^7$	$3.03x10^7$	11.5	$1.15x10^7$	$4.08x10^7$	23.6	$4.30x10^6$	$5.60x10^6$	29.2
4	$1.98x10^7$	$4.28x10^7$	2.1	$8.75x10^6$	$2.07x10^7$	2.3	$4.60x10^6$	$2.01x10^7$	0.7
5	$4.38x10^6$	$7.40x10^6$	2.6	$8.75x10^6$	$2.28x10^7$	1.9	$5.00x10^6$	$8.60x10^6$	1.3
6	$1.55x10^6$	$5.50x10^6$	0.8	$4.38x10^6$	$3.20x10^5$	74.2			
7	$4.75x10^6$	$6.60x10^6$	3.4						

Cells from a different horse were used for each replicate. Expected (Exp) MFI was calculated based on the measured MFI of the previous passage (Table 5.1), the number of cells seeded (initial # of cells) and the number of cells present when the cells were passaged (final # of cells). Exp MFI was higher than the MFI measured by flow cytometry for passages 2 and 3 (Table 5.1).

Table 5.3 Number of cells and time between passages for control and QD-labeled cells.

	Cell line A			Cell line B			Cell line C		
P	**Control**	**QD-labeled**	**CT**	**Control**	**QD-labeled**	**CT**	**Control**	**QD-labeled**	**CT**
1	$1.01x10^7$	$1.02x10^7$		$1.00x10^7$	$1.02x10^7$		$5.20x10^6$	$5.40x10^6$	
2	$1.98x10^7$	$2.04x10^7$	4	$5.74x10^7$	$5.76x10^7$	6	$1.25x10^7$	$1.23x10^7$	4
3	$2.98x10^7$	$3.03x10^7$	4	$4.10x10^7$	$4.08x10^7$	4	$5.40x10^6$	$5.60x10^6$	2
4	$4.20x10^7$	$4.28x10^7$	4	$2.05x10^7$	$2.07x10^7$	4	$2.00x10^7$	$2.01x10^7$	4
5	$7.40x10^6$	$7.40x10^6$	5	$2.25x10^7$	$2.28x10^7$	4	$8.40x10^6$	$8.60x10^6$	4
6	$5.30x10^6$	$5.50x10^6$	4	$3.00x10^5$	$3.20x10^5$	3	$1.96x10^7$	$1.95x10^7$	4
7	$6.50x10^6$	$6.60x10^6$	6						

The time between passages (CT- culture time in days) and the number of cells present at each passage was similar for QD-labeled and control cells. Cells from a different horse were used for each replicate.

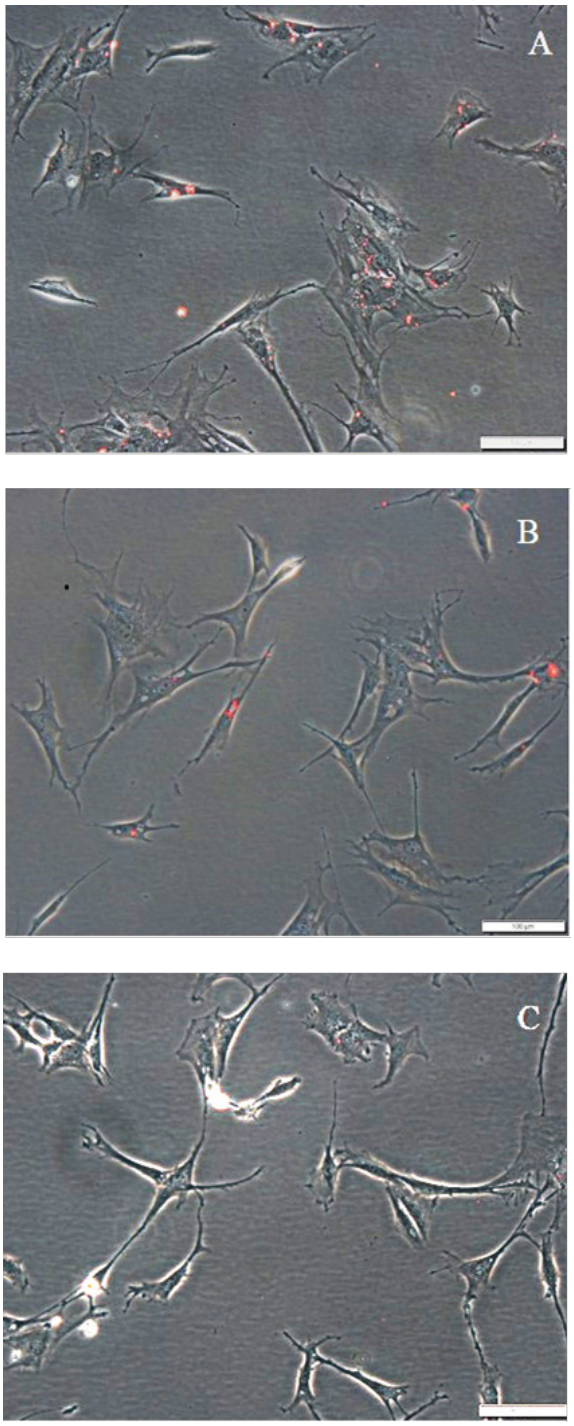

Figure 5.1 Dividing QD-labeled MSC cultures. Overlays of phase contrast and fluorescent images showing a rapid decrease in QD-labeled cells (Cell line A); QDs appear as red dots. A) 24 hr post-QD label; B) 3 d (P2) post-QD label; C) 8 d (P5) post-QD label. Original magnification 200 X, scale bar = 100 µm.

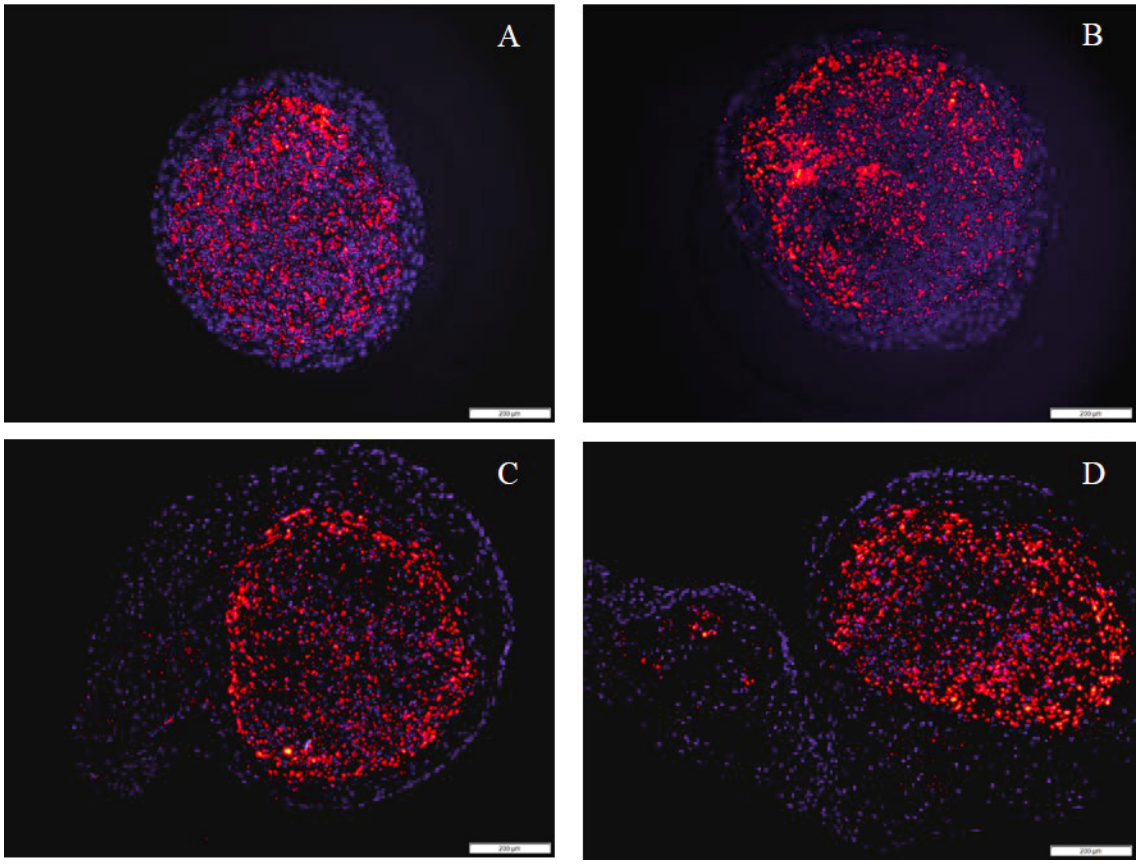

Figure 5.2 Non-dividing QD-labeled MSCs (chondrogenic pellets). Overlays of DAPI and fluorescent images showing persistence of QDs (red dots) in chondrogenic pellets. A) 2 wk post QD-label; B) 4 wk post-QD label; C) 6 wk post-QD label; D) 8 wk post-QD label. Original magnification 100 X, scale bar = 200 μm.

Adipogenic, Osteogenic and Chondrogenic Differentiation

Labeling MSCs with QDs did not affect the cells' ability to undergo trilineage differentiation into chondrogenic, adipogenic and osteogenic lineages, as assessed by visualizing positive staining for Toluidine Blue, Oil Red O, and Alizarin Red, respectively (Figure 5.3). QD-labeled cells harvested at the standard time allotted for differentiation into chondrocytes, adipocytes and osteocytes (21, 3, and 21 days, respectively), showed characteristic attributes of each type of cell, including round pellet

shape and extensive extracellular matrix in chondrogenic pellets, intracellular lipid droplets in adipocytes, and extracellular calcium deposition in osteocytes.

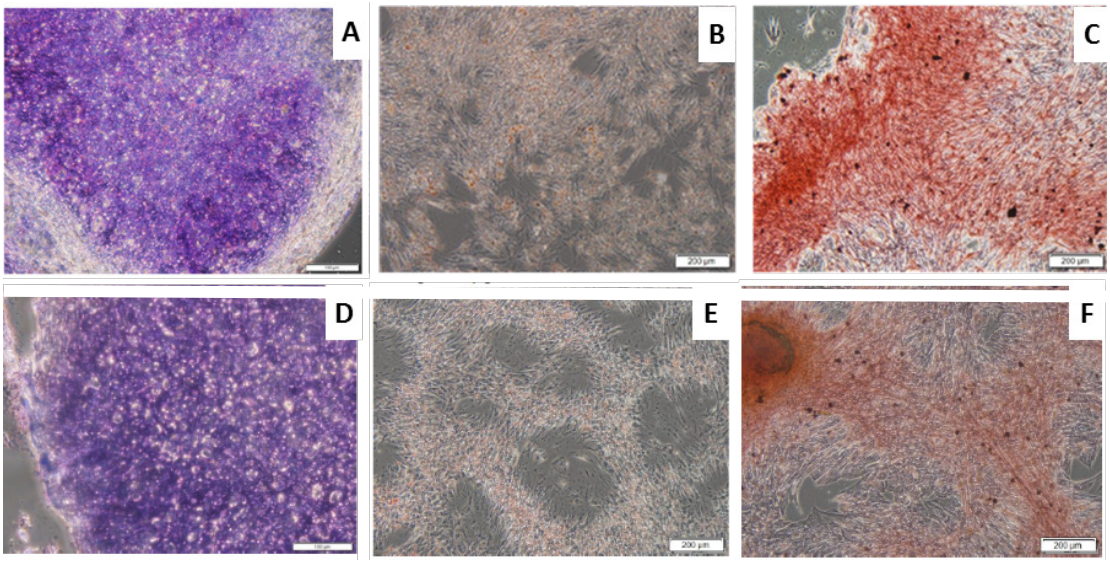

Figure 5.3 Trilineage differentiation of QD-labeled (A, B, C) and control (D, E, F) MSCs. A, D) chondrogenic- purple staining of cartilaginous extracellular matrix with Toluidine Blue (original magnification 200 X, scale bar = 100 µm) B, E) adipogenic- red staining of lipid droplets with Oil Red O (original magnification 100 X, scale bar = 200 µm) C, F) osteogenic- red staining of calcified extracellular matrix with 2% Alizarin Red (original magnification 100 X, scale bar = 200 µm).

Immunophenotyping

On immunophenotyping, the expression of CD29, CD44, and CD90 varied among control (unlabeled) cell lines, whereas CD45 was low in all three cell lines (Table 5.4). In QD-labeled cells, the percentage of cells expressing CD29 was high in all three cell lines, CD44 and CD90 varied among all cell lines, and CD45 was low in all three cell lines. Immunophenotyping of QD-labeled cells showed differences in CD expression from that of the control cells of that line; however, these differences were not

repeatable among cell lines (e.g. for Cell line A, CD44 was expressed in 86% of control cells vs 23% of cells with QDs; whereas for Cell line B, CD44 was expressed in 2% of control cells vs. 30% of cells with QDs). All cell lines in both control and QD treatments showed low expression of MHC II.

Table 5.4 Cell surface markers of control and QD-labeled MSCs determined by flow cytometry.

	Control (unlabeled)					QD-labeled				
	CD29	CD44	CD90	CD45	MHC II	CD29	CD44	CD90	CD45	MHC II
Cell line A	99.2	85.5	5.25	5.23	3.61	99.8	22.8	82.8	1.89	2.57
Cell line B	99.8	1.81	54.5	1.15	1.06	99.7	29.5	35.6	5.41	1.11
Cell line C	1.7	16.8	41.4	1.99	6.23	78.7	0	0.16	0	0

P4 cells were used; each cell line was from a different horse. Data are presented as % of cells positive for a given marker.

DISCUSSION

This study examined for the first time the use of QDs to label equine BM-MSCs and the factors affecting interpretation of results with this system. To be useful for MSC tracking, QDs must not interfere with cellular function or proliferation. We found that in monolayer culture conditions, QD-labeled MSCs continued to divide normally. However, they did not retain sufficient QD label to provide an effective method for cell tracking after the first 2 passages (4-6 days of *in vitro* culture). Similar results have been found with rat and human MSCs. Muller-Borer *et al.,* [217] reported that QD labeling was visible in live rat MSC cultures for up to 7 days. Seleverstov *et al.,* [222] reported a significant loss of fluorescence in QD-labeled human MSCs in culture 2-7 days after

labeling and Wang *et al.,* [223] recently reported a significant reduction in fluorescence in QD-labeled human MSCs after 24 h of culture. In contrast, Rosen *et al.,* [220] reported that proliferating human MSCs retained sufficient QDs to be easily imaged for more than 6 weeks *in vitro*. In the study of Rosen *et al.,* QDs were loaded into the cells by incubation of MSCs with QD labeling solution for 12-24 hr at 37 °C, rather than the one-h incubation used in the present study and that of Muller-Borer *et al.,* [217]. It is possible that the method used to label MSCs with QDs could have an effect on the persistence of the QDs; further studies are needed to determine the optimal method for labeling equine MSCs with QDs.

The proliferation of MSCs in culture likely leads to the dilution of QDs, as the cytoplasmic content of the parent cell is split between daughter cells at each division, reducing the concentration of QDs in progeny over time. Thus the MFI and the proportion of QD-labeled MSCs detected with flow cytometry decreases. In the present study, the expected MFI calculated based on the MFI of the previous passage and the initial and final numbers of cells, was notably higher at P2 and P3 than was the MFI measured by flow cytometry. These results suggest that QD-labeled cells died in culture and were rinsed out during medium changes, or that the cells ejected the QDs during culture. Because there was no difference in the time to reach confluence or in the number of cells at confluence in QD-labeled cells compared to control cells, the latter possibility may be more likely.

In contrast, non-dividing MSCs, i.e., MSCs that were induced to differentiate into chondrogenic pellets, retained QDs without an apparent decrease in label for up to 8

weeks (the length of the experiment). However, we noted that cells on the periphery of the pellet lost QD labeling; again, as the outermost cells are more likely to divide, these cells could have diluted the label via division, died and have been lost into the medium, or ejected the QDs into the medium. The retention of label in the chondrogenic pellets reflects the findings of Ohyabu at al. [286] who reported that chondrocytes, adipocytes and osteocytes (which also do not proliferate rapidly in culture), differentiated from human, rabbit, rat and monkey MSCs, retain strong QD label for 28 days *in vitro* and that chondrocytes differentiated from rat and rabbit MSCs retain QD label for 8 weeks after *in vivo* transplantation into experimentally-induced osteogenic defects. This indicates that QDs would be an effective method to track MSCs injected into areas in which, if they were retained, they would differentiate into non-dividing tissue types such as cartilage, adipose tissue or bone, or cells with limited capacity for division, such as cardiac muscle.

The results from the present study suggest that QD-labeled MSCs should be used immediately after QD labeling to maximize the QD load per injected cell, and that the majority of rapid loss of QD label is not directly related to cell proliferation, but could also be due to death of QD-labeled cells or to ejection of QDs by the cells. As the majority of the cells retained the QD-label in proliferating culture *in vitro* for only 4 to 6 days, a loss of QD label may occur after *in vivo* delivery of QD-labeled MSCs in this time, if cells proliferate after injection. Since the fate of MSCs after injection is unclear [182, 190, 191], histological examination of the target and other tissues (e.g. lymph nodes) within a week of delivery of QD-labeled cells should allow both tracking of the

MSCs and evaluation of their relative fluorescence intensity, which might be suggestive of the degree of proliferation the cells underwent after delivery. This finding might be useful to determine the fate of MSCs after injection.

Another requirement for use of QDs to label and track MSCs is that they must not affect the cells' trilineage potential and immunophenotypic characteristics. The results from the current study showed that the ability of equine BM-MSCs to differentiate into chondrocytes, adipocytes, and osteocytes was not affected by labeling with QDs. These results are similar to those from Ohyabu *et al.,* [286], Ranjbarvaziri *et al.,* [287] and Tautzenberger *et al.,* [288] for human, rabbit, rat, and monkey MSCs.

The immunophenotypic results in the present study were unexpected. According to the panel of immunophenotypic markers proposed by De Schauwer *et al.,* [203] and Schnabel *et al.,* [204] for equine MSCs, these cells tend to be positive for CD29, CD44 and CD90, negative for CD45, and heterogeneous (positive or negative) for MHC II. In the present study, all the cells used had low expression of CD45 and, interestingly, of MHC II; however, the cell lines varied in expression of CD29, CD44 and CD90. Notably, the lines cultured with QDs showed different immunophenotypes from the original cell line, although the effect of QDs was not consistent among cell lines. Whether this was due to an effect of QDs or to drift of the cell line immunophenotype over the passages in separate cultures is not clear, and further studies are needed in this area. While molecular markers continue to be used to characterize stem cell populations, recent studies with human MSCs indicate that cells isolated from different donors [289], or from different sites from the same donor [278, 290], and cells treated with different

enzymatic digestion methods for detachment [291] can have different surface antigen expression, and even MSCs with identical cell surface phenotype from different tissues and donors have distinct transcriptomic signatures and differentiation capacities, likely due to the broad overlap of cells with MSC markers with other cell populations [278, 279]. Thus, the immunophenotypic characterization of MSCs remains unclear and MSCs are currently best defined functionally.

In summary, while QD-labeled MSCs retain their ability to proliferate and differentiate, QDs as applied in this study do not appear to be a good option for long-term tracking of equine BM-MSCs *in vivo* for most indications, because the percentage of labeled cells and the MFI of the cells decreased rapidly in proliferating cells. This makes the absence of QD-labeled cells, such as was found in the study detailed in Chapter III (ovaries injected with QD-labeled MSCs showed no evidence of QDs seven months after injection) difficult to interpret- it cannot be determined if the cells were eliminated, migrated elsewhere, or proliferated *in situ* and lost their label. Further research is needed to determine if QDs can be used for short-term tracking of MSCs *in vivo* and to determine if the method used to label MSCs with QDs could have an effect on the long-term persistence on QDs in equine MSCs.

CHAPTER VI

CO-CULTURE OF EQUINE OVARIAN EXPLANTS WITH MESENCHYMAL STEM CELLS

INTRODUCTION

As discussed above, mesenchymal stem cells (MSCs) secrete a number of growth factors, some of which affect ovarian follicular growth [10, 11, 265-267]. Additionally, intra-ovarian injections of MSCs in rats [10] and systemic injections of MSCs in mice [11] induce mRNA and protein expression of genes that improve the function of ovaries compromised by chemotherapy. However, little is known about the effect of MSC injection on the aging ovary. This procedure has clinical relevance in the mare, as considerable interest exists in the equine industry to establish pregnancies from older, valuable mares. However, to the best of our knowledge, no information is available on the direct effect of *in vitro* co-culture of ovarian tissue with MSCs on ovarian gene expression, which is an essential step in determining the mechanism of action of MSCs *in vivo*.

Co-culture systems have been studied to simulate the *in vivo* microenvironment, and the transwell co-culture system has served as an effective method to determine the paracrine effects of MSCs on tissue. Lovati *et al.,* [292] co-cultured equine tendon tissue fragments in a transwell system with equine bone marrow-derived MSCs (BM-MSCs) for 7 and 15 days in serum-free medium. In that study, cells from tendon fragments in the transwell system showed the same viability as cells from tendon fragments grown in

monolayer as a control; gene expression, via real time PCR (RT-PCR), revealed that mRNA expression of collagen type 1 (*Col1*), tenomodulin (*Tnmd*) and tenascin-C (*Tnc*) genes was upregulated in the tendon fragments co-cultured with MSCs. Similarly, co-culture of equine articular chondrocytes with equine BM-MSCs revealed changes in chondrocyte gene expression as determined via RT-PCR; expression of collagen type 2 (*Col2*), aggrecan (*Acan*), and SRY-box 9 (*Sox9*) genes was upregulated in co-cultured tissue [293].

This study was conducted to determine if the transwell co-culture system would enable evaluation of the effect of soluble factors secreted by MSCs on gene expression of equine ovarian explants. Ovarian tissue was co-cultured in a transwell system with BM-MSCs, fibroblasts or media alone and differences in gene expression were evaluated by RNA-sequencing.

MATERIALS AND METHODS

BM-MSCs were obtained from sternebral aspirates, cultured, and frozen as described in Chapter III. Skin fibroblasts were obtained from a subcutaneous connective tissue biopsy sample. The biopsied tissue was cultured in DMEM/F12 (Invitrogen) supplemented with 10% FBS (Sigma-Aldrich) and 1% antibiotic-antimycotic (Invitrogen) which was changed every three to four days until growth of fibroblasts from the tissue was obtained. Cells from P3 were frozen in 90% DMEM/F12 with 10% DMSO.

Ovaries were obtained after euthanasia of mares aged 3 to 4 yr old, with normal reproductive tracts on palpation and ultrasonography per rectum. The ovaries were minced within 1 h of collection. Tissue explants (approximately 5 mm^3, 60-80 mg total wet weight/well) were maintained in the top well of 6-well 24-mm Transwell® permeable plates (Corning, Corning, NY). These plates have a permeable membrane which prevents cell-to-cell contact while allowing the diffusion of soluble factors between the two compartments. The tissue was cultured in a final volume of 2 ml DMEM/F12 (Invitrogen) supplemented with 10% FBS (Sigma-Aldrich) and 1% antibiotic-antimycotic (Invitrogen). The contents of the bottom well were 1) previously cryopreserved/thawed BM-MSCs (5.0×10^4 cells/well), 2) previously cryopreserved/thawed skin fibroblasts (5.0×10^4 cells/well), or 3) medium alone. The ovarian tissue was co-cultured at 37 °C in a humidified atmosphere of 5% CO_2 in air. After 4 days the tissue was flash-frozen in liquid nitrogen and stored at -80 ºC until RNA isolation was performed. Three replicates were performed.

RNA Isolation

RNA isolation from the co-cultured ovarian tissues was performed at the Texas A&M Institute for Genome Sciences and Society (TIGSS). Two different protocols were used. In Protocol 1, RNA was extracted using a Maxwell LEV SimplyRNA Tissue Kit (Promega, Madison, WI). Tissue was lysed using a TissueLyser II (Qiagen, Valencia, CA) and RNA was purified on the automated Maxwell 16 Instrument (Promega). Quantitative and qualitative parameters of the RNA preparations were assessed using a

Qubit 2.0 fluorometer (ThermoFisher; Invitrogen, Carlsbad, CA) and an Agilent RNA ScreenTape 2200 assay (Agilent Technologies, Santa Clara, CA). During the ScreenTape assay, RNA samples are loaded on top of a gel matrix contained in the ScreenTape lane and the samples are driven by a voltage gradient and separated by size according to the length of the RNA chain; smaller molecules migrate through the gel more quickly and therefore travel further than larger fragments. Dye molecules intercalate into the RNA strands and these complexes are detected by laser-induced fluorescence. Data is then translated into gel-like images (bands) and electropherograms (peaks). The qualitative parameter evaluated was RNA integrity as measured by the RNA integrity number (RIN) and the 28S/18S ribosomal RNA (rRNA) ratio. The RIN ranges from 1 to 10 with a score of 10 indicating no degradation, and a high 28S/18S ratio (> 2 is considered the benchmark) indicates that the purified RNA is intact and has not degraded (see Discussion for an explanation of these measures).

In Protocol 2, the ovarian tissues were pulverized with a biopulverizer (Cole-Parmer, Vernon Hills, IL) and RNA was extracted using a guanidinium thiocyanate-phenol-chloroform protocol (TRIzol Reagent; Life Technologies; Invitrogen). Samples were processed with a final silica-gel spin-column clean up and quantitative and qualitative parameters were assessed as in Protocol 1.

To determine if the poor-quality RNA obtained from co-cultured ovarian tissues (see Results) was due to an intrinsic nature of equine ovaries or to effects of processing of the tissue to obtain RNA vs an effect of tissue degradation over the time of co-culture, fresh ovarian tissue was recovered from one 9-yr old mare at euthanasia and snap-frozen

within 1 h of ovary removal. This tissue was processed by Protocol 2; quantitative and qualitative analysis of RNA was performed as described above.

RESULTS

When Protocol 1 was used, the concentration of RNA detected by the Qubit 2.0 was not adequate for analysis; therefore, gel-like images and electropherograms were not generated. When the ovarian tissues were pulverized via Protocol 2, adequate concentrations of RNA were obtained; however, the quality was poor due to RNA degradation (Figure 6.1). Highly intact RNA appears as sharp, compact bands as seen in the A0 (L) lane, whereas with progressive RNA degradation, the 28S and 18S bands become thinner, and highly degraded RNA appears as a diffuse smear extending into the lower molecular weight range of the lane (lanes A1 and B1), which correspond to two different co-cultured ovarian samples processed by Protocol 2. Similar results were obtained when a combination of methods from the two protocols was attempted. The electropherograms of samples A1 and B1 (Figure 6.2) showed that most of the RNA present was smaller than 200 nucleotides (nt), further indicating degradation of the samples.

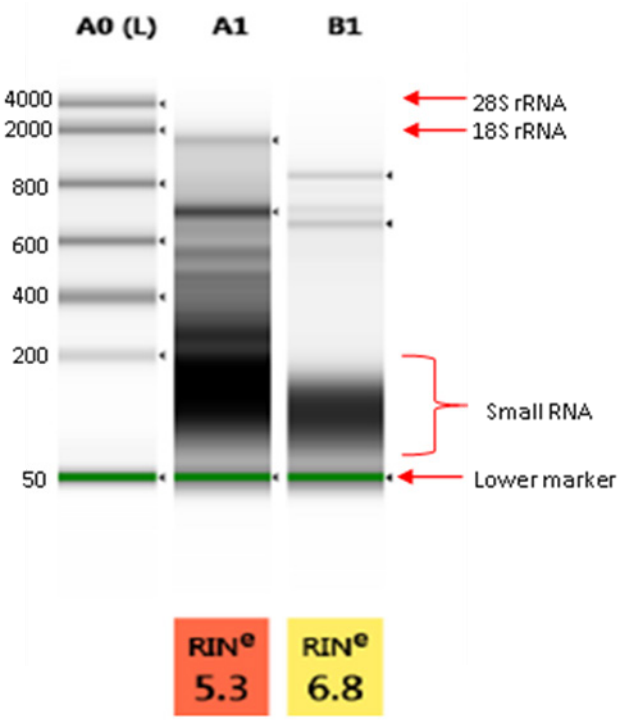

Well	RINe	28S/18S (Area)	Conc. [ng/µl]
A0	-	-	97.5
A1	5.3	0.3	463
B1	6.8	-	141

Figure 6.1 Quantitative and qualitative assessment of two RNA samples from ovarian tissue from two different mares. Although the RNA concentrations in the ovarian tissues (A1 and B1) were high, the quality of the RNA, as determined by the RIN and the 28S/18S rRNA ratio, was low. A1 and B1 represent two RNA samples from ovarian tissue from two different mares; both samples were pulverized and processed by Protocol 2. A0 (L) is the RNA ladder which sets the markers or standards against which the samples are compared.

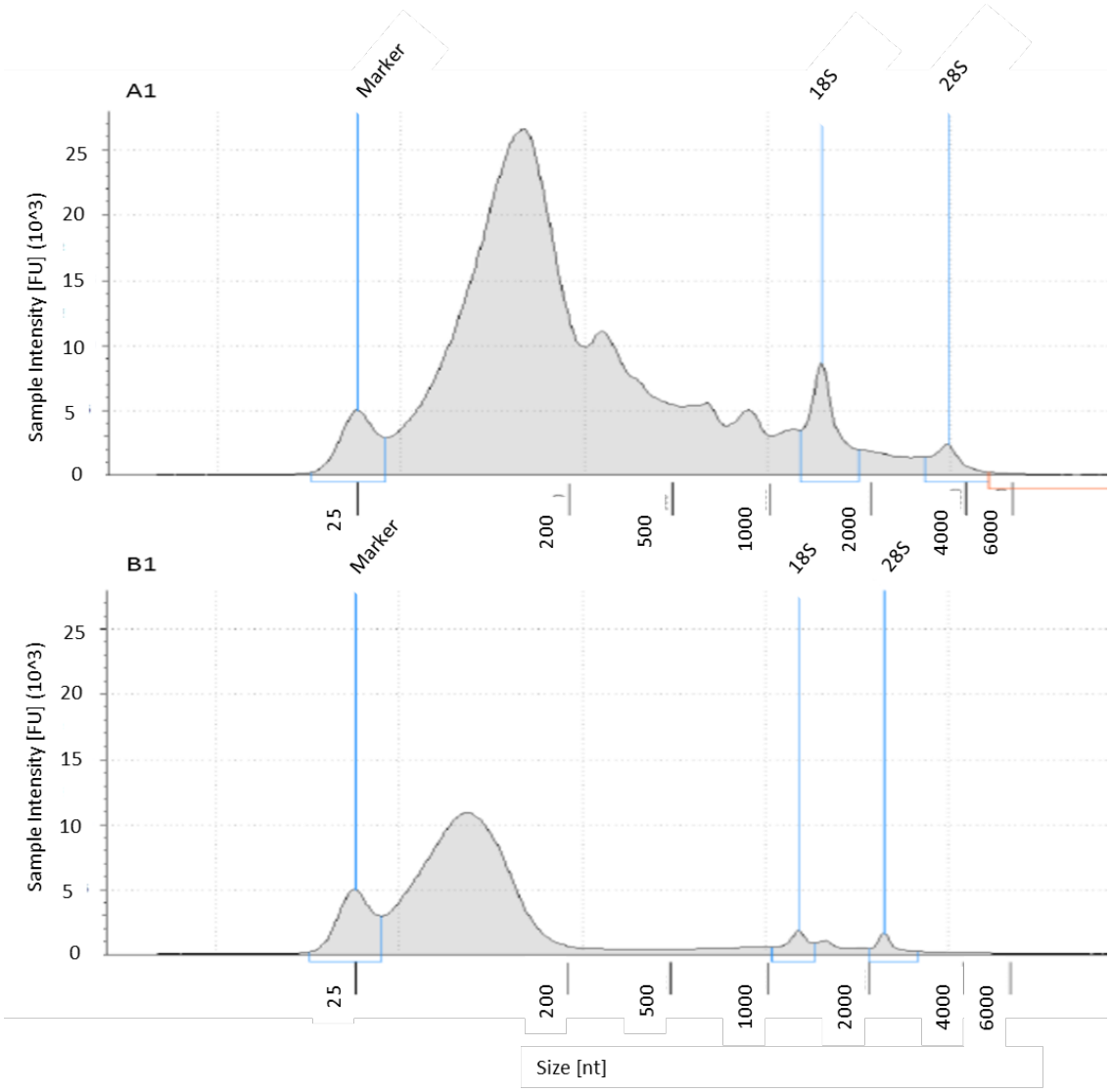

Figure 6.2. Electropherograms of two ovarian RNA samples (A1 and B1) from gel images shown in Figure 6.1. The y-axis represents fluorescence units (FU) and the x-axis represents the nucleotide length (nt) of the RNA fragments. As RNA degrades the 18S and 28S peaks become less sharp and smaller. The peaks generated prior to the 18S represent the small RNA fragments produced during RNA degradation; small fragments migrate faster through the gel and thus appear in the fast region of the electropherogram (see Figure 6.5). In both of these samples most of the RNA present was smaller than 200 nt and the 18S and 28S peaks were very small, both of these characteristics are indicative of degradation. These electropherograms can be compared to that shown in Figure 6.5 which corresponds to a sample of intact RNA with a RIN of 10.

In contrast to the co-cultured samples, when Protocol 2 was used to isolate RNA from equine ovaries that were not co-cultured (sample D1), RNA of adequate concentration and quality was obtained (Figures 6.3 and 6.4). The results of RNA-sequencing of this tissue are presented in Chapter VIII.

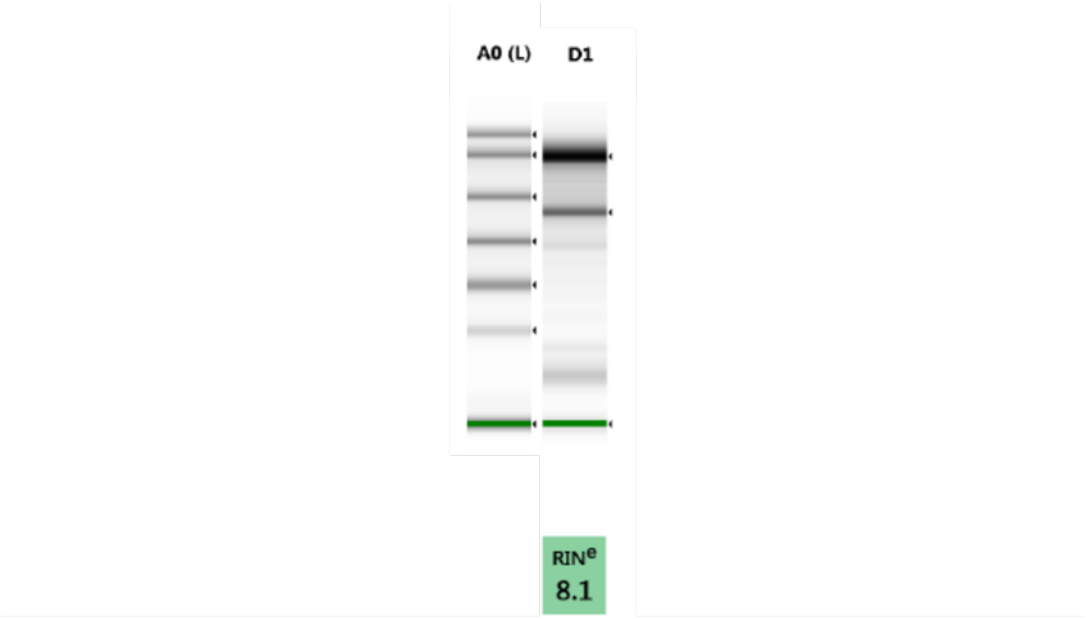

Well	RINe	28S/18S (Area)	Conc. [ng/µl]
D1	8.1	2.2	457

Figure 6.3. Quantitative and qualitative analysis of RNA obtained from equine ovaries that were not co-cultured. There are two sharp, compact bands corresponding to the 28S and 18S rRNAs. There is still some degradation present as seen by the slight smearing that extends into the lower molecular range of the lane; however, the RIN of 8.1 and the 28S/18S ratio of 2.2 are both indicative of high quality RNA that is adequate for RNA-sequencing analysis.

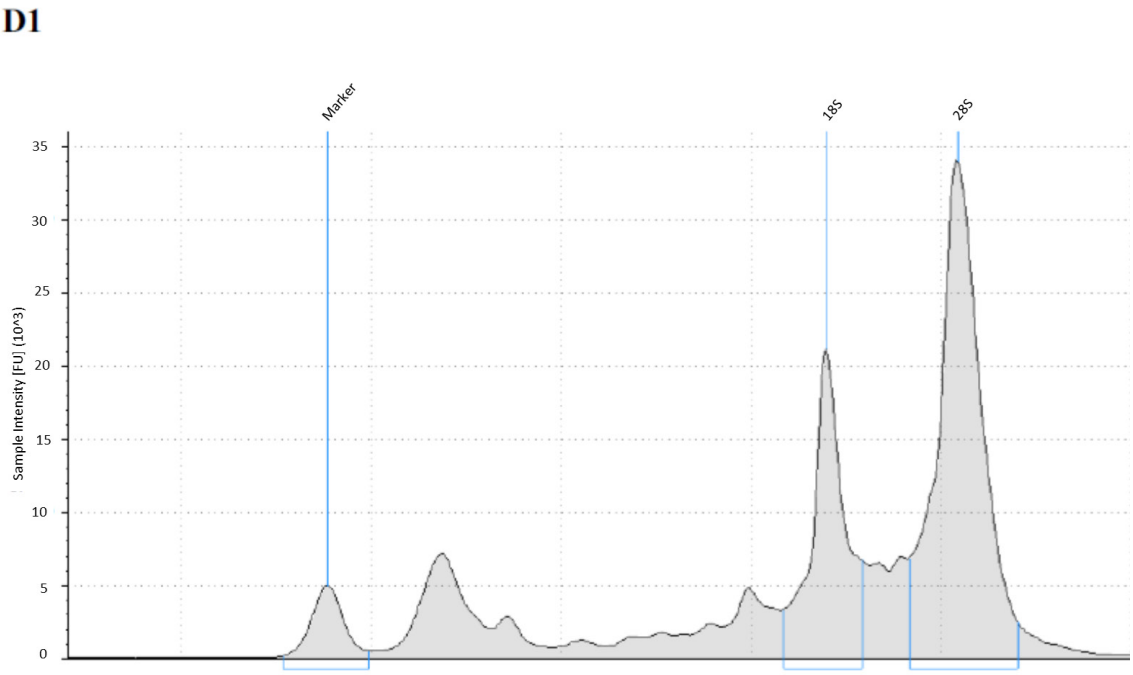

Figure 6.4 Electropherogram of equine ovarian sample from gel image shown in Figure 6.3. Unlike the electropherogram from the two degraded samples shown in Figure 6.2, this electropherogram has sharp 18S and 28S peaks. There is still a small amount of degradation present as seen by the small peaks generated prior to the 18S peak; however, the RIN, 28S/18S ratio and RNA concentrations were all indicative of high quality RNA.

DISCUSSION

This study was performed to evaluate whether co-culture of ovarian explants with BM-MSCs could be used to determine the effect of MSCs on gene expression of equine ovarian tissue in culture. To the best of my knowledge, this is the first attempt at this procedure using equine ovarian tissue. Information gathered in such a system, if effective, would serve as a first step in determining the mechanism of action of MSCs on ovarian tissue. While the transwell co-culture approach has been successful with other tissue, including equine tendon explants and equine cartilage tissue [292, 293], the

ovarian explants that we evaluated had degraded RNA, indicating that the explants had degenerated in culture. Equine ovaries, like tendons, are fibrous in nature [294]; the co-culture time of four days was selected based on previous co-culture studies in which equine tendon tissue fragments were co-cultured with MSCs for 7 and 15 days [292].

While the co-culture system was not effective due to tissue degradation, this study had value in determining methods for isolation of RNA from ovarian tissue. RNA isolation was problematic; when Protocol 1 was used, the RNA concentrations obtained were too low to be detected by the fluorometer. This was attributed to the fibrous nature of the equine ovary interfering with lysis by enzymatic digestion. This issue was resolved when the ovarian tissues were physically pulverized in Protocol 2. In this protocol, RNA isolation from the pulverized ovarian tissues was performed with guanidinium thiocyanate-phenol-chloroform. Even though there was significant RNA degradation, adequate RNA concentrations were obtained with this protocol even from the degenerating tissue, and it would appear to be the protocol of choice for future examination of equine ovarian tissue. To determine if the degradation seen was due to an intrinsic nature of RNA in equine ovaries or to sample processing, vs an effect of tissue degeneration during culture, ovarian tissues that were not co-cultured were pulverized and processed by Protocol 2. The RNA obtained from these ovaries was of high quality and adequate for RNA-sequencing (see RNA-sequencing results in Chapter VIII); therefore, it appears that the RNA degradation observed in co-cultured tissue was due to the ovarian tissue degrading during culture.

Integrity of RNA is summarized by two main statistics; 1) rRNA ratio (28S/18S),

and 2) RNA integrity number (RIN). Ribosomal RNA (rRNA) makes up > 80% of the total RNA in tissues. The majority of rRNA is comprised by the 28S and 18S rRNA species. The 28S and 18S rRNAs are produced in equal numbers by the cleavage of a single RNA transcript. Because mammalian 28S and 18S RNAs are approximately 5 kb and 2 kb in size, respectively, the theoretical 28S/18S mass ratio is approximately 2.7:1, but a 2:1 ratio has long been considered the benchmark for intact RNA that has not degraded [295]. The 28S RNA degrades more quickly than does the 18S RNA, so a decrease in mass ratio below 2:1 is considered a sign of RNA degradation; the lower the mass ratio, the greater the amount of degradation. In the RNA analyzed in the present study, the 28S/18S ratio was 0.3 and "unable to be detected," respectively, in the two ovarian samples that were co-cultured with MSCs; whereas it was 2.2 in the ovarian sample that was not co-cultured (desired is ≥ 2). This indicates that the RNA in co-cultured samples had undergone significant degradation over time in culture while RNA in the non-co-cultured sample was intact.

The RIN is a software algorithm that assigns integrity values to electrophoretic RNA measurements including; 1) total RNA ratio, which is calculated by taking the fraction of the area under the 18S and 28S rRNA peaks compared to the total area under the graph. A large number indicates that much of the rRNA is still at its initial (known) size and thus little to no degradation has occurred, 2) relative height of the 28S to 18S peaks which allows determination of the stage of degradation, as during degradation the 28S rRNA is degraded faster than the 18S rRNA; a large number is desired, 3) fast area ratio, which is the area under the curve between the 18S and 5S rRNA (which is the

smallest type of cytoplasmic rRNA) peaks. Initially as this value increases it indicates degradation of the 18S and 28S rRNA to an intermediate size (> 5S), however the ratio decreases as RNA degrades further to smaller sizes, and 4) marker height, which indicates the amount of RNA that has been degraded to small pieces, a small number, ie., short marker, is desired (Figure 6.5). From all these measurements, the RIN software will assign a final value between 1 and 10, with 1 being the most degraded and 10 being the most intact [296]. In the present study, the RIN numbers of co-cultured samples A1 and B1 were 5.3 and 6.8, respectively, and the non-co-cultured sample D1 had a RIN number of 8.1 (desired is > 8).

The methods used for co-culture may have an effect on the viability of the co-cultured tissue. In a recent study by Morgan *et al.,* [297] viability of intact neonatal mouse ovaries was maintained for up to six days in a specialized culture system. The ovaries were co-cultured with individual, intact ovarian follicles to study the interactions between primordial and growing follicles. The method used was floating polycarbonate membranes, which allow greater oxygenation of the tissue, and basic medium consisting of only αMEM and BSA, avoiding the use of serum. In a study by Riley *et al.,* [298] equine ovarian tissue explants were maintained in culture for 24 h on a hydrophilic mat in serum-free medium. Similarly, a study by Ricci *et al.,* [299] maintained rat ovarian explants in culture for 4 h in serum-free medium. In the present study, FBS was added to the co-culture media in order to support the MSCs and the Transwell® permeable plates were used based on positive results from previous equine tendon co-culture experiments. FBS-enriched media promotes the active proliferation of cells in culture [300, 301];

however, FBS also induces excessive tissue swelling [302], and suppresses the function and size of cultured granulosa [301, 303] and theca cells [300]. Furthermore, degradation of tissue matrix can occur during long-term maintenance with media supplemented with serum; matrix degradation is seen especially when cartilage from juvenile bovines and rats is cultured in FBS-supplemented media for up to 6 wk because juvenile tissue is more responsive to chemical stimuli than mature tissue [304]. In addition, it is harder to establish the involvement or contribution of certain growth factors when serum-enriched media is used because serum itself contains growth factors. Use of serum-free media should be investigated in future ovarian co-culture experiments.

Additional research is needed to determine if different co-culture systems and serum-free media would support the co-culture of equine ovarian explants and prevent the RNA degradation seen in the present study.

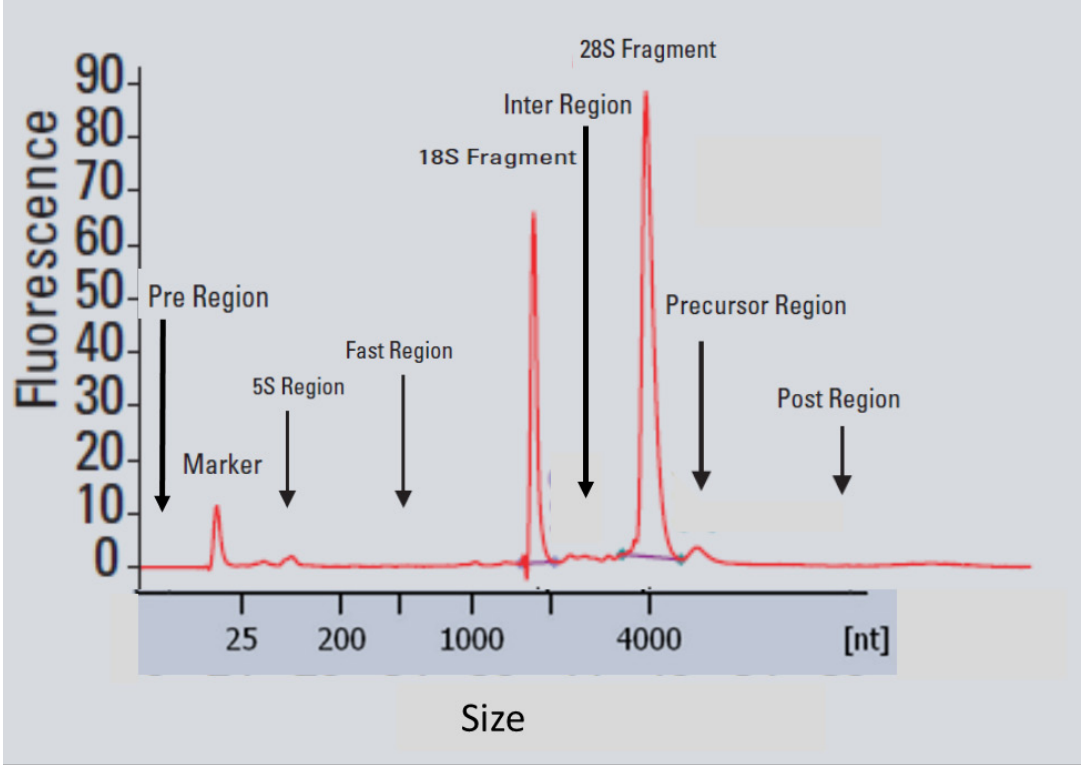

Figure 6.5. Electropherogram showing the regions used to compute the RIN, an indicative of RNA quality; figure from [296]. This electropherogram corresponds to an RNA sample with a RIN of 10. Common features of intact RNA include distinct 18S and 28S rRNA peaks, the absence of smaller peaks between the two ribosomal peaks, and a flat baseline prior to the 18S peak.

CHAPTER VII

EFFECT OF INTRA-OVARIAN INJECTION OF BONE MARROW-DERIVED MESENCHYMAL STEM CELLS ON OVARIAN FUNCTION IN OLD AND YOUNG MARES

INTRODUCTION

Age-related changes result in decreased follicle numbers and oocyte quality, reducing fertility in aging women [1]. The same changes have been reported to occur in mares [159]. As discussed in Chapter II, systemic and intra-ovarian injections of adult mesenchymal stem cells (MSCs) in mice [11] and rats [10] induce mRNA and protein expression of genes that improve the function of ovaries and rescue fertility following chemotherapy. However, little information is available on the effect of MSC injection on the aging ovary, an application which, if effective at increasing fertility, would have an impact on millions of women undergoing assisted reproduction because of age-related infertility. This application would also have clinical relevance in the mare, as considerable interest exists in the equine industry to establish pregnancies from older, valuable mares. Based on the results from the study presented in Chapter III showing that it is feasible to perform intra-ovarian injections of bone marrow-derived MSCs (BM-MSCs) in mares and that there is an apparent increase in follicle numbers in the 4 weeks after injection, a more comprehensive study that included both old and young mares was performed to determine if MSCs affect ovarian function in mares experiencing ovarian failure associated with aging.

MATERIALS AND METHODS

Animals

This study was performed from February 2015 to February 2016. Eight old mares, aged 20-29 yr, and six young mares, aged 7-12 yr, were housed in pens at the College of Veterinary Medicine Research Park and had *ad libitum* access to hay and fresh water throughout the study, and supplemental grain. Two yearling fillies were used as BM-MSC donors. All procedures were approved by the Texas A&M University Institutional Agricultural Animal Care and Use Committee, and were performed using guidelines set forth by the *United States Government Principles for the Utilization and Care of Vertebrate Animals Used in Testing, Research and Training.*

Experimental Design

The old mares were stratified by age and divided randomly into three treatment groups and assigned to intra-ovarian injection with: 1) BM-MSCs from filly A (n = 3), 2) BM-MSCs from filly B (n = 3), or 3) control (Vehicle injection, n = 2). The young mares were also stratified by age and divided similarly into these groups; n = 2, 2 and 2, respectively.

Bone marrow from the yearling donors was collected from sternebral aspirates and MSCs were isolated, expanded in culture, and cryopreserved in serum (autologous to the mare receiving the injection) as described in Chapter III. Aliquots of donor MSCs were induced to differentiate into chondrocytes, adipocytes and osteocytes and

characterized, and immunophenotyped by flow cytometry, as described in Chapters III and V.

Starting in February (~ 6 weeks before the beginning of the equine breeding season) the reproductive tracts of the old mares were evaluated by ultrasonography per rectum 3 times per week to determine the total number of follicles > 5 mm diameter in each ovary. Each ultrasound examination was recorded with a videotape recorder. The entire ovary was examined for ~15 sec (depending on the size of the ovary) of continuous taping. The videotapes were then viewed, on the same day that the recording was made, and the number of follicles > 5 mm in diameter in each ovary was counted.

Starting in March, blood was collected from the jugular vein of each old mare three times per week and the serum frozen for later evaluation of concentrations of anti-Müllerian hormone (AMH), FSH and total estrogens. Blood continued to be collected on this schedule until two weeks after the mares were ovariectomized at the end of the study. Mares were evaluated once every 14 days starting in mid-February, and if five or more follicles > 8 mm in diameter were present, transvaginal follicle aspiration (TVA) was performed to recover oocytes. All follicles > 8 mm diameter were aspirated; the aspirate was filtered and the granulosa cells from each ovary of MSC-injected mares were separately centrifuged and flash-frozen for later DNA analysis to determine the presence of DNA from the transferred BM-MSCs. Oocytes were recovered from the aspirates and matured *in vitro*, subjected to intracytoplasmic sperm injection (ICSI) and cultured to determine the blastocyst rate, as described in Chapter III.

Intra-ovarian injections were performed in the old mares starting in mid-April. Each mare had one ovary randomly assigned to be injected. Three mares underwent ovarian injection on Week 1, three mares on Week 3, and three mares on Week 5. The person performing the injections was blind as to treatment.

Twelve to sixteen weeks after the first injection, three MSC-injected mares received a second injection with MSCs from the alternate donor to that used in the first injection. The MSCs used in the second injection had been labeled with fluorescent nanoparticles (QDs) as described in Chapter III, before being frozen and subsequently thawed for injection.

The ovaries of all 8 old mares were removed by ovariectomy via colpotomy, as described in Chapter III, 14 to 19 weeks after the first injection. This was scheduled so that ovariectomies were performed two weeks after the second injection for the three mares in that treatment.

The young mares received one intra-ovarian injection. These mares similarly had their reproductive tracts evaluated by ultrasonography per rectum three times per week, and follicle counts obtained from video recordings, starting in June, 7 to 8 weeks before ovarian injection, and continuing until six months after ovarian injection. Blood was collected from young mares 3 times per week starting 5 to 7 weeks before ovarian injection and continuing for 8 weeks after injection. TVAs were performed in young mares having more than five follicles > 8 mm in diameter once every 14 days from June to August; however, the oocytes recovered were used for separate projects, thus maturation and blastocyst rates after ICSI were not available.

Ovarian Tissue Processing

Ovarian tissue processing was performed as detailed in Chapter III. Fragments (15 x 15 x 1 mm, 4 per ovary) of all the recovered ovaries were placed in Bouin's solution at room temperature, and after 24 h were placed in 70% ethanol and held until histological processing. Four slides from each ovary of each mare were submitted to the Texas A&M Veterinary Medical Diagnostic Laboratory (TVMDL) for histopathological analysis. For ovaries of the three old mares that received a second intra-ovarian injection, with QD-labeled MSCs, four additional slides from each ovary were examined under a fluorescent microscope for the presence of QDs.

Ovarian fragments (2 x 2 mm fragments, 5 per ovary per MSC-injected mare) were flash-frozen for later genetic analysis. The remainder of the ovarian tissue was minced into 5 x 5 mm fragments which were pulverized to extract RNA (see Chapter VIII).

Genetic Analysis

Hair samples from the BM-MSC donors underwent analysis of genomic and mitochondrial genotype at the Veterinary Genetics Laboratory at the University of California, Davis.

Genomic DNA was genotyped using loci for one sex-associated gene (AME), one X-linked marker (LEX3) and 16 microsatellite identification markers (AHT4, AHT5, ASB17, ASB2, ASB23, HMS2, HMS3, HMS6, HMS7, HTG10, HTG4, LEX33, TKY333, TKY374, TKY394 AND VHL20), for a total of 18 loci for each sample.

Mitochondrial (mt) genotype analysis was determined by sequencing a 744 bp fragment of mtDNA spanning bases 15382 through 16125 of the hypervariable region of the D-loop between tRNAPro and the large conserved sequence block (HVeqmitA 50-AACGTTTCCTCCCAAGGACT-30, HVeqmit B 50-GTAGTTGGGAGGGTTGCTGA-30).

The granulosa cells obtained on each TVA of the MSC-injected mares (pooled separately from each ovary) and the 5 samples from each ovary recovered via ovariectomy of the MSC-injected mares were then analyzed at the Veterinary Genetics Laboratory to identify any MSC-donor genomic or mitochondrial DNA in the samples.

Serum Hormone Analysis

Collected serum was sent to the Clinical Endocrinology Laboratory at the University of California for analysis of AMH and FSH, and to BET Labs (Lexington, KY) for analysis of total estrogens.

Statistical Analysis

A Bayesian model was implemented to evaluate a potential difference in follicle numbers in the injected ovary relative to the mare's untreated ovary. Ovary-specific follicle counts were modeled separately as Poisson distributions. The Poisson parameters were modeled as a function of the expected follicle count, with a within-mare, ovary-specific random effect, and a treatment effect. The 8-week period before injection (the first injection, for those mares injected twice) was considered the "Pre-treatment"

period; the 4-week period following injections were considered the "Treatment" period; and the 8-week period following the Treatment period was considered the "Post-treatment" period. The numbers of follicles in the MSC-injected ovary relative to the mare's non-injected ovary were compared at each period. For mares injected twice, the 4-week period before the second injection was considered the "Pre-treatment" period, and the 2-week period after injection until ovariectomy was considered the "Treatment" period. The number of follicles on the injected ovary was then compared within mare group (MSC vs Vehicle) among treatment periods.

For old mares, the oocyte recovery rate (oocytes recovered per follicle aspirated on TVA), proportion of oocytes reaching metaphase II in culture, and the proportion of oocytes developing to blastocyst after ICSI were compared among treatment periods within mare group (MSC or Vehicle) using Chi-square analysis, with Fisher's exact test used when a value < 5 was expected for any parameter.

Bayesian models were also implemented to evaluate AMH, FSH and total estrogen concentrations in relation to treatment. For hormone concentrations, in old mares the Pre-treatment period was the 4 wks before injection, the Treatment period was the 4 wks after injection, and the Post-treatment period was the 8 wks after the Treatment period. Significance level was defined as $P < 0.05$.

RESULTS

Mare Health and Ovarian Status

Intra-ovarian injections of allogeneic BM-MSCs (n = 10) or Vehicle (n = 4) in old or young mares were not associated with any observable signs of discomfort or systemic illness. Temperature, pulse and respiration rates were within normal limits for the 7-day period in which they were evaluated after injection. All the mares continued to appear bright, alert, responsive, and in good health for the duration of the study.

Of the 8 old mares, four mares (ages 20, 24, 20 and 20 yr) consistently had follicular activity as defined by the presence of antral follicles visible on ultrasonographic examinations; the other four mares (ages 22, 23, 29 and 29 yr) had no visible follicles throughout the study.

Gross examination of the ovaries of the old mares after ovariectomy revealed an abscess in the ovary of one of the mares. This mare had received two intra-ovarian MSC injections into the ovary in question, and had undergone a total of six TVA procedures. The rest of the ovaries showed no gross pathology. Histopathologic examination of the old mare ovaries revealed small areas of granulation tissue in ovaries in all categories (MSC-injected, vehicle-injected and non-injected), this was considered by the pathologist to be of no clinical significance.

On fluorescent microscopic evaluation of four sections from each ovary of the three mares injected with QD-labeled MSCs two weeks previous to ovariectomy, no QDs were detected in either the injected ovary or the contralateral ovary.

TVA was performed on 8 occasions after MSC injection of old mares: at 12 and 16 wks after injection in one mare; 2, 5, 8, and 10 wks after injection in a second mare; and at 4 and 11 weeks after injection in a third mare. At all other 14-day evaluations in these mares and all 14-day evaluation in the other three mares, there were insufficient follicles present (fewer than five follicles with a diameter > 8 mm) and TVA was not performed.

Characterization and Phenotypic Analysis of Donor MSCs

The MSCs isolated and used for intra-ovarian injections showed evidence of differentiation to chondrogenic, adipogenic and osteogenic cell lineages when cultured in appropriate conditions, as seen by the presence of cartilaginous extracellular matrix, intracytoplasmic lipid droplets, and calcified extracellular matrix, respectively (Figures 7.1 and 7.2).

Immunophenotypic analysis of MSCs at P3 by flow cytometry revealed that MSCs from both donors had a high expression of CD29 and CD90 markers, and low expression of CD44, CD45, and MHC II markers (Figures 7.3 and 7.4), consistent with results from equine MSCs as reported by De Schauwer [203] and Schnabel [204].

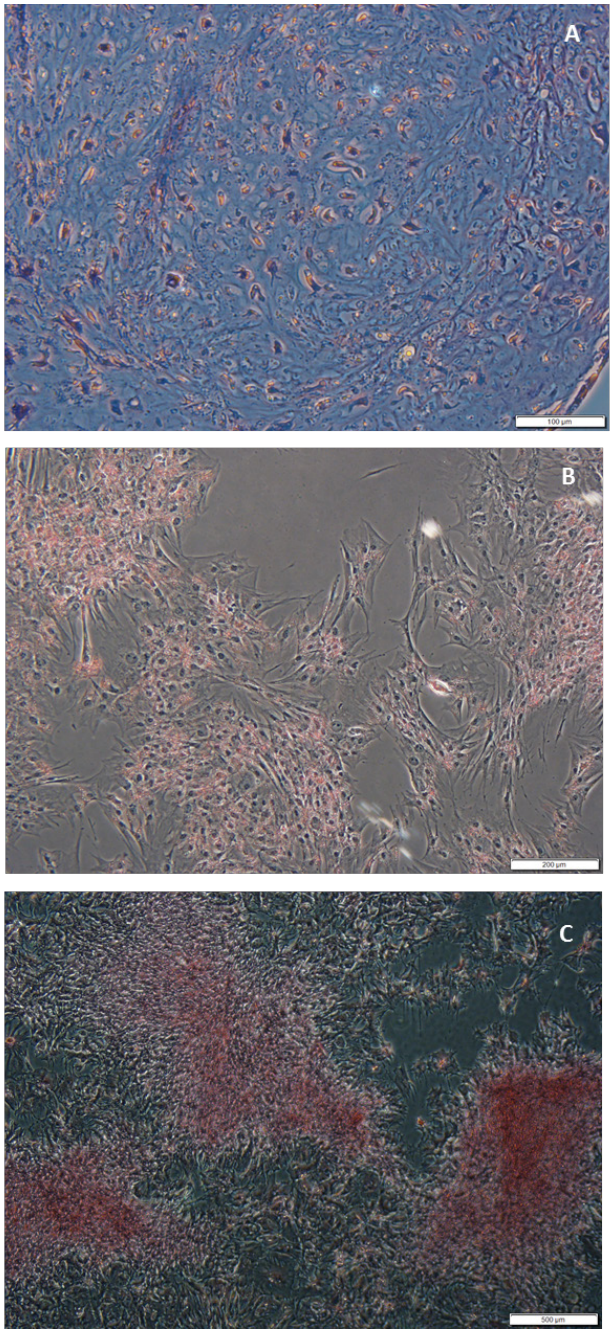

Figure 7.1 Trilineage differentiation of Donor A BM-MSCs. A) chondrogenic pellet stained with Toluidine Blue showing cartilaginous extracellular matrix (purple) and fibrous tissue (blue), original magnification 200 X, scale bar = 100 µm; B) adipogenic differentiation showing fat cells (red) stained with Oil Red O, original magnification 100 X, scale bar = 200 µm; and C) osteogenic differentiation showing calcified extracellular matrix and bone nodules (red) stained with 2% Alizarin Red, original magnification 40 X, scale bar = 500 µm.

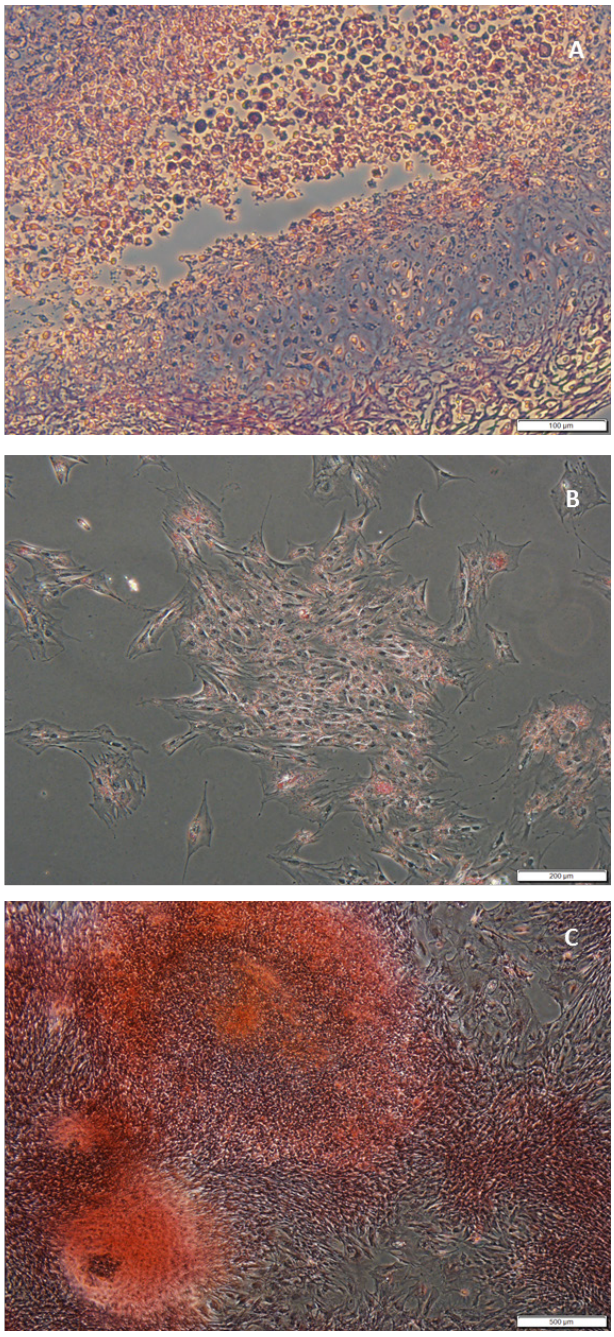

Figure 7.2 Trilineage differentiation of Donor B BM-MSCs. A) chondrogenic pellet stained with Toluidine Blue showing cartilaginous extracellular matrix (purple) and fibrous tissue (blue), original magnification 200 X, scale bar = 100 µm; B) adipogenic differentiation showing fat cells (red) stained with Oil Red O, original magnification 100 X, scale bar = 200 µm; and C) osteogenic differentiation showing calcified extracellular matrix and bone nodules (red) stained with 2% Alizarin Red, original magnification 40 X, scale bar = 500 µm.

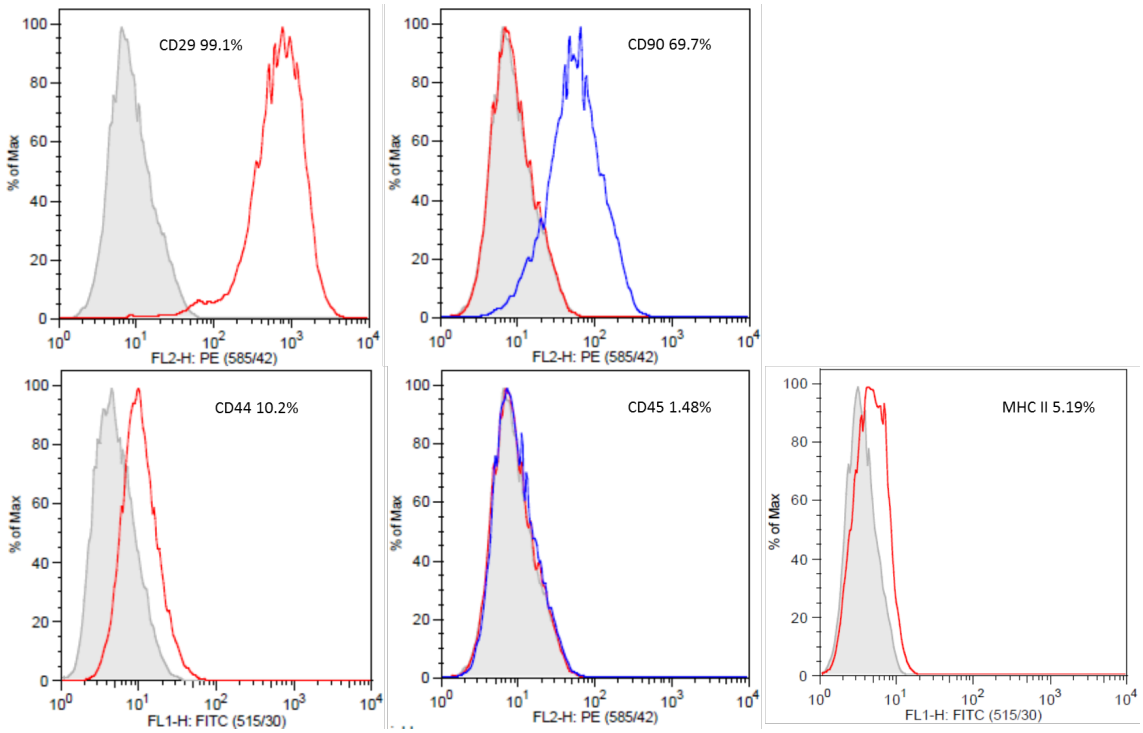

Figure 7.3 Flowcytometric histogram analyses of cell surface markers of Donor A BM-MSCs. For CD29, CD44 and MHC II the gray lines represent negative control staining and the red lines represent cell surface marker staining of MSCs. For CD90 and CD45the red lines represent secondary antibody staining and the blue lines represent cell surface marker staining of MSCs. The percentage of positive cells is indicated in each histogram.

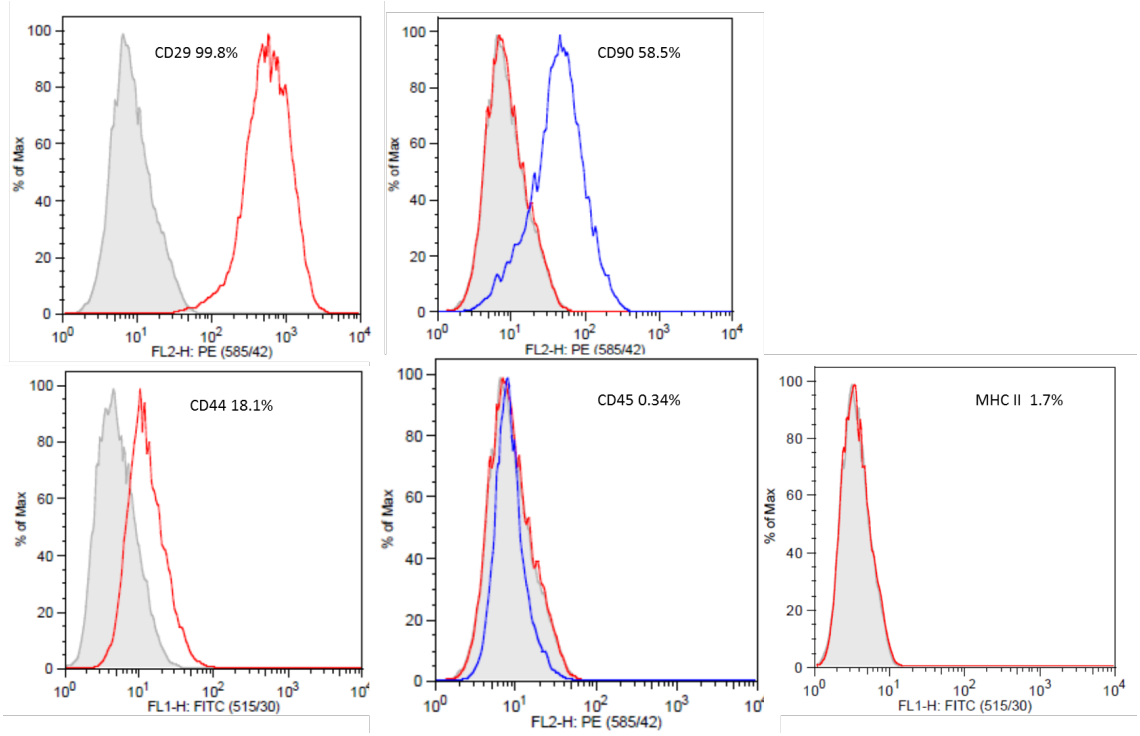

Figure 7.4 Flowcytometric histogram analyses of cell surface markers of Donor B BM-MSCs. For CD29, CD44 and MHC II the gray lines represent negative control staining and the red lines represent cell surface marker staining of MSCs. For CD90 and CD45 the red lines represent secondary antibody staining and the blue lines represent cell surface marker staining of MSCs. The percentage of positive cells is indicated in each histogram.

Follicle Numbers

Before injection, the number of ovarian follicles identified on the ovary designated for injection was not significantly different from the number of follicles identified on the contralateral ovary, for both old and young mares. This continued to be the case after injection within each MSC-injected mare, regardless of MSC donor (Figure 7.5). Because there were no significant differences in any parameter associated with the different MSC donors, mares injected with MSCs from either donor were

grouped as “MSC-injected mares.” Within group (MSC or Vehicle) there were no significant differences in the number of ovarian follicles in the injected ovary among the Pre-treatment, Treatment, and Post-treatment periods for either old or young mares (Figure 7.5). Similarly, after the second MSC injection in old mares there was no difference in follicle numbers between the Pre-treatment and Treatment periods (Figure 7.5).

Considering only the ovary that received the injection, regarding the first injection, old mares had a mean of 2.8 follicles (1, 4; lower 2.5% and upper 97.5% limits, respectively) in the Pre-treatment period, 1.7 follicles (1, 3) in the Treatment period, and 2.3 follicles (1, 4) in the Post-treatment period. Old mares that received Vehicle injection had a mean of 1.9 follicles (1, 2) in the Pre-treatment period, 1.8 follicles (1, 3) in the Treatment period, and 2 follicles in the Post-treatment period.

Old mares that received a second MSC injection had a mean of 1.4 follicles (0, 3.5) in the Pre-treatment prior to the second injection and 1.1 follicles (0, 3) in the 2-week Treatment period after this injection. There is no Post-treatment period for these mares since they were ovariectomized two weeks after the second injection.

Young mares that received one MSC injection had a mean of 4.1 follicles (2, 7) in the Pre-treatment period, 4.8 follicles (2, 7) in the Treatment period, and 4.1 follicles (2, 6) in the Post-treatment period. Young mares that received one Vehicle injection had a mean of 2.8 follicles (1, 4.25) in the Pre-treatment period, 1.8 follicles in the Treatment period, and 2.4 follicles (1, 4) in the Post-treatment period.

Follicle numbers in the young mares continued to be assessed three times weekly for 5 months after the Post-treatment period (7 months after injection). The number of follicles did not change significantly during this time. The number of follicles in each ovary for each mare throughout the study is represented in Figures 7.6 – 7.10.

Oocyte Recovery, Maturation and Blastocyst Formation

In old mares, there was no difference in oocyte recovery rate between the MSC-injected and Vehicle-injected mares in any period (Table 7.1). The overall oocyte maturation rate was 55% (99/179) in old MSC mares and 53.7% (29/54) in old Vehicle mares. Similarly, there were no significant differences among periods in oocyte recovery, maturation or blastocyst rates within either old MSC- or vehicle-injected mares (Table 7.1).

Genetic Analysis

The MSC donor fillies had distinguishable mtDNA sequences. Genetic analysis of granulosa cells recovered from MSC-injected mares on TVA, pooled separately from the injected ovary and from the non-injected ovary, revealed no genomic chimerism and no mitochondrial chimerism, in the 16 samples analyzed.

Separate genetic analysis of the 5 fragments from each of the 6 ovaries injected with BM-MSCs and of the 6 contralateral (non-injected) ovaries of these same mares revealed no genomic or mitochondrial chimerism in any fragment. Ovaries from the

mares that received a second MSC injection 2 weeks before ovariectomy had no evidence of chimerism for either MSC donor.

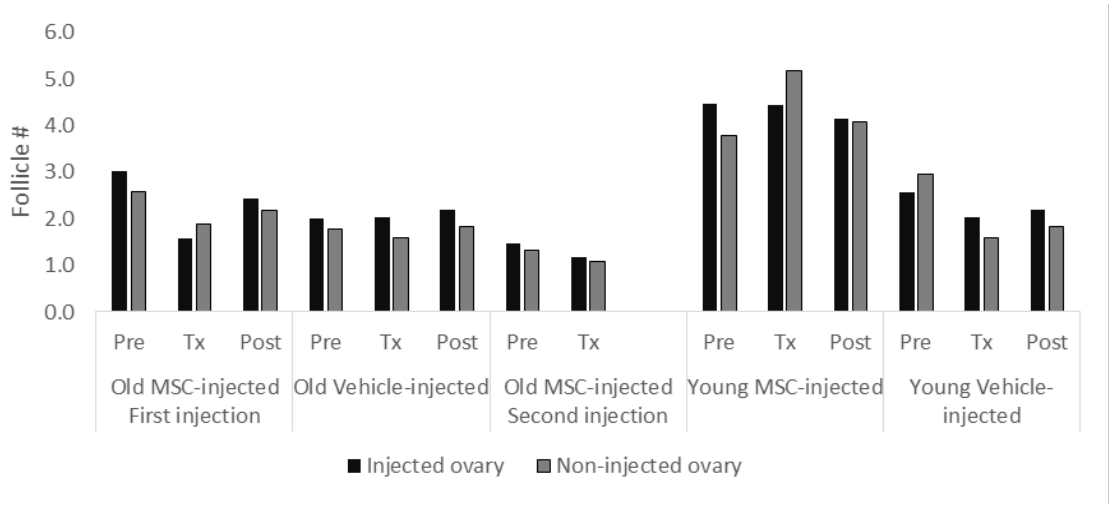

Figure 7.5 Mean follicle number in ovaries of MSC-injected and Vehicle-injected old and young mares over the period of the study. Pre-treatment period: the 8 weeks preceding the date of injection; Treatment: the 4 weeks following MSC-injection; Post-treatment: the 8 weeks after the Treatment period. Within mare group, there was no significant effect of period and there was no significant difference in follicle number between injected and non-injected ovaries ($P > 0.05$). Follicle graphs for individual mares are presented in Figures 7.6 to 7.10.

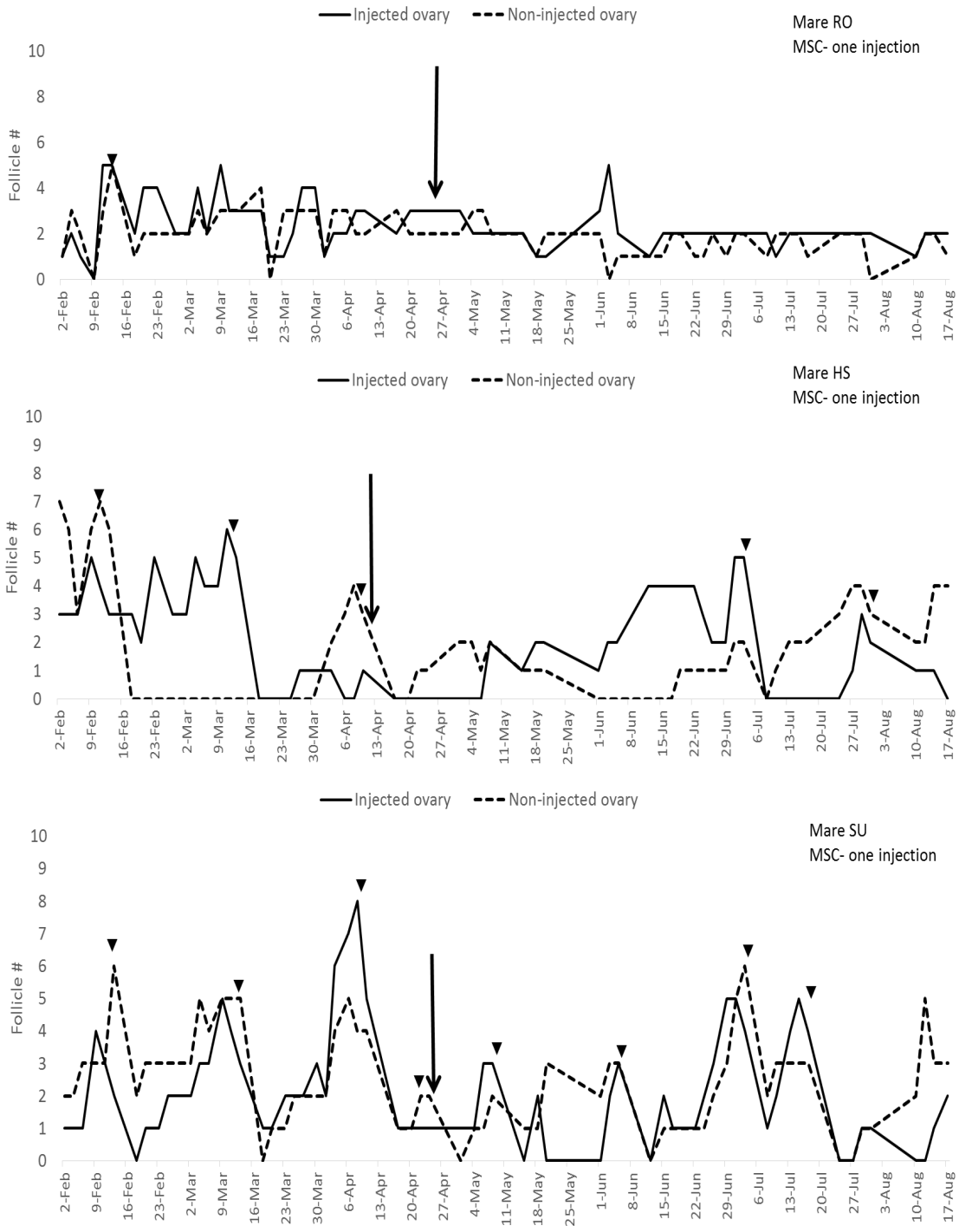

Figure 7.6 Follicle numbers of the injected and non-injected ovaries of old mares that received one MSC injection. Follicle numbers were those recorded during videotaping of ultrasound examinations. Arrows: dates on which MSC injections were performed. Arrow heads: dates on which TVAs were performed.

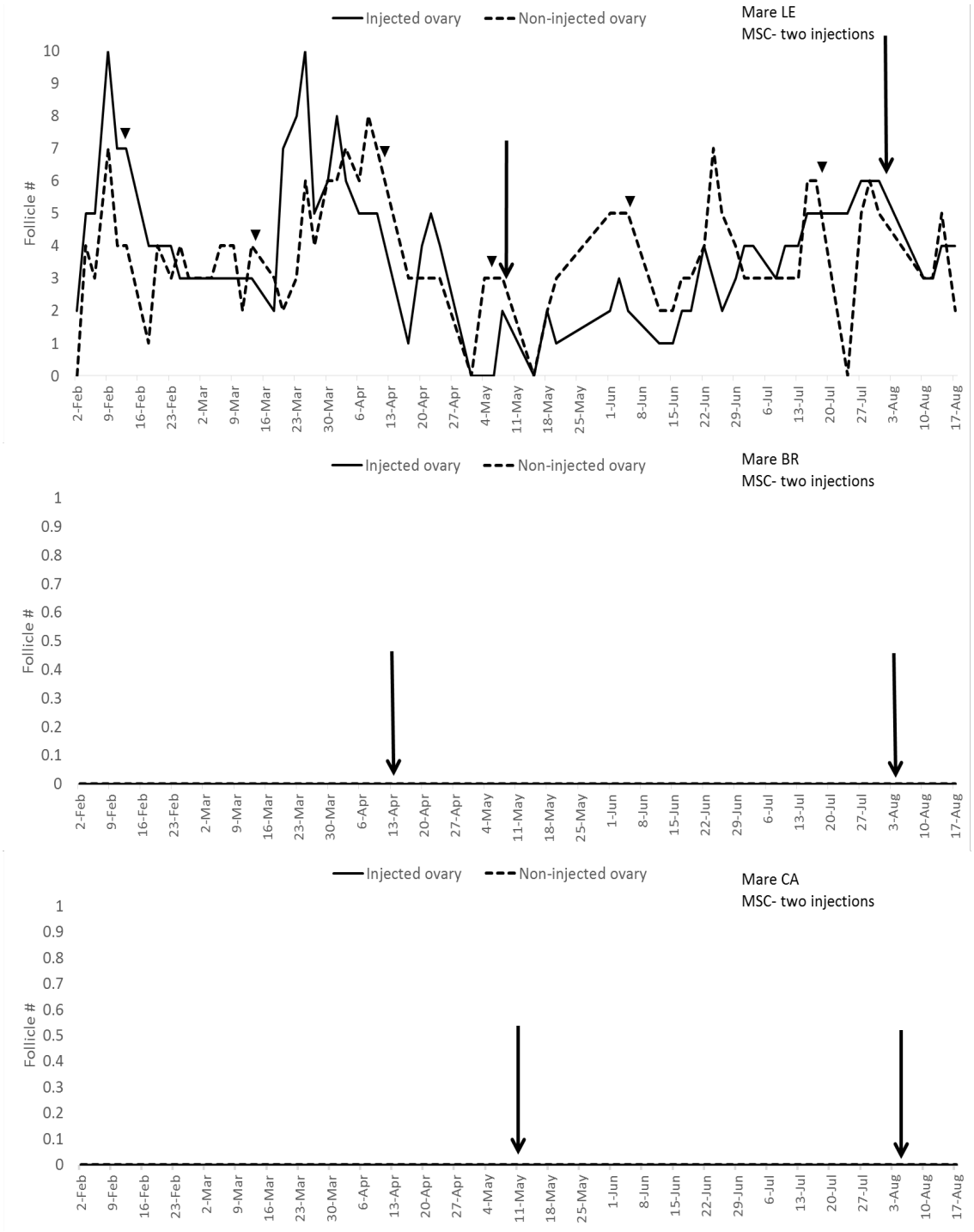

Figure 7.7 Follicle numbers of the injected and non-injected ovaries of old mares that received two MSC injections. Follicle numbers were those recorded during videotaping of ultrasound examinations. Arrows: dates on which MSC injections were performed. Arrow heads: dates on which TVAs were performed.

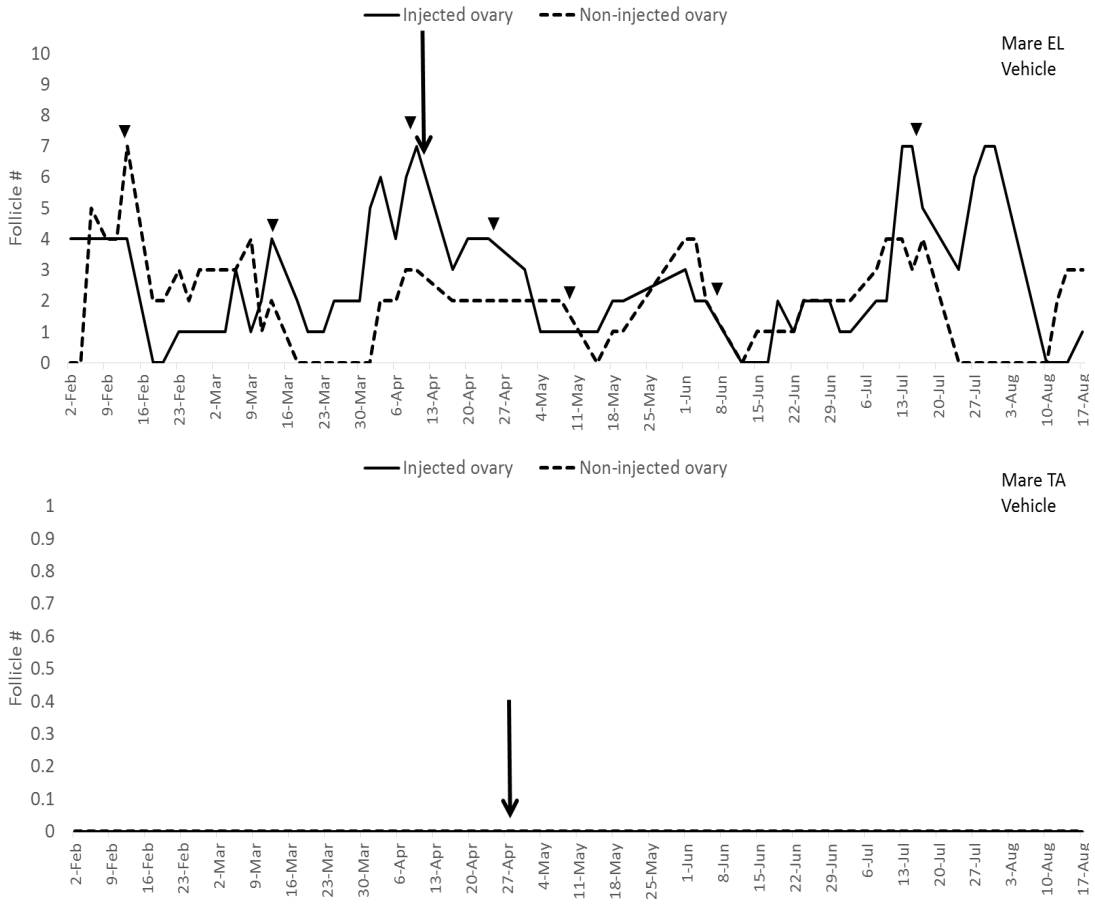

Figure 7.8 Follicle numbers of the injected and non-injected ovaries of old mares that received one vehicle injection. Follicle numbers were those recorded during videotaping of ultrasound examinations. Arrows: dates on which vehicle injections were performed. Arrow heads: dates on which TVAs were performed.

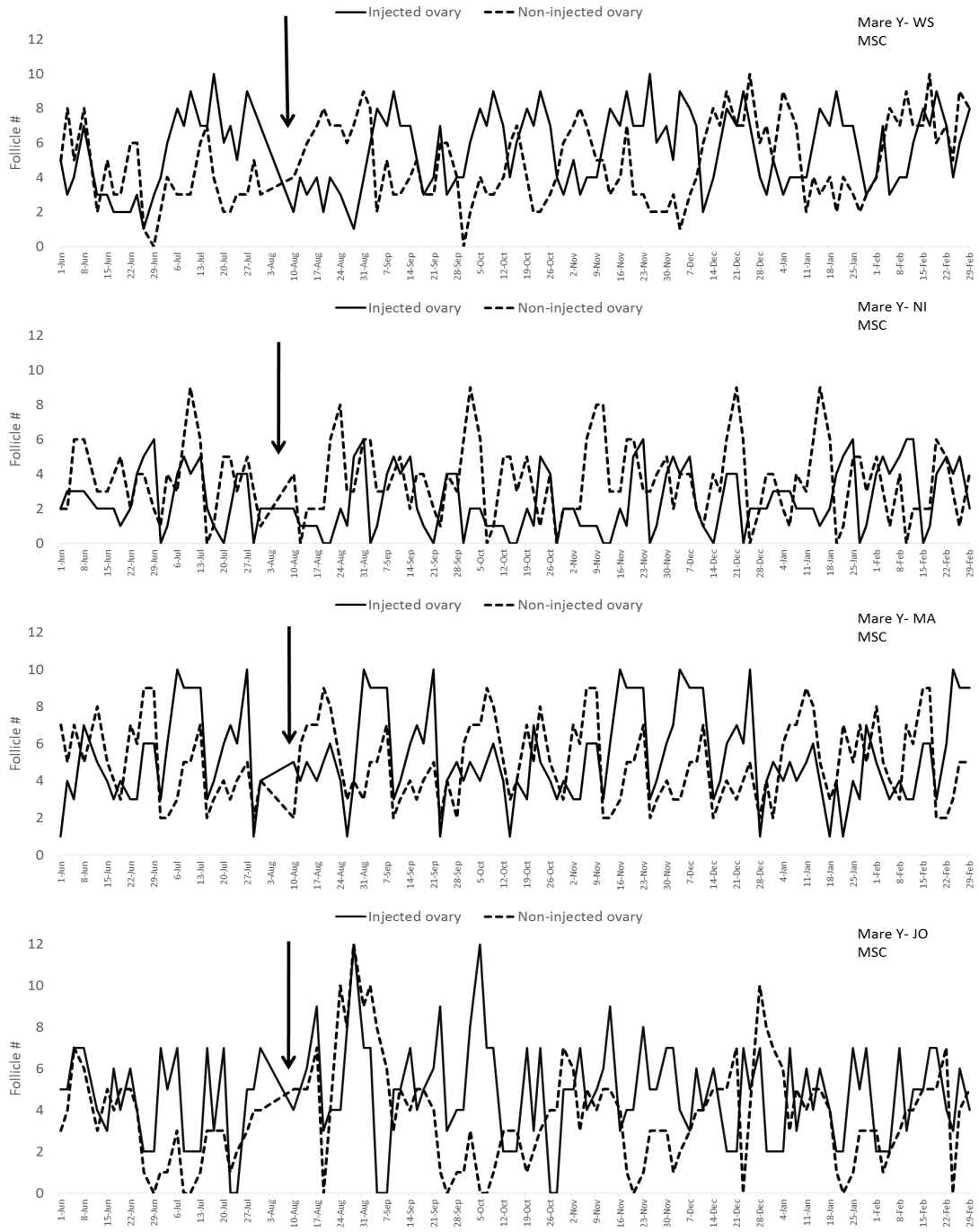

Figure 7.9 Follicle numbers of the injected and non-injected ovaries of young mares that received one MSC injection. Follicle numbers were those recorded during videotaping of ultrasound examinations. Arrows: dates on which MSC injections were performed. The ovarian activity of the mares continued to be assessed for 5 months after the Post-treatment period.

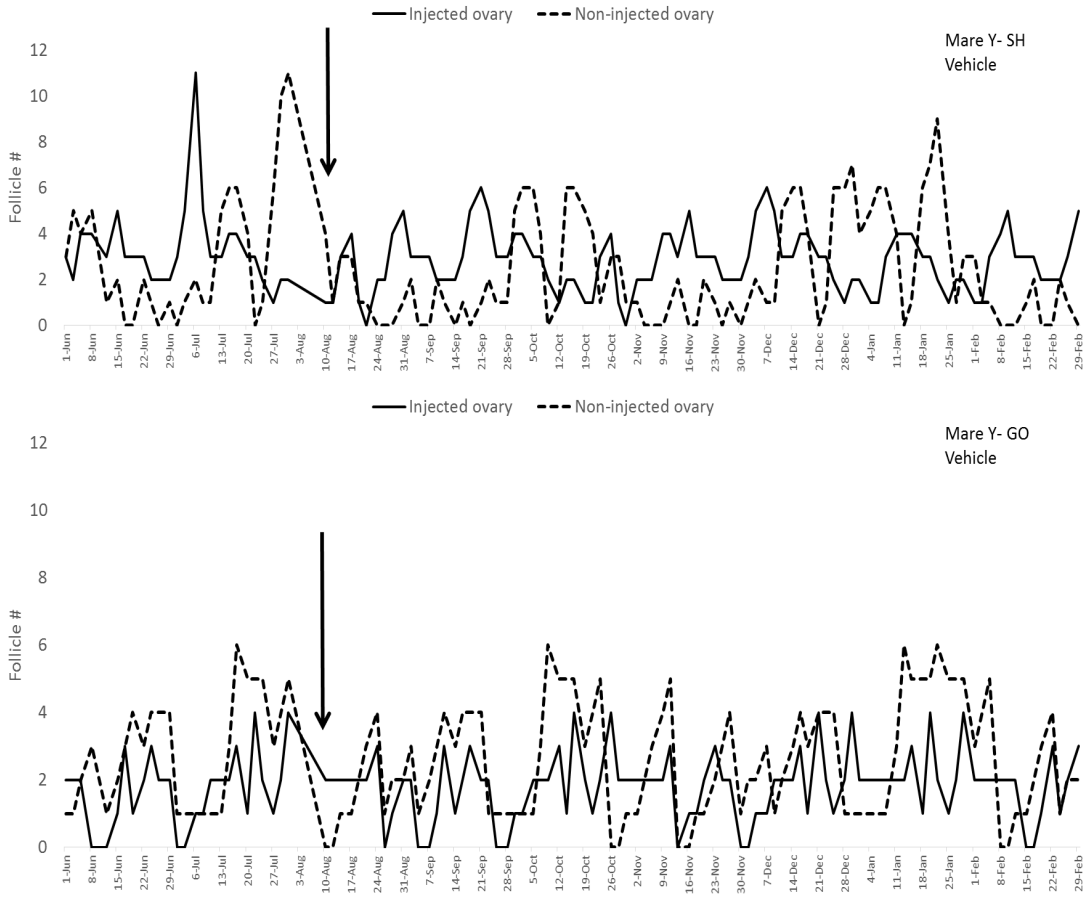

Figure 7.10 Follicle numbers of the injected and non-injected ovaries of young mares that received one vehicle injection. Follicle numbers were those recorded during videotaping of ultrasound examinations. Arrows: dates on which vehicle injections were performed. The ovarian activity of the mares continued to be assessed for 5 months after the Post-treatment period.

Table 7.1 Rates of oocyte recovery, *in vitro* maturation to metaphase II (MII), and blastocyst formation after ICSI of old MSC-injected and Vehicle-injected mares.

	MSC-injected			Vehicle-injected		
	Oocyte recovery	**Maturation to MII**	**Blastocyst**	**Oocyte recovery**	**Maturation to MII**	**Blastocyst**
Pre-treatment	56.1% (64/114)[a]	57.8% (37/64)[a]	29.7% (11/37)[a]	62.9% (17/27)[b]	58.8% (10/17)[b]	0/10[b]
Treatment	43.5% (10/23)[a]	50% (5/10)[a]	40% (2/5)[a]	45.5% (5/11)[b]	60% (3/5)[b]	0/3[b]
Post-treatment	59.5% (25/42)[a]	60% (15/25)[a]	13.3% (2/15)[a]	43.7% (7/16)[b]	85.7% (6/7)[b]	0/6[b]

There were no significant differences in oocyte recovery, maturation or blastocyst rates in either MSC-injected or Vehicle-injected mares among periods ($P > 0.05$).

Serum Hormone Levels

There was no significant difference in AMH, FSH or total estrogens among periods in old or young mares. Hormone concentrations for old and young mares throughout the study are presented in Figures 7.11 – 7.16. AMH values were reflective of follicle activity in the mares, in that the mares with no ovarian activity had basal AMH concentrations throughout the study, and AMH values for mares with follicle activity fell precipitously after ovariectomy (Figure 7.11). FSH values rose with the onset of the breeding season and were higher for mares with no follicular activity than for mares with follicular activity (Figure 7.12). Total estrogen levels tended to be higher in mares with follicular activity (Figure 7.13).

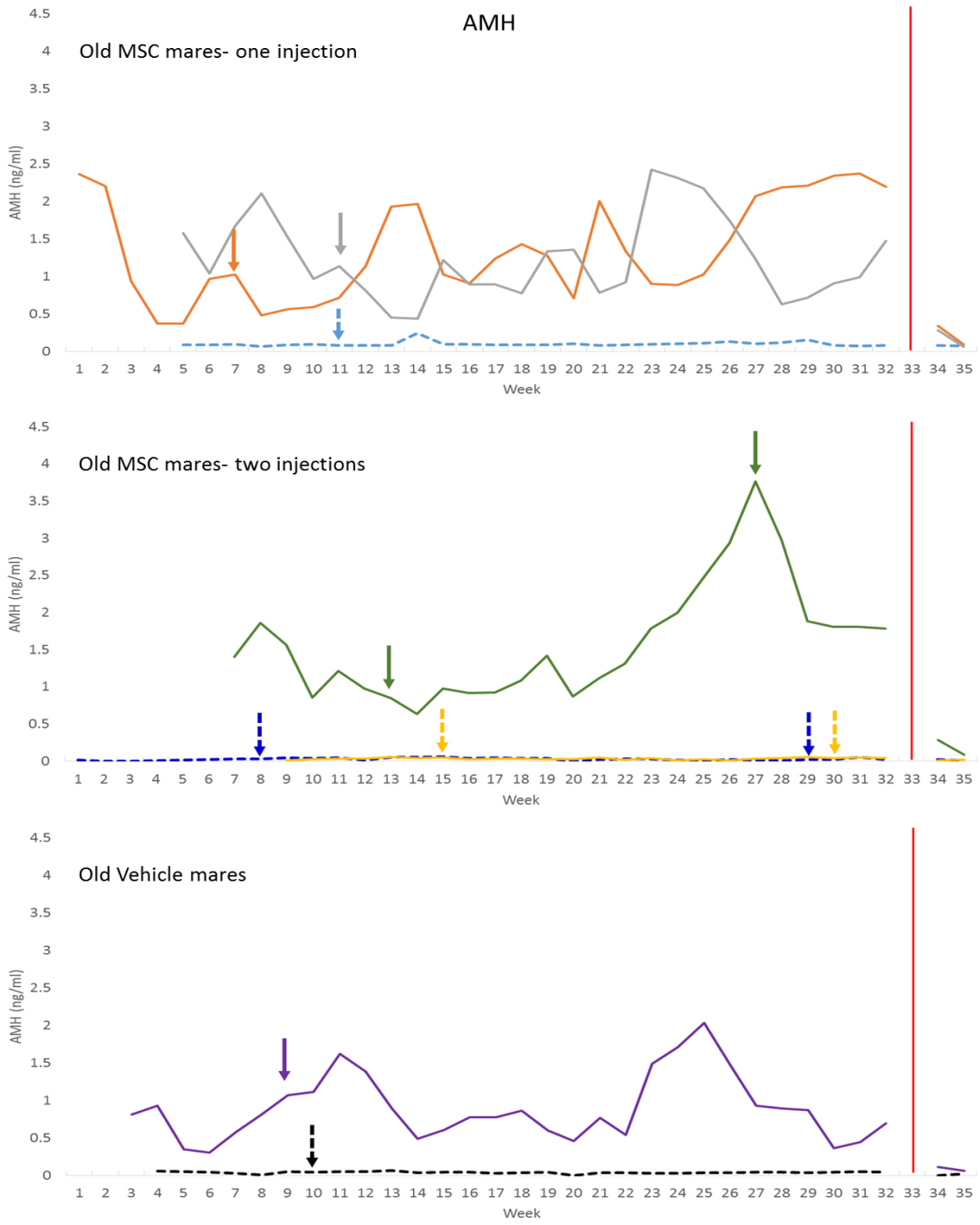

Figure 7.11 AMH concentrations for old mares injected once (top graph) or twice (middle graph) with MSCs or Vehicle (bottom graph). Solid lines: mares with follicular activity; Dashed lines: mares with no follicular activity; Arrows: dates on which injections were performed. Vertical line: date when ovariectomies were performed. Within mare group, there were no significant differences in AMH concentrations among the Pre-treatment, Treatment or Post-treatment periods.

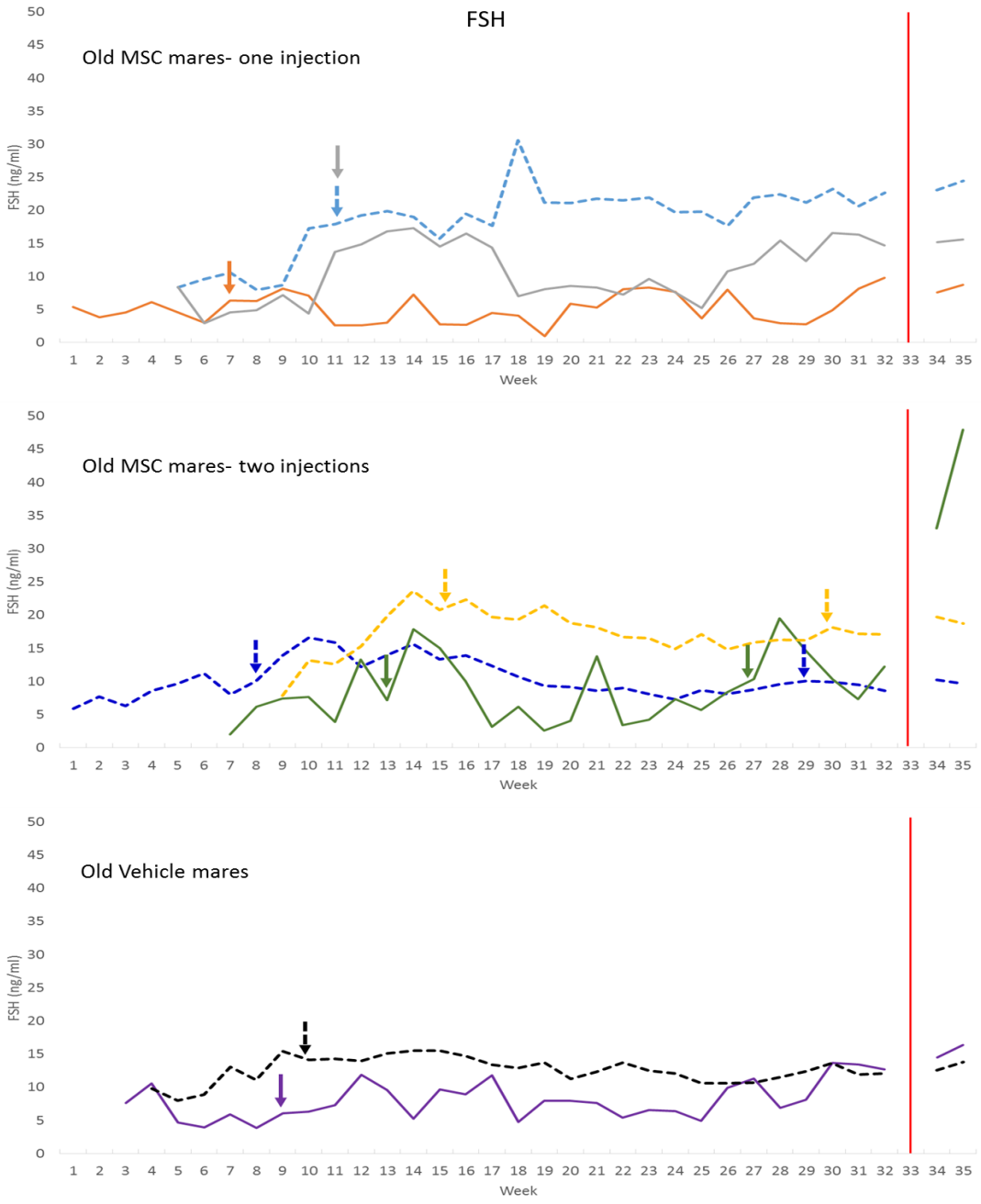

Figure 7.12 FSH concentrations for old mares injected once (top graph) or twice (middle graph) with MSCs or Vehicle (bottom graph). Solid lines: mares with follicular activity; Dashed lines: mares with no follicular activity; Arrows: dates on which injections were performed. Vertical line: date when ovariectomies were performed. Within mare group, there were no significant differences in FSH concentrations among the Pre-treatment, Treatment or Post-treatment periods.

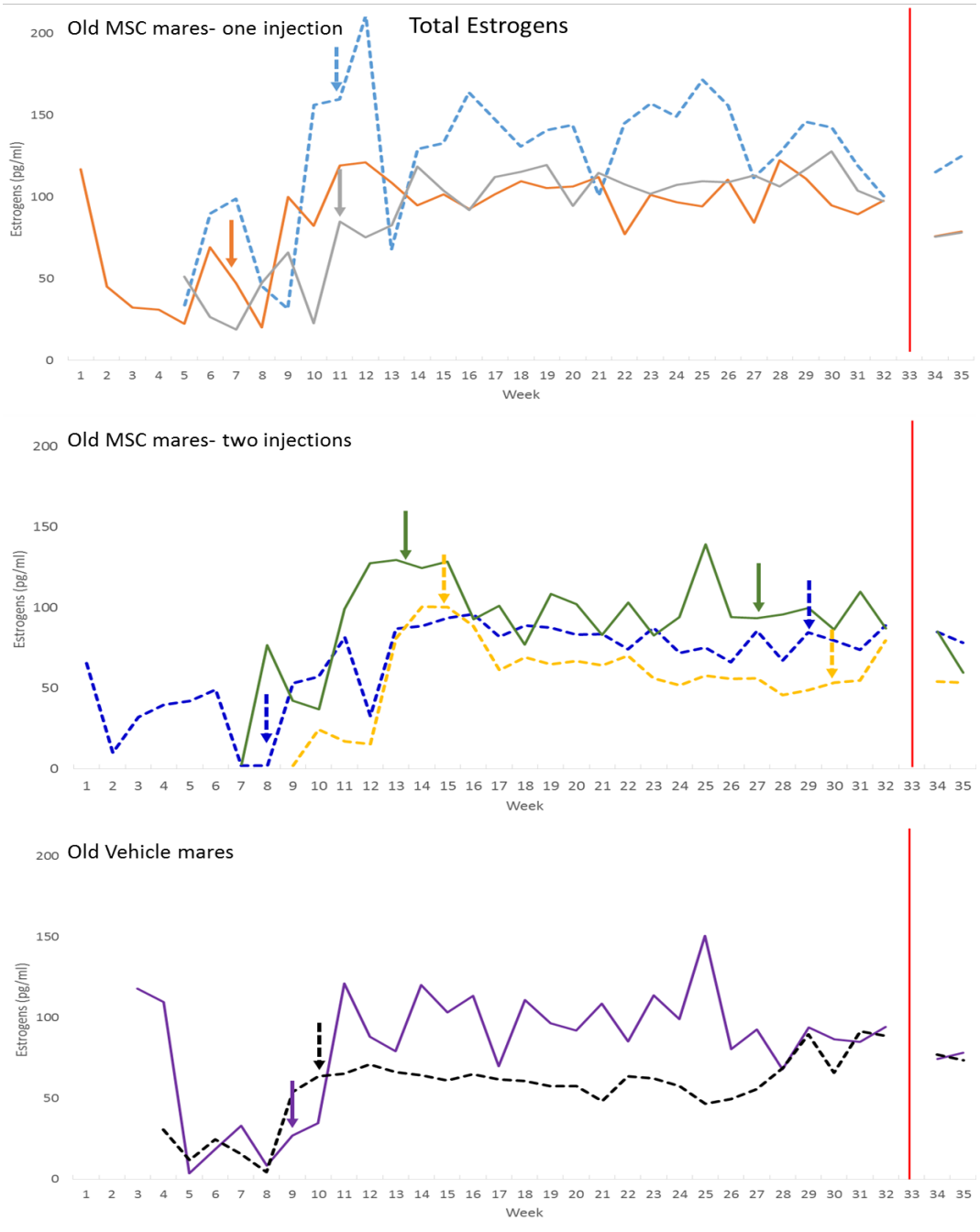

Figure 7.13 Total estrogens concentrations for old mares injected once (top graph) or twice (middle graph) with MSCs or Vehicle (bottom graph). Solid lines: mares with follicular activity; Dashed lines: mares with no follicular activity; Arrows: dates on which injections were performed. Vertical line: date when ovariectomies were performed. Within mare group, there were no significant differences in total estrogens concentrations among the Pre-treatment, Treatment or Post-treatment periods.

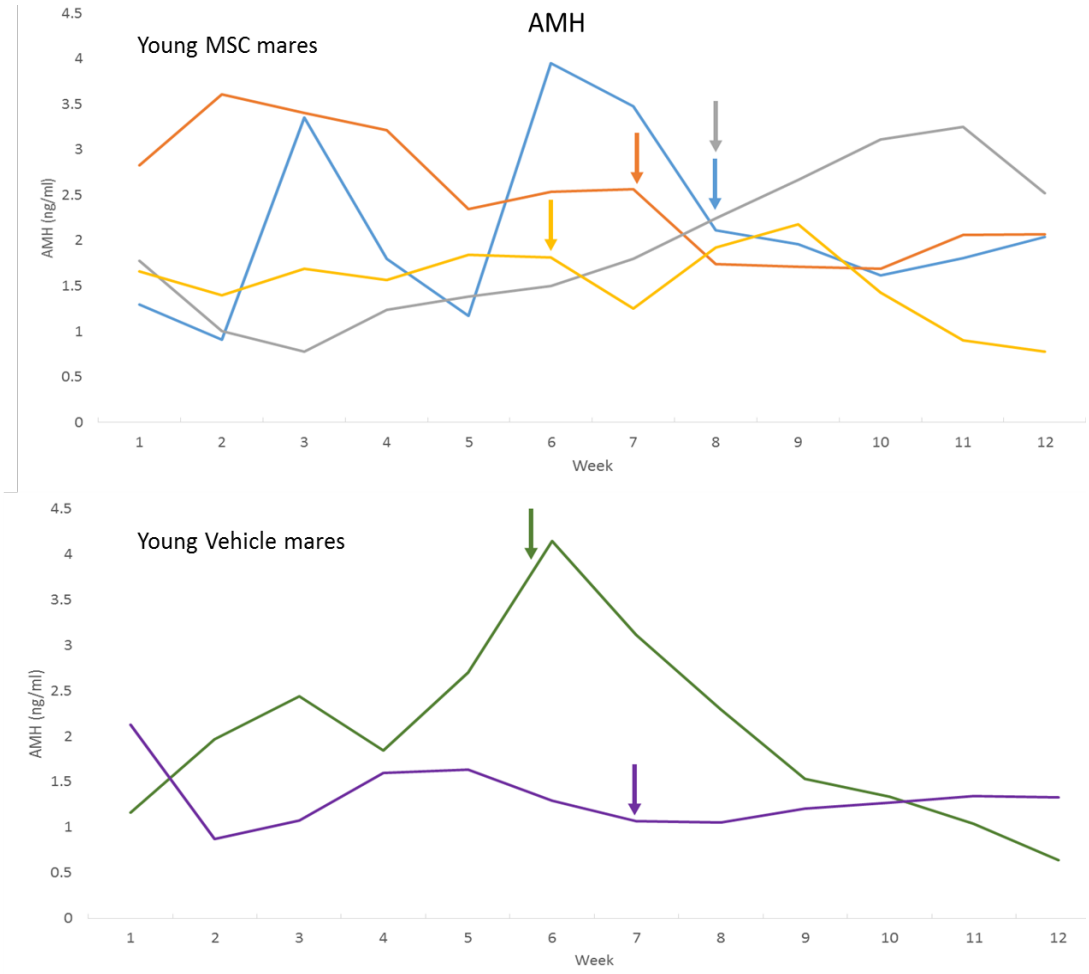

Figure 7.14 AMH for young mares injected with MSCs (top graph) or Vehicle (bottom graph). Arrows: dates on which injections were performed. Within mare group, there were no significant differences in AMH concentrations among the Pre-treatment, Treatment or Post-treatment periods.

Figure 7.15 FSH concentrations for young mares injected with MSCs (top graph) or Vehicle (bottom graph). Arrows: dates on which injections were performed. Within mare group, there were no significant differences in FSH concentrations among the Pre-treatment, Treatment or Post-treatment periods.

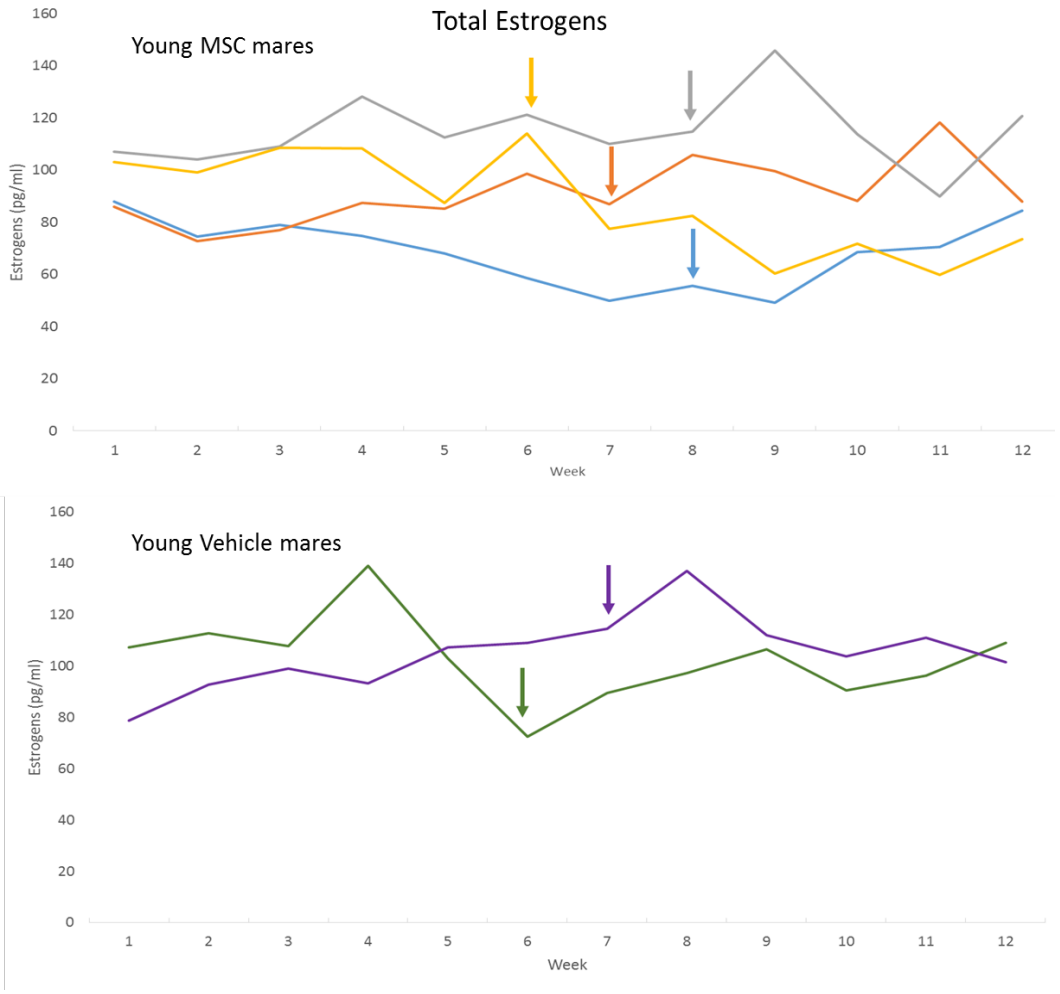

Figure 7.16 Total estrogens concentrations for young mares injected with MSCs (top graph) or Vehicle (bottom graph). Arrows: dates on which injections were performed. Within mare group, there were no significant differences in total estrogens concentrations among the Pre-treatment, Treatment or Post-treatment periods.

DISCUSSION

Supporting the preliminary study described in Chapter III, the results from this study indicate that intra-ovarian injections of allogeneic BM-MSCs are safe to perform in mares, as no detrimental effects were seen in mare health or ovarian status in injected mares. The exception to this is the abscess found in one ovary; this may have been related to either the MSC injections or the repeated TVAs. Abscess formation has been reported previously following TVA, but at a low incidence (~1 in 400 procedures) [305]. The small areas of granulation (scar tissue) found on histological examination of the ovarian tissue of the 8 old mares were considered to be of no significance by the pathologist. It is possible that these changes were intrinsic in these aged ovaries, or were the result of MSC injections, as this condition was observed in the ovaries of mares in which TVAs were not performed due to lack of follicles.

Injections of MSCs in other species have been associated with an improvement in ovarian function, as determined by an increase in ovarian follicles and fecundity, in females with ovaries compromised by chemotherapy [8-11, 262, 263]. In the preliminary study presented in Chapter III, there appeared to be a significant increase in follicle number 4 weeks after MSC injection in two randomly selected young mares. However, in the present study, there was no significant increase in follicle number after MSC injection in young or old mares. The ovarian activity of the young mares in the present study continued to be evaluated for 7 months after the injection, to detect any evidence of MSC stimulation of development of earlier-stage follicles, estimating 4 to 6 months

for growth from primordial to ovulatory follicle [22], but no increase in follicle numbers was seen during that time (Figure 7.9).

The lack of follicular response to MSC treatment is supported by the hormone concentrations, which were also not affected by MSC treatment. If MSCs had increased the number of growing follicles, we would have expected to see a concurrent increase in AMH, as concentrations of AMH are closely related to the total number of antral follicles present on the ovaries in mares, as in women [306]. Elevated FSH concentrations are a diagnostic finding in women with low follicle counts, as feedback from follicular inhibin is lost [307-309], and this is also true in other species such as cattle [310, 311]. The old mares that had no visible follicular activity on ultrasonography in the present study had correspondingly low AMH concentrations and high FSH concentrations.

Total estrogens were measured as this was the only commercial assay available to detect equine estrogen concentrations that we could identify; however, these values are less correlated with ovarian activity than are the AMH and FSH values. This assay is not specific for estradiol (the form of estrogen produced by antral follicles) and has a strong cross reactivity with adrenal estrogens; therefore, it is likely that much of the estrogen detected, including the high estrogen concentrations seen in the mare with no follicular activity, were not being produced by ovarian follicles but by another source, probably the adrenal glands. This is clearly shown by the persistence of moderate estrogen levels after ovariectomy.

The main question from evaluating the preliminary and main studies is: why did the two mares in the preliminary study have significantly higher follicle activity in the 4 weeks after MSC injection, whereas neither the old nor young mares in the main study showed an effect? One possible explanation for the lack of follicular number increase in the present study is that the mares in the preliminary study received two MSC injections (one in each ovary), i.e., in total they received twice the number of cells as the mares in the main study. Further research is needed to determine if there is an optimal number of cells needed to induce changes in follicle number. Another possible explanation is that the source of the MSCs used in the preliminary study and in the main study differed. The MSCs used in the preliminary study were obtained from a sexually-mature (7 yr) mare, whereas the MSCs used in the main study were obtained from two yearling fillies. We used these fillies as we felt that in young mares, MSC numbers in the BM aspirates would be higher, the cells would proliferate more readily, which was important as we had to produce sufficient cells for 13 injections, and the cells may have more stem-like properties. We used two different donor fillies in case there was a donor specific-effect. Unfortunately, by the time we obtained the results of the main study showing a lack of effect, the donor used in the preliminary study was no longer in the herd, and there were no remaining MSCs from that mare. Further research is needed to determine if MSCs from some categories of horses, or some individual donors, elicit changes in follicle numbers while MSCs from other donors do not.

The lack of donor MSC genomic DNA and mitochondrial chimerism detected in the ovaries of the old mares suggests that the injected MSCs did not persist or multiply

within the ovary; lack of chimerism in ovaries of mares injected two weeks before ovariectomy suggest that the MSCs do not persist for even this period. However, it is possible that MSCs were present in the ovarian tissue but at levels that were below the threshold detectable by the PCR performed.

We evaluated mitochondrial chimerism as it has been suggested that mitochondria from MSCs may be transferred to host cells [199]. Human alveolar epithelial cells with defective mitochondria or mutated mtDNA, which had rendered them incapable of aerobic respiration and growth, acquired functional mitochondria and regained their ability to propagate exponentially following 14 days of co-culture with human BM-MSCs [199]. Genetic analysis of the cells demonstrated the presence of mtDNA from the MSCs. As discussed in Chapter II, mitochondrial dysfunction and mtDNA mutations are thought to be a contributing factor or a hallmark of mammalian oocyte aging [95-100]. Therefore, transfer of mitochondria or mtDNA from the injected MSCs could have served to rescue or improve their function.

We also attempted to determine if MSCs colonize the ovary by labeling the cells with fluorescent nanoparticles (QDs) and then identifying cells containing these particles after ovary removal two weeks after injection. However, examination of ovarian sections in these mares post-ovariectomy did not reveal the presence of QDs. It is not possible to determine where the QD-labeled MSCs were injected, so the possibility exists that QDs were present and localized only to the area of injection, and were not in the examined ovarian sections. Although equine BM-MSCs have been shown to migrate *in vitro*, these

cells have been found to remain close to their site of injection following *in vivo* injection into artificially-induced tendon lesions [281].

In rat, mouse and rabbit ovaries damaged by chemotherapy, injection of MSCs increases ovarian function as indicated by an increase in follicle numbers [10, 11, 262]. However, in the present study there was no increase in follicle numbers following MSC injection. It is possible that MSCs have a different effect on chemotherapy-treated ovaries than in aged ovaries, or that rodent and rabbit ovaries react differently to MSCs than do equine ovaries.

It has also been reported that in rat and mouse ovaries damaged by chemotherapy, injection of MSCs induces changes in mRNA expression [10, 11]. Therefore we performed the study presented in Chapter VIII to determine if injection of BM-MSCs induces changes in gene expression in equine ovaries.

CHAPTER VIII

EFFECT OF INTRA-OVARIAN INJECTION OF BONE MARROW-DERIVED MESENCHYMAL STEM CELLS ON EQUINE OVARIAN GENE EXPRESSION

INTRODUCTION

Mesenchymal stem cells (MSCs) secrete factors that have the potential to affect follicular growth in ovaries; these include *Hgf* (hepatocyte growth factor), which induces angiogenesis and tissue regeneration [266], *Vegf* (vascular endothelial growth factor), which induces proliferation and migration of vascular endothelial cells and which has been found to inhibit apoptosis of rat cumulus cells [265], and *Igf1* (insulin-like growth factor 1), which is involved in mediating growth and development and has been shown to stimulate the proliferation of porcine cumulus cells [267]. Thus the possibility exists that injection of MSCs into ovaries could improve ovarian function. This has in fact been demonstrated repeatedly in ovaries damaged by chemotherapy. Protein and mRNA expression of *Hgf, Vegf,* and *Igf1* were higher in chemotherapy-damaged rat ovaries that had been injected with adipose-derived MSCs; additionally, expression of *Star* (steroidogenic acute regulator), which enhances the conversion of cholesterol to pregnenolone, was also increased [10]. Injection of ovaries with umbilical cord MSCs returned the RNA expression pattern of chemotherapy-damaged mouse ovaries back to that of control ovaries, and rescued the expression of important proteins from the aldo-keto reductase family 1, which catalyze the conversion of progesterone to 20-alpha

dihydroprogesterone [11]. These changes were associated with increased ovarian activity and fecundity in the MSC-treated mice and rats [10, 11].

The above-referenced studies indicate that intra-ovarian or systemic injection of MSCs in females with ovaries compromised by chemotherapy induces expression of mRNA and proteins that may improve ovarian function. However, little information is available on the effect of MSCs on gene expression of ovaries from old females. In the main study of this dissertation (detailed in Chapter VII), 8 old mares received intra-ovarian injections, in 1 ovary only, of MSCs or vehicle. The ovaries of these mares were removed via colpotomy and RNA sequencing was performed on the ovarian tissue to determine differences in gene expression between MSC-injected and vehicle-injected ovaries, and between these ovaries and the contralateral, non-injected, ovaries.

MATERIALS AND METHODS

In the study described in Chapter VII, intra-ovarian injections were performed in 8 old mares; of these, 6 mares had 1 ovary injected with MSCs and 2 mares had 1 ovary injected with vehicle. Of the 6 mares that had 1 ovary injected with MSCs, 3 mares received a second MSC injection into the same ovary 12 to 17 weeks after the first injection (MSC2 mares). Two weeks after the second injection to MSCs mares, both ovaries of all 8 old mares were removed by ovariectomy via colpotomy and ovarian tissue was processed as detailed in Chapter VII.

Samples

Samples were obtained by combining 5 tissue sections from each ovary, providing one combined sample for each ovary. This resulted in 3 samples from old mare ovaries injected once with MSCs (MSC1) and 3 samples from the contralateral ovaries of these mares (MSC1opp); 3 samples from old mares injected twice with MSCs (MSC2) and 3 samples from the contralateral ovaries of these mares (MSC2opp); 2 samples from old mares injected once with vehicle (V) and 2 samples from the contralateral ovaries of these mares (Vopp).

RNA Isolation and RNA-Sequencing

Isolation of RNA from pulverized ovarian tissues was performed by the Texas A&M Institute for Genomic Sciences and Society (TIGSS) as described in Chapter VI. The RNA samples were submitted to the Texas A&M AgriLife Genomics and Bioinformatics core for generation of RNA-Sequencing (RNA-Seq) libraries and for RNA-Seq reactions. RNA-Seq libraries were generated using the TruSeq RNA preparation kit (Illumina) with a polyA selection step; polyA mRNA was fragmented and reverse-transcribed to cDNA for sequencing. The samples were sequenced (50-base-pair, single-end sequencing) on 8 sequencing lanes of a HiSeq 2500 (Illumina).

Gene Expression Analysis

The raw data from the RNA-Seq reactions was processed by the TIGSS. Briefly, A total of 1.36 billion reads were checked to trim any adapter sequences and low quality

bases using Trimmomatic [312], resulting in approximately 1.31 billion filtered reads (96%) out of which a total of 1.18 billion filtered reads (approximately 87%) mapped to the equCab2 genome assembly. All samples had Phred scores > 20. The quality of the bases is determined by a Phred score, which represents the probability that a given base call is incorrect. Quality scores range from 4 to 60, with higher values corresponding to higher quality; the scores are linked to error probabilities. A Phred score of 20 represents a 1 in 100 probability that the base is called wrong, i.e., a 99% accuracy of the base call. High quality bases are those with a Phred score ≥ 20 [313]. Read mapping was performed using HISAT version 2.0.5 [314]. HTSeq [315] was used to generate raw read counts per gene using intersection-nonempty parameters to account for ambiguous read mappings. Differential gene expression tests were then performed using DESeq2 [316]; differentially expressed genes were defined as those having a false discovery rate (FDR) ≤ 0.5 and log2FC +/- 1. Plots were generated using R programming language.

Biological pathway analysis was performed by the PI at the Equine Embryo Laboratory, using the Ingenuity Pathway Analysis tool-kit (QIAGEN, Venlo, Netherlands; www.ingenuity.com Application Build 261899, Content Version 18030641).

RESULTS

Analysis of Gene Expression

To determine the effects of MSCs on equine ovarian gene expression, we first compared the gene expression of MSC1 (injected once with MSCs) ovaries to V

(injected once with vehicle) ovaries. There were 93 significantly different genes with 57 upregulated and 36 downregulated in MSC1 ovaries compared to V ovaries, and these two groups shared 1270 genes in common (Figure 8.1). Pathway analysis revealed biological processes involving cell-to-cell signaling and interaction (17 genes), small molecule biochemistry (14 genes), cellular assembly and organization (12 genes), cellular function and maintenance (12 genes), and lipid metabolism (9 genes; Table 8.1). The twenty most highly differentially-regulated genes between MSC1 and V ovaries are presented individually in Table 8.2.

To determine if the injected MSCs may have a systemic effect, we compared the gene expression between MSC1opp (contralateral ovary of MSC1 mares) and Vopp (contralateral ovary of V mares) ovaries. There were 286 significantly different genes with 75 upregulated and 211 downregulated in MSC1opp ovaries compared to Vopp ovaries, and these two groups shared 2135 genes in common (Figure 8.3). Pathway analysis revealed biological processes involving cellular development (64 genes), cell morphology (61 genes), cellular growth and proliferation (56 genes), cellular assembly and organization (44 genes), and cell cycle (37 genes; Table 8.3). The twenty most highly regulated genes between MSC1opp and Vopp ovaries are presented individually in Table 8.4.

To determine whether there were differences in the acute and long-term effects of MSC injection, we compared gene expression between MSC2 (injected twice with MSCs) and MSC1 ovaries. There were 261 significantly different genes with 200 upregulated and 61 downregulated in MSC2 ovaries as compared to MSC1, and these

two groups shared 1618 genes in common (Figure 8.5). Pathway analysis revealed biological processes involving cellular function and maintenance (85 genes), cell-to-cell signaling and interaction (84 genes), cellular movement (76 genes), cellular development (75 genes), and cellular growth and proliferation (72 genes; Table 8.5). The twenty most highly regulated genes in MSC2 ovaries are presented individually in Table 8.6.

All the differentially-expressed genes identified for each of the comparisons mentioned above are presented, in alphabetical order, in Appendix Tables A-2 to A-4. The complete list of identified genes in each group is given in Supplementary Table S-1.

Other comparisons were reviewed to detect any pronounced differences in gene expression; the most prominent was *Tac1* (tachykinin precursor). This gene, which was the most highly upregulated gene in MSC2 ovaries vs MSC1 ovaries (Table 8.6), was also the most highly upregulated gene in MSC2 ovaries vs V ovaries (3.99, 1.81E-15; log2FC, P-value, respectively; Figure 8.4), and in MSC2opp (contralateral ovary of MSC2 mares) vs Vopp ovaries (3.70, 1.72E-13; Figure 8.5).

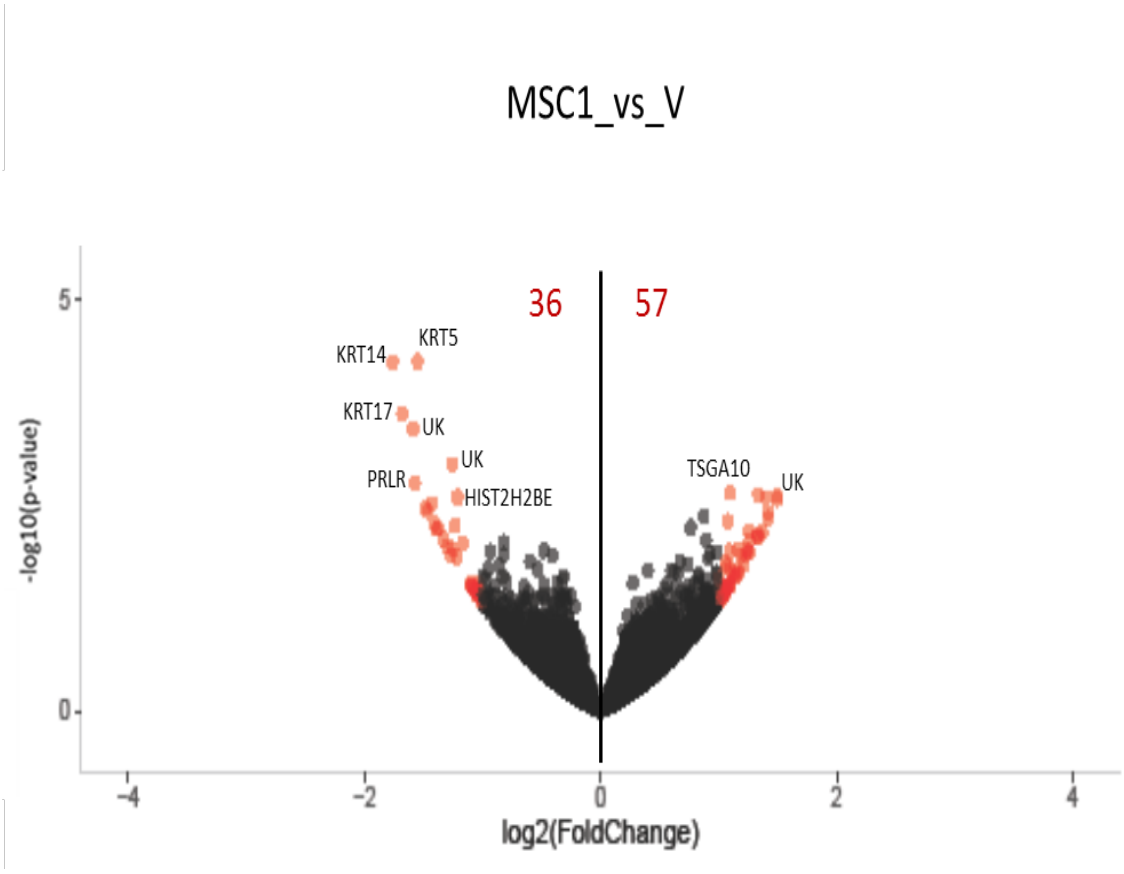

Figure 8.1 Volcano plot of upregulated and downregulated genes in ovaries injected once with MSCs (MSC1) compared to ovaries injected once with Vehicle (V). There were 57 upregulated genes and 36 downregulated genes. The 10 most differentially-regulated genes are given in the figure: KRT (keratin 5, 14, and 17); PRLR (prolactin receptor); TSGA10 (testis specific 10); HIST2H2BE (histone cluster 2 H2B family member e). Unknown gene products are designated by "UK."

Table 8.1 Biological processes representative of the top five functional annotation clusters among genes differentially expressed in ovaries injected once with MSCs (MSC1) versus ovaries injected once with Vehicle (V).

			Genes	
Biological Process	**Gene count**	**P-value**	**Upregulated**	**Downregulated**
Cell-to-cell signaling and interaction	17	3.65E-05	*CNTN5, CTNND2, ERBB4, GRM5, IL33, LRRTM2, MSLN, NR1H4, SEMA3E, TLR1*	*ADCY1, ASGR1, CAMSAP3, CCR3, KRT17, PIGR, PRLR*
Cellular assembly and organization	12	2.97E-04	*CNTN5, CTNND2, ERBB4, GRM5, IL33, KCNK2, LRRTM2, SEMA3E, NR1H4*	*CAMPSAP3, PRLR, HIST2H2BE*
Cellular function and maintenance	12	2.97E-04	*CTNND2, ERBB4, GRM5, LRRTM2, IL33, SEMA3E, SLC1A2, SLC4A9,*	*ASGR1, CAMSAP3, PIGR, SCNN1G*
Lipid metabolism	9	4.68E-04	*AKR1D1, ERBB4, GRM5, IL33, NR1H4, TLR1*	*CCR3, DPEP2, PRLR*
Small molecule biochemistry	14	4.68E-04	*AKR1D1, CNTNAP5, ERBB4, GRM5, NR1H4, IL33, SLC1A2, TLR1*	*ADCY1, CCR3, DPEP2 KRT14, NMNAT2, PRLR,*

Table 8.2 The twenty most differentially-expressed genes identified by DESeq2 in MSC1 ovaries compared to Vehicle-injected ovaries.

Gene symbol	Log2FC	P-value	Gene description
KRT5	-1.55	5.70E-05	keratin 5
KRT14	-1.76	5.80E-05	keratin 14
KRT17	-1.68	2.47E-04	keratin 17
PRLR	-1.57	1.72E-03	prolactin receptor
TSGA10	1.10	2.24E-03	testis specific 10
HIST2H2BE	-1.21	2.53E-03	histone cluster 2 H2B family member e
CNTN5	1.40	2.55E-03	contactin 5
CISH	-1.43	3.03E-03	cytokine inducible SH2 containing protein
ASB15	-1.48	3.42E-03	Ankyrin repeat and SOCS box containing 15
DCST2	1.42	4.59E-03	DC-STAMP domain containing 2
RASSF9	1.07	4.98E-03	Ras association domain family member 9
RNF17	-1.41	5.39E-03	ring finger protein 17
EPS8L3	1.26	6.71E-03	EPS8 like 3
MSLN	1.37	6.76E-03	mesothelin
ERBB4	1.34	7.10E-03	erb-b2 receptor tyrosine kinase 4
SLC4A9	1.32	7.66E-03	solute carrier family 4 member 9
ADCY1	-1.17	9.33E-03	adenyl cyclase 1
TLR1	1.09	1.14E-02	toll like receptor 1
IL33	1.25	1.16E-02	interleukin 33
ACVR1C	1.26	1.20E-02	activing A receptor type 1C

FC fold-change.

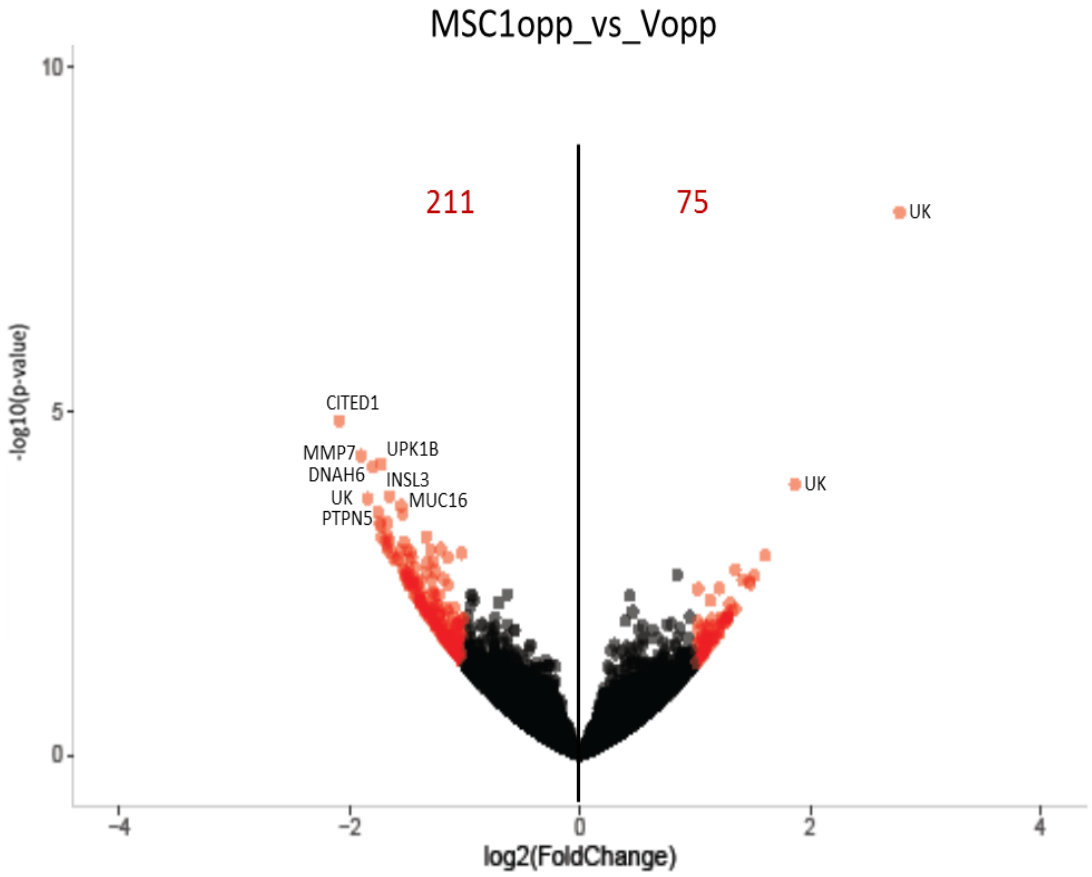

Figure 8.2 Volcano plot of upregulated and downregulated genes in MSC1opp ovaries compared to Vopp ovaries. There were 75 upregulated genes and 211 downregulated genes. The 10 most differentially-regulated genes are given in the figure: CITED (Cnp/p300 interacting transactivator with Glu/Asp rich carboxy-terminal doimain 1); MMP7 (matrix metallopeptidase 7); UPK1B (uroplakin 1B); DNAH6 (dynein axonemal heavy chain 6); INSL3 (insulin like 3); MUC16 (mucin 16); PTPN5 (protein tyrosine phosphatase, non-receptor type 5). Unknown gene products are designated by "UK."

Table 8.3 Biological processes representative of the top five functional annotation clusters among genes differentially expressed in MSC1opp versus Vopp ovaries.

			Genes	
Biological Process	**Gene count**	**P-value**	**Upregulated**	**Downregulated**
Cellular development	64	1.11E-08	*ADAD1, FABP7, FGL1, FOXC2, , HSF4, IL22RA1, IL2RG, ITIH4, LTB, NOV*	*ADAMTS9, AQP5, BMP7, BNC1, BUB1, CCNB2, CDCA5, CDH1, CDHR2, CDKN3, CITED1, CLDN2, COL1A1, CXADR, DPP4, DSC1, DSP, E2F1, EHF, EPHA1, ESRP1, ESRP2, FGF5, FOXJ1, FOXM1, FST, GABRP, GGT1, GRHL2, HMMR, HPN, INHA, INHBB, INSL3, KIF20A, LPAR3, LRP8, MMP7, MUC16, MUC4, OPRK1, PAX8, PCLAF, PKP3, PPP1R1B, PRLR, PTPRQ, RAB25, SP6, ST14, TNC, UPK1B, WFDC2, WWC1*
Cell cycle	37	5.94E-07	*IL2RG, UBD*	*ANLN, BMP7, BUB1, BUB1B, CEP55, CCNB2, CCNB3, CDC20, CDCA5, CDH1, CDKN3, CENPF, CKAP2, COL1A1, DPP4, DUOXA1,E2F1, EHF, EXO1, FOXM1, HJURP, HMMR, INHA, KIF11, KIF20A, MIS18A, PAX8, PCLAF, PKMYT1, PRC1, PRR11, TNC, TOP2A, WWC1*
Cell morphology	60	1.03E-06	*CD36, CD8B, FGL1, FOXC2, HSF4, IL2RG, IL33, LTB, MPO, MYOC, NOV, PRKG2,*	*AP1M2, AQP5, BMP7, BNC1, BUB1, CADPS, CDH1, CLDN2, CNTN2, COL1A1, COL3A1, CX3CR1, CXADR, CYP17A1, DKK2, DPP4, E2F1, ELOVL3, EXO1, FCMR, FOXJ1, FOXM1, FST, GRHL2, GRIN3A, HPN, INHA, INHBB, KIF11, KIF20A, LPAR3, LRP8, MUC4, NEFH, NRCAM, PAX8, PCLAF, PIGR, PRLR, PTPRQ, SERINC2, SLC2A2, SLC4A4, SP6, SPTA1, SPTBN2, ST14, TNC*
Cellular growth and proliferation	55	2.55E-06	*ADAD1, FABP7, FGL1, FOXC2, HSF4, IL22RA2, IL2RG, ITIH4, LTB, , NOV*	*AQP5, BMP7, BNC1, BUB1, CCNB2, CDCA5, CDH1, CDKN3, CITED1, CLDN2, COL1A1, CXADR, DPP4, E2F1, EHF, EPHA1, ESRP1, ESRP2, FGF5, FOXM1, FST, GABRP, GGT1, GRHL2, HMMR, HPN, INHA, INHBB, INSL3, KIF20A, LPAR3, LRP8, MMP7, MUC16, MUC4, PAX8, PCLAF, PKP3, PPP1R1B, PRLR, PTPRQ, SP6, TNC, WFDC2, WWC1*
Cellular assembly and organization	44	1.09E-05	*FOXC2, IL33, MYOC*	*ADCY1, AQP5, BMP7, BUB1, BUB1B, CAMSAP3, CCDC113, CCNB2, CDC20, CDH1, CENPF, CKAP2, CNTN2, CNTN4, COL1A1, COL3A1, CXADR, DSP, EPHA8, ESRP2, EXO1, FOXJ1, FOXM1, FTCD, GRIN3A, HJURP, HMMR, KIF11, KIF20A, LRP8, MIS18A, MMP7, NEFH, NRCAM, PRC1, PTPRQ, SPTA1, SPTBN2, ST14, TNC, TOP2A*

Table 8.4 The twenty most differentially-expressed genes identified by DESeq2 in MSC1opp ovaries compared to Vopp ovaries.

Gene symbol	Log2FC	P-value	Gene description
CITED2	-2.09	1.38E-05	Cbp/p300 interacting transactivator with Glu/Asp rich carboxy-terminal domain 1
MMP7	-1.90	4.47E-05	matrix metallopeptidase 7
UPK1B	-1.73	5.85E-05	uroplakin 1B
DNAH6	-1.80	6.54E-05	dynein axonemal heavy chain 6
INSL3	-1.65	1.72E-04	insulin like 3
MUC16	-1.55	2.37E04	mucin 16, cell surface associated
PTPN5	-1.75	2.91E-04	protein tyrosine phosphatase, non-receptor type 5
LRRN4	-1.74	4.25E-04	leucine rich repeat neuronal 4
CILP	-1.73	4.62E-04	cartilage intermediate layer protein
UNC45B	-1.72	6.69E-04	unc-45 myosin chaperone B
OPRK1	-1.33	6.76E-04	opioid receptor kappa 1
PIGR	-1.65	7.58E-04	polymeric immunoglobulin receptor
MUC4	-1.53	8.22E-04	mucin 4, cell surface associated
SERINC2	-1.68	9.80E-04	serine incorporator 2
C6ORF118	-1.50	1.03E-03	chromosome 6 open reading frame 118
THAP12	-1.30	1.04E-03	THAP domain containing 12
DAW1	-1.56	1.07E-03	dynein assembly factor with WD repeats 1
FBXO47	-1.65	1.11E-03	F-box protein 47
ESRP2	-1.03	1.15E-03	epithelial splicing regulatory protein 2
BNC1	-1.15	1.31E-03	basonuclin 1

FC fold-change.

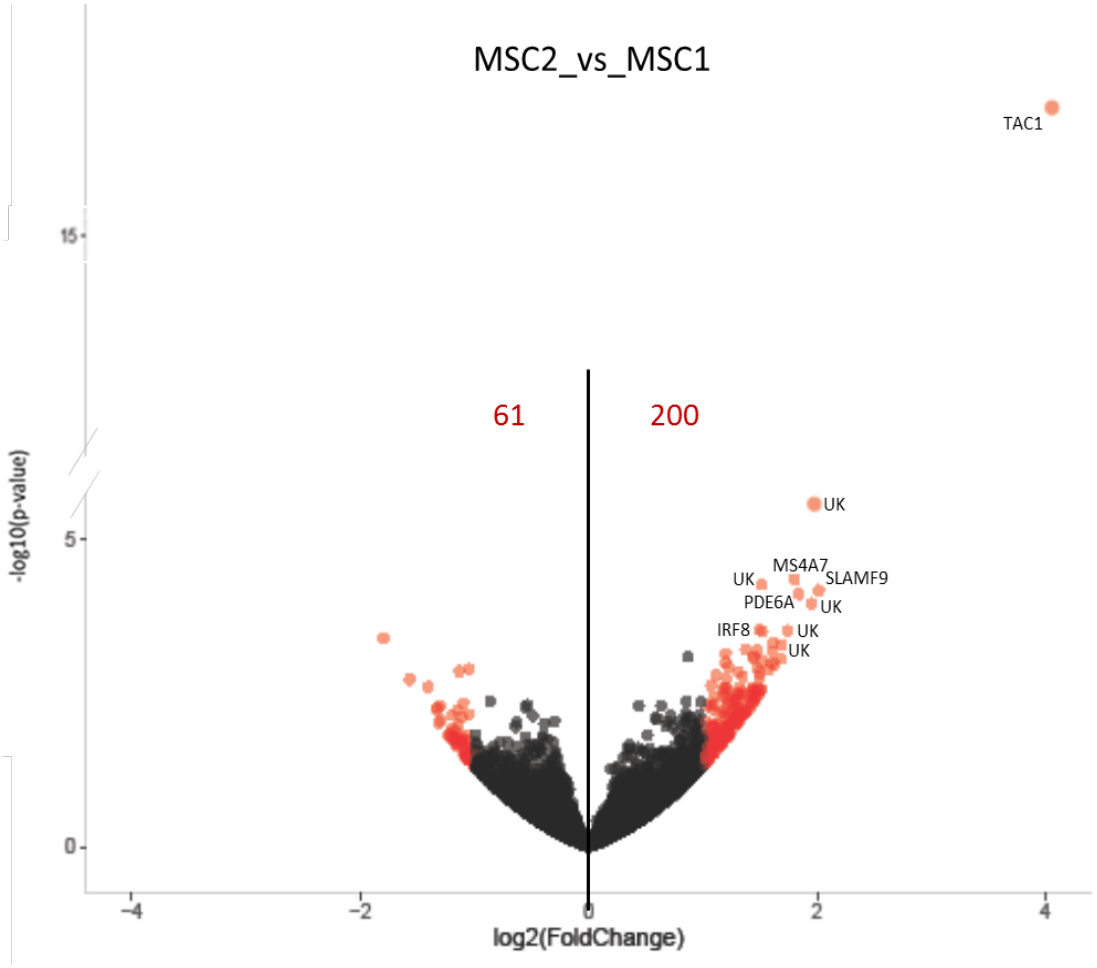

Figure 8.3 Volcano plot of upregulated and downregulated genes in ovaries injected twice with MSCs (MSC2) compared to ovaries injected once with MSCs (MSC1). There were 200 upregulated genes and 61 downregulated genes. The 10 most differentially-regulated genes are given in the figure: TAC1 (tachykinin precursor); MS4A7 (membrane spanning 4-domains A7); SLAMF9 (SLAM family member 9); PDE6A (phosphodiesterase 6A); IRF8 (interferon regulatory factor 8). Unknown gene products are designated by "UK."

Table 8.5 Biological processes representative of the top five functional annotation clusters among genes differentially expressed in ovaries injected twice with MSCs (MSC2) versus ovaries injected once with MSCs (MSC1).

			Genes	
Biological Process	**Gene count**	**P-value**	**Upregulated**	**Downregulated**
Cellular movement	76	6.23E-31	*ACP5, ALOX5, BATF, BTLA, C3AR1, CCL2, C5AR1, CASP1, CD86, CD300LB, CSF1R, CCR3, CX3CR1, CD48, CEBPE, CHI3L1, CLEC7A, CTSS, CXCL9, CXCL11, CYBB, EEF1A2, FCER1G, FLT3, GHSR, HCK, HCLS1, HMGA1, HPSE, IL10RA, IL1A, IL1RN, IRF5, IRF8, ITGAX, ITGB2, LCP1, LTF, MUC2, NCF4, NCKAP1L, P2RY12, POU2AF1, RAC2, RASGRP4, RGS1, SERPINB1, SLAMF8, ST14, TAC1, THBS1, TLR2, TLR7, TNFSF8, TNFSF9, TNFSF15, TREM2, TRPM2,TYROBP, UCP2, VAV1, VDR, XCR1*	*CAV3, CCL20, CHRM3 FOXC2, GFRA3, IL2, IL33, KCNMA1, KISS1, MEOX2, MPZ, SELL, SEMA3E*
Cell-to-cell signaling and interaction	84	9.26E-29	*ALOX5, ASGR1, BCL2A1, BTLA, C1QA, C3AR1, C5AR1, CACNA1B, CASP1, CCL2, CCL20, CCR3, CD163, CD180, CD300LB, CD48, CD68, CD84, CD86, CEBPE, CHI3L1, CLEC6A, CLEC7A, CP, CSF1R, CTSS, CX3CR1, CXCL11, CXCL9, CYBB, EEF1A2, FCER1G, FLT3, GHSR, HCK, HCLS1, HNF4A, HPSE, IL10RA, IL1A, IL1RN, IL27, IRF5, IRF8, ITGAX, ITGB2, LAT2, LCP1, LTF, NCF4, P2RY12, PLA2G2D, PLD4, POU2AF1, RAC2, RASGRP4, RGS1, SELL, SIGLEC1, SLAMF6, TAC1, THBS1, TIGIT, TLR2, TLR7, TLR8, TNFSF15, TNFSF8, TNFSF9, TREM2, TRPM2, TYROBP, UCP2, VAV1, VDR*	*FOXC2, IL2, IL33, KCNMA1, KISS1, LGALS4, MEOX2, MPZ MSLN*
Cell function and maintenance	85	2.37E-28	*AIM2, ASGR1, BATF, BCL2A1, BTLA, C1QA, C3AR1, C5AR1, CASP1, CCL2, CCL20, CCR3, CD163, CD48, CD84, CD86, CEBPE, CHI3L1, CLEC6A, CLEC7A, CP, CSF1R, CTSS, CX3CR1, CXCL9, CYBB, FCER1G, FLT3, GHSR, GPR65, HCK, HMGA1, HNF4A, IFI30, IL10RA, IL1A, IL1RN, IL27, IRF5, IRF8, ITGAX, ITGB2, LAT2, LCP1, LY9, NCKAP1L, P2RX2, P2RY12, PLA2G2D, PLD4, POU2AF1, RAC2, RASGRP4, RGS1, SELL, SIGLEC1, SLAMF6, SLAMF8, SLC46A2, TAC1, THBS1, TIGIT, TLR2, TLR7, TLR8, TNFSF15, TNFSF8, TREM2, TRPM2, TYROBP, UCP2, VAV1, VDR, XCR1*	*CAV3, CHRM3, FOXC2, IL2, IL33, JPH2, KCNMA1, KISS1, MPZ, PPP1R3C, SEMA3E*

Table 8.5 continued

			Genes	
Biological Process	**Gene count**	**P-value**	**Upregulated**	**Downregulated**
Cellular development	75	4.02E-25	*ALOX5, BATF, BCL2A1, BTLA, C1QC, C3AR1, C5AR1, CASP1, CCL2, CCL20, CD163, CD180, CD48, CD84, CD86, CEBPE, CLEC6A, CLEC7A, CSF1R, CXCL11, EEF1A2, FCER1G, FLT3, HCK, HCLS1, HMGA1, HNF4A, IL10RA, IL1A, IL1RN, IL27, IRF5, IRF8, ISG20, ITGAX, ITGB2, LAT2, LCP1, LTF, LY86, LY9, MNDA, MUC2, MUSK, NCKAP1L, NFAM1, PIK3AP1, PLA2G2D, POU2AF1, RAC2, RASGRP4, SELL, SEZ6L2, SIGLEC1, SLAMF6, SLAMF7, SLC46A2, TAC1, THBS1, TIGIT, TLR2, TLR7, TLR8, TNFSF15, TNFSF8, TNFSF9, TREM2, TRPM2, TYROBP, VAV1, VDR*	*IL2, IL33, KCNMA1, LGALS4*
Cellular growth and proliferation	72	4.02E-25	*ALOX5, BATF, BCL2A1, BTLA, C1QC, C3AR1, C5AR1, CASP1, CCL2, CCL20, CD163, CD180, CD48, CD84, CD86, CEBPE, CHI3L1, CLEC6A, CSF1R, CXCL11, EEF1A2, FCER1G, FLT3, HCK, HCLS1, HMGA1, IL10RA, IL1A, IL1RN, IL27, IRF5, IRF8, ISG20, ITGAX, ITGB2, LAT2, LCP1, LTF, LY86, LY9, MNDA, MUSK, NCKAP1L, NFAM1, PIK3AP1, PLA2G2D, POU2AF1, RAC2, RASGRP4, SELL, SIGLEC1, SLAMF6, SLAMF7, SLC46A2, TAC1, THBS1, TIGIT, TLR2, TLR7, TNFSF15, TNFSF8, TNFSF9, TREM2, TRPM2, TYROBP, VAV1, VDR*	*IL2, IL33, KISS1, LGALS4, MSLN*

Table 8.6 The twenty most differentially-expressed genes identified by DESeq2 in MSC2 ovaries compared to MSC1 ovaries.

Gene symbol	Log2FC	P value	Gene description
TAC1	4.36	7.79E-18	tachykinin precursor
MS4A7	1.80	4.52E-05	membrane spanning 4-domains A7
SLAMF9	2.01	6.82E-05	SLAM family member 9
PDE6A	1.84	7.89E-05	phosphodiesterase 6A
IRF8	1.49	3.00E-04	interferon regulatory factor 8
LGALS4	-1.80	4.12E-04	galectin 4
SIGLEC1	1.38	6.34E-04	sialic acid binding IG like lectin 1
PLD4	1.48	6.53E-04	phospholipase D family member 4
LAT2	1.20	7.23E-04	linker for activation of T-cells family member 2
GPR31	1.45	8.08E-04	G protein-coupled receptor 31
VAV1	1.44	8.60E-04	vav guanine nucleotide exchange factor 1
CD300LB	1.69	8.95E-04	CD300 molecule like family member b
CD163	1.52	9.80E-04	CD163 molecule
RHBG	1.63	1.08E-03	Rh family B glycoprotein (gene/pseudogene)
GPR151	1.22	1.19E-03	G protein-coupled receptor 151
CD86	1.47	1.23E-03	CD86 molecule
CRADD	-1.05	1.30E-03	CASP2 and RIPK1 domain containing adaptor with death domain
SLAMF7	1.58	1.32E-03	SLAM family member 7
RASSF9	-1.13	1.40E-03	Ras association domain family member 9
CYBB	1.50	1.51E-03	cytochrome b-245 beta chain

FC fold-change.

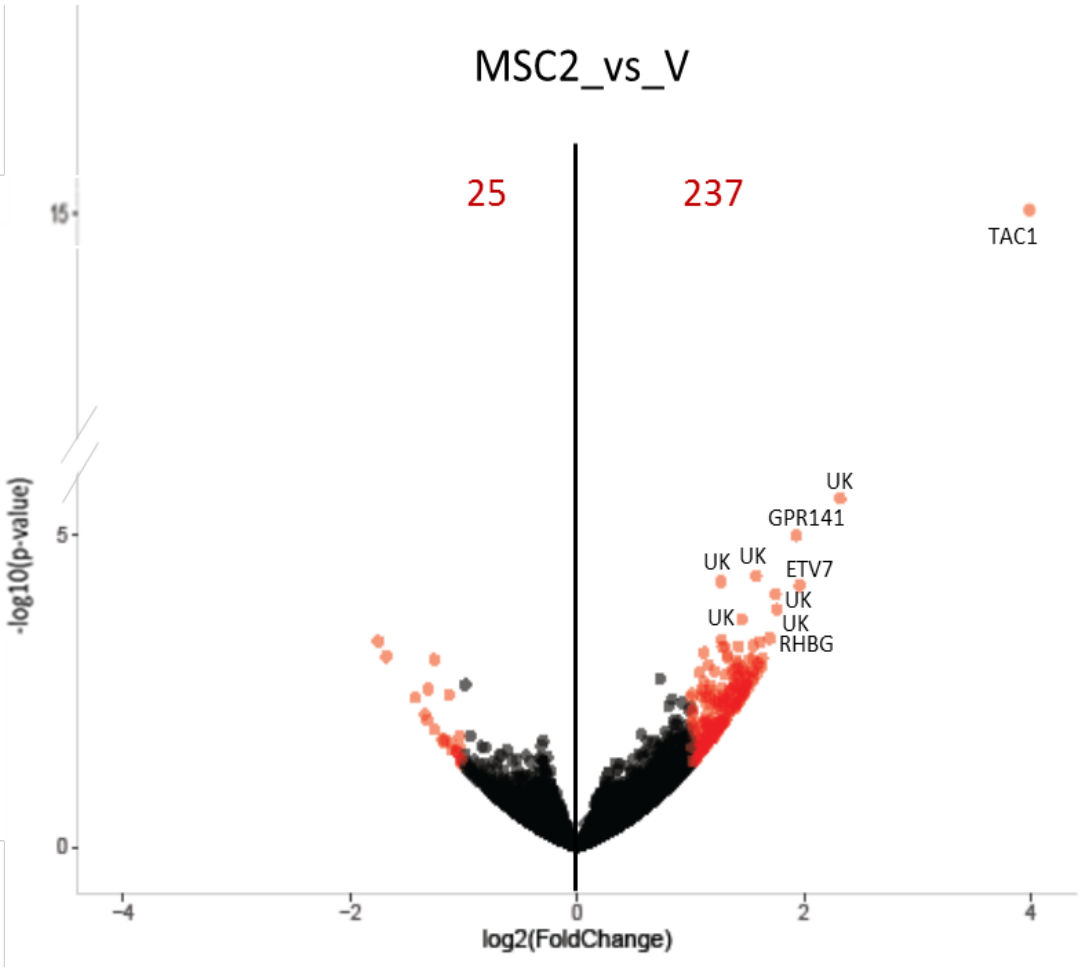

Figure 8.4 Volcano plot of upregulated and downregulated genes in ovaries injected twice with MSCs (MSC2) compared to ovaries injected once with Vehicle (V). There were 237 upregulated genes and 25 downregulated genes. The 10 most differentially-regulated genes are given in the figure: TAC1 (tachykinin precursor); GPR141 (G protein-coupled receptor 141); ETV7 (ETS variant 7); and RHGB (Rh family B glycoprotein (gene/pseudogene)). Unknown gene products designated by "UK."

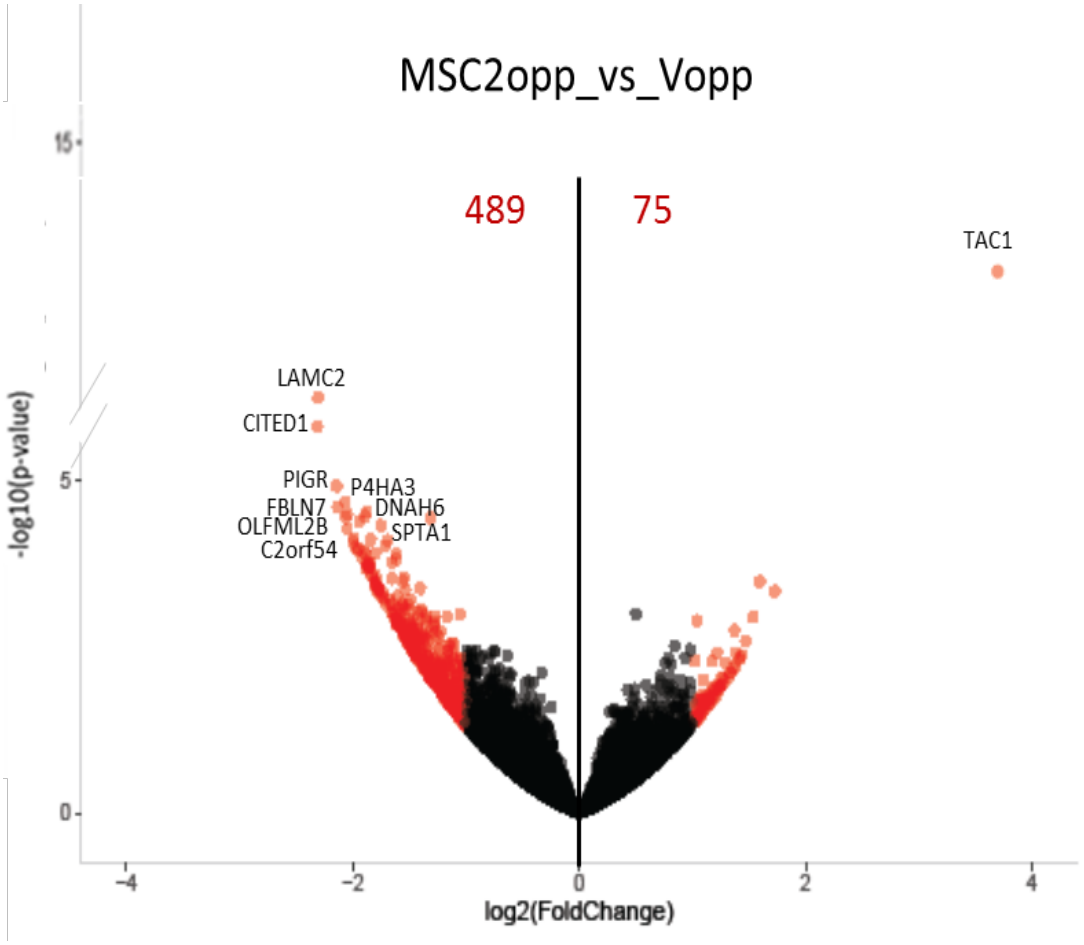

Figure 8.5 Volcano plot of upregulated and downregulated genes in MSC2opp ovaries compared to Vopp ovaries. There were 75 upregulated genes and 489 downregulated genes. The 10 most differentially-regulated genes are given in the figure: TAC1 (tachykinin precursor); LAMC2 (laminin subunit gamma 2); CITED1 (Cbp/p300 interacting transactivator with Glu/Asp rich carboxy-terminal domain 1); PIGR (polymeric immunoglobulin receptor); FBLN7 (fibulin 7); P4HA3 (prolyl 4-hydroxylase subunit alpha 3); DNAH6 (dynein axonemal heavy chain 6); OLFML2B (olfactomedin like 2B); C2orf54 (chromosome 2 open reading frame 54); and SPTA1 (spectrin alpha, erythocytic 1).

DISCUSSION

This study presents some of the first data on global gene expression in equine ovaries. Three of the most highly differentially-expressed genes in MSC1 ovaries were keratin 5, 14 and 17, all of which were downregulated when compared to Vehicle-injected ovaries. These genes encode keratin proteins, which are intermediate filament proteins involved in cellular assembly and organization [317]. While we could find no data on these specific keratin proteins as they relate to ovarian or MSC function, the expression of *Krt8* (keratin 8) in cumulus cells has been associated with embryos that arrested at the 2- to 8-cell stage during *in vitro* culture, and thus has been proposed as a marker of poor oocyte quality [317, 318]. DMSO itself has been shown to downregulate *Krt15* (keratin 15) in embryonic stem cells [319], however, both MSC1 and V mares received the vehicle (DMSO) at relatively the same time before tissue collection, so the downregulation observed is related to the MSCs rather than the DMSO.

Prolactin receptor (*PRLR*) was also among the differentially-expressed genes being downregulated in MSC1 ovaries compared to V ovaries. Prolactin (PRL) is a polypeptide hormone that, in addition to stimulating mammary gland development and lactation, is involved in folliculogenesis in mice [320]. The effects of prolactin are mediated through its interaction with the PRLR. In mice, the interaction of PRL with PRLR is a key component in folliculogenesis and the regulation of corpora luteal (CL) function [320]. Although it is not clear whether PL/PRLR play a role in folliculogenesis in mares, follicular diameter has been found to be highly correlated with plasma prolactin concentrations, and PRL seems to play a role in the transition out of anestrus

[321]. Therefore, the downregulation of *PRLR* in the present study would not seem to argue for a stimulatory role of MSCs on folliculogenesis. Again, DMSO (1-5%) has been shown to cause a dose-dependent decrease in prolactin receptor levels in other tissue (normal mammary cells [322]) but both MSC1 and V ovaries received DMSO at the same time before ovariectomy.

Among the 20 most differentially-expressed genes, testis specific 10 (*TSGA10*) was upregulated in MSC1 ovaries vs V ovaries. *TSGA10* is a gene that was once considered testis restricted, i.e., expressed exclusively in adult testes. However, it has since been shown to be expressed in normal tissues, including undifferentiated embryonic stem cells [323], and in a wide range of neoplasms, including ovarian cancer [324]. In the testis, TSGA10 is related to spermatogenesis and has been used as a marker of active spermatogenesis *in vivo* and *in vitro* [325]. In embryonic stem cells, the expression of *TSGA10* increases during transition from the proliferation phase to the differentiation phase [323]. In cancer cells, *TSGA10* may be involved in angiogenesis, cell growth and division, motility and migration, all of which are factors important for tumor metastasis and invasion [326]. The increased expression of *TSGA10* appears to be an effect of MSCs; the upregulation of *TSGA10* was localized only to the MSC-injected ovaries and was not seen in the non-injected contralateral ovaries. To the best of our knowledge, this is the first report of *TSGA10* expression in the ovary.

Another interesting finding was that *RASSF9* (Ras-association domain family member 9) was upregulated in MSC1 ovaries compared to both V and MSC2 ovaries. RASSF genes encode proteins that control cellular processes including membrane

trafficking, apoptosis, and proliferation [327]. Although the expression and functional significance of *RASSF9* is not well known, *Rassf9*-deficient mice exhibit signs of senescence, including alopecia, growth retardation, and decreased lifespan [328]. In the present study, upregulation of *RASSF9* in MSC1 ovaries appears to be an effect of MSCs and may indicate an anti-senescence effect of these cells.

Activin A receptor type 1C (*ACVR1C,* formerly known as *ALK7*) was also upregulated in the ovaries of old mares injected with MSCs, in comparison to those injected with vehicle. Activins belong to the TGF-β (transforming growth factor-beta) family of cytokines, and expression patterns during post-natal follicular development in rodents and humans indicate that activin A stimulates the differentiation of primordial follicles into antral follicles [329-331]. The ACVR1C is involved in Nodal signaling in early embryo development [332], and it has been found in mare luteal tissue, in which it may play a role in luteolysis [333]. *ACVR1C* is expressed in human pre-antral follicles [334] and mouse granulosa cells [335]. It serves as a receptor for not only TGF-beta ligands, but also bone morphogenic proteins, which play an important role in ovarian function and germ line differentiation [336].

From the above gene expression findings, we can conclude that while increased antral follicle growth was not observed after MSC injection in the present study (see results from Chapter VII), some proliferative and folliculogenic effects of MSCs on gene expression were evident.

Studies performed in mice [11] and rabbits [262] have shown that in females with chemotherapy-damaged ovaries, both systemic (tail- or ear-vein) injection and

intra-ovarian injection of MSCs have resulted in restored ovarian function (increased number of follicles) and fecundity. In the present study, we decided to perform intra-ovarian injection rather than systemic injection for several reasons: A) intra-ovarian injection allowed us to deliver a meaningful number of cells to the ovary, whereas systemic injections using a peripheral vein would have required a markedly higher number of cells than was available in order to deliver the same number to the ovary; B) methods to deliver the cells to an artery immediately serving the ovary, as done in humans via ultrasound-guided catheterization from the common femoral artery [337] have not been developed in the horse; and C) the technique of transvaginal ultrasound-guided ovarian injection is well-established in our laboratory. The possibility exists that MSCs injected in the ovary could be distributed in the bloodstream and thus have a systemic effect. Therefore, to determine any systemic effects of MSCs, we compared the contralateral non-injected ovary of MSC1 mares (MSC1opp) to the contralateral non-injected ovary of Vehicle mares (Vopp). If MSCs had had a systemic effect, we would have expected the same genes that were differentially-regulated in MSC-injected ovaries (MSC1) to be differentially-regulated in the contralateral ovary (MSC1opp) when compared to Vopp. Analysis of differentially-regulated genes between the two comparisons (Tables 8.2 and 8.4) show that there was no overlap in these sets; none of the 20 most differentially-expressed genes in the MSC1-injected ovary, vs V, were among the most differentially-expressed genes in MSC1opp vs Vopp. This suggests that there were limited systemic effects of MSCs 14 to 19 weeks after MSC injection.

To determine whether there were differences in the acute and long-term effects of MSCs, we compared the gene expression between ovaries of mares that received one MSC injection (MSC1) and ovaries of mares that received two MSC injections (MSC2). Tissue collection and processing for RNA analysis was performed 14 to 19 weeks after the first injection and 2 weeks after the second injection. There were 200 upregulated genes and 61 downregulated genes in MSC2 ovaries compared to MSC1 ovaries.

One of the most striking findings on evaluation of gene expression in MSC2 and MSC2opp ovaries was the expression of tachykinin precursor (*TAC1*). Expression of this gene was highly significantly upregulated in MSC2 compared to both MSC1 (P = 7.79E-18) and V (P = 1.81E-15); and in MSC2opp compared to Vopp (P = 1.72E-13). *TAC1* encodes four neurally-active gene products, including substance P. Substance P is a neuropeptide, and is also a well-known mediator of response to inflammation and injury [338]. However, substance P has also been shown to stimulate cell growth, including proliferation of bone marrow cells, lymphocytes and endothelial cells, and to promote angiogenesis [339]. The MSC2 mares received the second injection two weeks before being ovariectomized, raising the possibility that *TAC1* was upregulated in MSC2 in response to the trauma of injection; however, the MSC2opp ovary had not been injected and *TAC1* was equally upregulated in the MSC2opp vs the Vopp ovaries. Additionally, one of the V mares, to which the MSC2 ovaries were compared, had undergone a TVA in which both ovaries were subjected to ovarian puncture 4 weeks before the ovariectomy with similar ovarian trauma as for the mares receiving MSCs. Treatment with DMSO has been shown to decrease levels of substance P [340]. Thus, it appears

that this notable increase in *TAC1* is acutely associated with the injection of MSCs, and that is a systemic effect, as it was seen in both the injected and non-injected ovary.

Another remarkable finding in MSC2 mares was that one of the 20 most differentially-expressed genes, *CRADD*, which was significantly downregulated in MSC2 compared to MSC1, encodes a protein containing a death domain motif which recruits caspase 2/ICH1 to the cell death signal transduction complex to promote apoptosis. This suggests an acute anti-apoptotic effect of MSC injection. Some of the genes that were upregulated, including *SIGLEC1, PLD4, LAT2, CD300LB,* and *CD86* encode products involved in immunomodulation. In general, there was a pronounced difference in the acute and long-term effects of MSC injection, as ovaries that had been injected 2 weeks prior to ovariectomy had upregulation of genes involved in immune responses, and downregulation of genes involved in apoptosis, in comparison to ovaries that had been injected 14 to 19 weeks before ovariectomy.

As mentioned above, *RASSF9* was upregulated in MSC1 ovaries compared to both V and MSC2, suggesting that upregulation of this gene in MSC1 is an effect of MSCs. However, it is not clear why *RASSF9* was upregulated only in MSC1 and not acutely, in MSC2 ovaries.

In rat and mouse ovaries damaged by chemotherapy, injection of MSCs increases the expression of factors known to affect ovarian function, including *Vegf, Hgf, Igf1* and *Star*, and these changes are associated with an increase in ovarian activity and fecundity [10, 11]. However, in the present study, changes in the expression of these genes was not seen after MSC injection, and MSC injection was not associated with

increases in follicle numbers in old or young mares (results presented in Chapter VII). It is possible that rodent ovaries react differently to MSCs than do equine ovaries, or that MSCs have a different effect on chemotherapy-treated ovaries than in aged ovaries. This latter may be related to the finding that it is necessary to induce prior injury to tissues to clear the target tissue's cell niches in order to enable engraftment of donor stem cells [341]. It is possible that chemotherapy causes injury to the ovarian tissue that allows MSC engraftment in functional niches, whereas injection of MSCs in an intact aged ovary does not support MSC engraftment. Thus, it is tempting to speculate that MSCs would improve ovarian function in chemotherapy-damaged ovaries but not in aging ovaries. Additional studies are needed to investigate this.

In the present study, the vehicle used to inject the cells (DMSO) has been shown to have direct effects on gene regulation [319, 340]. A vehicle control was included for the MSC1 group, but not for the MSC2 group. The possible contribution of the DMSO confounds the interpretation of the data. In future studies, use of non-frozen MSCs, or MSCs rinsed to remove DMSO prior to injection, would minimize any potential effect of DMSO. In the present study, with the exception of *TAC1* in the MSC2 and MSC2opp ovaries, there did not appear to be a systemic effect of MSC injection, as the gene expression in the contralateral non-injected ovaries was different than the gene expression in the injected ovaries. There seemed to be a difference in the acute and long-term effects of MSCs, as ovaries that had been injected 2 weeks prior to ovariectomy had upregulation of genes involved in immune responses, and downregulation of genes

involved in apoptosis, in comparison to ovaries that had been injected 14 to 19 weeks prior to ovariectomy.

In conclusion, in contrast to the effects seen in rats, mice, and rabbits with chemotherapy-damaged ovaries, intra-ovarian injection of MSCs in old mares did not regulate the same subset of genes known to be involved in the improvement of ovarian function. Further research is needed to explore the potential of MSC injection on improving ovarian function in aged mares.

CHAPTER IX

CONCLUSIONS

The research presented in this dissertation examined the effects of MSCs on equine ovarian function and gene expression. In a preliminary study there was an apparent increase in follicle numbers four weeks after MSC injection in 2 young mares. However, in a more comprehensive study that included both old and young mares there were no increases in follicle numbers. One possible explanation for the different results obtained between these 2 studies is that the mares in the preliminary study received 2 MSC injections (one in each ovary), i.e., in total they received twice the number of cells as the old or young mares in the subsequent study. Another possible explanation is that the source of the MSCs used in the preliminary study and in the main study differed; it is possible that some categories of horses, or some individual donors, elicit changes in follicle numbers while MSCs from other donors do not.

Intra-ovarian injection of MSCs in old mares did not increase the expression of factors known to improve ovarian function, in contrast to what has been reported in rodent studies, which indicate that the systemic of intra-ovarian injection of MSCs in females with chemotherapy-damaged ovaries induces expression of mRNA and proteins that may improve ovarian function. It is possible that rodent ovaries react differently to MSC injection than do equine ovaries, or that MSC injection improves ovarian function after chemotherapy-induced damage, perhaps due to clearance of a cellular niche which

the injected MSCs can occupy, but not in females experiencing ovarian failure associated with aging.

We evaluated the use of fluorescent QDs to label equine MSCs. Although QDs did not interfere with the proliferation and differentiation capacity of MSCs, QDs did not appear to be an effective method to track and label MSCs long-term. We also determined that when recording MSC viability, it is best to do so within 60 min post-thaw; alternatively, the cells can be rinsed to remove DMSO and held on ice for up to 120 min without an effect on viability. Although the co-culture system we utilized has been used successfully with other tissues, this system was not effective when equine ovarian tissue was co-cultured with MSCs. Nonetheless, this study had value in determining methods for isolation of RNA from ovarian tissue which was problematic due to the fibrous nature of the equine ovary interfering with lysis by enzymatic digestion.

Further research is needed to study alternative methods to label and track MSCs, to determine if different co-culture systems would support co-culture of equine ovarian explants, and to better understand the mechanism of action of MSCs on follicular populations and ovarian gene expression in mares.

REFERENCES

1. Fitzgerald, C., A.E. Zimon, and E.E. Jones, Aging and reproductive potential in women. Yale J Biol Med, 1998. 71(5): p. 367-381.

2. te Velde, E., D. Habbema, H. Leridon, and M. Eijkemans, The effect of postponement of first motherhood on permanent involuntary childlessness and total fertility rate in six European countries since the 1970s. Hum Reprod, 2012. 27(4): p. 1179-1183.

3. Vanderwall, D. and G. Woods. *Age-related subfertility in the mare*. in *Proceedings of the annual convention of the American Association of Equine Practitioners*. 1990.

4. Salooja, N., R. Chatterjee, A.K. McMillan, S.M. Kelsey, A.C. Newland, D.W. Milligan, I.M. Franklin, R.M. Hutchinson, D.C. Linch, and A.H. Goldstone, Successful pregnancies in women following single autotransplant for acute myeloid leukemia with a chemotherapy ablation protocol. Bone Marrow Transplant, 1994. 13(4): p. 431-435.

5. Salooja, N., R.M. Szydlo, G. Socie, B. Rio, R. Chatterjee, P. Ljungman, M.T. Van Lint, R. Powles, G. Jackson, M. Hinterberger-Fischer, H.J. Kolb, and J.F. Apperley, Pregnancy outcomes after peripheral blood or bone marrow transplantation: a retrospective survey. Lancet, 2001. 358(9278): p. 271-276.

6. Sanders, J.E., J. Hawley, W. Levy, T. Gooley, C.D. Buckner, H.J. Deeg, K. Doney, R. Storb, K. Sullivan, R. Witherspoon, and F.R. Appelbaum, Pregnancies following high-dose cyclophosphamide with or without high-dose busulfan or total-body irradiation and bone marrow transplantation. Blood, 1996. 87(7): p. 3045-3052.

7. Hershlag, A. and M.W. Schuster, Return of fertility after autologous stem cell transplantation. Fertil Steril, 2002. 77(2): p. 419-421.

8. Lee, H.-J., K. Selesniemi, Y. Niikura, T. Niikura, R. Klein, D.M. Dombkowski, and J.L. Tilly, Bone marrow transplantation generates immature oocytes and rescues long-term fertility in a preclinical mouse model of chemotherapy-induced premature ovarian failure. J Clin Oncol, 2007. 25(22): p. 3198-3204.

9. Fu, X., Y. He, C. Xie, and W. Liu, Bone marrow mesenchymal stem cell transplantation improves ovarian function and structure in rats with chemotherapy-induced ovarian damage. Cytotherapy, 2008. 10(4): p. 353-363.

10. Takehara, Y., A. Yabuuchi, K. Ezoe, T. Kuroda, R. Yamadera, C. Sano, N. Murata, T. Aida, K. Nakama, F. Aono, N. Aoyama, K. Kato, and O. Kato, The restorative effects of adipose-derived mesenchymal stem cells on damaged ovarian function. Lab Invest, 2013. 93(2): p. 181-193.

11. Wang, S., L. Yu, M. Sun, S. Mu, C. Wang, D. Wang, and Y. Yao, The therapeutic potential of umbilical cord mesenchymal stem cells in mice premature ovarian failure. Biomed Res Int, 2013. 2013: p. 690491.

12. Selesniemi, K., H.J. Lee, T. Niikura, and J.L. Tilly, Young adult donor bone marrow infusions into female mice postpone age-related reproductive failure and improve offspring survival. Aging (Albany NY), 2009. 1(1): p. 49-57.

13. Mohammed Ali, A.F., et al., Fertility Treatment of Aged Women By Laparoscopic Intra Ovarian Injection of Peripheral Blood Mononuclear Cell (PBMNC) a New Modality, in *Fertility Magazine*. 2013, IVFonline: Guelph, Ontario, Canada. p. 52-55.

14. Johnson, J., J. Canning, T. Kaneko, J.K. Pru, and J.L. Tilly, Germline stem cells and follicular renewal in the postnatal mammalian ovary. Nature, 2004. 428(6979): p. 145-150.

15. Baker, T.G., A quantitative and cytological study of germ cells in human ovaries. Proc R Soc Lond B Biol Sci, 1963. 158: p. 417-433.

16. Block, E., Quantitative morphological investigations of the follicular system in women; variations at different ages. Acta Anat (Basel), 1952. 14(1-2): p. 108-123.

17. Navot, D., P.A. Bergh, M.A. Williams, G.J. Garrisi, I. Guzman, B. Sandler, and L. Grunfeld, Poor oocyte quality rather than implantation failure as a cause of age-related decline in female fertility. Lancet, 1991. 337(8754): p. 1375-1377.

18. Sauer, M.V., Pregnancy wastage and reproductive aging: the oocyte donation model. Curr Opin Obstet Gynecol, 1996. 8(3): p. 226-229.

19. Sauer, M.V., R.J. Paulson, and R.A. Lobo, Reversing the natural decline in human fertility. An extended clinical trial of oocyte donation to women of advanced reproductive age. JAMA, 1992. 268(10): p. 1275-1279.

20. Rotsztejn, D.A. and R.H. Asch. *Effect of aging on assisted reproductive technologies (ART): experience from egg donation*. in *Seminars in reproductive endocrinology*. 1991. Thieme.

21. Carnevale, E. and O. Ginther, Defective oocytes as a cause of subfertility in old mares. Biol Reprod Mono 1, 1995: p. 209-214.

22. Gosden, R., Oocyte development throughout life, in *Gametes—The Oocyte*, J.G.G.a.J.L. Yovich, Editor. 1995, Cambridge University Press: Cambridge, UK. p. 119-149.

23. Beaumont, H.M. and A.M. Mandl, A quantitative and cytological study of oogonia and oocytes in the foetal and neonatal rat. Proceedings of the Royal Society of London B: Biological Sciences, 1962. 155(961): p. 557-579.

24. Matzuk, M.M., Eggs in the balance. Nat Genet, 2001. 28(4): p. 300-301.

25. Ratts, V., J. Flaws, R. Kolp, C. Sorenson, and J. Tilly, Ablation of bcl-2 gene expression decreases the numbers of oocytes and primordial follicles established in the post-natal female mouse gonad. Endocrinology, 1995. 136(8): p. 3665-3668.

26. Greenfeld, C.R., M.E. Pepling, J.K. Babus, P.A. Furth, and J.A. Flaws, BAX regulates follicular endowment in mice. Reproduction, 2007. 133(5): p. 865-876.

27. Bergeron, L., G.I. Perez, G. Macdonald, L. Shi, Y. Sun, A. Jurisicova, S. Varmuza, K.E. Latham, J.A. Flaws, and J.C. Salter, Defects in regulation of apoptosis in caspase-2-deficient mice. Genes Dev, 1998. 12(9): p. 1304-1314.

28. Coticchio, G., D.F. Albertini, and L. De Santis, Oogenesis. 2013: Springer.

29. De Pol, A., F. Vaccina, A. Forabosco, E. Cavazzuti, and L. Marzona, Apoptosis of germ cells during human prenatal oogenesis. Hum Reprod, 1997. 12(10): p. 2235-2241.

30. Tilly, J.L., K.I. Kowalski, A.L. Johnson, and A.J. Hsueh, Involvement of apoptosis in ovarian follicular atresia and postovulatory regression. Endocrinology, 1991. 129(5): p. 2799-2801.

31. Manabe, N., Y. Imai, H. Ohno, Y. Takahagi, M. Sugimoto, and H. Miyamoto, Apoptosis occurs in granulosa cells but not cumulus cells in the atretic antral follicles in pig ovaries. Experientia, 1996. 52(7): p. 647-651.

32. Palumbo, A. and J. Yeh, In situ localization of apoptosis in the rat ovary during follicular atresia. Biol Reprod, 1994. 51(5): p. 888-895.

33. Hughes JR, F.M., Gorospe WC, Biochemical Identification of Apoptosis (Programmed Cell Death) in Granulosa Cells: Evidence for a Potential Mechanism Underlying Follicular Atresia*. Endocrinology, 1991. 129(5): p. 2415-2422.

34. Yuan, W. and L.C. Giudice, Programmed cell death in human ovary is a function of follicle and corpus luteum status 1. The Journal of Clinical Endocrinology & Metabolism, 1997. 82(9): p. 3148-3155.

35. Dell'Aquila, M.E., M. Albrizio, F. Maritato, P. Minoia, and K. Hinrichs, Meiotic competence of equine oocytes and pronucleus formation after intracytoplasmic sperm injection (ICSI) as related to granulosa cell apoptosis. Biol Reprod, 2003. 68(6): p. 2065-2072.

36. Nandedkar, T.D., M.S. Rajadhyaksha, R.R. Mukhopadhya, S. Rao, and D. Joshf, Apoptosis in granulose cells induced by intrafollicular peptide. J Biosci, 1998. 23(3): p. 271-277.

37. Mintz, B. and E.S. Russell, Gene-induced embryological modifications of primordial germ cells in the mouse. J Exp Zool, 1957. 134(2): p. 207-237.

38. McCoshen, J. and D. McCallion, A study of the primordial germ cells during their migratory phase in Steel mutant mice. Experientia, 1975. 31(5): p. 589-590.

39. Besmer, P., K. Manova, R. Duttlinger, E.J. Huang, A. Packer, C. Gyssler, and R.F. Bachvarova, The kit-ligand (steel factor) and its receptor c-kit/W: pleiotropic roles in gametogenesis and melanogenesis. Development, 1993. 119(Supplement): p. 125-137.

40. Horie, K., K. Takakura, S. Taii, K. Narimoto, Y. Noda, S. Nishikawa, H. Nakayama, J. Fujita, and T. Mori, The expression of c-kit protein during oogenesis and early embryonic development. Biol Reprod, 1991. 45(4): p. 547-552.

41. Joyce, I.M., F.L. Pendola, K. Wigglesworth, and J.J. Eppig, Oocyte regulation of kit ligand expression in mouse ovarian follicles. Dev Biol, 1999. 214(2): p. 342-353.

42. Manova, K., E.J. Huang, M. Angeles, V. De Leon, S. Sanchez, S.M. Pronovost, P. Besmer, and R.F. Bachvarova, The expression pattern of the c-kit ligand in gonads of mice supports a role for the c-kit receptor in oocyte growth and in proliferation of spermatogonia. Dev Biol, 1993. 157(1): p. 85-99.

43. Manova, K., K. Nocka, P. Besmer, and R.F. Bachvarova, Gonadal expression of c-kit encoded at the W locus of the mouse. Development, 1990. 110(4): p. 1057-1069.

44. Yoshida, H., N. Takakura, H. Kataoka, T. Kunisada, H. Okamura, and S.-I. Nishikawa, Stepwise requirement ofc-kit tyrosine kinase in mouse ovarian follicle development. Dev Biol, 1997. 184(1): p. 122-137.

45. Parrott, J.A. and M.K. Skinner, Kit-ligand/stem cell factor induces primordial follicle development and initiates folliculogenesis 1. Endocrinology, 1999. 140(9): p. 4262-4271.

46. Accili, D. and K.C. Arden, FoxOs at the crossroads of cellular metabolism, differentiation, and transformation. Cell, 2004. 117(4): p. 421-426.

47. Reddy, P., L. Shen, C. Ren, K. Boman, E. Lundin, U. Ottander, P. Lindgren, Y.-x. Liu, Q.-y. Sun, and K. Liu, Activation of Akt (PKB) and suppression of FKHRL1 in mouse and rat oocytes by stem cell factor during follicular activation and development. Dev Biol, 2005. 281(2): p. 160-170.

48. Castrillon, D.H., L. Miao, R. Kollipara, J.W. Horner, and R.A. DePinho, Suppression of ovarian follicle activation in mice by the transcription factor Foxo3a. Science, 2003. 301(5630): p. 215-218.

49. John, G.B., T.D. Gallardo, L.J. Shirley, and D.H. Castrillon, Foxo3 is a PI3K-dependent molecular switch controlling the initiation of oocyte growth. Dev Biol, 2008. 321(1): p. 197-204.

50. Reddy, P., L. Liu, D. Adhikari, K. Jagarlamudi, S. Rajareddy, Y. Shen, C. Du, W. Tang, T. Hämäläinen, and S.L. Peng, Oocyte-specific deletion of Pten causes premature activation of the primordial follicle pool. Science, 2008. 319(5863): p. 611-613.

51. Kissel, H., I. Timokhina, M.P. Hardy, G. Rothschild, Y. Tajima, V. Soares, M. Angeles, S.R. Whitlow, K. Manova, and P. Besmer, Point mutation in kit receptor tyrosine kinase reveals essential roles for kit signaling in spermatogenesis and oogenesis without affecting other kit responses. The EMBO journal, 2000. 19(6): p. 1312-1326.

52. Liu, L., S. Rajareddy, P. Reddy, C. Du, K. Jagarlamudi, Y. Shen, D. Gunnarsson, G. Selstam, K. Boman, and K. Liu, Infertility caused by retardation of follicular development in mice with oocyte-specific expression of Foxo3a. Development, 2007. 134(1): p. 199-209.

53. Brenkman, A.B. and B.M. Burgering, FoxO3a eggs on fertility and aging. Trends Mol Med, 2003. 9(11): p. 464-467.

54. Georges, A., A. Auguste, L. Bessière, A. Vanet, A.-L. Todeschini, and R.A. Veitia, FOXL2: a central transcription factor of the ovary. J Mol Endocrinol, 2014. 52(1): p. R17-R33.

55. Schmidt, D., C.E. Ovitt, K. Anlag, S. Fehsenfeld, L. Gredsted, A.-C. Treier, and M. Treier, The murine winged-helix transcription factor Foxl2 is required for granulosa cell differentiation and ovary maintenance. Development, 2004. 131(4): p. 933-942.

56. Uda, M., C. Ottolenghi, L. Crisponi, J.E. Garcia, M. Deiana, W. Kimber, A. Forabosco, A. Cao, D. Schlessinger, and G. Pilia, Foxl2 disruption causes mouse ovarian failure by pervasive blockage of follicle development. Hum Mol Genet, 2004. 13(11): p. 1171-1181.

57. Visser, J.A., F.H. de Jong, J.S. Laven, and A.P. Themmen, Anti-Müllerian hormone: a new marker for ovarian function. Reproduction, 2006. 131(1): p. 1-9.

58. Durlinger, A.L., P. Kramer, B. Karels, F.H. de Jong, J.T.J. Uilenbroek, J.A. Grootegoed, and A.P. Themmen, Control of Primordial Follicle Recruitment by Anti-Müllerian Hormone in the Mouse Ovary. Endocrinology, 1999. 140(12): p. 5789-5796.

59. Durlinger, A.L., M.J. Gruijters, P. Kramer, B. Karels, H.A. Ingraham, M.W. Nachtigal, J.T.J. Uilenbroek, J.A. Grootegoed, and A.P. Themmen, Anti-Mullerian hormone inhibits initiation of primordial follicle growth in the mouse ovary. Endocrinology, 2002. 143(3): p. 1076-1084.

60. Visser, J.A., Shaping up the function of anti-Müllerian hormone in ovaries of mono-ovulatory species. Hum Reprod, 2016. 31(7): p. 1403-1405.

61. Chang, H.-M., C. Klausen, and P.C. Leung, Antimüllerian hormone inhibits follicle-stimulating hormone-induced adenylyl cyclase activation, aromatase expression, and estradiol production in human granulosa-lutein cells. Fertil Steril, 2013. 100(2): p. 585-592. e581.

62. Pellatt, L., S. Rice, N. Dilaver, A. Heshri, R. Galea, M. Brincat, K. Brown, E.R. Simpson, and H.D. Mason, Anti-Müllerian hormone reduces follicle sensitivity to follicle-stimulating hormone in human granulosa cells. Fertil Steril, 2011. 96(5): p. 1246-1251. e1241.

63. Guertin, D.A. and D.M. Sabatini, Defining the role of mTOR in cancer. Cancer Cell, 2007. 12(1): p. 9-22.

64. Wullschleger, S., R. Loewith, and M.N. Hall, TOR signaling in growth and metabolism. Cell, 2006. 124(3): p. 471-484.

65. Adhikari, D., W. Zheng, Y. Shen, N. Gorre, T. Hämäläinen, A.J. Cooney, I. Huhtaniemi, Z.-J. Lan, and K. Liu, Tsc/mTORC1 signaling in oocytes governs the quiescence and activation of primordial follicles. Hum Mol Genet, 2010. 19(3): p. 397-410.

66. Adhikari, D., G. Flohr, N. Gorre, Y. Shen, H. Yang, E. Lundin, Z. Lan, M.J. Gambello, and K. Liu, Disruption of Tsc2 in oocytes leads to overactivation of the entire pool of primordial follicles. Mol Hum Reprod, 2009. 15(12): p. 765-770.

67. Hunter, N., Meiotic recombination: the essence of heredity. Cold Spring Harb Perspect Biol, 2015. 7(12): p. a016618.

68. Clift, D. and M. Schuh, Restarting life: fertilization and the transition from meiosis to mitosis. Nature reviews Molecular cell biology, 2013. 14(9): p. 549-562.

69. Angell, R.R., Predivision in human oocytes at meiosis I: a mechanism for trisomy formation in man. Hum Genet, 1991. 86(4): p. 383-387.

70. Kuliev, A., Z. Zlatopolsky, I. Kirillova, J. Spivakova, and J.C. Janzen, Meiosis errors in over 20,000 oocytes studied in the practice of preimplantation aneuploidy testing. Reproductive Biomedicine Online, 2011. 22(1): p. 2-8.

71. Hall, J.E., Neuroendocrine physiology of the early and late menopause. Endocrinol Metab Clin North Am, 2004. 33(4): p. 637-659.

72. Vialard, F., F. Boitrelle, D. Molina-Gomes, and J. Selva, Predisposition to aneuploidy in the oocyte. Cytogenetic and genome research, 2011. 133(2-4): p. 127-135.

73. Bernstein, L., A. Mackenzie, C. Chaffin, and I. Merchenthaler, An FSH-lowering activin disrupting therapy prevents egg chromosome and spindle misalignments that predispose to aneuploidy, and increases fertility, in a mouse model of midlife reproductive aging. Fertil Steril, 2015. 104(3): p. e63.

74. Van Blerkom, J. and P. Davis, Differential effects of repeated ovarian stimulation on cytoplasmic and spindle organization in metaphase II mouse oocytes matured in vivo and in vitro. Hum Reprod, 2001. 16(4): p. 757-764.

75. Roberts, R., A. Iatropoulou, D. Ciantar, J. Stark, D.L. Becker, S. Franks, and K. Hardy, Follicle-stimulating hormone affects metaphase I chromosome alignment and increases aneuploidy in mouse oocytes matured in vitro. Biol Reprod, 2005. 72(1): p. 107-118.

76. Hammoud, I., F. Vialard, M. Bergere, M. Albert, D.M. Gomes, M. Adler, L. Malagrida, M. Bailly, R. Wainer, and J. Selva, Follicular fluid protein content (FSH, LH, PG4, E2 and AMH) and polar body aneuploidy. J Assist Reprod Genet, 2012. 29(10): p. 1123-1134.

77. Xu, Y.-W., Y.-T. Peng, B. Wang, Y.-H. Zeng, G.-L. Zhuang, and C.-Q. Zhou, High follicle-stimulating hormone increases aneuploidy in human oocytes matured in vitro. Fertil Steril, 2011. 95(1): p. 99-104.

78. Duncan, F.E., J.E. Hornick, M.A. Lampson, R.M. Schultz, L.D. Shea, and T.K. Woodruff, Chromosome cohesion decreases in human eggs with advanced maternal age. Aging cell, 2012. 11(6): p. 1121-1124.

79. Zielinska, A.P., Z. Holubcova, M. Blayney, K. Elder, and M. Schuh, Sister kinetochore splitting and precocious disintegration of bivalents could explain the maternal age effect. Elife, 2015. 4: p. e11389.

80. Patel, J., S.L. Tan, G.M. Hartshorne, and A.D. McAinsh, Unique geometry of sister kinetochores in human oocytes during meiosis I may explain maternal age-associated increases in chromosomal abnormalities. Biology open, 2016. 5(2): p. 178-184.

81. Sakakibara, Y., S. Hashimoto, Y. Nakaoka, A. Kouznetsova, C. Höög, and T.S. Kitajima, Bivalent separation into univalents precedes age-related meiosis I errors in oocytes. Nature communications, 2015. 6.

82. Lister, L.M., A. Kouznetsova, L.A. Hyslop, D. Kalleas, S.L. Pace, J.C. Barel, A. Nathan, V. Floros, C. Adelfalk, and Y. Watanabe, Age-related meiotic segregation errors in mammalian oocytes are preceded by depletion of cohesin and Sgo2. Curr Biol, 2010. 20(17): p. 1511-1521.

83. Chiang, T., F.E. Duncan, K. Schindler, R.M. Schultz, and M.A. Lampson, Evidence that weakened centromere cohesion is a leading cause of age-related aneuploidy in oocytes. Curr Biol, 2010. 20(17): p. 1522-1528.

84. Garcia-Cruz, R., M. Brieno, I. Roig, M. Grossmann, E. Velilla, A. Pujol, L. Cabero, A. Pessarrodona, J. Barbero, and M.G. Caldes, Dynamics of cohesin proteins REC8, STAG3, SMC1β and SMC3 are consistent with a role in sister chromatid cohesion during meiosis in human oocytes. Hum Reprod, 2010: p. deq180.

85. Chiang, T., R.M. Schultz, and M.A. Lampson, Meiotic origins of maternal age-related aneuploidy. Biol Reprod, 2012. 86(1): p. 1-7.

86. Revenkova, E., M. Eijpe, C. Heyting, C.A. Hodges, P.A. Hunt, B. Liebe, H. Scherthan, and R. Jessberger, Cohesin SMC1β is required for meiotic chromosome dynamics, sister chromatid cohesion and DNA recombination. Nat Cell Biol, 2004. 6(6): p. 555-562.

87. Hodges, C.A., E. Revenkova, R. Jessberger, T.J. Hassold, and P.A. Hunt, SMC1β-deficient female mice provide evidence that cohesins are a missing link in age-related nondisjunction. Nat Genet, 2005. 37(12): p. 1351-1355.

88. Chiang, T., R.M. Schultz, and M.A. Lampson, Age-dependent susceptibility of chromosome cohesion to premature separase activation in mouse oocytes. Biol Reprod, 2011. 85(6): p. 1279-1283.

89. Tarin, J.J., Cell cycle: Aetiology of age-associated aneuploidy: a mechanism based on the 'free radical theory of ageing'. Hum Reprod, 1995. 10(6): p. 1563-1565.

90. Harman, D., Free radical theory of aging: an update. Ann N Y Acad Sci, 2006. 1067(1): p. 10-21.

91. Gaziev, A.I., S. Abdullaev, and A. Podlutsky, Mitochondrial function and mitochondrial DNA maintenance with advancing age. Biogerontology, 2014. 15(5): p. 417-438.

92. Kujoth, G., A. Hiona, T. Pugh, S. Someya, K. Panzer, S. Wohlgemuth, T. Hofer, A. Seo, R. Sullivan, and W. Jobling, Mitochondrial DNA mutations, oxidative stress, and apoptosis in mammalian aging. Science, 2005. 309(5733): p. 481-484.

93. Trifunovic, A., A. Wredenberg, M. Falkenberg, J.N. Spelbrink, A.T. Rovio, C.E. Bruder, M. Bohlooly-Y, S. Gidlöf, A. Oldfors, and R. Wibom, Premature ageing in mice expressing defective mitochondrial DNA polymerase. Nature, 2004. 429(6990): p. 417-423.

94. Takeuchi, T., Q.V. Neri, Y. Katagiri, Z. Rosenwaks, and G.D. Palermo, Effect of treating induced mitochondrial damage on embryonic development and epigenesis. Biol Reprod, 2005. 72(3): p. 584-592.

95. Murakoshi, Y., K. Sueoka, K. Takahashi, S. Sato, T. Sakurai, H. Tajima, and Y. Yoshimura, Embryo developmental capability and pregnancy outcome are related to the mitochondrial DNA copy number and ooplasmic volume. J Assist Reprod Genet, 2013. 30(10): p. 1367-1375.

96. Wells, D., K. Kaur, J. Grifo, M. Glassner, J.C. Taylor, E. Fragouli, and S. Munne, Clinical utilisation of a rapid low-pass whole genome sequencing technique for the diagnosis of aneuploidy in human embryos prior to implantation. J Med Genet, 2014. 51(8): p. 553-562.

97. Chappel, S., The role of mitochondria from mature oocyte to viable blastocyst. Obstet Gynecol Int, 2013. 2013.

98. Simsek-Duran, F., F. Li, W. Ford, R.J. Swanson, H.W. Jones, Jr., and F.J. Castora, Age-associated metabolic and morphologic changes in mitochondria of individual mouse and hamster oocytes. PLoS One, 2013. 8(5): p. e64955.

99. Rambags, B.P., D.C. van Boxtel, T. Tharasanit, J.A. Lenstra, B. Colenbrander, and T.A. Stout, Advancing maternal age predisposes to mitochondrial damage and loss during maturation of equine oocytes in vitro. Theriogenology, 2014. 81(7): p. 959-965.

100. Rebolledo-Jaramillo, B., M.S.-W. Su, N. Stoler, J.A. McElhoe, B. Dickins, D. Blankenberg, T.S. Korneliussen, F. Chiaromonte, R. Nielsen, and M.M. Holland, Maternal age effect and severe germ-line bottleneck in the inheritance of human mitochondrial DNA. Proceedings of the National Academy of Sciences, 2014. 111(43): p. 15474-15479.

101. Babayev, E., T. Wang, K. Szigeti-Buck, K. Lowther, H.S. Taylor, T. Horvath, and E. Seli, Reproductive aging is associated with changes in oocyte mitochondrial dynamics, function, and mtDNA quantity. Maturitas, 2016. 93: p. 121-130.

102. Wilding, M., B. Dale, M. Marino, L. di Matteo, C. Alviggi, M.L. Pisaturo, L. Lombardi, and G. De Placido, Mitochondrial aggregation patterns and activity in human oocytes and preimplantation embryos. Hum Reprod, 2001. 16(5): p. 909-917.

103. Santonocito, M., M.R. Guglielmino, M. Vento, M. Ragusa, D. Barbagallo, P. Borzi, I. Casciano, P. Scollo, M. Romani, C. Tatone, M. Purrello, and C. Di Pietro, The apoptotic transcriptome of the human MII oocyte: characterization and age-related changes. Apoptosis, 2013. 18(2): p. 201-211.

104. Zhang, X., X.Q. Wu, S. Lu, Y.L. Guo, and X. Ma, Deficit of mitochondria-derived ATP during oxidative stress impairs mouse MII oocyte spindles. Cell Res, 2006. 16(10): p. 841-850.

105. Wang, L., F. Wang, L. Robinson, Y. Kramer, M. Seth-Smith, N. Sachdev, and D. Keefe, In human germinal vesicle oocytes mitochondrial stress disrupts meiotic spindles without affecting mean telomere length. Fertil Steril, 2016. 106(3): p. e289.

106. Atef, A., P. Francois, V. Christian, and S. Marc-André, The potential role of gap junction communication between cumulus cells and bovine oocytes during in vitro maturation. Mol Reprod Dev, 2005. 71(3): p. 358-367.

107. Tanghe, S., A. Van Soom, H. Nauwynck, M. Coryn, and A. de Kruif, Minireview: Functions of the cumulus oophorus during oocyte maturation, ovulation, and fertilization. Mol Reprod Dev, 2002. 61(3): p. 414-424.

108. Gilchrist, R.B., M. Lane, and J.G. Thompson, Oocyte-secreted factors: regulators of cumulus cell function and oocyte quality. Hum Reprod Update, 2008. 14(2): p. 159-177.

109. Hyttel, P., T. Fair, H. Callesen, and T. Greve, Oocyte growth, capacitation and final maturation in cattle. Theriogenology, 1997. 47(1): p. 23-32.

110. Mermillod, P., Croissance et maturation de l'ovocyte in vivo et in vitro. La Reproduction Chez les Mammifères et lHomme.: Ellipses, 2001: p. 348-366.

111. Sirard, M.-A., S. Desrosier, and M. Assidi, In vivo and in vitro effects of FSH on oocyte maturation and developmental competence. Theriogenology, 2007. 68: p. S71-S76.

112. Sirard, M.-A., F. Richard, P. Blondin, and C. Robert, Contribution of the oocyte to embryo quality. Theriogenology, 2006. 65(1): p. 126-136.

113. Balaban, B. and B. Urman, Effect of oocyte morphology on embryo development and implantation. Reproductive Biomedicine Online, 2006. 12(5): p. 608-615.

114. Borini, A., C. Lagalla, M. Cattoli, E. Sereni, R. Sciajno, C. Flamigni, and G. Coticchio, Predictive factors for embryo implantation potential. Reproductive Biomedicine Online, 2005. 10(5): p. 653-668.

115. Ebner, T., M. Moser, M. Sommergruber, and G. Tews, Selection based on morphological assessment of oocytes and embryos at different stages of preimplantation development: a review. Hum Reprod Update, 2003. 9(3): p. 251-262.

116. Vassena, R., R.J. Mapletoft, S. Allodi, J. Singh, and G.P. Adams, Morphology and developmental competence of bovine oocytes relative to follicular status. Theriogenology, 2003. 60(5): p. 923-932.

117. Warriach, H.M. and K.R. Chohan, Thickness of cumulus cell layer is a significant factor in meiotic competence of buffalo oocytes. J Vet Sci, 2004. 5(3): p. 247-251.

118. Gasca, S., F. Pellestor, S. Assou, V. Loup, T. Anahory, H. Dechaud, J. De Vos, and S. Hamamah, Identifying new human oocyte marker genes: a microarray approach. Reproductive Biomedicine Online, 2007. 14(2): p. 175-183.

119. Gasca, S., L. Reyftmann, F. Pellestor, T. Rème, S. Assou, T. Anahory, H. Dechaud, B. Klein, J. De Vos, and S. Hamamah, Total fertilization failure and molecular abnormalities in metaphase II oocytes. Reproductive Biomedicine Online, 2008. 17(6): p. 772-781.

120. Wells, D., M. Bermudez, N. Steuerwald, A. Thornhill, D. Walker, H. Malter, J. Delhanty, and J. Cohen, Expression of genes regulating chromosome segregation, the cell cycle and apoptosis during human preimplantation development. Hum Reprod, 2005. 20(5): p. 1339-1348.

121. Assou, S., D. Haouzi, K. Mahmoud, A. Aouacheria, Y. Guillemin, V. Pantesco, T. Reme, H. Dechaud, J. De Vos, and S. Hamamah, A non-invasive test for assessing embryo potential by gene expression profiles of human cumulus cells: a proof of concept study. Mol Hum Reprod, 2008. 14(12): p. 711-719.

122. Feuerstein, P., V. Cadoret, R. Dalbies-Tran, F. Guerif, R. Bidault, and D. Royere, Gene expression in human cumulus cells: one approach to oocyte competence. Hum Reprod, 2007. 22(12): p. 3069-3077.

123. McKenzie, L., S. Pangas, S. Carson, E. Kovanci, P. Cisneros, J. Buster, P. Amato, and M. Matzuk, Human cumulus granulosa cell gene expression: a predictor of fertilization and embryo selection in women undergoing IVF. Hum Reprod, 2004. 19(12): p. 2869-2874.

124. Cillo, F., T.A. Brevini, S. Antonini, A. Paffoni, G. Ragni, and F. Gandolfi, Association between human oocyte developmental competence and expression levels of some cumulus genes. Reproduction, 2007. 134(5): p. 645-650.

125. Assidi, M., M. Montag, K. Van Der Ven, and M.-A. Sirard, Biomarkers of human oocyte developmental competence expressed in cumulus cells before ICSI: a preliminary study. J Assist Reprod Genet, 2011. 28(2): p. 173-188.

126. Lucidi, P., N. Bernabò, M. Turriani, B. Barboni, and M. Mattioli, Cumulus cells steroidogenesis is influenced by the degree of oocyte maturation. Reprod Biol Endocrinol, 2003. 1(1): p. 1.

127. Teves, M.E., H.A. Guidobaldi, D.R. Uñates, R. Sanchez, W. Miska, S.J. Publicover, A.A.M. Garcia, and L.C. Giojalas, Molecular mechanism for human sperm chemotaxis mediated by progesterone. PLoS One, 2009. 4(12): p. e8211.

128. Assidi, M., I. Dufort, A. Ali, M. Hamel, O. Algriany, S. Dielemann, and M.-A. Sirard, Identification of potential markers of oocyte competence expressed in bovine cumulus cells matured with follicle-stimulating hormone and/or phorbol myristate acetate in vitro. Biol Reprod, 2008. 79(2): p. 209-222.

129. Huo, L.-J., H.-Y. Fan, C.-G. Liang, L.-Z. Yu, Z.-S. Zhong, D.-Y. Chen, and Q.-Y. Sun, Regulation of ubiquitin-proteasome pathway on pig oocyte meiotic maturation and fertilization. Biol Reprod, 2004. 71(3): p. 853-862.

130. Russell, D.L., K.M. Doyle, S.A. Ochsner, J.D. Sandy, and J.S. Richards, Processing and localization of ADAMTS-1 and proteolytic cleavage of versican during cumulus matrix expansion and ovulation. J Biol Chem, 2003. 278(43): p. 42330-42339.

131. Tsafriri, A., Ovulation as a tissue remodelling process, in *Tissue renin-angiotensin systems*. 1995, Springer. p. 121-140.

132. Franciosi, F., S. Manandhar, and M. Conti, FSH regulates mRNA translation in mouse oocytes and promotes developmental competence. Endocrinology, 2015. 157(2): p. 872-882.

133. Chen, J., S. Torcia, F. Xie, C.-J. Lin, H. Cakmak, F. Franciosi, K. Horner, C. Onodera, J.S. Song, and M.I. Cedars, Somatic cells regulate maternal mRNA translation and developmental competence of mouse oocytes. Nat Cell Biol, 2013. 15(12): p. 1415-1423.

134. Cakmak, H., F. Franciosi, A.M. Zamah, M.I. Cedars, and M. Conti, Dynamic secretion during meiotic reentry integrates the function of the oocyte and cumulus cells. Proceedings of the National Academy of Sciences, 2016. 113(9): p. 2424-2429.

135. Fortune, J., Ovarian follicular growth and development in mammals. Biol Reprod, 1994. 50(2): p. 225-232.

136. Preis, K.A., G. Seidel, and D.K. Gardner, Metabolic markers of developmental competence for in vitro-matured mouse oocytes. Reproduction, 2005. 130(4): p. 475-483.

137. Zachut, M., P. Sood, Y. Levin, and U. Moallem, Proteomic analysis of preovulatory follicular fluid reveals differentially abundant proteins in less fertile dairy cows. J Proteomics, 2016. 139: p. 122-129.

138. Jinno, M., M. Takeuchi, A. Watanabe, K. Teruya, J. Hirohama, N. Eguchi, and A. Miyazaki, Advanced glycation end-products accumulation compromises embryonic development and achievement of pregnancy by assisted reproductive technology. Hum Reprod, 2011. 26(3): p. 604-610.

139. Takeo, S., R. Kawahara-Miki, H. Goto, F. Cao, K. Kimura, Y. Monji, T. Kuwayama, and H. Iwata, Age-associated changes in gene expression and developmental competence of bovine oocytes, and a possible countermeasure against age-associated events. Mol Reprod Dev, 2013. 80(7): p. 508-521.

140. Tatone, C., T. Heizenrieder, G. Di Emidio, P. Treffon, F. Amicarelli, T. Seidel, and U. Eichenlaub-Ritter, Evidence that carbonyl stress by methylglyoxal exposure induces DNA damage and spindle aberrations, affects mitochondrial integrity in mammalian oocytes and contributes to oocyte ageing. Hum Reprod, 2011. 26(7): p. 1843-1859.

141. Liu, Y., X.-Q. He, X. Huang, L. Ding, L. Xu, Y.-T. Shen, F. Zhang, M.-B. Zhu, B.-H. Xu, and Z.-Q. Qi, Resveratrol protects mouse oocytes from methylglyoxal-induced oxidative damage. PLoS One, 2013. 8(10): p. e77960.

142. Goodacre, R., S. Vaidyanathan, W.B. Dunn, G.G. Harrigan, and D.B. Kell, Metabolomics by numbers: acquiring and understanding global metabolite data. Trends Biotechnol, 2004. 22(5): p. 245-252.

143. Gkogkolou, P. and M. Böhm, Advanced glycation end products: Key players in skin aging? Dermatoendocrinol, 2012. 4(3): p. 259-270.

144. Shi, L., X. Yu, H. Yang, and X. Wu, Advanced glycation end products induce human corneal epithelial cells apoptosis through generation of reactive oxygen species and activation of JNK and p38 MAPK pathways. PLoS One, 2013. 8(6): p. e66781.

145. Stensen, M.H., T. Tanbo, R. Storeng, and P. Fedorcsak, Advanced glycation end products and their receptor contribute to ovarian ageing. Hum Reprod, 2014. 29(1): p. 125-134.

146. Pertynska-Marczewska, M. and E. Diamanti-Kandarakis, Aging ovary and the role for advanced glycation end products. Menopause, 2016. 24(3): p. 345-351.

147. Noce, T., S. Okamoto-Ito, and N. Tsunekawa, Vasa homolog genes in mammalian germ cell development. Cell Struct Funct, 2001. 26(3): p. 131-136.

148. White, Y.A.R., D.C. Woods, Y. Takai, O. Ishihara, H. Seki, and J.L. Tilly, Oocyte formation by mitotically active germ cells purified from ovaries of reproductive-age women. Nat Med, 2012. 18(3): p. 413-421.

149. Sunderdam, S., Kissin, D. M., Crawford, S. B., Folger, S. G., Jamieson, D. J., Warner, L., Barfield, W. D., Assited Reproductive Technology Surveillance-United States 2012, in *Morbidity and Mortality Weekly Report*, S.A. Rasmussen, Editor. 2015, Centers for Disease Control and Prevention: Atlanta, GA. p. 1-32.

150. Medicine, P.C.o.t.A.S.f.R., Definitions of infertility and recurrent pregnancy loss: a committee opinion. Fertil Steril, 2013. 99(1): p. 63.

151. Sunderam, S., D.M. Kissin, S.B. Crawford, S.G. Folger, D.J. Jamieson, L. Warner, and W.D. Barfield, Assisted Reproductive Technology Surveillance - United States, 2013. MMWR Surveill Summ, 2015. 64(11): p. 1-25.

152. Carnevale, E., D. Bergfelt, and O. Ginther, Follicular activity and concentrations of FSH and LH associated with senescence in mares. Anim Reprod Sci, 1994. 35(3): p. 231-246.

153. Physick-Sheard, P.W., Demographic analysis of the Canadian Standardbred broodmare herd. Prev Vet Med, 1995. 24(4): p. 285-299.

154. Hutton, C.A. and T. Meacham, Reproductive efficiency on fourteen horse farms. J Anim Sci, 1968. 27(2): p. 434-438.

155. McDowell, K., D. Powell, and C. Baker, Effect of book size and age of mare and stallion on foaling rates in thoroughbred horses. J Equine Vet Sci, 1992. 12(6): p. 364-367.

156. Carnevale, E.M., D.R. Bergfelt, and O.J. Ginther, Aging effects on follicular activity and concentrations of FSH, LH, and progesterone in mares. Anim Reprod Sci, 1993. 31(3–4): p. 287-299.

157. Carnevale, E., M.C. Da Silva, D. Panzani, J. Stokes, and E. Squires, Factors affecting the success of oocyte transfer in a clinical program for subfertile mares. Theriogenology, 2005. 64(3): p. 519-527.

158. Wesson, J.A. and O. Ginther, Influence of season and age on reproductive activity in pony mares on the basis of a slaughterhouse survey. J Anim Sci, 1981. 52(1): p. 119-129.

159. Carnevale, E.M., The mare model for follicular maturation and reproductive aging in the woman. Theriogenology, 2008. 69(1): p. 23-30.

160. Carnevale, E., M. Uson, J. Bozzola, S. King, S. Schmitt, and H. Gates, Comparison of oocytes from young and old mares with light and electron microscopy. Theriogenology, 1999. 51(1): p. 299.

161. Altermatt, J., T. Suh, J. Stokes, and E. Carnevale, Effects of age and equine follicle-stimulating hormone (eFSH) on collection and viability of equine oocytes assessed by morphology and developmental competency after intracytoplasmic sperm injection (ICSI). Reproduction, Fertility and Development, 2009. 21(4): p. 615-623.

162. Ruggeri, E., K.F. DeLuca, C. Galli, G. Lazzari, J.G. DeLuca, and E.M. Carnevale, Cytoskeletal alterations associated with donor age and culture interval for equine oocytes and potential zygotes that failed to cleave after intracytoplasmic sperm injection. Reproduction, Fertility and Development, 2015. 27(6): p. 944-956.

163. Yi, K., B. Rubinstein, J.R. Unruh, F. Guo, B.D. Slaughter, and R. Li, Sequential actin-based pushing forces drive meiosis I chromosome migration and symmetry breaking in oocytes. The Journal of cell biology, 2013. 200(5): p. 567-576.

164. Yu, X.-J., Z. Yi, Z. Gao, D. Qin, Y. Zhai, X. Chen, Y. Ou-Yang, Z.-B. Wang, P. Zheng, and M.-S. Zhu, The subcortical maternal complex controls symmetric division of mouse zygotes by regulating F-actin dynamics. Nature communications, 2014. 5.

165. Yi, K. and R. Li, Actin cytoskeleton in cell polarity and asymmetric division during mouse oocyte maturation. Cytoskeleton, 2012. 69(10): p. 727-737.

166. Holubcová, Z., G. Howard, and M. Schuh, Vesicles modulate an actin network for asymmetric spindle positioning. Nat Cell Biol, 2013. 15(8): p. 937-947.

167. Coticchio, G., M.C. Guglielmo, D.F. Albertini, M. Dal Canto, M.M. Renzini, E. De Ponti, and R. Fadini, Contributions of the actin cytoskeleton to the emergence of polarity during maturation in human oocytes. Mol Hum Reprod, 2014. 20(3): p. 200-207.

168. Campos-Chillon, F., T.A. Farmerie, G.J. Bouma, C.M. Clay, and E.M. Carnevale, Effects of aging on gene expression and mitochondrial DNA in the equine oocyte and follicle cells. Reproduction, Fertility and Development, 2015. 27(6): p. 925-933.

169. da Silveira, J.C., D.R. Veeramachaneni, Q.A. Winger, E.M. Carnevale, and G.J. Bouma, Cell-secreted vesicles in equine ovarian follicular fluid contain miRNAs and proteins: a possible new form of cell communication within the ovarian follicle. Biol Reprod, 2012. 86(3): p. 71.

170. da Silveira, J.C., Q.A. Winger, G.J. Bouma, and E.M. Carnevale, Effects of age on follicular fluid exosomal microRNAs and granulosa cell transforming growth factor-β signalling during follicle development in the mare. Reproduction, Fertility and Development, 2015. 27(6): p. 897-905.

171. Sessions-Bresnahan, D.R. and E.M. Carnevale, Age-associated changes in granulosa cell transcript abundance in equine preovulatory follicles. Reproduction, Fertility and Development, 2015. 27(6): p. 906-913.

172. Jin, S.-L.C., F.J. Richard, W.-P. Kuo, A.J. D'Ercole, and M. Conti, Impaired growth and fertility of cAMP-specific phosphodiesterase PDE4D-deficient mice. Proceedings of the National Academy of Sciences, 1999. 96(21): p. 11998-12003.

173. Stevens, L.C. and C.C. Little, Spontaneous Testicular Teratomas in an Inbred Strain of Mice. Proc Natl Acad Sci U S A, 1954. 40(11): p. 1080-1087.

174. Caplan, A.I. and J.E. Dennis, Mesenchymal stem cells as trophic mediators. J Cell Biochem, 2006. 98(5): p. 1076-1084.

175. Haynesworth, S.E., J. Goshima, V.M. Goldberg, and A.I. Caplan, Characterization of cells with osteogenic potential from human marrow. Bone, 1992. 13(1): p. 81-88.

176. Yoo, J.U., T.S. Barthel, K. Nishimura, L. Solchaga, A.I. Caplan, V.M. Goldberg, and B. Johnstone, The chondrogenic potential of human bone-marrow-derived mesenchymal progenitor cells. J Bone Joint Surg Am, 1998. 80(12): p. 1745-1757.

177. Dennis, J.E., A. Merriam, A. Awadallah, J.U. Yoo, B. Johnstone, and A.I. Caplan, A quadripotential mesenchymal progenitor cell isolated from the marrow of an adult mouse. J Bone Miner Res, 1999. 14(5): p. 700-709.

178. Rubinstein, P., R.E. Rosenfield, J.W. Adamson, and C.E. Stevens, Stored placental blood for unrelated bone marrow reconstitution. Blood, 1993. 81(7): p. 1679-1690.

179. Zuk, P.A., M. Zhu, P. Ashjian, D.A. De Ugarte, J.I. Huang, H. Mizuno, Z.C. Alfonso, J.K. Fraser, P. Benhaim, and M.H. Hedrick, Human adipose tissue is a source of multipotent stem cells. Mol Biol Cell, 2002. 13(12): p. 4279-4295.

180. Wilke, M.M., D.V. Nydam, and A.J. Nixon, Enhanced early chondrogenesis in articular defects following arthroscopic mesenchymal stem cell implantation in an equine model. J Orthop Res, 2007. 25(7): p. 913-925.

181. Smith, R.K., N.J. Werling, S.G. Dakin, R. Alam, A.E. Goodship, and J. Dudhia, Beneficial effects of autologous bone marrow-derived mesenchymal stem cells in naturally occurring tendinopathy. PLoS One, 2013. 8(9): p. e75697.

182. Schnabel, L.V., M.E. Lynch, M.C. van der Meulen, A.E. Yeager, M.A. Kornatowski, and A.J. Nixon, Mesenchymal stem cells and insulin-like growth factor-I gene-enhanced mesenchymal stem cells improve structural aspects of healing in equine flexor digitorum superficialis tendons. J Orthop Res, 2009. 27(10): p. 1392-1398.

183. Kunter, U., S. Rong, Z. Djuric, P. Boor, G. Muller-Newen, D. Yu, and J. Floege, Transplanted mesenchymal stem cells accelerate glomerular healing in experimental glomerulonephritis. J Am Soc Nephrol, 2006. 17(8): p. 2202-2212.

184. Lee, R.H., M.J. Seo, R.L. Reger, J.L. Spees, A.A. Pulin, S.D. Olson, and D.J. Prockop, Multipotent stromal cells from human marrow home to and promote repair of pancreatic islets and renal glomeruli in diabetic NOD/scid mice. Proc Natl Acad Sci U S A, 2006. 103(46): p. 17438-17443.

185. Lian, W.S., W.T. Cheng, C.C. Cheng, F.S. Hsiao, J.J. Chen, C.F. Cheng, and S.C. Wu, In vivo therapy of myocardial infarction with mesenchymal stem cells modified with prostaglandin I synthase gene improves cardiac performance in mice. Life Sci, 2011. 88(9-10): p. 455-464.

186. Emmert, M.Y., B. Weber, P. Wolint, T. Frauenfelder, S.M. Zeisberger, L. Behr, S. Sammut, J. Scherman, C.E. Brokopp, R. Schwartlander, V. Vogel, P. Vogt, J. Grunenfelder, H. Alkadhi, V. Falk, A. Boss, and S.P. Hoerstrup, Intramyocardial transplantation and tracking of human mesenchymal stem cells in a novel intra-uterine pre-immune fetal sheep myocardial infarction model: a proof of concept study. PLoS One, 2013. 8(3): p. e57759.

187. Welt, F.G., R. Gallegos, J. Connell, J. Kajstura, D. D'Amario, R.Y. Kwong, O. Coelho-Filho, R. Shah, R. Mitchell, A. Leri, L. Foley, P. Anversa, and M.A. Pfeffer, Effect of cardiac stem cells on left-ventricular remodeling in a canine model of chronic myocardial infarction. Circ Heart Fail, 2013. 6(1): p. 99-106.

188. Alestalo, K., R. Korpi, J. Makela, S. Lehtonen, T. Makela, F. Yannopoulos, K. Ylitalo, M. Haapea, T. Juvonen, V. Anttila, E. Lappi-Blanco, R. Blanco Sequeiros, and P. Lehenkari, High number of transplanted stem cells improves myocardial recovery after AMI in a porcine model. Scand Cardiovasc J, 2015. 49(2): p. 82-94.

189. Phinney, D.G. and I. Isakova, Plasticity and therapeutic potential of mesenchymal stem cells in the nervous system. Curr Pharm Des, 2005. 11(10): p. 1255-1265.

190. Iso, Y., J.L. Spees, C. Serrano, B. Bakondi, R. Pochampally, Y.H. Song, B.E. Sobel, P. Delafontaine, and D.J. Prockop, Multipotent human stromal cells improve cardiac function after myocardial infarction in mice without long-term engraftment. Biochem Biophys Res Commun, 2007. 354(3): p. 700-706.

191. Kurtz, A., Mesenchymal stem cell delivery routes and fate. Int J Stem Cells, 2008. 1(1): p. 1-7.

192. Ortiz, L.A., M. Dutreil, C. Fattman, A.C. Pandey, G. Torres, K. Go, and D.G. Phinney, Interleukin 1 receptor antagonist mediates the antiinflammatory and antifibrotic effect of mesenchymal stem cells during lung injury. Proc Natl Acad Sci U S A, 2007. 104(26): p. 11002-11007.

193. Shyu, K.G., B.W. Wang, H.F. Hung, C.C. Chang, and D.T. Shih, Mesenchymal stem cells are superior to angiogenic growth factor genes for improving myocardial performance in the mouse model of acute myocardial infarction. J Biomed Sci, 2006. 13(1): p. 47-58.

194. Tang, J., Q. Xie, G. Pan, J. Wang, and M. Wang, Mesenchymal stem cells participate in angiogenesis and improve heart function in rat model of myocardial ischemia with reperfusion. Eur J Cardiothorac Surg, 2006. 30(2): p. 353-361.

195. Mahmood, A., D. Lu, and M. Chopp, Marrow stromal cell transplantation after traumatic brain injury promotes cellular proliferation within the brain. Neurosurgery, 2004. 55(5): p. 1185-1193.

196. Crigler, L., R.C. Robey, A. Asawachaicharn, D. Gaupp, and D.G. Phinney, Human mesenchymal stem cell subpopulations express a variety of neuro-regulatory molecules and promote neuronal cell survival and neuritogenesis. Exp Neurol, 2006. 198(1): p. 54-64.

197. Inoue, Y., A. Iriyama, S. Ueno, H. Takahashi, M. Kondo, Y. Tamaki, M. Araie, and Y. Yanagi, Subretinal transplantation of bone marrow mesenchymal stem cells delays retinal degeneration in the RCS rat model of retinal degeneration. Exp Eye Res, 2007. 85(2): p. 234-241.

198. Hung, S.C., R.R. Pochampally, S.C. Chen, S.C. Hsu, and D.J. Prockop, Angiogenic effects of human multipotent stromal cell conditioned medium activate the PI3K-Akt pathway in hypoxic endothelial cells to inhibit apoptosis, increase survival, and stimulate angiogenesis. Stem Cells, 2007. 25(9): p. 2363-2370.

199. Spees, J.L., S.D. Olson, M.J. Whitney, and D.J. Prockop, Mitochondrial transfer between cells can rescue aerobic respiration. Proc Natl Acad Sci U S A, 2006. 103(5): p. 1283-1288.

200. Friedenstein, A.J., R.K. Chailakhjan, and K.S. Lalykina, The development of fibroblast colonies in monolayer cultures of guinea-pig bone marrow and spleen cells. Cell Tissue Kinet, 1970. 3(4): p. 393-403.

201. Pittenger, M.F., A.M. Mackay, S.C. Beck, R.K. Jaiswal, R. Douglas, J.D. Mosca, M.A. Moorman, D.W. Simonetti, S. Craig, and D.R. Marshak, Multilineage potential of adult human mesenchymal stem cells. Science, 1999. 284(5411): p. 143-147.

202. Dominici, M., K. Le Blanc, I. Mueller, I. Slaper-Cortenbach, F. Marini, D. Krause, R. Deans, A. Keating, D. Prockop, and E. Horwitz, Minimal criteria for defining multipotent mesenchymal stromal cells. The International Society for Cellular Therapy position statement. Cytotherapy, 2006. 8(4): p. 315-317.

203. De Schauwer, C., S. Piepers, G.R. Van de Walle, K. Demeyere, M.K. Hoogewijs, J.L. Govaere, K. Braeckmans, A. Van Soom, and E. Meyer, In search for cross-reactivity to immunophenotype equine mesenchymal stromal cells by multicolor flow cytometry. Cytometry A, 2012. 81(4): p. 312-323.

204. Schnabel, L.V., L.M. Pezzanite, D.F. Antczak, M.J. Felippe, and L.A. Fortier, Equine bone marrow-derived mesenchymal stromal cells are heterogeneous in MHC class II expression and capable of inciting an immune response in vitro. Stem Cell Res Ther, 2014. 5(1): p. 13.

205. Rowley, S.D., Z. Feng, L. Chen, L. Holmberg, S. Heimfeld, B. MacLeod, and W.I. Bensinger, A randomized phase III clinical trial of autologous blood stem cell transplantation comparing cryopreservation using dimethylsulfoxide vs dimethylsulfoxide with hydroxyethylstarch. Bone Marrow Transplant, 2003. 31(11): p. 1043-1051.

206. Mandumpal, J.B., C.A. Kreck, and R.L. Mancera, A molecular mechanism of solvent cryoprotection in aqueous DMSO solutions. Phys Chem Chem Phys, 2011. 13(9): p. 3839-3842.

207. Fleming, K.K. and A. Hubel, Cryopreservation of hematopoietic and non-hematopoietic stem cells. Transfus Apher Sci, 2006. 34(3): p. 309-315.

208. Balint, B., Z. Ivanovic, M. Petakov, J. Taseski, G. Jovcic, N. Stojanovic, and P. Milenkovic, The cryopreservation protocol optimal for progenitor recovery is not optimal for preservation of marrow repopulating ability. Bone Marrow Transplant, 1999. 23(6): p. 613-619.

209. Berz, D., E.M. McCormack, E.S. Winer, G.A. Colvin, and P.J. Quesenberry, Cryopreservation of hematopoietic stem cells. Am J Hematol, 2007. 82(6): p. 463-472.

210. Ginis, I., B. Grinblat, and M.H. Shirvan, Evaluation of bone marrow-derived mesenchymal stem cells after cryopreservation and hypothermic storage in clinically safe medium. Tissue Eng Part C Methods, 2012. 18(6): p. 453-463.

211. Pal, R., M. Hanwate, and S.M. Totey, Effect of holding time, temperature and different parenteral solutions on viability and functionality of adult bone marrow-derived mesenchymal stem cells before transplantation. J Tissue Eng Regen Med, 2008. 2(7): p. 436-444.

212. Hill, R.S., C.A. Mackinder, B.F. Postlewaight, and H.A. Blacklock, The survival of cryopreserved human bone marrow stem cells. Pathology, 1979. 11(3): p. 361-367.

213. Bos, C., Y. Delmas, A. Desmouliere, A. Solanilla, O. Hauger, C. Grosset, I. Dubus, Z. Ivanovic, J. Rosenbaum, P. Charbord, C. Combe, J.W. Bulte, C.T. Moonen, J. Ripoche, and N. Grenier, In vivo MR imaging of intravascularly injected magnetically labeled mesenchymal stem cells in rat kidney and liver. Radiology, 2004. 233(3): p. 781-789.

214. Stodilka, R.Z., K.J. Blackwood, and F.S. Prato, Tracking transplanted cells using dual-radionuclide SPECT. Phys Med Biol, 2006. 51(10): p. 2619-2632.

215. Templin, C., D. Kotlarz, F. Marquart, J. Faulhaber, V. Brendecke, A. Schaefer, D. Tsikas, T. Bonda, D. Hilfiker-Kleiner, L. Ohl, H.Y. Naim, R. Foerster, H. Drexler, and F.P. Limbourg, Transcoronary delivery of bone marrow cells to the infarcted murine myocardium: feasibility, cellular kinetics, and improvement in cardiac function. Basic Res Cardiol, 2006. 101(4): p. 301-310.

216. Laflamme, M.A. and C.E. Murry, Regenerating the heart. Nat Biotechnol, 2005. 23(7): p. 845-856.

217. Muller-Borer, B.J., M.C. Collins, P.R. Gunst, W.E. Cascio, and A.P. Kypson, Quantum dot labeling of mesenchymal stem cells. J Nanobiotechnology, 2007. 5: p. 9.

218. Wang, Y., C. Xu, and H. Ow, Commercial nanoparticles for stem cell labeling and tracking. Theranostics, 2013. 3(8): p. 544-560.

219. Donegan, J. and Y. Rakovich, Cadmium Telluride Quantum Dots: Advances and Applications. 2013: CRC Press.

220. Rosen, A.B., D.J. Kelly, A.J. Schuldt, J. Lu, I.A. Potapova, S.V. Doronin, K.J. Robichaud, R.B. Robinson, M.R. Rosen, P.R. Brink, G.R. Gaudette, and I.S. Cohen, Finding fluorescent needles in the cardiac haystack: tracking human mesenchymal stem cells labeled with quantum dots for quantitative in vivo three-dimensional fluorescence analysis. Stem Cells, 2007. 25(8): p. 2128-2138.

221. Costa, C.R., M.L. Feitosa, D.O. Bezerra, Y.K. Carvalho, R.F. Olivindo, P.B. Fernando, G.C. Silva, M.L. Silva, C.E. Ambrósio, and A.M.C. Júnior, Labeling of adipose-derived stem cells with quantum dots provides stable and long-term fluorescent signal for ex vivo cell tracking. In Vitro Cellular & Developmental Biology-Animal, 2016: p. 1-8.

222. Seleverstov, O., O. Zabirnyk, M. Zscharnack, L. Bulavina, M. Nowicki, J.-M. Heinrich, M. Yezhelyev, F. Emmrich, R. O'Regan, and A. Bader, Quantum dots for human mesenchymal stem cells labeling. A size-dependent autophagy activation. Nano letters, 2006. 6(12): p. 2826-2832.

223. Wang, Z.-G., S.-L. Liu, Y.-J. Hu, Z.-Q. Tian, B. Hu, Z.-L. Zhang, and D.-W. Pang, Dissecting the Factors Affecting the Fluorescence Stability of Quantum Dots in Live Cells. ACS applied materials & interfaces, 2016. 8(13): p. 8401-8408.

224. Larson, D.R., W.R. Zipfel, R.M. Williams, S.W. Clark, M.P. Bruchez, F.W. Wise, and W.W. Webb, Water-soluble quantum dots for multiphoton fluorescence imaging in vivo. Science, 2003. 300(5624): p. 1434-1436.

225. Hossain, M.A., T. Chowdhury, and A. Bagul, Imaging modalities for the in vivo surveillance of mesenchymal stromal cells. J Tissue Eng Regen Med, 2015. 9(11): p. 1217-1224.

226. Byrne, J., T.R. Fears, M.H. Gail, D. Pee, R.R. Connelly, D.F. Austin, G.F. Holmes, F.F. Holmes, H.B. Latourette, and J.W. Meigs, Early menopause in long-term survivors of cancer during adolescence. Am J Obstet Gynecol, 1992. 166(3): p. 788-793.

227. Meirow, D., H. Lewis, D. Nugent, and M. Epstein, Subclinical depletion of primordial follicular reserve in mice treated with cyclophosphamide: clinical importance and proposed accurate investigative tool. Hum Reprod, 1999. 14(7): p. 1903-1907.

228. Chiarelli, A.M., L.D. Marrett, and G. Darlington, Early menopause and infertility in females after treatment for childhood cancer diagnosed in 1964-1988 in Ontario, Canada. Am J Epidemiol, 1999. 150(3): p. 245-254.

229. Petrek, J.A., M.J. Naughton, L.D. Case, E.D. Paskett, E.Z. Naftalis, S.E. Singletary, and P. Sukumvanich, Incidence, time course, and determinants of menstrual bleeding after breast cancer treatment: a prospective study. J Clin Oncol, 2006. 24(7): p. 1045-1051.

230. Letourneau, J.M., E.E. Ebbel, P.P. Katz, K.H. Oktay, C.E. McCulloch, W.Z. Ai, A.J. Chien, M.E. Melisko, M.I. Cedars, and M.P. Rosen, Acute ovarian failure underestimates age-specific reproductive impairment for young women undergoing chemotherapy for cancer. Cancer, 2012. 118(7): p. 1933-1939.

231. Meirow, D. and D. Nugent, The effects of radiotherapy and chemotherapy on female reproduction. Hum Reprod Update, 2001. 7(6): p. 535-543.

232. Meirow, D., H. Biederman, R.A. Anderson, and W.H. Wallace, Toxicity of chemotherapy and radiation on female reproduction. Clin Obstet Gynecol, 2010. 53(4): p. 727-739.

233. Fan, W., Possible mechanisms of paclitaxel-induced apoptosis. Biochem Pharmacol, 1999. 57(11): p. 1215-1221.

234. Stumm, S., A. Meyer, M. Lindner, G. Bastert, D. Wallwiener, and B. Gückel, Paclitaxel treatment of breast cancer cell lines modulates Fas/Fas ligand expression and induces apoptosis which can be inhibited through the CD40 receptor. Oncology, 2004. 66(2): p. 101-111.

235. Lopes, F., R. Smith, R.A. Anderson, and N. Spears, Docetaxel induces moderate ovarian toxicity in mice, primarily affecting granulosa cells of early growing follicles. Mol Hum Reprod, 2014. 20(10): p. 948-959.

236. Roti, E.C.R., S.K. Leisman, D.H. Abbott, and S.M. Salih, Acute doxorubicin insult in the mouse ovary is cell-and follicle-type dependent. PLoS One, 2012. 7(8): p. e42293.

237. Kalich-Philosoph, L., H. Roness, A. Carmely, M. Fishel-Bartal, H. Ligumsky, S. Paglin, I. Wolf, H. Kanety, B. Sredni, and D. Meirow, Cyclophosphamide triggers follicle activation and "burnout"; AS101 prevents follicle loss and preserves fertility. Sci Transl Med, 2013. 5(185): p. 185ra162-185ra162.

238. Chen, X.-Y., H.-X. Xia, H.-Y. Guan, B. Li, and W. Zhang, Follicle loss and apoptosis in cyclophosphamide-treated mice: what's the matter? Int J Mol Sci, 2016. 17(6): p. 836.

239. Makarovsky, D., Y. Kalechman, T. Sonino, I. Freidkin, S. Teitz, M. Albeck, M. Weil, R. GEFFEN-ARICHA, G. Yadid, and B. Sredni, Tellurium compound AS101 induces PC12 differentiation and rescues the neurons from apoptotic death. Ann N Y Acad Sci, 2003. 1010(1): p. 659-666.

240. Roness, H., Z. Gavish, Y. Cohen, and D. Meirow, Ovarian follicle burnout: a universal phenomenon? Cell Cycle, 2013. 12(20): p. 3245-3246.

241. Roness, H.D.-H., S; Gavish, Z; Meirow, D., Anti-Mullerian c-treatment to prevent chemotherapy-induced activation and loss. Abstracts of the 31st Annual Meeting of the European Society of Human Reproduction and Embryology., 2015.

242. Utsunomiya, T., T. Tanaka, H. Utsunomiya, and N. Umesaki, A novel molecular mechanism for anticancer drug-induced ovarian failure: Irinotecan HCl, an anticancer topoisomerase I inhibitor, induces specific FasL expression in granulosa cells of large ovarian follicles to enhance follicular apoptosis. Int J Oncol, 2008. 32(5): p. 991-1000.

243. Perez, G.I., C.M. Knudson, L. Leykin, S.J. Korsmeyer, and J.L. Tilly, Apoptosis-associated signaling pathways are required for chemotherapy-mediated female germ cell destruction. Nat Med, 1997. 3(11): p. 1228-1232.

244. Depalo, R., L. Nappi, G. Loverro, S. Bettocchi, M.L. Caruso, A.M. Valentini, and L. Selvaggi, Evidence of apoptosis in human primordial and primary follicles. Hum Reprod, 2003. 18(12): p. 2678-2682.

245. Morita, Y., G.I. Perez, F. Paris, S.R. Miranda, D. Ehleiter, A. Haimovitz-Friedman, Z. Fuks, Z. Xie, J.C. Reed, and E.H. Schuchman, Oocyte apoptosis is suppressed by disruption of the acid sphingomyelinase gene or by sphingosine-1-phosphate therapy. Nat Med, 2000. 6(10): p. 1109-1114.

246. Kurita, T., G.R. Cunha, S.J. Robboy, A.A. Mills, and R.T. Medina, Differential expression of p63 isoforms in female reproductive organs. Mech Dev, 2005. 122(9): p. 1043-1055.

247. Suh, E.-K., A. Yang, A. Kettenbach, C. Bamberger, A.H. Michaelis, Z. Zhu, J.A. Elvin, R.T. Bronson, C.P. Crum, and F. McKeon, p63 protects the female germ line during meiotic arrest. Nature, 2006. 444(7119): p. 624-628.

248. Livera, G., B. Petre-Lazar, M.-J. Guerquin, E. Trautmann, H. Coffigny, and R. Habert, p63 null mutation protects mouse oocytes from radio-induced apoptosis. Reproduction, 2008. 135(1): p. 3-12.

249. Gonfloni, S., L. Di Tella, S. Caldarola, S.M. Cannata, F.G. Klinger, C. Di Bartolomeo, M. Mattei, E. Candi, M. De Felici, and G. Melino, Inhibition of the c-Abl–TAp63 pathway protects mouse oocytes from chemotherapy-induced death. Nat Med, 2009. 15(10): p. 1179-1185.

250. Kim, S.-Y., M. Cordeiro, V. Serna, K. Ebbert, L.M. Butler, S. Sinha, A.A. Mills, T.K. Woodruff, and T. Kurita, Rescue of platinum-damaged oocytes from programmed cell death through inactivation of the p53 family signaling network. Cell Death Differ, 2013. 20(8): p. 987-997.

251. Kerr, J.B., K.J. Hutt, E.M. Michalak, M. Cook, C.J. Vandenberg, S.H. Liew, P. Bouillet, A. Mills, C.L. Scott, and J.K. Findlay, DNA damage-induced primordial follicle oocyte apoptosis and loss of fertility require TAp63-mediated induction of Puma and Noxa. Mol Cell, 2012. 48(3): p. 343-352.

252. Soleimani, R., E. Heytens, Z. Darzynkiewicz, and K. Oktay, Mechanisms of chemotherapy-induced human ovarian aging: double strand DNA breaks and microvascular compromise. Aging-Us, 2011. 3(8): p. 782-793.

253. Marcello, M.F., G. Nuciforo, R. Romeo, G. Di Dino, I. Russo, A. Russo, G. Palumbo, and G. Schiliro, Structural and ultrastructural study of the ovary in childhood leukemia after successful treatment. Cancer, 1990. 66(10): p. 2099-2104.

254. Ben-Aharon, I., I. Meizner, T. Granot, S. Uri, N. Hasky, S. Rizel, R. Yerushalmi, A. Sulkes, and S.M. Stemmer, Chemotherapy-induced ovarian failure as a prototype for acute vascular toxicity. The oncologist, 2012. 17(11): p. 1386-1393.

255. Bar-Joseph, H., I. Ben-Aharon, M. Tzabari, G. Tsarfaty, S.M. Stemmer, and R. Shalgi, In vivo bioimaging as a novel strategy to detect doxorubicin-induced damage to gonadal blood vessels. PLoS One, 2011. 6(9): p. e23492.

256. Meirow, D., J. Dor, B. Kaufman, A. Shrim, J. Rabinovici, E. Schiff, H. Raanani, J. Levron, and E. Fridman, Cortical fibrosis and blood-vessels damage in human ovaries exposed to chemotherapy. Potential mechanisms of ovarian injury. Hum Reprod, 2007. 22(6): p. 1626-1633.

257. Soleimani, R., E. Heytens, and K. Oktay, Enhancement of neoangiogenesis and follicle survival by sphingosine-1-phosphate in human ovarian tissue xenotransplants. PLoS One, 2011. 6(4): p. e19475.

258. Oktay, K., G. Karlikaya, O. Akman, G.K. Ojakian, and M. Oktay, Interaction of extracellular matrix and activin-A in the initiation of follicle growth in the mouse ovary. Biol Reprod, 2000. 63(2): p. 457-461.

259. Oktem, O. and K. Oktay, The role of extracellular matrix and activin-A in in vitro growth and survival of murine preantral follicles. Reprod Sci, 2007. 14(4): p. 358-366.

260. Roness, H., O. Kashi, and D. Meirow, Prevention of chemotherapy-induced ovarian damage. Fertil Steril, 2016. 105(1): p. 20-29.

261. Sanders, J.E., C.D. Buckner, D. Amos, W. Levy, F.R. Appelbaum, K. Doney, R. Storb, K.M. Sullivan, R.P. Witherspoon, and E.D. Thomas, Ovarian function following marrow transplantation for aplastic anemia or leukemia. J Clin Oncol, 1988. 6(5): p. 813-818.

262. Abd-Allah, S.H., S.M. Shalaby, H.F. Pasha, A.S. El-Shal, N. Raafat, S.M. Shabrawy, H.A. Awad, M.G. Amer, M.A. Gharib, E.A. El Gendy, A.A. Raslan, and H.M. El-Kelawy, Mechanistic action of mesenchymal stem cell injection in the treatment of chemically induced ovarian failure in rabbits. Cytotherapy, 2013. 15(1): p. 64-75.

263. Ghadami, M., E. El-Demerdash, D. Zhang, S.A. Salama, A.A. Binhazim, A.E. Archibong, X. Chen, B.R. Ballard, M.R. Sairam, and A. Al-Hendy, Bone marrow transplantation restores follicular maturation and steroid hormones production in a mouse model for primary ovarian failure. PLoS One, 2012. 7(3): p. e32462.

264. Buigues, A.H., S; Romeu, M; Martinez, S; Solves, P; Martinez, L; Pellicer, A., Optimization of the ovarian reserve in Poor Responder patients by ovarian autologous transplantation of mobilized-bone marrow derived stem cells. Abstracts of the 32nd Annual Meeting of the European Society of Human Reproduction and Embryology., 2016. 31(Supp 1): p. i4-i5.

265. Shin, S.Y., J.Y. Lee, E. Lee, J. Choi, B.K. Yoon, D. Bae, and D. Choi, Protective effect of vascular endothelial growth factor (VEGF) in frozen-thawed granulosa cells is mediated by inhibition of apoptosis. Eur J Obstet Gynecol Reprod Biol, 2006. 125(2): p. 233-238.

266. Uzumcu, M., Z. Pan, Y. Chu, P.E. Kuhn, and R. Zachow, Immunolocalization of the hepatocyte growth factor (HGF) system in the rat ovary and the anti-apoptotic effect of HGF in rat ovarian granulosa cells in vitro. Reproduction, 2006. 132(2): p. 291-299.

267. Mao, J., M.F. Smith, E.B. Rucker, G.M. Wu, T.C. McCauley, T.C. Cantley, R.S. Prather, B.A. Didion, and B.N. Day, Effect of epidermal growth factor and insulin-like growth factor I on porcine preantral follicular growth, antrum formation, and stimulation of granulosal cell proliferation and suppression of apoptosis in vitro. J Anim Sci, 2004. 82(7): p. 1967-1975.

268. Ortiz, L.A., F. Gambelli, C. McBride, D. Gaupp, M. Baddoo, N. Kaminski, and D.G. Phinney, Mesenchymal stem cell engraftment in lung is enhanced in response to bleomycin exposure and ameliorates its fibrotic effects. Proc Natl Acad Sci U S A, 2003. 100(14): p. 8407-8411.

269. Minguell, J.J. and A. Erices, Mesenchymal stem cells and the treatment of cardiac disease. Exp Biol Med (Maywood), 2006. 231(1): p. 39-49.

270. Bruck, I., K. Raun, B. Synnestvedt, and T. Greve, Follicle aspiration in the mare using a transvaginal ultrasound-guided technique. Equine Vet J, 1992. 24(1): p. 58-59.

271. Jacobson, C.C., Y.-H. Choi, S.S. Hayden, and K. Hinrichs, Recovery of mare oocytes on a fixed biweekly schedule, and resulting blastocyst formation after intracytoplasmic sperm injection. Theriogenology, 2010. 73(8): p. 1116-1126.

272. Choi, Y., L. Love, D. Varner, and K. Hinrichs, Holding immature equine oocytes in the absence of meiotic inhibitors: effect on germinal vesicle chromatin and blastocyst development after intracytoplasmic sperm injection. Theriogenology, 2006. 66(4): p. 955-963.

273. Choi, Y.-H., P. Ross, I.C. Velez, B. Macias-Garcia, F.L. Riera, and K. Hinrichs, Cell lineage allocation in equine blastocysts produced in vitro under varying glucose concentrations. Reproduction, 2015. 150(1): p. 31-41.

274. Choi, Y., Y. Chung, S. Walker, M. Westhusin, and K. Hinrichs, In vitro development of equine nuclear transfer embryos: effects of oocyte maturation media and amino acid composition during embryo culture. Zygote, 2003. 11(01): p. 77-86.

275. Slone, D.E., Jr., Ovariectomy, ovariohysterectomy, and cesarean section in mares. Vet Clin North Am Equine Pract, 1988. 4(3): p. 451-459.

276. Alves, K.A., B.G. Alves, C.D. Rocha, M. Visonna, R.F. Mohallem, M.O. Gastal, J.O. Jacomini, M.E. Beletti, J.R. Figueiredo, M.L. Gambarini, and E.L. Gastal, Number and density of equine preantral follicles in different ovarian histological section thicknesses. Theriogenology, 2015. 83(6): p. 1048-1055.

277. De Schauwer, C., E. Meyer, G.R. Van de Walle, and A. Van Soom, Markers of stemness in equine mesenchymal stem cells: a plea for uniformity. Theriogenology, 2011. 75(8): p. 1431-1443.

278. Sacchetti, B., A. Funari, C. Remoli, G. Giannicola, G. Kogler, S. Liedtke, G. Cossu, M. Serafini, M. Sampaolesi, and E. Tagliafico, No identical "Mesenchymal Stem Cells" at different times and sites: human committed progenitors of distinct origin and differentiation potential are incorporated as adventitial cells in microvessels. Stem Cell Reports, 2016. 6(6): p. 897-913.

279. Assoni, A., G. Coatti, M.C. Valadares, M. Beccari, J. Gomes, M. Pelatti, M. Mitne-Neto, V.M. Carvalho, and M. Zatz, Different donors Mesenchymal Stromal Cells secretomes reveal heterogeneous profile of relevance for therapeutic use. Stem Cells and Development, 2016.

280. Burk, J., I. Ribitsch, C. Gittel, H. Juelke, C. Kasper, C. Staszyk, and W. Brehm, Growth and differentiation characteristics of equine mesenchymal stromal cells derived from different sources. The Veterinary Journal, 2013. 195(1): p. 98-106.

281. Guest, D., M. Smith, and W. Allen, Equine embryonic stem-like cells and mesenchymal stromal cells have different survival rates and migration patterns following their injection into damaged superficial digital flexor tendon. Equine Vet J, 2010. 42(7): p. 636-642.

282. Hanna, J. and A. Hubel, Preservation of stem cells. Organogenesis, 2009. 5(3): p. 134-137.

283. Naaldijk, Y., M. Staude, V. Fedorova, and A. Stolzing, Effect of different freezing rates during cryopreservation of rat mesenchymal stem cells using combinations of hydroxyethyl starch and dimethylsulfoxide. BMC Biotechnol, 2012. 12: p. 49.

284. Heng, B.C., Effect of Rho-associated kinase (ROCK) inhibitor Y-27632 on the post-thaw viability of cryopreserved human bone marrow-derived mesenchymal stem cells. Tissue Cell, 2009. 41(5): p. 376-380.

285. Collins, M.C., P.R. Gunst, W.E. Cascio, A.P. Kypson, and B.J. Muller-Borer, Labeling and imaging mesenchymal stem cells with quantum dots. Methods Mol Biol, 2012. 906: p. 199-210.

286. Ohyabu, Y., Z. Kaul, T. Yoshioka, K. Inoue, S. Sakai, H. Mishima, T. Uemura, S.C. Kaul, and R. Wadhwa, Stable and nondisruptive in vitro/in vivo labeling of mesenchymal stem cells by internalizing quantum dots. Hum Gene Ther, 2009. 20(3): p. 217-224.

287. Ranjbarvaziri, S., S. Kiani, A. Akhlaghi, A. Vosough, H. Baharvand, and N. Aghdami, Quantum dot labeling using positive charged peptides in human hematopoetic and mesenchymal stem cells. Biomaterials, 2011. 32(22): p. 5195-5205.

288. Tautzenberger, A., S. Lorenz, L. Kreja, A. Zeller, A. Musyanovych, H. Schrezenmeier, K. Landfester, V. Mailander, and A. Ignatius, Effect of functionalised fluorescence-labelled nanoparticles on mesenchymal stem cell differentiation. Biomaterials, 2010. 31(8): p. 2064-2071.

289. Szepesi, Á., Z. Matula, A. Szigeti, G. Várady, J. Szalma, G. Szabó, F. Uher, B. Sarkadi, and K. Német, In Vitro Characterization of Human Mesenchymal Stem Cells Isolated from Different Tissues with a Potential to Promote Complex Bone Regeneration. Stem Cells International, 2016. 2016.

290. Hatakeyama, A., S. Uchida, H. Utsunomiya, M. Tsukamoto, H. Nakashima, E. Nakamura, C. Pascual-Garrido, I. Sekiya, and A. Sakai, Isolation and Characterization of Synovial Mesenchymal Stem Cell Derived from Hip Joints: A Comparative Analysis with a Matched Control Knee Group. Stem Cells International, 2017. 2017.

291. Tsuji, K., M. Ojima, K. Otabe, M. Horie, H. Koga, I. Sekiya, and T. Muneta, Effects of different cell detaching methods on the viability and cell surface antigen expression of synovial mesenchymal stem cells. Cell Transplant, 2017.

292. Lovati, A.B., B. Corradetti, F. Cremonesi, D. Bizzaro, and A.L. Consiglio, Tenogenic differentiation of equine mesenchymal progenitor cells under indirect co-culture. Int J Artif Organs, 2012. 35(11): p. 996-1005.

293. Lettry, V., K. Hosoya, S. Takagi, and M. Okumura, Coculture of equine mesenchymal stem cells and mature equine articular chondrocytes results in improved chondrogenic differentiation of the stem cells. Jpn J Vet Res, 2010. 58(1): p. 5-15.

294. Samuelson, D.A., Textbook of Veterinary Histology Saunders. 1st ed ed. 2007, St. Louis, MO, USA: Saunders Elsevier.

295. Palmer, M.a.P., E. Assesing RNA Quality. 2016 [cited 2016 09/22]; Available from: https://www.thermofisher.com/us/en/home/references/ambion-tech-support/rna-isolation/tech-notes/assessing-rna-quality.html.

296. Mueller, O., S. Lightfoot, and A. Schroeder, RNA integrity number (RIN)–standardization of RNA quality control. Agilent application note, publication, 2004: p. 1-8.

297. Morgan, S., L. Campbell, V. Allison, A. Murray, and N. Spears, Culture and co-culture of mouse ovaries and ovarian follicles. J Vis Exp, 2015(97).

298. Riley, S.C., R. Thomassen, S.E. Bae, R. Leask, H.G. Pedersen, and E.D. Watson, Matrix metalloproteinase-2 and -9 secretion by the equine ovary during follicular growth and prior to ovulation. Anim Reprod Sci, 2004. 81(3-4): p. 329-339.

299. Ricci, A.G., M.P. Di Yorio, and A.G. Faletti, Inhibitory effect of leptin on the rat ovary during the ovulatory process. Reproduction, 2006. 132(5): p. 771-780.

300. Ikeda, H., Serum-free medium conditions for steroidogenesis of bovine follicular thecal cells cultured on collagen gel matrix. In Vitro Cell Dev Biol, 1990. 26(2): p. 193-200.

301. Hulshof, S.C.J., J.R. Figueiredo, J.F. Beckers, M.M. Bevers, J.A. van der Donk, and R. van den Hurk, Effects of fetal bovine serum, FSH and 17β-estradiol on the culture of bovine preantral follicles. Theriogenology, 1995. 44(2): p. 217-226.

302. Sah, R.L., S.B. Trippel, and A.J. Grodzinsky, Differential effects of serum, insulin-like growth factor-I, and fibroblast growth factor-2 on the maintenance of cartilage physical properties during long-term culture. J Orthop Res, 1996. 14(1): p. 44-52.

303. Orly, J. and G. Sato, Fibronectin mediates cytokinesis and growth of rat follicular cells in serum-free medium. Cell, 1979. 17(2): p. 295-305.

304. Bian, L., E.G. Lima, S.L. Angione, K.W. Ng, D.Y. Williams, D. Xu, A.M. Stoker, J.L. Cook, G.A. Ateshian, and C.T. Hung, Mechanical and biochemical characterization of cartilage explants in serum-free culture. J Biomech, 2008. 41(6): p. 1153-1159.

305. Velez, I., C. Arnold, C. Jacobson, J. Norris, Y. Choi, J. Edwards, S. Hayden, and K. Hinrichs, Effects of repeated transvaginal aspiration of immature follicles on mare health and ovarian status. Equine Vet J, 2012. 44(S43): p. 78-83.

306. Claes, A., B.A. Ball, K.E. Scoggin, A. Esteller-Vico, J.J. Kalmar, A.J. Conley, E.L. Squires, and M.H. Troedsson, The interrelationship between anti-Mullerian hormone, ovarian follicular populations and age in mares. Equine Vet J, 2014.

307. Lenton, E., L. Sexton, S. Lee, and I. Cooke, Progressive changes in LH and FSH and LH: FSH ratio in women throughout reproductive life. Maturitas, 1988. 10(1): p. 35-43.

308. Sherman, B.M., J.H. WEST, and S.G. KORENMAN, The menopausal transition: analysis of LH, FSH, estradiol, and progesterone concentrations during menstrual cycles of older women. The Journal of Clinical Endocrinology & Metabolism, 1976. 42(4): p. 629-636.

309. Giannini, A., A.R. Genazzani, and T. Simoncini, Neuroendocrine Basis of the Hypothalamus–Pituitary–Ovary Axis Aging, in *Frontiers in Gynecological Endocrinology*. 2016, Springer. p. 91-95.

310. Mossa, F., S. Walsh, S. Butler, D. Berry, F. Carter, P. Lonergan, G. Smith, J. Ireland, and A. Evans, Low numbers of ovarian follicles≥ 3mm in diameter are associated with low fertility in dairy cows. J Dairy Sci, 2012. 95(5): p. 2355-2361.

311. Jimenez-Krassel, F., J. Folger, J. Ireland, G. Smith, X. Hou, J. Davis, P. Lonergan, A. Evans, and J. Ireland, Evidence that high variation in ovarian reserves of healthy young adults has a negative impact on the corpus luteum and endometrium during estrous cycles in cattle. Biol Reprod, 2009. 80(6): p. 1272-1281.

312. Bolger, A.M., M. Lohse, and B. Usadel, Trimmomatic: a flexible trimmer for Illumina sequence data. Bioinformatics, 2014: p. btu170.

313. Bokulich, N.A., S. Subramanian, J.J. Faith, D. Gevers, J.I. Gordon, R. Knight, D.A. Mills, and J.G. Caporaso, Quality-filtering vastly improves diversity estimates from Illumina amplicon sequencing. Nature methods, 2013. 10(1): p. 57-59.

314. Kim, D., B. Langmead, and S.L. Salzberg, HISAT: a fast spliced aligner with low memory requirements. Nat Meth, 2015. 12(4): p. 357-360.

315. Anders, S., P.T. Pyl, and W. Huber, HTSeq–a Python framework to work with high-throughput sequencing data. Bioinformatics, 2014: p. 166-169.

316. Love, M., S. Anders, and W. Huber, Differential analysis of count data–the DESeq2 package. Genome Biol, 2014. 15: p. 550.

317. Kussano, N., L. Leme, A. Guimarães, M. Franco, and M. Dode, Molecular markers for oocyte competence in bovine cumulus cells. Theriogenology, 2016. 85(6): p. 1167-1176.

318. Bunel, A., E. Jorssen, E. Merckx, J. Leroy, P. Bols, and M. Sirard, Individual bovine in vitro embryo production and cumulus cell transcriptomic analysis to distinguish cumulus-oocyte complexes with high or low developmental potential. Theriogenology, 2015. 83(2): p. 228-237.

319. Pal, R., M.K. Mamidi, A.K. Das, and R. Bhonde, Diverse effects of dimethyl sulfoxide (DMSO) on the differentiation potential of human embryonic stem cells. Arch Toxicol, 2012. 86(4): p. 651-661.

320. Binart, N., A. Bachelot, and J. Bouilly, Impact of prolactin receptor isoforms on reproduction. Trends Endocrinol Metab, 2010. 21(6): p. 362-368.

321. Nequin, L., S. King, A. Johnson, G. Gow, and G. Ferreira-Dias, Prolactin may play a role in stimulating the equine ovry during the spring reproductive transition. J Equine Vet Sci, 1993. 13(11): p. 631-635.

322. Costlow, M.E., Differentiation-inducing agents decrease cryptic prolactin receptors in cultured rat mammary tumor cells. Exp Cell Res, 1984. 155(1): p. 17-23.

323. Behnam, B., M.H. Modarressi, V. Conti, K.E. Taylor, A. Puliti, and J. Wolfe, Expression of Tsga10 sperm tail protein in embryogenesis and neural development: from cilium to cell division. Biochem Biophys Res Commun, 2006. 344(4): p. 1102-1110.

324. Mobasheri, M.B., I. Jahanzad, M.A. Mohagheghi, M. Aarabi, S. Farzan, and M.H. Modarressi, Expression of two testis-specific genes, TSGA10 and SYCP3, in different cancers regarding to their pathological features. Cancer Detect Prev, 2007. 31(4): p. 296-302.

325. Miryounesi, M., K. Nayernia, M.B. Mobasheri, M. Dianatpour, R. Oko, S. Savad, and M.H. Modarressi, Evaluation of in vitro spermatogenesis system effectiveness to study genes behavior: monitoring the expression of the testis specific 10 (Tsga10) gene as a model. Archives of Iranian Medicine (AIM), 2014. 17(10).

326. Tanaka, R., T. Ono, S. Sato, T. Nakada, F. Koizumi, K. Hasegawa, K. Nakagawa, H. Okumura, T. Yamashita, and M. Ohtsuka, Over-Expression of the Testis-Specific Gene TSGA10 in Cancers and Its Immunogenicity. Microbiol Immunol, 2004. 48(4): p. 339-345.

327. Volodko, N., M. Gordon, M. Salla, H.A. Ghazaleh, and S. Baksh, RASSF tumor suppressor gene family: biological functions and regulation. FEBS Lett, 2014. 588(16): p. 2671-2684.

328. Lee, C.-M., P. Yang, L.-C. Chen, C.-C. Chen, S.-C. Wu, H.-Y. Cheng, and Y.-S. Chang, A novel role of RASSF9 in maintaining epidermal homeostasis. PLoS One, 2011. 6(3): p. e17867.

329. Woodruff, T.K., R.J. Lyon, S.E. Hansen, G.C. Rice, and J.P. Mather, Inhibin and activin locally regulate rat ovarian folliculogenesis. Endocrinology, 1990. 127(6): p. 3196-3205.

330. Roberts, V.J., S. Barth, A. el-Roeiy, and S. Yen, Expression of inhibin/activin subunits and follistatin messenger ribonucleic acids and proteins in ovarian follicles and the corpus luteum during the human menstrual cycle. The Journal of Clinical Endocrinology & Metabolism, 1993. 77(5): p. 1402-1410.

331. Drummond, A.E., M.T. Le, J.-F. Ethier, M. Dyson, and J.K. Findlay, Expression and localization of activin receptors, Smads, and βglycan to the postnatal rat ovary. Endocrinology, 2002. 143(4): p. 1423-1433.

332. Reissmann, E., H. Jörnvall, A. Blokzijl, O. Andersson, C. Chang, G. Minchiotti, M.G. Persico, C.F. Ibáñez, and A.H. Brivanlou, The orphan receptor ALK7 and the Activin receptor ALK4 mediate signaling by Nodal proteins during vertebrate development. Genes Dev, 2001. 15(15): p. 2010-2022.

333. Galvão, A., D. Skarzynski, and G. Ferreira-Dias, Nodal Promotes Functional Luteolysis via Down-Regulation of Progesterone and Prostaglandins E2 and Promotion of PGF2α Synthetic Pathways in Mare Corpus Luteum. Endocrinology, 2015. 157(2): p. 858-871.

334. Kristensen, S.G., K. Andersen, C.A. Clement, S. Franks, K. Hardy, and C.Y. Andersen, Expression of TGF-beta superfamily growth factors, their receptors, the associated SMADs and antagonists in five isolated size-matched populations of preantral follicles from normal human ovaries. Mol Hum Reprod, 2013: p. gat089.

335. Sandoval-Guzmán, T., C. Göngrich, A. Moliner, T. Guo, H. Wu, C. Broberger, and C.F. Ibáñez, Neuroendocrine control of female reproductive function by the activin receptor ALK7. The FASEB Journal, 2012. 26(12): p. 4966-4976.

336. Chang, H.-M., J. Qiao, and P.C. Leung, Oocyte–somatic cell interactions in the human ovary—novel role of bone morphogenetic proteins and growth differentiation factors. Hum Reprod Update, 2016.

337. Santamaria, X., S. Cabanillas, I. Cervelló, C. Arbona, F. Raga, J. Ferro, J. Palmero, J. Remohí, A. Pellicer, and C. Simón, Autologous cell therapy with CD133+ bone marrow-derived stem cells for refractory Asherman's syndrome and endometrial atrophy: a pilot cohort study. Hum Reprod, 2016: p. dew042.

338. Mashaghi, A., A. Marmalidou, M. Tehrani, P.M. Grace, C. Pothoulakis, and R. Dana, Neuropeptide substance P and the immune response. Cell Mol Life Sci, 2016. 73(22): p. 4249-4264.

339. Ziche, M., L. Morbidelli, M. Pacini, P. Geppetti, G. Alessandri, and C.A. Maggi, Substance P stimulates neovascularization in vivo and proliferation of cultured endothelial cells. Microvasc Res, 1990. 40(2): p. 264-278.

340. Şimşek, E., E.A. Aydemir, N. İmir, O. Koçak, A. Kuruoğlu, and K. Fışkın, Dimethyl sulfoxide-caused changes in pro-and anti-angiogenic factor levels could contribute to an anti-angiogenic response in HeLa cells. Neuropeptides, 2015. 53: p. 37-43.

341. Rosen, C., E. Shezen, A. Aronovich, Y.Z. Klionsky, Y. Yaakov, M. Assayag, I.E. Biton, O. Tal, G. Shakhar, and H. Ben-Hur, Preconditioning allows engraftment of mouse and human embryonic lung cells, enabling lung repair in mice. Nat Med, 2015. 21(8): p. 869-879.

APPENDIX

Table A-1 Percent MSC viability for each treatment group.

	Immediately	15 min	30 min	45 min	60 min	120 min
DMSO	83.0 ± 3.99	81.2 ± 4.19	77.7 ± 5.18	75.3 ± 4.46	71.8 ± 4.34	46.9 ± 7.48
Rinse	79.4 ± 3.39	79.0 ± 2.94	76.5 ± 2.90	76.4 ± 3.55	73.1 ± 2.94	69.5 ± 5.52
Dil1	83.0 ± 5.04	79.9 ± 3.17	81.1 ± 4.57	79.2 ± 4.53	75.9 ± 3.31	71.7 ± 4.20
Dil2	81.8 ± 4.18	81.5 ± 3.20	76.9 ± 2.48	80.0 ± 3.06	75.5 ± 2.95	65.4 ± 7.95

Values represent the mean ± SE for six independent replicates with cells from a different horse used for each replicate.

Table A-2 Differentially expressed genes identified by DESeq2 in ovaries injected once with MSCs (MSC1) compared to ovaries injected once with Vehicle (V).

ID	log2FC	P-value	Gene Description
Acvr1c	1.26	1.20E-02	activin A receptor type 1C
Adcy1	-1.17	9.33E-03	adenylate cyclase 1
Akr1d1	1.02	3.66E-02	aldo-keto reductase family 1 member D1
Angptl7	1.00	4.41E-02	angiopoietin like 7
Asb15	-1.48	3.42E-03	ankyrin repeat and SOCS box containing 15
Asgr1	-1.10	2.96E-02	asialoglycoprotein receptor 1
C21orf62	1.03	3.18E-02	chromosome 21 open reading frame 62
C6orf163	-1.04	3.56E-02	chromosome 6 open reading frame 163
Camsap3	-1.06	3.56E-02	calmodulin regulated spectrin associated protein family member 3
Ccdc102b	1.23	1.28E-02	coiled-coil domain containing 102B
Ccr3	-1.04	3.95E-02	C-C motif chemokine receptor 3
Cish	-1.43	3.03E-03	cytokine inducible SH2 containing protein
Cntn5	1.40	2.55E-03	contactin 5
Cntnap5	1.05	3.82E-02	contactin associated protein like 5
Ct83	-1.00	4.74E-02	cancer/testis antigen 83
Ctnnd2	1.09	2.88E-02	catenin delta 2
Dcst2	1.42	4.59E-03	DC-STAMP domain containing 2
Depdc4	1.04	3.76E-02	DEP domain containing 4
Dll3	-1.06	3.52E-02	delta like canonical Notch ligand 3
Dpep2	-1.22	1.34E-02	dipeptidase 2
Ensecag00000000093	1.05	3.56E-02	
Ensecag00000000422	1.07	1.74E-02	
Ensecag00000000778	-1.04	3.80E-02	
Ensecag00000001271	-1.30	1.02E-02	
Ensecag00000001947	1.07	3.07E-02	
Ensecag00000002196	-1.06	3.35E-02	
Ensecag00000003457	-1.25	1.06E-02	
Ensecag00000003763	1.25	1.09E-02	
Ensecag00000004041	1.34	7.63E-03	
Ensecag00000004103	1.16	1.09E-02	
Ensecag00000004574	1.16	2.14E-02	
Ensecag00000005577	1.14	2.38E-02	
Ensecag00000006200	1.14	2.09E-02	
Ensecag00000006631	-1.26	1.01E-03	
Ensecag00000007937	-1.59	3.81E-04	
Ensecag00000008828	1.26	8.62E-03	
Ensecag00000011121	1.17	1.99E-02	
Ensecag00000011772	1.42	3.92E-03	
Ensecag00000012375	1.21	1.69E-02	
Ensecag00000012909	-1.39	6.19E-03	
Ensecag00000014202	1.50	2.45E-03	
Ensecag00000014719	1.03	3.60E-02	
Ensecag00000015570	1.01	4.02E-02	
Ensecag00000016810	-1.47	3.75E-03	
Ensecag00000018574	-1.38	6.01E-03	
Ensecag00000018854	-1.24	5.62E-03	
Ensecag00000019820	1.00	4.63E-02	

Table A-2 continued

ID	log2FC	P-value	Gene Description
Ensecag00000022656	1.15	2.28E-02	
Ensecag00000022921	-1.03	2.84E-02	
Ensecag00000023091	1.49	2.68E-03	
Ensecag00000024042	1.06	3.42E-02	
Ensecag00000024765	1.34	2.37E-03	
Ensecag00000026593	1.01	4.52E-02	
Ensecag00000027051	1.06	2.96E-02	
Ensecag00000027178	1.02	4.00E-02	
Eps8l3	1.26	6.71E-03	EPS8 like 3
Erbb4	1.34	7.10E-03	erb-b2 receptor tyrosine kinase 4
Grm5	1.04	3.67E-02	glutamate metabotropic receptor 5
Hand2	1.05	3.35E-02	heart and neural crest derivatives expressed 2
Hist1h2bn	1.10	1.91E-02	histone cluster 1 H2B family member n
Hist2h2be	-1.21	2.53E-03	histone cluster 2 H2B family member e
Il33	1.25	1.16E-02	interleukin 33
Ilt11b	1.00	3.55E-02	
Kcnk2	1.05	3.85E-02	potassium two pore domain channel subfamily K member 2
Kctd19	-1.09	3.23E-02	potassium channel tetramerization domain containing 19
Krt14	-1.76	5.80E-05	keratin 14
Krt17	-1.68	2.47E-04	keratin 17
Krt5	-1.55	5.70E-05	keratin 5
Lrrtm2	1.19	1.29E-02	leucine rich repeat transmembrane neuronal 2
Lyg1	1.10	2.88E-02	lysozyme g1
Msln	1.37	6.76E-03	mesothelin
Myhc-Alpha	-1.33	8.11E-03	
Nalcn	1.01	2.45E-02	sodium leak channel, non-selective
Nmnat2	-1.02	4.16E-02	nicotinamide nucleotide adenylyltransferase 2
Notum	-1.00	4.58E-02	NOTUM, palmitoleoyl-protein carboxylesterase
Nr1h4	1.06	1.59E-02	nuclear receptor subfamily 1 group H member 4
P2rx6	-1.10	3.07E-02	purinergic receptor P2X 6
Pigr	-1.04	3.27E-02	polymeric immunoglobulin receptor
Prame	-1.09	2.86E-02	preferentially expressed antigen in melanoma
Prlr	-1.57	1.72E-03	prolactin receptor
Prr16	1.07	3.19E-02	proline rich 16
Rassf9	1.07	4.98E-03	Ras association domain family member 9
Rnf17	-1.41	5.39E-03	ring finger protein 17
Scnn1g	-1.09	3.02E-02	sodium channel epithelial 1 gamma subunit
Scrg1	1.02	4.28E-02	stimulator of chondrogenesis 1
Sema3e	1.10	3.00E-02	semaphorin 3E
Slc1a2	1.03	4.06E-02	solute carrier family 1 member 2
Slc44a5	1.07	3.48E-02	solute carrier family 44 member 5
Slc4a9	1.32	7.66E-03	solute carrier family 4 member 9
Snord41	-1.27	1.26E-02	small nucleolar RNA, C/D box 41
Tlr1	1.09	1.14E-02	toll like receptor 1
Tsga10	1.10	2.24E-03	testis specific 10
Wdr87	1.02	4.22E-02	WD repeat domain 87

Table A-3 Differentially expressed genes identified by DESeq2 in MSC1opp ovaries versus Vopp ovaries.

ID	log2FC	P-value	Gene Description
7sk	1.05	2.17E-02	
Abcg5	1.12	2.58E-02	ATP binding cassette subfamily G member 5
Acp5	1.21	1.67E-02	acid phosphatase 5, tartrate resistant
Adad1	1.30	6.27E-03	adenosine deaminase domain containing 1
Adamts9	-1.02	3.87E-02	ADAM metallopeptidase with thrombospondin type 1 motif 9
Adcy1	-1.28	4.29E-03	adenylate cyclase 1
Ankrd34b	1.03	4.10E-02	ankyrin repeat domain 34B
Ankrd55	-1.20	1.81E-02	ankyrin repeat domain 55
Anln	-1.17	1.91E-02	anillin actin binding protein
Ano9	-1.52	2.42E-03	anoctamin 9
Ap1m2	-1.02	1.28E-02	adaptor related protein complex 1 mu 2 subunit
Aqp5	-1.03	3.99E-02	aquaporin 5
Arid5a	1.29	9.87E-03	AT-rich interaction domain 5A
Armc3	-1.20	1.19E-02	armadillo repeat containing 3
Asb11	1.12	2.03E-02	ankyrin repeat and SOCS box containing 11
Asgr2	-1.10	3.04E-02	asialoglycoprotein receptor 2
Atp13a4	-1.26	4.81E-03	ATPase 13A4
Atp13a5	-1.15	3.33E-03	ATPase 13A5
Atp2c2	-1.37	6.64E-03	ATPase secretory pathway Ca2+ transporting 2
Bmp7	-1.52	2.11E-03	bone morphogenetic protein 7
Bnc1	-1.15	1.31E-03	basonuclin 1
Bub1	-1.01	4.20E-02	BUB1 mitotic checkpoint serine/threonine kinase
Bub1b	-1.15	2.26E-02	BUB1 mitotic checkpoint serine/threonine kinase B
C17orf72	-1.39	6.13E-03	chromosome 18 open reading frame 63
C18orf63	-1.00	2.85E-02	chromosome 22 open reading frame 31
C22orf31	-1.48	2.24E-03	chromosome 2 open reading frame 54
C2orf54	-1.43	1.85E-03	chromosome 4 open reading frame 22
C4orf22	-1.15	1.49E-02	chromosome 6 open reading frame 118
C6orf118	-1.50	1.03E-03	calcium dependent secretion activator
C9orf9	-1.54	2.02E-03	calmodulin regulated spectrin associated protein family member 3
Cadps	-1.07	3.40E-02	coiled-coil domain containing 113
Camsap3	-1.49	3.37E-03	coiled-coil domain containing 116
Ccdc113	-1.14	1.78E-02	cyclin B2
Ccdc116	1.02	2.30E-02	cyclin B3
Ccnb2	-1.27	1.13E-02	CD36 molecule
Ccnb3	-1.45	3.51E-03	CD8b molecule
Cd36	1.29	8.92E-03	cell division cycle 20
Cd8b	1.18	1.93E-02	cell division cycle associated 5
Cdc20	-1.02	2.72E-02	cadherin 1
Cdca5	-1.16	2.24E-02	cadherin related family member 2
Cdh1	-1.41	3.38E-03	cadherin related family member 4
Cdhr2	-1.39	4.98E-03	cyclin dependent kinase inhibitor 3
Cdhr4	-1.02	4.31E-02	centromere protein F
Cdkn3	-1.07	3.17E-02	centrosomal protein 55

Table A-3 continued

ID	log2FC	P-value	Gene Description
Cenpf	-1.13	2.55E-02	choline dehydrogenase
Cep55	-1.13	2.49E-02	cartilage intermediate layer protein
Chdh	-1.01	3.12E-02	Cbp/p300 interacting transactivator with Glu/Asp rich carboxy-terminal domain 1
Cilp	-1.73	4.62E-04	cytoskeleton associated protein 2
Cited1	-2.09	1.38E-05	claudin 2
Ckap2	-1.02	3.91E-02	claudin 7
Cldn2	-1.26	1.22E-02	contactin 2
Cldn7	-1.62	1.32E-03	contactin 4
Cntn2	-1.31	9.01E-03	collagen type I alpha 1 chain
Cntn4	-1.05	3.66E-02	collagen type XXI alpha 1 chain
Col1a1	-1.09	3.20E-02	collagen type III alpha 1 chain
Col21a1	-1.07	1.23E-02	collagen type VI alpha 6 chain
Col3a1	-1.00	4.51E-02	copine 7
Col6a6	-1.50	3.11E-03	chondroitin sulfate proteoglycan 5
Cpne7	1.01	3.95E-02	C-X3-C motif chemokine receptor 1
Cspg5	-1.22	9.46E-03	coxsackie virus and adenovirus receptor
Cx3cr1	-1.05	2.68E-02	cytochrome P450 family 17 subfamily A member 1
Cxadr	-1.03	3.52E-02	dynein assembly factor with WD repeats 1
Cyp17a1	-1.50	2.30E-03	DEP domain containing 4
Daw1	-1.56	1.07E-03	dickkopf WNT signaling pathway inhibitor 2
Depdc4	1.18	1.81E-02	dynein axonemal heavy chain 6
Dkk2	-1.41	4.77E-03	dynein axonemal intermediate chain 1
Dnah6	-1.80	6.54E-05	dipeptidyl peptidase 4
Dnai1	-1.45	4.37E-03	desmocollin 1
Dpp4	-1.32	9.54E-03	desmoplakin
Dsc1	-1.16	1.44E-02	dual oxidase 1
Dsp	-1.48	3.31E-03	dual oxidase maturation factor 1
Duox1	-1.15	2.09E-02	E2F transcription factor 1
Duoxa1	-1.22	9.52E-03	ATP binding cassette subfamily G member 5
E2f1	-1.05	3.60E-02	acid phosphatase 5, tartrate resistant
Eca-Mir-492-1	-1.84	1.87E-04	
Ehf	-1.35	5.20E-03	ETS homologous factor
Elovl3	-1.24	6.73E-03	ELOVL fatty acid elongase 3
Ensecag00000000778	-1.15	2.15E-02	
Ensecag00000000799	-1.11	2.95E-02	
Ensecag00000000929	-1.35	7.80E-03	
Ensecag00000001091	1.05	3.49E-02	
Ensecag00000001271	-1.42	5.01E-03	
Ensecag00000001639	-1.26	1.28E-02	
Ensecag00000002139	-1.18	1.95E-02	
Ensecag00000002196	1.09	2.81E-02	
Ensecag00000002402	-1.28	1.05E-02	
Ensecag00000004041	1.52	2.47E-03	
Ensecag00000004126	-1.26	7.35E-03	
Ensecag00000004696	-1.47	1.12E-03	
Ensecag00000005122	-1.14	7.96E-03	
Ensecag00000006099	-1.05	3.11E-02	

Table A-3 continued

ID	log2FC	P-value	Gene Description
Ensecag00000006291	-1.37	5.77E-03	
Ensecag00000006785	1.06	1.91E-02	
Ensecag00000006816	-1.58	1.39E-03	
Ensecag00000007832	-1.01	2.31E-02	
Ensecag00000008432	-1.02	3.69E-02	
Ensecag00000008785	-1.14	2.14E-02	
Ensecag00000009152	-1.68	6.31E-04	
Ensecag00000010934	1.28	9.75E-03	
Ensecag00000011121	1.21	1.57E-02	
Ensecag00000011256	-1.05	2.47E-02	
Ensecag00000011685	-1.05	3.29E-02	
Ensecag00000012503	-1.54	3.11E-04	
Ensecag00000013193	-1.02	4.31E-02	
Ensecag00000014165	1.03	1.50E-02	
Ensecag00000015137	-1.08	2.94E-02	
Ensecag00000016395	1.03	3.57E-02	
Ensecag00000016799	1.07	1.27E-02	
Ensecag00000016992	-1.25	6.50E-03	
Ensecag00000017155	-1.70	7.83E-04	
Ensecag00000018391	1.10	2.58E-02	
Ensecag00000018753	-1.23	1.49E-02	
Ensecag00000019052	1.28	1.07E-02	
Ensecag00000020268	-1.19	1.90E-02	
Ensecag00000020734	-1.21	9.99E-04	
Ensecag00000020802	1.26	1.16E-02	
Ensecag00000021531	-1.39	2.96E-03	
Ensecag00000021775	-1.24	1.28E-02	
Ensecag00000021806	1.11	2.30E-02	
Ensecag00000022318	-1.03	1.57E-02	
Ensecag00000022324	-1.34	2.26E-03	
Ensecag00000022656	1.14	2.31E-02	
Ensecag00000022921	-1.00	2.72E-02	
Ensecag00000023653	1.87	1.16E-04	
Ensecag00000023710	-1.28	1.55E-03	
Ensecag00000024557	1.09	3.00E-02	
Ensecag00000026387	1.01	3.41E-02	
Ensecag00000026830	-1.11	2.92E-02	
Ensecag00000027051	1.24	1.18E-02	
Ensecag00000027105	1.15	1.05E-02	
Ensecag00000027132	1.05	3.53E-02	
Ensecag00000027336	1.61	1.25E-03	
Ensecag00000027466	1.09	2.32E-02	
Ensecag00000027547	2.78	1.28E-08	
Ensecag00000027634	1.23	9.95E-03	
Epha1	-1.18	1.79E-02	EPH receptor A1
Epha8	-1.27	1.22E-02	EPH receptor A8
Esrp1	-1.11	9.75E-03	epithelial splicing regulatory protein 1
Esrp2	-1.03	1.15E-03	epithelial splicing regulatory protein 2
Exo1	-1.10	2.46E-02	exonuclease 1

Table A-3 continued

ID	log2FC	P-value	Gene Description
Fabp7	1.10	1.37E-02	fatty acid binding protein 7
Fads3	-1.18	1.79E-02	fatty acid desaturase 3
Faim3	1.16	2.17E-02	family with sequence similarity 216 member B
Fam216b	-1.26	2.11E-03	family with sequence similarity 92 member B
Fam92b	-1.49	2.72E-03	fatty acyl-CoA reductase 2
Far2	-1.16	2.08E-02	FAT atypical cadherin 2
Fat2	-1.33	7.10E-03	F-box protein 47
Fbxo47	-1.65	1.11E-03	Fc fragment of IgM receptor
Fgf5	-1.12	1.76E-02	fibroblast growth factor 5
Fgl1	1.10	1.96E-02	fibrinogen like 1
Fibin	1.05	1.97E-02	fin bud initiation factor homolog (zebrafish)
Foxc2	1.19	1.30E-02	forkhead box C2
Foxj1	-1.17	2.14E-02	forkhead box J1
Foxm1	-1.02	3.92E-02	forkhead box M1
Fst	-1.10	3.01E-02	follistatin
Fstl4	-1.20	1.76E-02	follistatin like 4
Ftcd	-1.10	2.96E-02	formimidoyltransferase cyclodeaminase
Fxyd2	-1.21	1.73E-02	FXYD domain containing ion transport regulator 2
Gabrp	-1.05	1.15E-02	gamma-aminobutyric acid type A receptor pi subunit
Gcnt3	-1.13	1.83E-02	glucosaminyl (N-acetyl) transferase 3, mucin type
Gdap1l1	-1.23	1.34E-02	ganglioside induced differentiation associated protein 1 like 1
Ggt1	-1.17	1.98E-02	gamma-glutamyltransferase 1
Gpr84	1.04	3.40E-02	G protein-coupled receptor 84
Grhl2	-1.32	1.63E-03	grainyhead like transcription factor 2
Grin3a	-1.06	3.27E-02	glutamate ionotropic receptor NMDA type subunit 3A
Gzmh	1.41	2.82E-03	granzyme H
Hjurp	-1.04	3.03E-02	Holliday junction recognition protein
Hmmr	-1.12	2.66E-02	hyaluronan mediated motility receptor
Hpn	-1.30	8.96E-03	hepsin
Hsf4	1.11	1.84E-02	heat shock transcription factor 4
Hspa6	1.35	7.53E-03	heat shock protein family A (Hsp70) member 6
Htr1e	-1.45	3.12E-03	5-hydroxytryptamine receptor 1E
Igj	-1.07	2.79E-02	interleukin 22 receptor subunit alpha 1
Il22ra1	-1.31	1.02E-02	interleukin 22 receptor subunit alpha 2
Il22ra2	1.28	1.01E-02	interleukin 2 receptor subunit gamma
Il2rg	1.03	3.84E-03	interleukin 33
Il33	1.02	3.97E-02	inhibin alpha subunit
Inha	-1.34	8.41E-03	inhibin beta B subunit
Inhbb	-1.14	2.10E-02	insulin like 3
Insl3	-1.65	1.72E-04	inter-alpha-trypsin inhibitor heavy chain 2
Itih2	-1.12	1.24E-02	inter-alpha-trypsin inhibitor heavy chain family member 4
Itih4	1.14	2.19E-02	joining chain of multimeric IgA and IgM
Kiaa0101	-1.28	7.78E-03	kinesin family member 11

Table A-3 continued

ID	log2FC	P-value	Gene Description
Kif11	-1.12	2.46E-02	kinesin family member 20A
Kif20a	-1.14	2.21E-02	keratin 77
Krt77	-1.02	1.72E-02	laminin subunit gamma 2
Lamc2	-1.46	1.37E-03	leucine rich repeat LGI family member 4
Lgi4	1.07	2.84E-02	lysophosphatidic acid receptor 3
Lpar3	-1.28	6.68E-03	LDL receptor related protein 8
Lrp8	-1.02	3.15E-02	leucine rich repeat containing 43
Lrrc43	-1.20	1.56E-02	leucine rich repeat containing 56
Lrrc56	-1.26	1.29E-02	leucine rich repeat neuronal 4
Lrrn4	-1.74	4.25E-04	lymphotoxin beta
Ltb	1.13	5.70E-03	MACRO domain containing 1
Macrod1	1.03	1.15E-02	mediator complex subunit 12 like
Med12l	-1.06	1.21E-02	methyltransferase like 11B
Mettl11b	-1.27	4.33E-03	EPH receptor A1
Mhc-1	-1.03	4.01E-02	
Mip-2beta	1.01	4.60E-02	
Mis18a	-1.02	4.36E-02	MIS18 kinetochore protein A
Mmp7	-1.90	4.47E-05	matrix metallopeptidase 7
Mpo	1.12	1.29E-02	myeloperoxidase
Ms4a1	1.29	1.01E-02	membrane spanning 4-domains A1
Muc16	-1.55	2.37E-04	mucin 16, cell surface associated
Muc20	-1.02	1.06E-02	mucin 20, cell surface associated
Muc4	-1.53	8.22E-04	mucin 4, cell surface associated
Muc5b	1.08	3.19E-02	mucin 5B, oligomeric mucus/gel-forming
Mybphl	1.21	3.75E-03	myosin binding protein H like
Myhc-Alpha	-1.67	8.89E-04	
Myoc	1.08	3.37E-02	myocilin
Myt1l	-1.20	1.75E-02	myelin transcription factor 1 like
Napsa	1.01	4.16E-02	napsin A aspartic peptidase
Nefh	-1.11	2.33E-02	neurofilament heavy
Nov	1.09	3.05E-02	nephroblastoma overexpressed
Nr0b2	-1.18	2.03E-02	nuclear receptor subfamily 0 group B member 2
Nrcam	-1.03	3.50E-02	neuronal cell adhesion molecule
Oprk1	-1.33	6.76E-04	opioid receptor kappa 1
Paqr5	-1.35	7.44E-03	progestin and adipoQ receptor family member 5
Pax8	-1.07	1.27E-02	paired box 8
Pde4c	1.12	1.47E-02	PCNA clamp associated factor
Pi16	1.05	3.66E-02	phosphodiesterase 4C
Pigr	-1.65	7.58E-04	peptidase inhibitor 16
Pinlyp	-1.04	3.08E-02	polymeric immunoglobulin receptor
Pkmyt1	-1.04	1.86E-02	phospholipase A2 inhibitor and LY6/PLAUR domain containing
Pkp3	-1.01	1.04E-02	protein kinase, membrane associated tyrosine/threonine 1
Ppp1r1b	-1.39	5.52E-03	plakophilin 3
Prc1	-1.06	3.48E-02	protein phosphatase 1 regulatory inhibitor subunit 1B

Table A-3 continued

ID	log2FC	P-value	Gene Description
Prkg2	1.26	1.00E-02	protein regulator of cytokinesis 1
Prkrir	-1.30	1.04E-03	protein kinase, cGMP-dependent, type II
Prlr	-1.60	1.46E-03	prolactin receptor
Prom2	-1.16	7.44E-03	prominin 2
Prr11	-1.10	2.80E-02	proline rich 11
Prss54	-1.08	3.23E-02	proline rich 29
Ptpn5	-1.75	2.91E-04	protease, serine 54
Ptprq	-1.16	1.95E-02	protein tyrosine phosphatase, non-receptor type 5
Qpct	-1.05	3.41E-02	protein tyrosine phosphatase, receptor type Q
Rab25	-1.40	3.20E-03	glutaminyl-peptide cyclotransferase
Rbm47	-1.35	7.46E-03	RAB25, member RAS oncogene family
Rgs8	-1.03	4.26E-02	RNA binding motif protein 47
Rgs9	-1.04	3.20E-02	regulator of G-protein signaling 8
Rnase_MRP	1.47	2.96E-03	
Rnasep_Nuc	1.32	7.76E-03	
Rnf43	-1.40	5.72E-03	ring finger protein 43
Ropn1l	-1.12	2.51E-02	rhophilin associated tail protein 1 like
S100a14	-1.24	1.40E-02	S100 calcium binding protein A14
Scarna17	1.08	3.12E-02	small Cajal body-specific RNA 17
Scarna2	1.35	1.99E-03	small Cajal body-specific RNA 2
Scnn1g	-1.01	4.47E-02	sodium channel epithelial 1 gamma subunit
Serinc2	-1.68	9.80E-04	serine incorporator 2
Slc13a2	-1.21	8.57E-03	solute carrier family 13 member 2
Slc22a16	-1.23	4.65E-03	solute carrier family 22 member 16
Slc2a2	-1.49	1.45E-03	solute carrier family 2 member 2
Slc35g1	-1.33	8.39E-03	solute carrier family 35 member G1
Slc4a4	-1.07	1.87E-02	solute carrier family 4 member 4
Slc8a2	1.16	1.93E-02	solute carrier family 8 member A2
Snora43	-1.19	9.46E-03	small nucleolar RNA, H/ACA box 17B
Snord74	1.09	2.16E-02	small nucleolar RNA, C/D box 74
Snou2-30	1.01	4.45E-02	
Sp6	-1.20	1.44E-02	Sp6 transcription factor
Spint1	-1.20	1.70E-02	**serine peptidase inhibitor, Kunitz type 1**
Spla2	-1.67	4.19E-04	
Spta1	-1.51	2.62E-03	spectrin alpha, erythrocytic 1
Sptbn2	-1.19	2.74E-03	spectrin beta, non-erythrocytic 2
St14	-1.38	4.30E-03	suppression of tumorigenicity 14
Svopl	-1.09	7.19E-03	SVOP like
Syce1l	1.48	3.19E-03	synaptonemal complex central element protein 1 like
Tepp	1.11	1.92E-02	testis, prostate and placenta expressed
Thsd7b	-1.06	3.40E-02	THAP domain containing 12
Tmem200a	-1.05	3.80E-02	thrombospondin type 1 domain containing 7B
Tmem54	-1.05	3.04E-02	transmembrane protein 200A
Tnc	-1.44	2.98E-03	transmembrane protein 54
Top2a	-1.03	3.35E-02	tenascin C
Ttc21a	-1.29	2.75E-03	topoisomerase (DNA) II alpha
Tubb2b	-1.07	1.57E-02	tetratricopeptide repeat domain 21A

Table A-3 continued

ID	log2FC	P-value	Gene Description
U6atac	1.25	1.22E-02	
Ubd	1.21	1.39E-02	ubiquitin D
Unc45b	-1.72	6.69E-04	unc-45 myosin chaperone B
Upk1b	-1.73	5.85E-05	uroplakin 1B
Upk3b	-1.46	2.53E-03	uroplakin 3B
Vwa3a	-1.14	1.96E-02	von Willebrand factor A domain containing 3A
Vwa3b	-1.39	6.02E-03	von Willebrand factor A domain containing 3B
Wfdc2	-1.05	2.26E-02	WAP four-disulfide core domain 2
Wwc1	-1.38	6.37E-03	WW and C2 domain containing 1
Xg	1.03	2.47E-02	Xg blood group
Zdhhc23	-1.09	1.98E-02	zinc finger DHHC-type containing 23

Table A-4 Differentially expressed genes identified by DESeq2 in ovaries injected twice with MSCs (MSC2) versus ovaries injected once with MSCs (MSC1).

ID	log2FC	P-value	Gene Description
ABCD2	-1.57	1.92E-03	ATP binding cassette subfamily D member 2
ACP5	1.37	6.46E-03	acid phosphatase 5, tartrate resistant
ACSBG2	1.07	2.07E-02	acyl-CoA synthetase bubblegum family member 2
ADCY1	1.15	7.05E-03	adenylate cyclase 1
AGBL4	-1.03	2.28E-02	adhesion G protein-coupled receptor E3
AIM2	1.03	3.38E-02	ATP/GTP binding protein like 4
ALOX5	1.31	5.78E-03	absent in melanoma 2
ASB15	1.22	1.65E-02	arachidonate 5-lipoxygenase
ASGR1	1.24	1.49E-02	ankyrin repeat and SOCS box containing 15
BATF	1.13	1.98E-02	asialoglycoprotein receptor 1
BCL2A1	1.14	2.29E-02	basic leucine zipper ATF-like transcription factor
BCL2L14	1.32	8.73E-03	BCL2 related protein A1
BPIFC	1.26	9.18E-03	BCL2 like 14
BRINP2	-1.04	3.15E-02	BPI fold containing family C
BTBD16	-1.00	4.86E-02	BMP/retinoic acid inducible neural specific 2
BTLA	1.15	2.19E-02	BTB domain containing 16
C1QA	1.17	6.38E-03	B and T lymphocyte associated
C1QB	1.20	7.23E-03	complement C1q A chain
C1QC	1.34	3.39E-03	complement C1q B chain
C21orf62	-1.41	2.52E-03	complement C1q C chain
C3AR1	1.04	4.97E-03	chromosome 21 open reading frame 62
C5AR1	1.08	1.04E-02	complement C3a receptor 1
CA8	1.09	1.80E-02	complement C5a receptor 1
CACNA1B	1.38	6.55E-03	carbonic anhydrase 8
CASP1	1.20	1.87E-03	calcium voltage-gated channel subunit alpha1 B
CAV3	-1.05	3.67E-02	caspase 1
CCL2	1.03	4.33E-02	caveolin 3
CCL20	1.08	1.15E-02	C-C motif chemokine ligand 2
CCR3	1.44	4.50E-03	C-C motif chemokine ligand 20
CD163	1.52	9.80E-04	C-C motif chemokine receptor 3
CD163L1	1.03	3.91E-02	CD163 molecule
CD180	1.49	3.45E-03	CD163 molecule like 1
CD300LB	1.69	8.95E-04	CD180 molecule
CD48	1.50	2.85E-03	CD300 molecule like family member b
CD53	1.11	1.15E-02	CD48 molecule
CD68	1.13	1.60E-02	CD53 molecule
CD84	1.09	1.59E-02	CD68 molecule
CD86	1.47	1.23E-03	CD84 molecule
CEBPE	1.04	1.54E-02	CD86 molecule
CECR1	1.31	5.84E-03	CCAAT/enhancer binding protein epsilon
CHI3L1	1.32	5.69E-03	cat eye syndrome chromosome region, candidate 1
CHRM3	-1.31	9.61E-03	chitinase 3 like 1

Table A-4 continued

ID	log2FC	P-value	Gene Description
CLDN20	1.00	4.70E-02	cholinergic receptor muscarinic 3
CLEC6A	1.47	3.55E-03	claudin 20
CLEC7A	1.30	8.72E-03	C-type lectin domain family 6 member A
CNTN5	-1.09	2.47E-02	C-type lectin domain family 7 member A
CP	1.01	1.72E-02	contactin 5
CRABP1	-1.08	3.05E-02	ceruloplasmin
CRADD	-1.05	1.30E-03	cellular retinoic acid binding protein 1
CRHBP	1.51	2.88E-03	CASP2 and RIPK1 domain containing adaptor with death domain
CSF1R	1.17	3.60E-03	corticotropin releasing hormone binding protein
CTSS	1.01	1.73E-02	colony stimulating factor 1 receptor
CX3CR1	1.04	2.15E-02	cathepsin S
CXCL11	1.21	1.60E-02	C-X3-C motif chemokine receptor 1
CXCL9	1.50	1.77E-03	C-X-C motif chemokine ligand 11
CYBB	1.50	1.51E-03	C-X-C motif chemokine ligand 9
CYTH4	1.22	2.70E-03	cytochrome b-245 beta chain
DENND1C	1.10	3.62E-03	cytohesin 4
DEPDC4	-1.01	4.76E-02	DENN domain containing 1C
DPEP2	1.22	1.07E-02	DEP domain containing 4
EEF1A2	1.03	3.03E-02	dipeptidase 2
EIF4E1B	1.22	1.09E-02	eukaryotic translation elongation factor 1 alpha 2
EMR3	1.37	6.64E-03	
ENSECAG00000000339	1.31	6.80E-03	
ENSECAG00000000422	-1.04	2.73E-02	
ENSECAG00000000649	-1.06	3.43E-02	
ENSECAG00000001489	-1.15	1.67E-02	
ENSECAG00000001649	1.61	6.69E-04	
ENSECAG00000003088	1.34	7.35E-03	
ENSECAG00000003180	1.07	2.69E-02	
ENSECAG00000003446	1.02	2.90E-02	
ENSECAG00000003447	1.22	1.55E-02	
ENSECAG00000003466	1.07	1.56E-02	
ENSECAG00000004548	-1.05	3.89E-02	
ENSECAG00000004863	1.46	3.96E-03	
ENSECAG00000005231	1.62	4.84E-04	
ENSECAG00000005400	1.02	4.26E-02	
ENSECAG00000005562	1.23	9.90E-03	
ENSECAG00000006200	-1.04	3.98E-02	
ENSECAG00000006663	1.52	3.19E-04	
ENSECAG00000006701	1.08	2.65E-02	
ENSECAG00000006708	-1.11	1.74E-02	
ENSECAG00000007937	1.35	3.86E-03	
ENSECAG00000007943	1.08	5.09E-03	
ENSECAG00000008615	1.43	3.11E-03	
ENSECAG00000009228	-1.10	4.67E-03	
ENSECAG00000009271	1.60	1.06E-03	
ENSECAG00000009404	1.29	8.76E-03	

Table A-4 continued

ID	log2FC	P-value	Gene Description
ENSECAG00000009816	1.13	2.23E-02	
ENSECAG00000009954	-1.18	1.60E-02	
ENSECAG00000010357	1.46	3.16E-03	
ENSECAG00000011121	-1.18	1.69E-02	
ENSECAG00000011772	-1.13	1.84E-02	
ENSECAG00000012199	1.30	3.13E-03	
ENSECAG00000012204	-1.32	5.62E-03	
ENSECAG00000012222	1.22	1.13E-02	
ENSECAG00000012909	1.42	4.63E-03	
ENSECAG00000013056	1.08	2.18E-02	
ENSECAG00000014250	1.26	1.22E-02	
ENSECAG00000014546	1.98	4.79E-08	
ENSECAG00000014585	1.20	1.00E-03	
ENSECAG00000015201	-1.30	8.84E-03	
ENSECAG00000015451	-1.08	3.32E-02	
ENSECAG00000015462	-1.09	1.92E-02	
ENSECAG00000016000	-1.05	1.85E-02	
ENSECAG00000016712	1.01	2.61E-02	
ENSECAG00000016970	1.95	1.13E-04	
ENSECAG00000017969	1.17	2.08E-02	
ENSECAG00000018516	1.44	2.95E-03	
ENSECAG00000018574	1.69	5.16E-04	
ENSECAG00000018848	-1.05	3.84E-02	
ENSECAG00000019100	1.18	1.80E-02	
ENSECAG00000019352	1.24	1.05E-02	
ENSECAG00000019488	1.13	1.58E-02	
ENSECAG00000020136	1.29	1.02E-02	
ENSECAG00000020640	1.23	1.50E-02	
ENSECAG00000020862	-1.21	1.47E-02	
ENSECAG00000021110	1.52	5.49E-05	
ENSECAG00000021202	1.74	3.10E-04	
ENSECAG00000021713	1.02	4.37E-02	
ENSECAG00000022087	1.01	4.45E-02	
ENSECAG00000022716	1.23	1.44E-02	
ENSECAG00000022781	-1.16	2.04E-02	
ENSECAG00000023091	-1.06	3.68E-02	
ENSECAG00000023126	1.04	3.29E-02	
ENSECAG00000023214	1.02	3.21E-02	
ENSECAG00000023307	-1.05	3.83E-02	
ENSECAG00000023653	-1.19	1.22E-02	
ENSECAG00000024765	-1.30	5.07E-03	
ENSECAG00000024790	1.16	1.35E-02	
ENSECAG00000024882	1.31	1.45E-03	
ENSECAG00000024996	1.04	4.09E-02	
ENSECAG00000025064	-1.13	1.99E-02	
EQMHCC1	-1.05	3.44E-02	
ETV7	1.44	2.59E-03	ETS variant 7
FAT2	1.01	3.40E-02	FAT atypical cadherin 2
FCER1G	1.28	4.18E-03	Fc fragment of IgE receptor Ig

Table A-4 continued

ID	log2FC	P-value	Gene Description
FLT3	1.07	2.38E-03	fms related tyrosine kinase 3
FOXC2	-1.00	2.91E-02	forkhead box C2
FTCDNL1	1.00	4.21E-02	formiminotransferase cyclodeaminase N-terminal like
GALNTL6	-1.08	3.33E-02	polypeptide N-acetylgalactosaminyltransferase-like 6
GBP6	1.05	2.74E-02	guanylate binding protein family member 6
GFRA3	-1.20	7.32E-03	GDNF family receptor alpha 3
GFRA4	1.07	3.07E-02	GDNF family receptor alpha 4
GHSR	1.18	1.50E-02	growth hormone secretagogue receptor
GPR141	1.02	9.22E-03	G protein-coupled receptor 141
GPR151	1.22	1.19E-03	G protein-coupled receptor 151
GPR31	1.45	8.08E-04	G protein-coupled receptor 31
GPR65	1.22	4.68E-03	G protein-coupled receptor 65
GRIA4	1.07	2.78E-02	glutamate ionotropic receptor AMPA type subunit 4
HCK	1.20	1.41E-02	HCK proto-oncogene, Src family tyrosine kinase
HCLS1	1.08	5.80E-03	hematopoietic cell-specific Lyn substrate 1
HIST1H2BB	-1.11	1.96E-02	histone cluster 1 H2B family member b
HIST1H2BN	-1.10	2.36E-02	histone cluster 1 H2B family member n
HIST2H2BE	1.08	1.14E-02	histone cluster 2 H2B family member e
HMGA1	1.48	2.55E-03	high mobility group AT-hook 1
HNF4A	1.03	4.23E-02	hepatocyte nuclear factor 4 alpha
HPSE	1.23	1.45E-02	heparanase
HPSE2	-1.08	3.29E-02	heparanase 2 (inactive)
HS6ST3	1.28	6.07E-03	heparan sulfate 6-O-sulfotransferase 3
HSPA6	1.43	4.96E-03	heat shock protein family A (Hsp70) member 6
IFI30	1.11	1.65E-03	IFI30, lysosomal thiol reductase
IGF2BP2	1.29	8.41E-03	insulin like growth factor 2 mRNA binding protein 2
IGFBPL1	1.30	9.66E-03	insulin like growth factor binding protein like 1
IL10RA	1.19	5.67E-03	interleukin 10 receptor subunit alpha
IL1A	1.10	2.99E-02	interleukin 1 alpha
IL1RN	1.37	6.37E-03	interleukin 1 receptor antagonist
IL2	-1.15	2.29E-02	interleukin 2
IL27	1.16	2.21E-02	interleukin 27
IL33	-1.33	5.83E-03	interleukin 33
ILT11A	1.29	9.93E-03	
IRF5	1.20	2.61E-03	interferon regulatory factor 5
IRF8	1.49	3.00E-04	interferon regulatory factor 8
ISG20	1.32	7.63E-03	interferon stimulated exonuclease gene 20
ITGAX	1.27	7.82E-03	integrin subunit alpha X
ITGB2	1.19	3.08E-03	integrin subunit beta 2
JPH2	-1.07	1.51E-02	junctophilin 2
KCNMA1	-1.17	1.30E-02	potassium calcium-activated channel subfamily M alpha 1

Table A-4 continued

ID	log2FC	P-value	Gene Description
KCTD19	1.33	7.56E-03	potassium channel tetramerization domain containing 19
KISS1	-1.06	2.79E-02	KiSS-1 metastasis-suppressor
KLC3	-1.18	1.87E-02	kinesin light chain 3
KRT26	1.18	1.90E-02	keratin 26
KYNU	1.00	3.58E-02	kynureninase
LAT2	1.20	7.23E-04	linker for activation of T-cells family member 2
LCP1	1.13	1.41E-02	lymphocyte cytosolic protein 1
LGALS4	-1.80	4.12E-04	galectin 4
LRRC10B	-1.03	2.84E-02	leucine rich repeat containing 10B
LTF	1.24	7.24E-03	lactotransferrin
LY86	1.17	1.15E-02	lymphocyte antigen 86
LY9	1.05	2.85E-02	lymphocyte antigen 9
MCOLN2	1.02	4.31E-02	mucolipin 2
MEOX2	-1.21	1.62E-02	mesenchyme homeobox 2
MNDA	1.02	1.41E-02	myeloid cell nuclear differentiation antigen
MPEG1	1.35	7.60E-03	macrophage expressed 1
MPZ	-1.09	3.13E-02	myelin protein zero
MS4A7	1.80	4.52E-05	membrane spanning 4-domains A7
MSLN	-1.20	1.75E-02	mesothelin
MUC2	1.51	2.80E-03	mucin 2, oligomeric mucus/gel-forming
MUSK	1.07	3.57E-02	muscle associated receptor tyrosine kinase
MX2	1.08	2.72E-02	MX dynamin like GTPase 2
NAT16	1.07	3.53E-02	N-acetyltransferase 16 (putative)
NCF4	1.35	1.72E-03	neutrophil cytosolic factor 4
NCKAP1L	1.32	2.56E-03	NCK associated protein 1 like
NFAM1	1.19	1.26E-02	NFAT activating protein with ITAM motif 1
NUP210	1.10	4.86E-03	nucleoporin 210
NXPE4	1.43	2.81E-03	neurexophilin and PC-esterase domain family member 4
NYAP2	1.23	1.09E-02	neuronal tyrosine-phosphorylated phosphoinositide-3-kinase adaptor 2
OVOL1	1.08	2.85E-02	ovo like transcriptional repressor 1
P2RX2	1.10	3.09E-02	purinergic receptor P2X 2
P2RY12	1.38	4.52E-03	purinergic receptor P2Y12
PDE6A	1.84	7.89E-05	phosphodiesterase 6A
PIK3AP1	1.27	3.80E-03	phosphoinositide-3-kinase adaptor protein 1
PLA2G2D	1.18	2.63E-03	phospholipase A2 group IID
PLD4	1.48	6.53E-04	phospholipase D family member 4
POU2AF1	1.44	3.54E-03	POU class 2 associating factor 1
PPFIA2	-1.11	7.82E-03	PTPRF interacting protein alpha 2
PPP1R3C	-1.14	1.04E-02	protein phosphatase 1 regulatory subunit 3C
RAC2	1.20	3.67E-03	ras-related C3 botulinum toxin substrate 2 (rho family, small GTP binding protein Rac2)
RASGRP4	1.01	3.43E-02	RAS guanyl releasing protein 4
RASSF9	-1.13	1.40E-03	Ras association domain family member 9

Table A-4 continued

ID	log2FC	P-value	Gene Description
RBM44	-1.05	7.11E-03	RNA binding motif protein 44
RGS1	1.14	1.57E-02	regulator of G-protein signaling 1
RHBG	1.63	1.08E-03	Rh family B glycoprotein (gene/pseudogene)
SBSPON	-1.23	1.49E-02	somatomedin B and thrombospondin type 1 domain containing
SELL	1.01	4.66E-02	selectin L
SEMA3E	-1.16	2.19E-02	semaphorin 3E
SERPINB1	1.01	4.50E-02	serpin family B member 1
SEZ6L2	1.06	3.20E-02	seizure related 6 homolog like 2
SIGLEC1	1.38	6.34E-04	sialic acid binding Ig like lectin 1
SLAMF6	1.06	3.42E-02	SLAM family member 6
SLAMF7	1.58	1.32E-03	SLAM family member 7
SLAMF8	1.13	1.61E-02	SLAM family member 8
SLAMF9	2.01	6.82E-05	SLAM family member 9
SLC46A2	1.09	1.08E-02	solute carrier family 46 member 2
SLCO4C1	1.12	2.61E-02	solute carrier organic anion transporter family member 4C1
SPI1/PU.1	1.15	1.09E-02	
SPNS3	1.29	3.97E-03	sphingolipid transporter 3 (putative)
ST14	1.13	1.62E-02	suppression of tumorigenicity 14
SYT17	-1.15	5.95E-03	synaptotagmin 17
TAC1	4.36	7.79E-18	tachykinin precursor 1
TFEC	1.40	5.95E-03	transcription factor EC
THBS1	1.15	1.56E-02	thrombospondin 1
TIGIT	1.08	3.25E-02	T-cell immunoreceptor with Ig and ITIM domains
TLR2	1.28	5.25E-03	toll like receptor 2
TLR7	1.30	3.43E-03	toll like receptor 7
TLR8	1.03	4.07E-02	toll like receptor 8
TMEM82	1.05	2.38E-02	transmembrane protein 82
TNFSF15	1.04	4.10E-02	tumor necrosis factor superfamily member 15
TNFSF8	1.23	8.12E-03	tumor necrosis factor superfamily member 8
TNFSF9	1.02	3.54E-02	tumor necrosis factor superfamily member 9
TREM2	1.44	4.01E-03	triggering receptor expressed on myeloid cells 2
TRPM2	1.34	3.01E-03	transient receptor potential cation channel subfamily M member 2
TYROBP	1.24	4.47E-03	TYRO protein tyrosine kinase binding protein
U4	1.03	3.31E-02	
UCP2	1.13	1.02E-02	uncoupling protein 2
VAV1	1.44	8.60E-04	vav guanine nucleotide exchange factor 1
VDR	1.32	7.76E-03	vitamin D (1,25- dihydroxyvitamin D3) receptor
XCR1	1.15	2.05E-02	X-C motif chemokine receptor 1
XPNPEP2	-1.16	1.69E-02	X-prolyl aminopeptidase 2
ZMAT4	-1.07	3.62E-02	zinc finger matrin-type 4